A POWER LAW MODEL FOR TIME DEPENDENT BEHAVIOR OF SOILS

A Dissertation

by

GANG BI

Submitted to the Office of Graduate and Professional Studies of
Texas A&M University
in partial fulfillment of the requirements for the degree of

DOCTOR OF PHILOSOPHY

Chair of Committee,	Jean-Louis Briaud
Co-Chair of Committee,	Marcelo Sanchez
Committee Members,	Charles Aubeny
	Mark Everett
Head of Department,	Robin Autenrieth

December 2015

Major Subject: Civil Engineering

ABSTRACT

The research focuses on a difference between Federal Highway Administration (FHWA) guidelines and Texas Department of Transportation (TxDOT) design practices for soil nail walls in high plasticity (i.e., plasticity index (PI) ≥ 15) clays. It will be going to validate TxDOT's design approach, and then extending the topic to study time dependent behavior of soils, specifically the creep failure and the prediction of long-term deformation, followed by proposing some methods to reduce deformation caused by creep in practice.

A power law model is proposed to describe time dependent behavior of soils. The proposed model is fully demonstrated through enormous laboratory tests on three different soils, data from literature, four kinds of field tests and one field practice.

All objectives are fulfilled in this dissertation. The outcome of this research will give a support to TxDOT's design practice then clarify (or even remove) the creep behavior restrictions in high PI clays in later revision of GEC#7. It will also increase the understanding of time dependent behavior of soils and its application in areas and circumstances where it was previously ignored. Besides, it will be useful to researchers and engineers for being able to reasonably predict long-term deformation in practice with the power law model. It also suggests three methods to reduce creep deformation in practice.

DEDICATION

To my lovely wife, Lei Zhou

To my dear parents, Sheng-xi Bi and Bing-zhen Tian

To my dear parents in law, Bing Zhou and Zong-bi Lei

ACKNOWLEDGEMENTS

I would like to express my gratitude to my advisor, Dr. Jean-Louis Briaud, and my co-advisor, Dr. Marcelo Sanchez, for the chance to involve this project and to focus on the topic of “creep”. Without their support and guidance, this dissertation would not have been accomplished.

Great appreciation goes to my other two committee members, Dr. Charles Aubeny and Dr. Mark Everett, for serving on my committee. I really appreciate their advice and help.

I also would like to acknowledge all staffs in our department and Texas A&M Transportation Institute (TTI) for their help and assistance during my PhD study. Special thanks go to Mr. Mike Linger for guidance on laboratory tests, Mr. Gary Gerke and Mr. Eddie Haug for help on field tests, and Ms. Maria Medrano, Ms. Theresa Taeger, Ms. Kelsey McCoy, Ms. Maria Bunch and Ms. Laura Byrd for assistance on paperworks.

A very special thanks is due to my dear parents, Mr. Sheng-xi Bi and Ms. Bing-zhen Tian, and my father and mother in law, Mr. Bing Zhou and Ms. Zong-bi Lei, for their unconditional support and continuous encouragement over years.

Finally, I would like to show my great gratitude to my lovely, adorable, gorgeous and wise wife, Ms. Lei Zhou, for her love and faith in me. She is always there with me. I couldn’t be any more lucky to have her in my life.

I could not have completed my research without the support of my family, and the dissertation is dedicated to my family.

TABLE OF CONTENTS

Page

LIST OF FIGURES

Page

LIST OF TABLES

Page

1. INTRODUCTION

1.1. Problem Statement

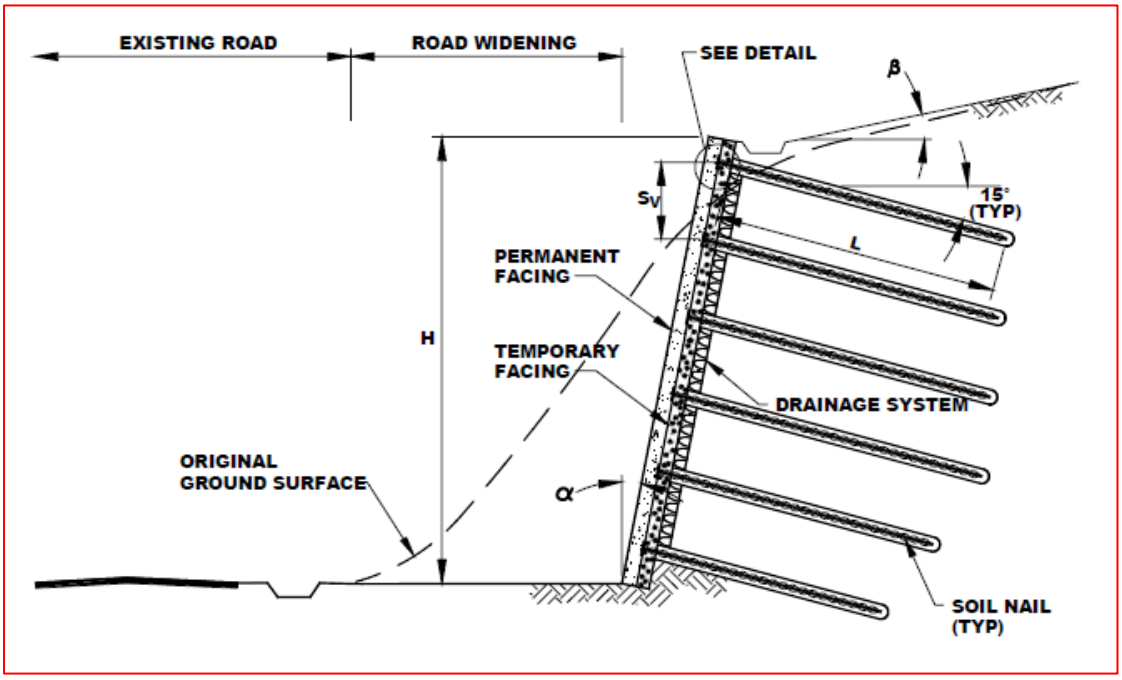

Figure 1-1. Widen road adjacent to a slope, GEC#7 (FHWA, 2003, 2015)

One application of soil nail wall is to widen road either adjacent to a slope (figure 1-1) or under existing bridge abutments (figure 1-2). Soil nail wall is widely adopted in Texas for the construction of common "Texas Turn Around" under piled bridge abutments.

An aspect of particular concern in the current FHWA guidelines "Geotechnical Engineering Circular No. 7 - Soil Nail Walls" (GEC#7) (FHWA, 2003, 2015) is the creep behavior of soil nail systems in high plasticity clays (i.e., plasticity index (PI) ≥

15), and the associated long-term deformations. According to GEC#7, creep behavior is directly associated with the presence of high plasticity clays regardless of the stress level.

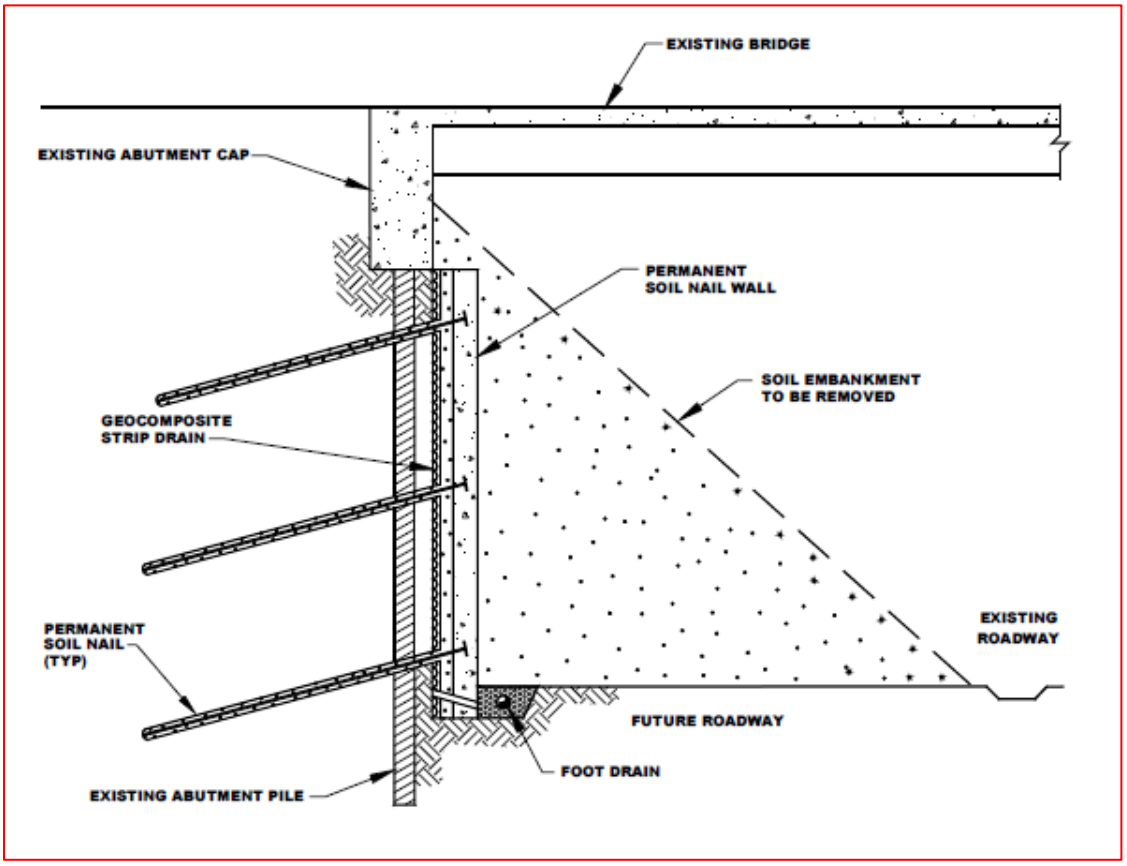

Figure 1-2. Widen road under existing bridge abutments, GEC#7 (FHWA, 2003, 2015)

In total, it is mentioned five times in 2003 version of GEC#7:

- Page 14: "*To minimize potential long-term lateral displacements of the soil nail wall, find-grained soils should be of relatively low plasticity [i.e., in*

*general, plasticity index **(PI) < 15**]*";

- Page 15: "*Long-term deformations (creep) of the soils may be a concern for **highly plastic clays***";
- Page 17: "*Soil nails can be installed in engineered fill if it is a mixture of well-graded granular material (approximately 90 percent of the mix or more) and fine-grained soil with low plasticity (typically, **PI < 15)***";
- Page 38: "*However, practice has shown that soils with potential for creep include: 1. Find-grained soils with a liquid limit (LL) ≥ 50; 2. fine-grained soils with plasticity index **(PI) ≥ 20***";
- Page 107: " *Fine-grained soils of high-plasticity (i.e., approximately **PI > 20)** and high water contents (such that LI > 0.2) tend to incur deformation for longer periods of time*";

It is also mentioned five times in 2015 version of GEC#7:

- Page 27: "*The potential for excessive long-term, creep-like, lateral displacements of soil nail walls is low in fine-grained soil with a **plasticity index (PI) of less than 15***";
- Page 27: "*Soil nails can be installed in existing engineered, structural fill if this material is a mixture of well-graded granular material (approximately 90 percent of the mix or more) and fine-grained soil with Liquid Limit (LL) and **PI** values of **less than** 40 and **20**, respectively*";
- Page 29: "*Long-term deformations such as creep may be a concern with **highly plastic clays***";

- Page 87: "*Although there are no definitive criteria to estimate before construction which soil nails would creep, it is considered that creep may occur in soils that meet one of the following: LL ≥ 50;* ***PI ≥ 20***";
- Page 142: " *Fine-grained soils of high-plasticity (approximately* ***PI > 20)*** *and high water contents (such that LI > 0.2) tend to incur deformation for longer periods of time due to their potential for creep*";

However, TxDOT has successfully designed and constructed numerous soil nail walls in soils with PIs greater than 20. In typical soil nail designs, TxDOT has limited the bond strength of the soil nail to a "safe" load level, thus reducing the potential of creep behavior (Galvan, 2012). It is thought that the current TxDOT's design practice leads to service load that are much less than the load level required for initiating creep behavior. The ratio of service load over ultimate load for TxDOT's design approach is around one third. Because high PI clays are very common in Texas, it is necessary to study the creep behavior of high PI clays and to validate the TxDOT's design approach.

It should be noted that soils are divided into groups of highly plastic (PI > 30), medium plastic (15 < PI ≤ 30), slightly plastic (3 < PI ≤ 15), and nonplastic (PI ≤ 3), according to Sowers (1979); however, high PI clays in this research are clays with PI ≥ 15, which follows GEC#7, and low PI clays in this research are clays with PI < 15.

1.2. Research Objectives

The first objective is to validate TxDOT's design approach. Remaining objectives are:

- Study the time and possibility for creep failure at various stress level;
- Predict long-term deformation in practice;
- Propose some methods to reduce deformation caused by creep;

1.3. Significance of the Research

Overall, the research will not also benefit TxDOT, but also contribute to new knowledge.

1.3.1. Benefit TxDOT and Most State DOTs

If creep is not a problem for soil nails in high PI clays, soil nails could be applied in the high PI clays where they were once restricted. It will save TxDOT plenty of money, because one great advantage of soil nail walls is their cost-effectiveness over other alternatives. Because most state DOTs follow GEC#7, a revision clarifying (or even removing) the creep behavior restrictions in high PI clays would increase the understanding and application of soil nail walls in areas and circumstances where they were previously ignored. Besides, when long-term loads and their associated durations are known, being able to reasonably predict the state of stresses, and associated deformations, would be useful to designers.

1.3.2. Quantify the Time and Possibility for Creep Failure at Any Stress Level

Time and possibility for creep failure at any stress level will be readily quantified with the proposed power law model (figure 1-3) in detail in Chapter five.

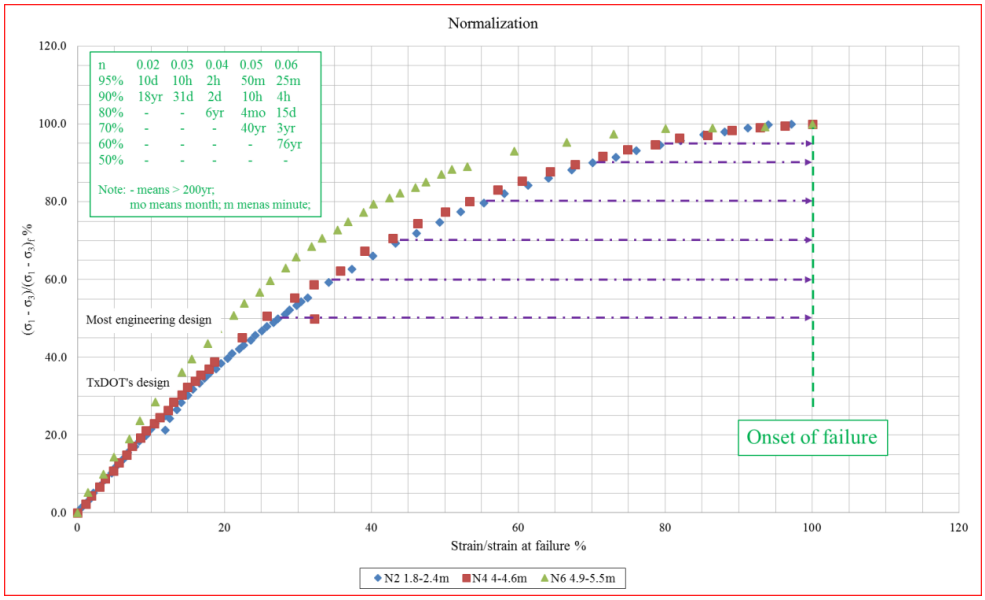

Figure 1-3. Quantify the time and possibility for creep failure

1.3.3. Forecast Long-term Deformation in Practice

Not only will the proposed power law model quantify the time and possibility for creep failure at any stress level, but also it will forecast long-term deformation in practice after a given duration (figure 1-4). It will be presented in detail in Chapter four and Chapter five.

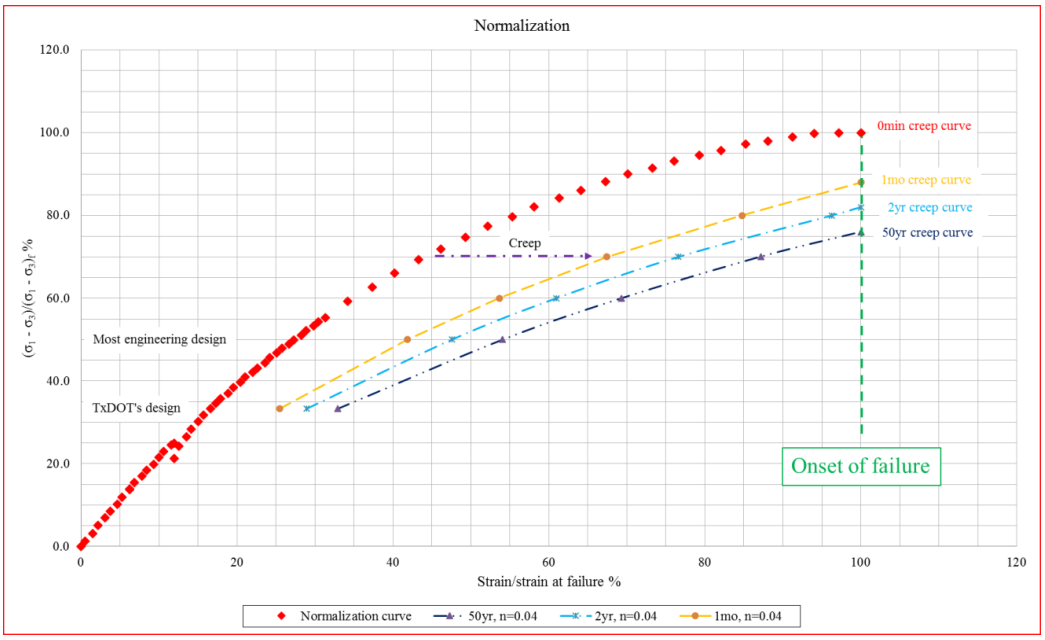

Figure 1-4. Forecast long-term deformation in practice

1.3.4. Separate Creep in Primary Consolidation

There is a long debate where creep starts in consolidation. Data from this research supports the view that creep should be taken into account during the whole consolidation process. Besides, deformation associated with creep is readily separated from deformation associated with consolidation (i.e., excess pore pressure dissipation) in primary consolidation.

1.3.5. Constant N Value at Different Stress Levels

N value is the exponent in proposed power law model (see Chapter three). N value whether from laboratory tests and field tests is found to be independent of stress (load)

level, and the same n value from different kinds of tests may be considered as a soil property.

1.3.6. Propose Methods to Reduce Creep Deformation in Practice

Except the way of limiting stress (load) under a "safe" level to reduce creep deformation (i.e., TxDOT's design approach), another two methods are prestressing (preloading) and cycles which will be demonstrated in this research.

1.4. Methodology

A power law model is proposed to describe time dependent behavior of soils. It will be fully demonstrated through two kinds of laboratory tests on three different soils, other data from literature, four kinds of field tests and one field practice. All laboratory tests and part of field tests will be performed by this research team, and remaining field tests had been performed by previous students of Dr. Jean-Louis Briaud. Data from literature will be collected by the PhD candidate.

1.5. Organization of Dissertation

The dissertation is organized into nine chapters. Chapter one is introduction, including problem statement, research objectives, significance of the research and methodology. Chapter two is literature review, covering creep mechanism, general review, creep failure criteria and current models. Chapter three is proposed power law model presented in detail. Chapter four focuses on one-dimensional (1D) consolidation

test and 1D compression test in laboratory on three different soils, including but not limited to test data, n value-stress curve, separating creep in primary consolidation, long-term prediction from laboratory to field, and one field practice (San Jacinto monument). Chapter five focuses on triaxial creep test in laboratory on three different soils, covering from test results, normalization curve, n value-stress level curve, predicting time to creep failure, forecasting long-term deformation, and reducing creep deformation by prestressing. Chapter six is applying power law model to other data from literature to demonstrate that the model is generally feasible. Chapter seven focuses on spread footing test, ground anchor pullout test, soil nail pullout test and cyclic lateral load test, including load-deformation (settlement, movement, etc.) curve, deformation-time curve, n value-load level curve and equation relating cycle to creep. Chapter eight is numerical implementation of power law model. Chapter nine is summary and conclusion of dissertation. Recommendation for future research is also made.

2. LITERATURE REVIEW

Literature review in this chapter will cover several topics: creep mechanism, general review, creep failure criteria, and current models.

2.1. Creep Mechanism

For clay, the physical clay model proposed by Pusch (1978) implied that creep was the break-down of a certain number of particle links and to slip between particles. The rheological model of type H/(H-N) (Christensen et al., 1990) was applied to explain the process of gradually yielding of bonds at particle contacts. Vermeer and Neher (1999) and Havel (2004) had proposed several different 1D creep models to simulate creep behavior in numerical modelling basing on the logarithmic creep law for secondary compression. Wong and Varatharajan (2014) studied secondary compression with the classical rheological model (e.g., Maxwell, Kelvin-Voight and Bingham model) by choosing the void ratio at the end of primary consolidation. Yin (1999) developed a one-dimension elastic visco-plastic (1D EVP) model with the equivalent-time concept and implemented this model in a 1D consolidation analysis. The model used a logarithmic function to fit oedometer test (i.e., 1D consolidation test) data of vertical strain (or void ratio) versus time after the completion of primary consolidation.

There has been a debate on how creep contributes to 1D consolidation. Some researchers (Mesri and Choi, 1985) believe creep (secondary compression) occurs only after primary consolidation, while others (Bjerrum, 1967; Crawford, 1986; Kabbaj et al.,

1988; Yin and Graham, 1989, 1994, 1996; Wahls, 1965) insist creep should be considered throughout the whole consolidation process.

In most cases, creep is defined as continuous deformation under constant effective stress. The total stress rather than the effective stress is constant in the primary consolidation of 1D consolidation test, and it consists of two different deformations: deformation because of excess pore pressure dissipation which is usually called consolidation; deformation because of the adjustment of soil particle positions with respect to each other which should be called creep. These two deformations should be distinguished and separated to be compared.

For sand, creep was viewed as the elastoplastic transition associated with the onset and progression of particle crushing (Pestana and Whittle 1995, 1998; Sanzeni et al., 2012). The proposed rate-independent model described the compression of freshly deposited cohesionless soils with the observation that sand specimens would approach a unique limiting compression curve regardless of its initial density. Triaxial compression tests were performed on dense sand at low (250kPa) and high (8000kPa) confining pressures by Karimpour and Lade (2013), it showed that no grain crushing at low confining pressures.

In the view of the PhD candidate, creep is the process soil particles adjust their positions with respect to each other, to reach a denser, stiffer, stronger (higher strength) state which tries to resist the applied constant stress in order to reach a steady state. If by creep, the soil can’t reach a state to maintain the applied constant stress, it will fail, which is called creep failure. The power law model proposed in the research will

describe the time dependent behavior of soils in a global level rather than microscope level (i.e., without focusing the creep mechanism).

2.2. General Review

The author would like to list three pioneering researches in detail.

2.2.1. Casagrande and Wilson (1951)

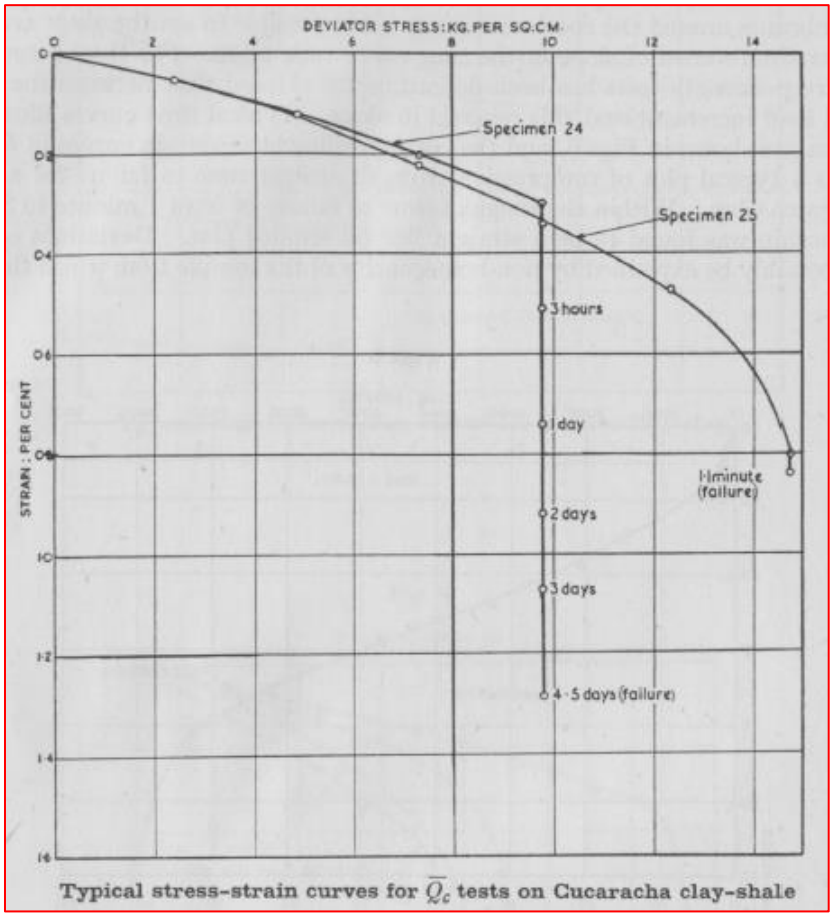

Figure 2-1. Creep-strength test, CU (Casagrande and Wilson, 1951)

Note: 1kg/cm^2=98.1kPa

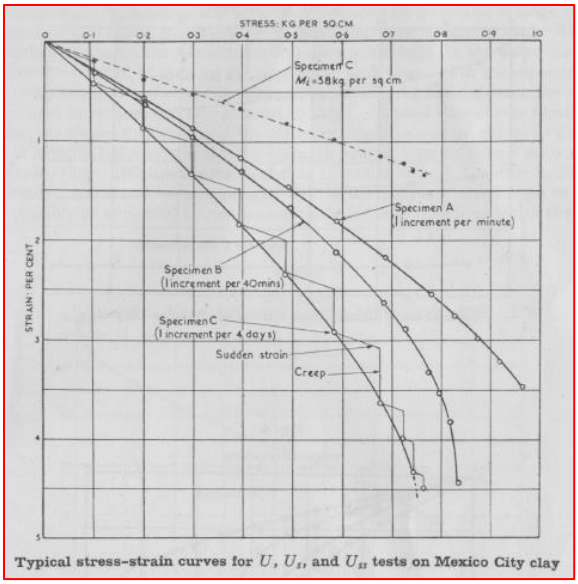

Figure 2-2. Long-term compression test, UC (Casagrande and Wilson, 1951)

Note: $1kg/cm^2$=98.1kPa

In 1951, Casagrande and Wilson carried out two kinds of tests: creep-strength test (figure 2-1) and long-term compression test (figure 2-2). A creep-strength test is one in which a load is built up quickly and maintained constant until the specimen fails, while a long-term compression test is one in which the specimen is subjected to incremental axial loading, the elapsed time between increments of load varying for different tests. Thus, the impact of rate of loading on ultimate strength is studied by long-term compression test, and creep behavior is studied by creep-strength test. Creep-strength test includes triaxial unconfined-compression (UC) test, triaxial unconsolidated-undrained (UU) test, and triaxial consolidated-undrained (CU) test, while long-term

strength test only includes triaxial UC test. To note, it seems Casagrande and Wilson is the first one to conduct creep test.

Stress at which creep failure happens versus time to failure (i.e., duration of creep) was plotted in figure 2-3. The author doubts whether the straight line drawn by Casagrande and Wilson is reasonable. Besides, it is worth noting that it was mentioned in the journal paper that creep failure didn't happen for stress 0.45kg/cm^2~0.55kg/cm^2 (i.e., 45kPa~55kPa) after 30d duration. In this case, stress threshold for creep failure in 30d is stress level equal to 60% (i.e., 0.45/0.75, where 0.75kg/cm^2 is the strength at 1min duration).

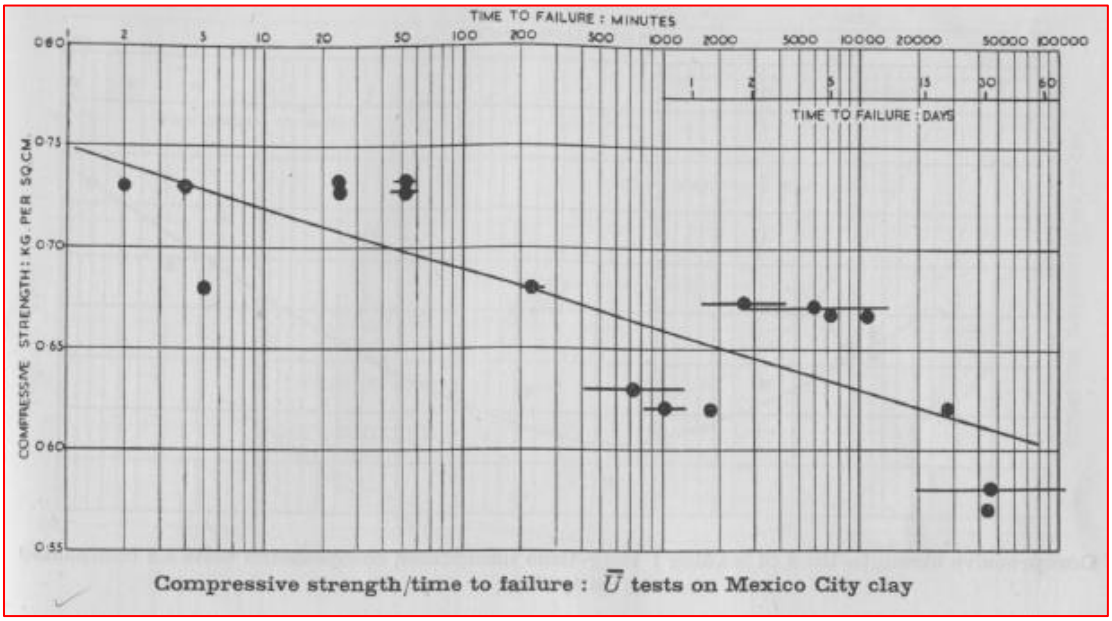

Figure 2-3. Creep strength versus time to failure, UC (Casagrande and Wilson, 1951)

Note: 1kg/cm^2=98.1kPa

Strength ratio versus time to failure for six soils was plotted in figure 2-4. Again, the author doubts whether it is reasonable to draw straight lines. Strength ratio is defined as the ratio of the compressive strength acquired in a creep test to the estimated compressive strength corresponding to a normal rate of loading.

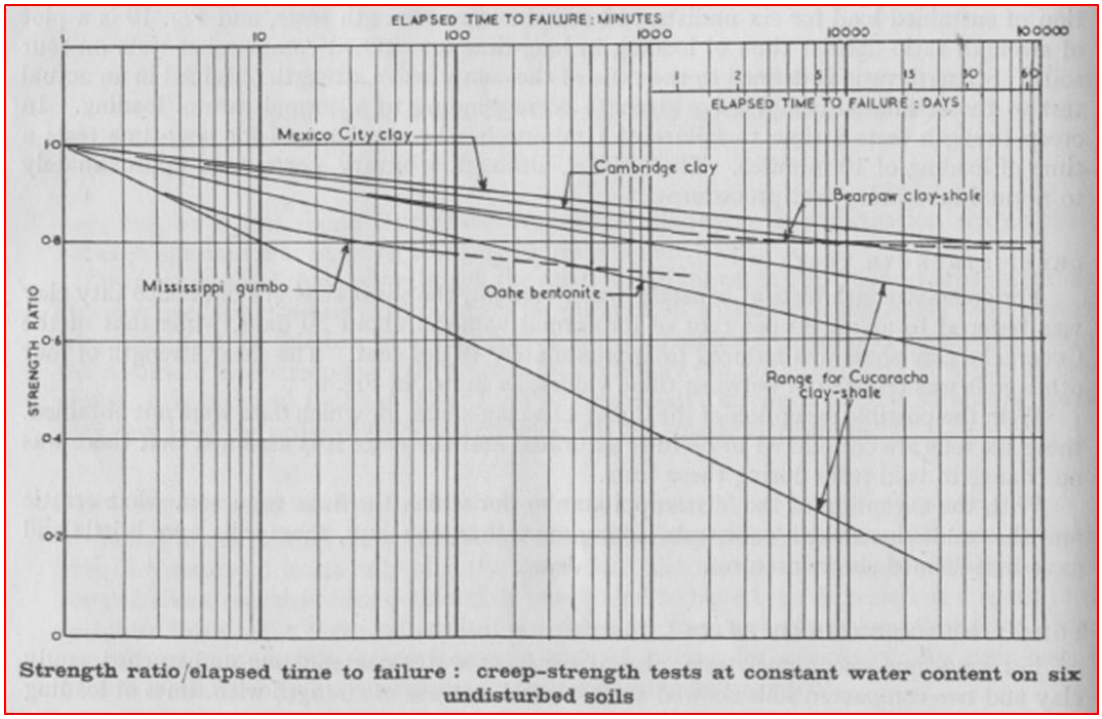

Figure 2-4. Strength ratio versus time to failure (Casagrande and Wilson, 1951)

Note: $1kg/cm^2$=98.1kPa

2.2.2. Bishop (1966, 1969)

In vote of thanks for the sixth Rankine lecture by Bishop (1966), Professor Hansen

commented that failure criterion would probably be expressed in strains rather than in stresses.

Triaxial consolidated-drained (CD) creep test had been conducted on overconsolidated London clay with duration up to 3.5yr. Strain-time curve was plotted in figure 2-5 (Bishop, 1969). The stress level, for example 90~106%, is sustained stress over peak stress from conventional triaxial shear test. Six conventional triaxial shear tests were carried out to obtain the peak stress, while two of them had a higher peak value than that of the remaining four. Thus the average of two higher and the average of remaining four were both adopted to calculate stress level. Besides, it should be noted that triaxial creep test was conducted on six specimens (labelled C1, C2 …, C6) rather than on one specimen. Bishop (1969) stated there was no apparent threshold value of stress below which time dependent deformation did not occur.

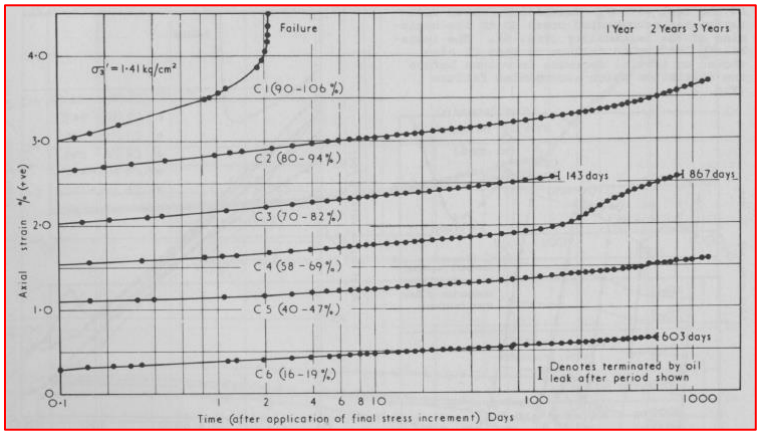

Figure 2-5. Strain-time curves (Bishop, 1969)

Note: 1kg/cm^2=98.1kPa

Strain rate-time curve was plotted in figure 2-6 (Bishop, 1969). The curve seems to be a straight line before creep failure in semi-log scales. Besides, Bishop (1969) claimed the bump on the curve of C4 was fundamental behavior of soils. It was not a mistake made by tester. The same phenomenon was shown on strain-time curve (figure 2-7). It should be noted data up to 168d on figure 2-7 was presented by Bishop (1966), and based on the linear behavior of strain-time curve of data up to 168d, a model was proposed by Singh and Mitchell (1968) to describe time dependent behavior of soil. However, the complete data on figure 2-7 (Bishop, 1969) didn't support the assumption made by Singh and Mitchell (1968).

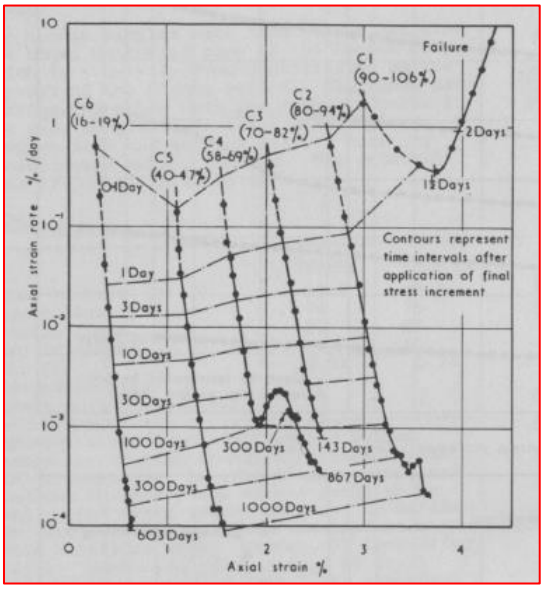

Figure 2-6. Strain rate-strain curves (Bishop, 1969)

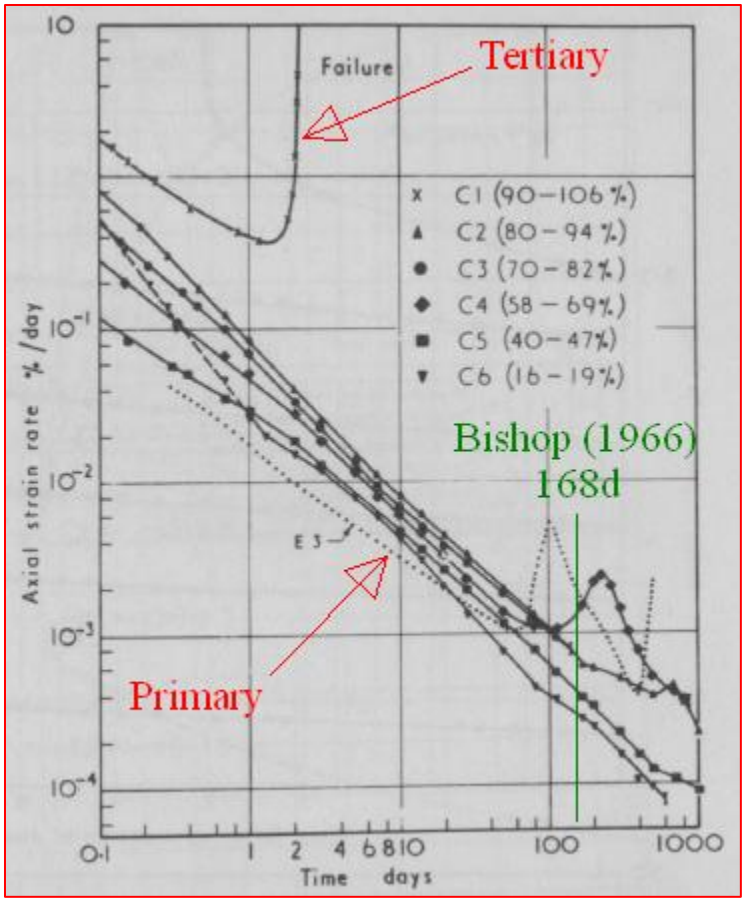

Figure 2-7. Strain rate-time curves, after Bishop (1969)

In usual, creep is subdivided into three parts - primary creep, secondary creep, and tertiary creep - on strain-time curves (figure 2-8). However, Bishop (1969) claimed that secondary creep disappeared on strain rate-time curve (log-log scales) (figure 2-7). Many studies carried out by other researchers (Adachi and Takase, 1981; Campanella and Vaid, 1974; Murayama and Shibata, 1958) supported this view.

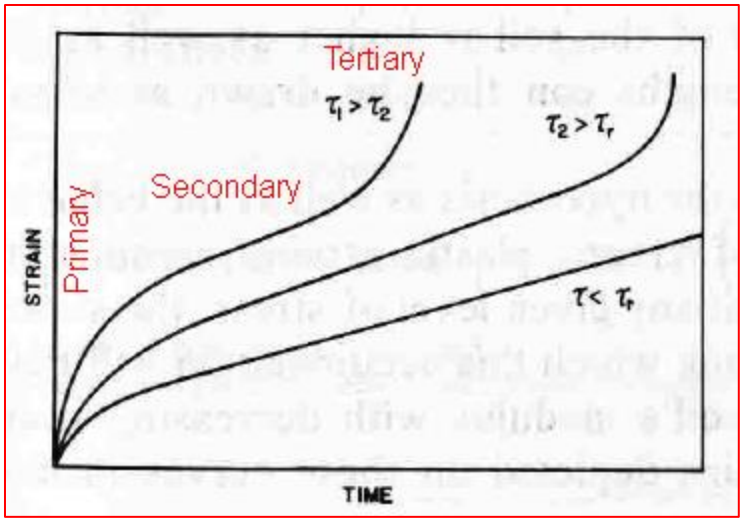

Figure 2-8. Primary creep, secondary creep, and tertiary creep

2.2.3. Skempton (1964, 1970, 1977)

Skempton (1964) reported three cutting slopes failed after 19yr, 29yr, and 49yr, respectively on the fourth Rankine lecture.

One important concept was the back-calculated strength at failure of these first-time slides was higher than residual strength, and this back-calculated strength was named as "fully softened strength" by Skempton (1964). Besides, Skempton (1964) introduced the "residual factor' (equation 2-1) to measure fully softened strength with respect to peak strength and residual strength, in other words, the proportion of the total slip surface in the clay along which its strength has fallen to the residual value (figure 2-9 and figure 2-10).

$$R = \frac{s_f - \bar{s}}{s_f - s_r} \tag{2-1}$$

Where,

R: Residual factor;

s_f : Peak strength;

s_r : Residual strength;

$\bar{s}$: Fully softened strength.

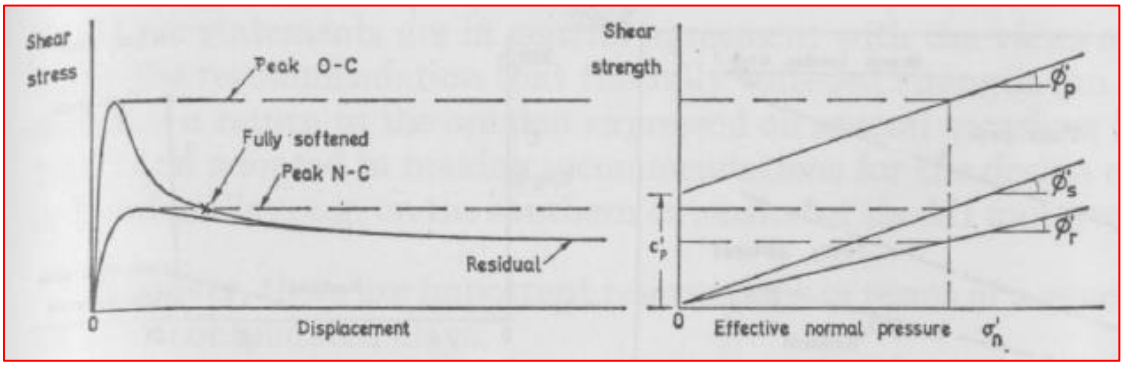

Figure 2-9. Fully softened strength (Skempton, 1970)

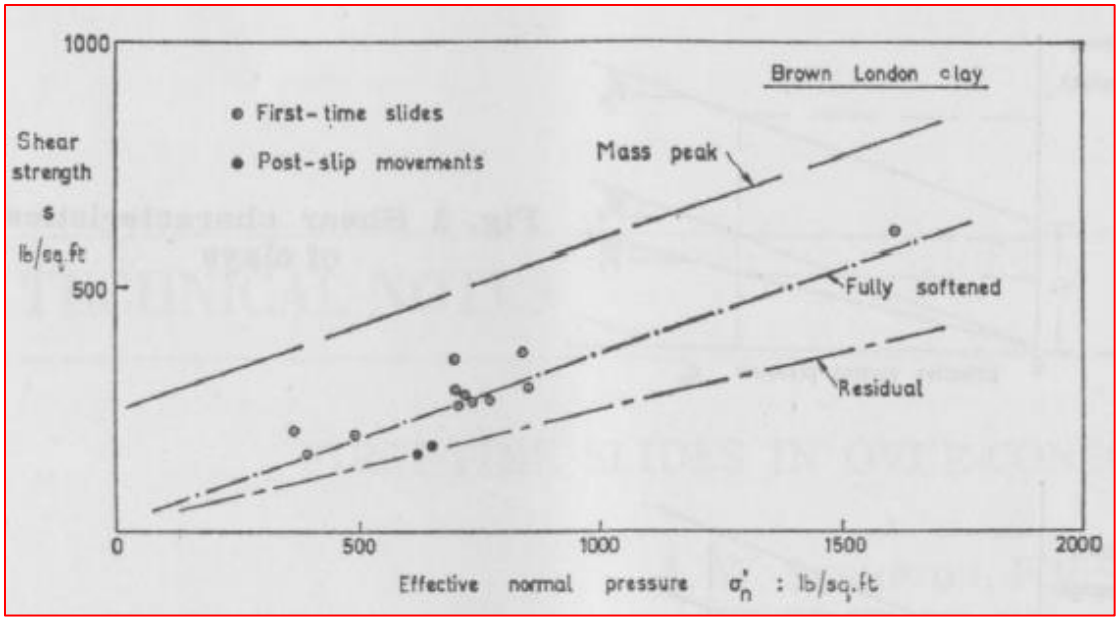

Figure 2-10. Fully softened strength with back-calculated data (Skempton, 1970)

It was believed failures of three cutting slopes were combination of creep failure and progressive failure. Skempton (1970) said:

"Tests by Bishop (1969) indicate clay samples will not cross the peak when kept at stresses lower than peak but higher than fully softened strength or residual strength. It emphasizes the necessity for a progressive failure process if a clay is to fail at strengths well below the undisturbed peak value."

Thus, this fully softened strength was the stress threshold for the first-time slides. Skempton (1977) added that the delayed failure was caused by very slow rate of excess pore pressure equilibration.

Dr. Suklje at Geotechnical Conference (Oslo, 1967) discussed:

"In soils with constant peak value the failure develops either by successive mobilization and degradation of the peak value in Different parts of the failure zone or as a creep process leading to the decrease of the peak value, or by a combination of both effects.

In stationary loading conditions the progressive failure caused by successive stress concentrations beyond the peak value is expected to develop with a speed of the order of magnitude close to the rate of the failure process observed on the specimen.

The retardation of the failure as proved by Skempton's data is to be interpreted either by periodical local stressing of short duration up to the peak strength, with long intervals of lower stressing, or by a slow creep leading to the reduction of the peak value with time."

Bjerrum (1967) agreed the viewpoint that progressive failure and creep failure were concurrent on slides. Dornfest et al. (2000) presented figure 2-11 that creep failure at point B caused by creeping from point A to point B would result in progressive failure at point E after local stress equilibrium from point D to point E, which would further result in progressive failure at point K.

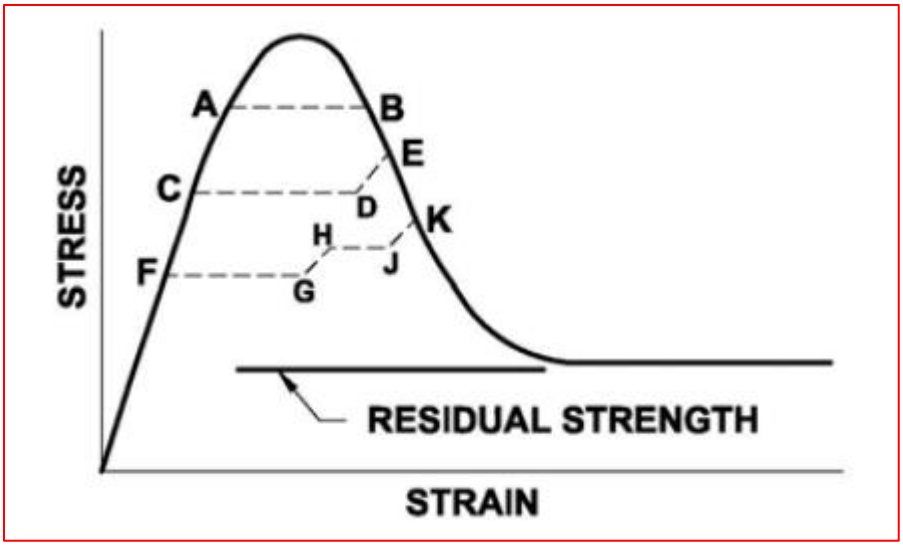

Figure 2-11. Progressive failure and creep failure coexist (Dornfest et al., 2007)

2.3. Creep Failure Criteria

Two common creep failure criteria were stress threshold and critical strain, which were presented in detail below.

2.3.1. Stress Threshold

Some researchers claimed that there was a stress threshold for creep failure, if the applied stress was above stress threshold, it would creep to fail in a limited time, and if the applied stress was below stress threshold, the creep failure wouldn't happen. However, in views of different researchers, the stress threshold was different.

Many researchers believed stress threshold was the residual strength. Adachi and Takase (1981) argued that no creep failure occurred under stress state below the residual

strength surface. Dornfest et al. (2007) demonstrated that the back-calculated shear strength along the failure plane appeared to be reaching a value of residual strength (figure 2-11). Nelson and Thompson (1977) pointed out the shear strength of the soil would have been reduced to its residual strength after creep failure.

Besides, there were other definitions of stress threshold. Hunter and Khalili (2000) agreed that creep to failure could occur at less than peak strength, with the limiting strength possible being as low as the fully soften (or critical state) strength, which was defined by Skempton (1964, 1970, 1977). Philibert (1976) and Lefebvre (1981) suggested the stress threshold was the post-peak strength, which was defined at or around 8% axial deformation on the stress-strain curve of triaxial consolidated drained tests. Campanella and Vaid (1974) came out the concept of creep stress, which was also termed the upper yield strength by Murayama and Shibata (1961), which was expressed as the principal stress difference normalized with respect to the vertical effective stress during consolidation (i.e., $q = (\sigma_1 - \sigma_3)/\sigma_{1c}'$) during triaxial consolidated undrained tests. Based on their test data, the stress threshold was $q = 0.482$. A yield strength of a clay (Arulanandan et al., 1971; Briaud et al., 1998; Suroor, 1998) was defined as the point before the peak of the log stress versus log strain curve where the curvature was maximum because the stress-strain curve continued to show a decrease in stress until 20% strain without a clear plateau (i.e., residual strength is unclear), and this yield strength was stress threshold for creep failure.

Besides, Singh and Mitchell (1968) introduced the m value that related to stress level as the stress threshold for creep failure, and creep failure would happen if m was less than 1.

To recall, stress threshold based on Casagrande and Wilson (1951) was stress level equal to 60%.

2.3.2. Critical Strain

In vote of thanks for the sixth Rankine lecture given by Bishop (1966), Professor Hansen commented that creep failure criterion would probably be expressed in strains rather than in stresses.

Nelson and Thompson (1977) pointed that on the basis of creep data that had been published by Murayama and Shibata (1961) there was evidence that some critical strain existed at which point all of the internal bonds in the soil would have failed. Furthermore, Nelson and Thompson (1977) stated that it was seen that for most soils the point of accumulated plastic strains at which tertiary creep (i.e., onset of creep failure) began was relatively independent of stress. Singh and Mitchell (1968; 1969) thought that for a given soil the value of ε_f which caused failure was fairly independent of stress level. Varnes (1982) commented that for creep tests on the same material at different deviatoric stress levels, the strain at which inflection (of the strain rate on the log-log scales of strain rate-time curve, that is, onset of creep failure) occurred was more or less constant.

Not only did some researchers believe the existence of critical strain, but also they stated it was strain corresponding to peak stress in conventional triaxial shear test. Campanella and Vaid (1974) observed that for a given test type, irrespective of the creep test level, failure occurred at approximately the same magnitude of axial strain, which was equal to the failure strain in conventional constant strain rate triaxial undrained shear test. Hunter and Khalili (2000) proposed the creep failure criterion that the level of shear strain at which the onset of failure due to creep occurred was equivalent to the shear strain at peak stress in the equivalent conventional strength test. Philibert (1976) and Lefebvre (1981) stated that creep failure was usually predicted in terms of stresses but could also be based on strain (Mitchell, 1970; Tavenas and Leroueil, 1977) or on strain energy (Tavenas et al., 1979). Results of triaxial consolidated isotropically drained creep tests clearly showed that for samples which had remained stable with time, the maximum axial deformation under creep had remained lower than the value recorded at failure in conventional triaxial shear tests. It indicated that accumulated axial deformations under creep loading of less than the axial deformation to peak in the conventional triaxial consolidated isotropically drained tests for all samples that did not fail.

The implicit assumption of critical strain for creep failure equal to strain corresponding to peak stress in conventional triaxial shear test, is that the conventional triaxial shear test could be compared and provide the reference to triaxial creep test, however, it seemed that nobody had it demonstrated so for.

2.4. Current Models

2.4.1. Adachi and Takase (1981)

Adachi and Takase (1981) proposed a method to predict the long-term strength of soft sedimentary rock based on the empirical evidences found from triaxial drained creep test results on Ohya-stone (porous tuff) deposited in Tertiary period.

According to figure 2-12, mean stress and deviatoric stress have a relationship as below:

$$\sigma_1 - \sigma_3 = \alpha \cdot \sigma_m^{'\beta} \tag{2-2}$$

Where, $\sigma_1 - \sigma_3$ is Deviatoric stress; $\sigma_m^{'}$ is Mean stress; and α and β are Parameters.

According to figure 2-13, minimum creep strain rate and deviatoric stress have a relationship as follows,

$$\log \dot{\varepsilon} = A \cdot \left(\sigma_1 - \sigma_3\right) + B \tag{2-3}$$

Where, $\dot{\varepsilon}$ is Minimum creep strain rate; A is parameter; and B is parameter.

Combing equation 2-2 and equation 2-3, minimum creep strain rate will depend on stress level, if mean stress is normalized (figure 2-14).

Adachi and Takase (1981) stated minimum creep strain rate and time to creep failure satisfied equation proposed by Saito and Uezawa (1961), as follows,

$$\dot{\varepsilon} \cdot t_f = C \tag{2-4}$$

Where, t_f is time to failure; and C is a material constant.

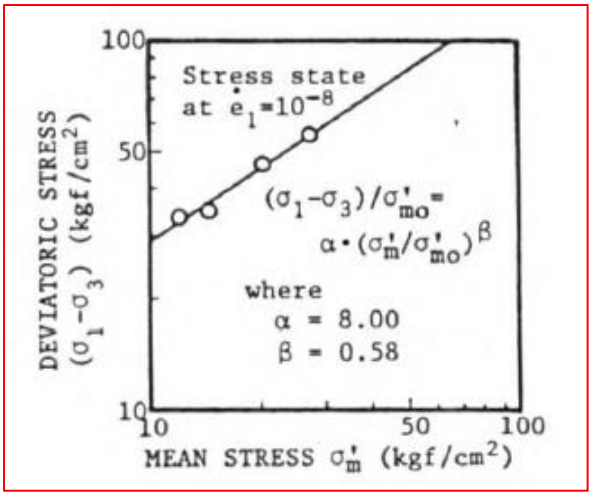

Figure 2-12. Stress state at minimum creep strain rate (Adachi and Takase, 1981)

Note: 1kgf/cm^2=98.1kPa

2.4.2. Campanella and Vaid (1974)

A study of the creep failure characteristic of a saturated, normally consolidated, undisturbed marine clay has been carried out under triaxial isotropically consolidated undrained test by Campanella and Vaid (1974). An equation to estimate time to creep failure was introduced as follows based on figure 2-15.

$$\dot{\varepsilon}\cdot t_f = k / 2.303 \tag{2-5}$$

Where, $\dot{\varepsilon}$ is strain rate; t_f is time to creep failure; and k is a constant equal to 4.54.

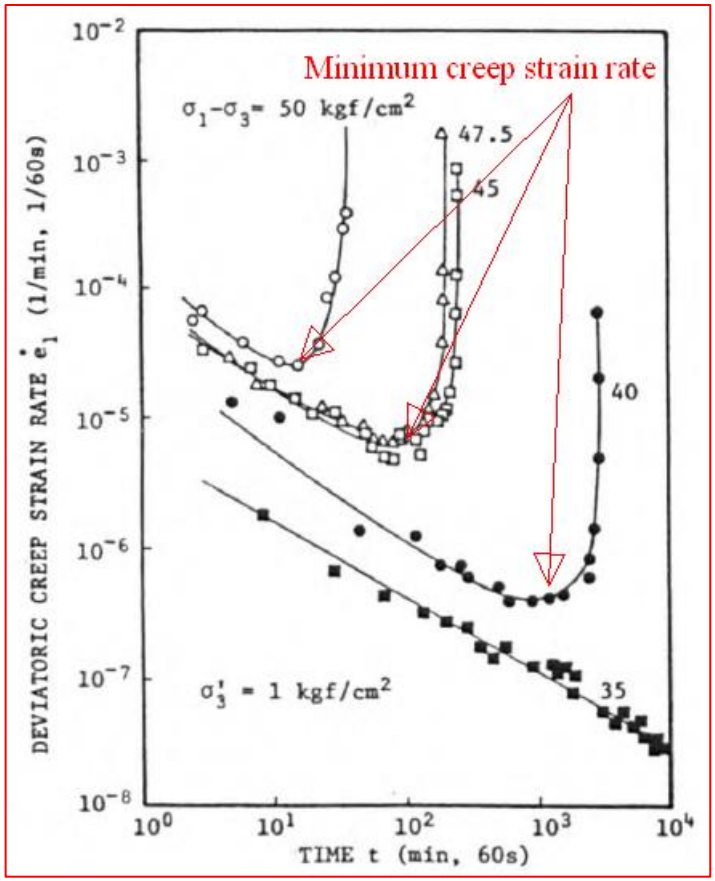

Figure 2-13. Creep strain rate versus time curves (Adachi and Takase, 1981)

Note: 1kgf/cm^2=98.1kPa

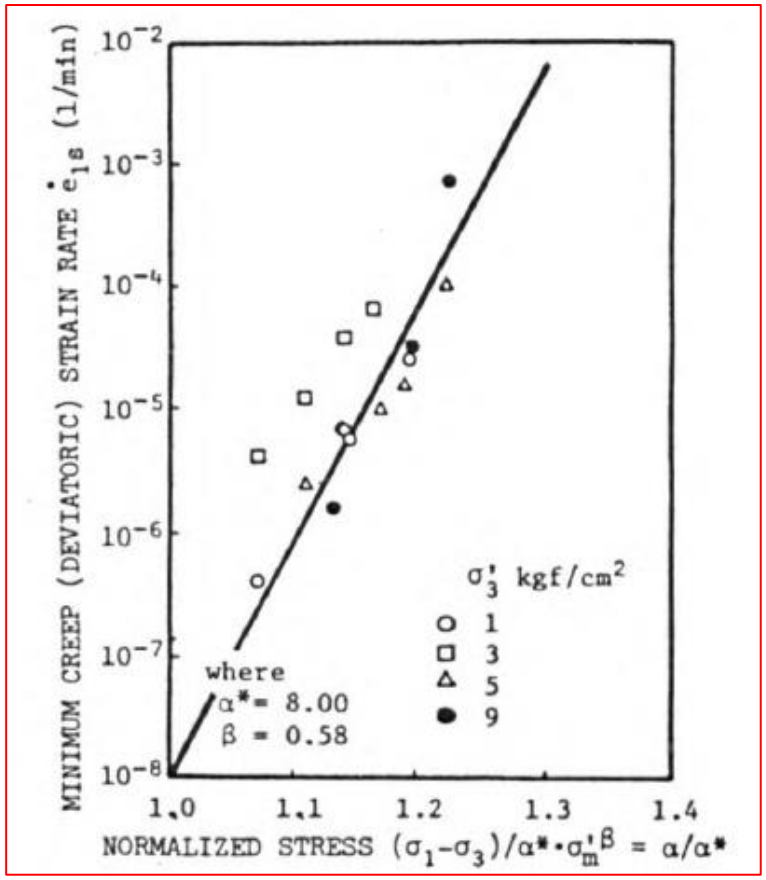

Figure 2-14. Relationship between minimum creep strain rate and stress level (Adachi and Takase, 1981)

Note: 1kgf/cm^2=98.1kPa

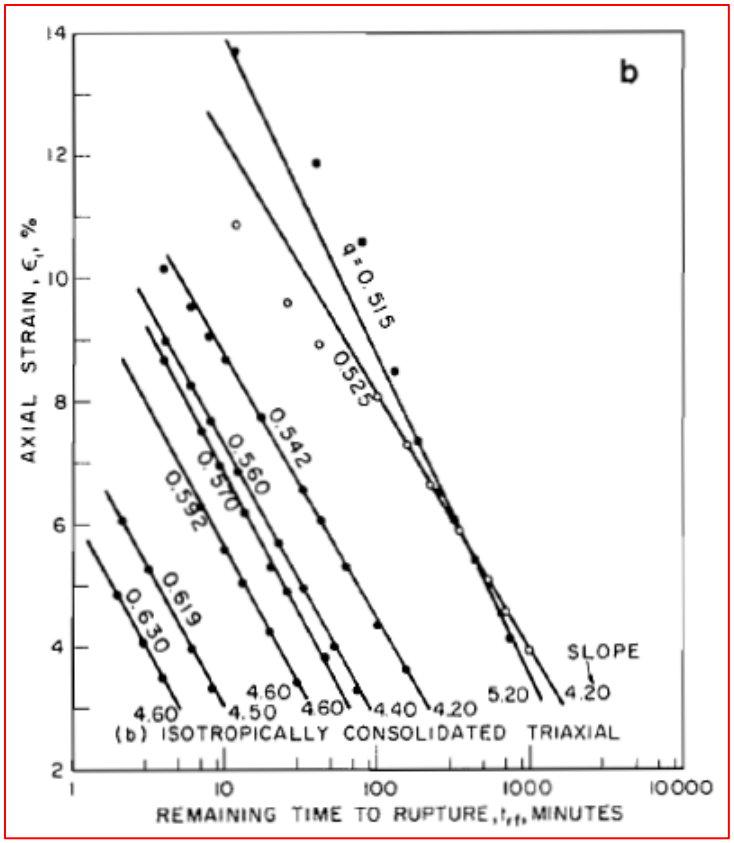

Figure 2-15. Relationship between strain rate and time to creep failure (Campanella and Vaid, 1974)

2.4.3. Hunter and Khalili (2000)

Hunter and Khalili (2000) summarized studies by previous researchers, and proposed a model (figure 2-16) as follows to estimate time to creep failure,

$$t_f = \frac{\varepsilon_f}{\dot{\varepsilon}} \tag{2-6}$$

Where, t_f is time to creep failure; $\dot{\varepsilon}$ is minimum strain rate; and ε_f is critical strain which corresponds to peak stress on stress-strain curve of conventional triaxial shear test.

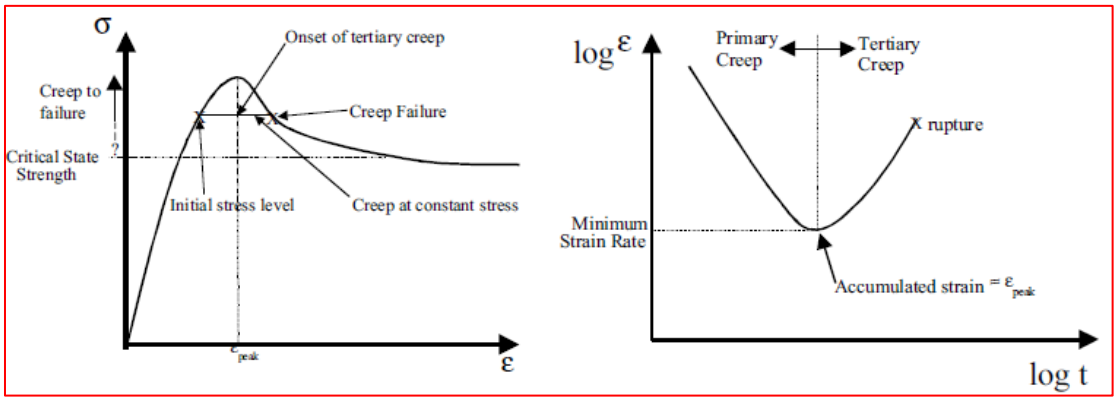

Figure 2-16. Creep failure model (Hunter and Khalili, 2000)

Table 2-1. Summary of laboratory triaxial drained creep tests (Hunter and Khalili, 2000)

Material	Material Type	Author/s	Figure Reference	Deviatoric Stress Level (% of peak)	Normalised Strain at Minimum Strain Rate	Normalised Strain at Intersection of Primary and Tertiary Creep[*1]
Nicolet Clay	Sensitive, structured clay	Lefebvre (1981)	Figure 4	77%	1.04	1.0 (power), 0.96 (log)
London Clay	Heavily over consolidated	Bishop and Lovenbury (1969)	Figure 5	90 – 106%	1.0	1.0 (log)
Saint Alban Clay	Sensitive, structured clay (OCR≈5)	Tavenas et al (1978)	Figure 6	104%	0.97	0.81 (log)
				100%	0.76	-
				93%	1.42	-
Umeda Clay	Alluvial clay, tested over-consolidated	Murayama & Shibata (1958)	Figure 7	110%	1.26	1.26 (power)
				100%	0.99	1.02 (power)
				95%	0.95	0.97 (power)
				83%	-	1.08 (power)

Data of triaxial drained creep tests in laboratory were collected to verify the proposed model (table 2-1), and it seemed that the model worked pretty well (figure 2-17).

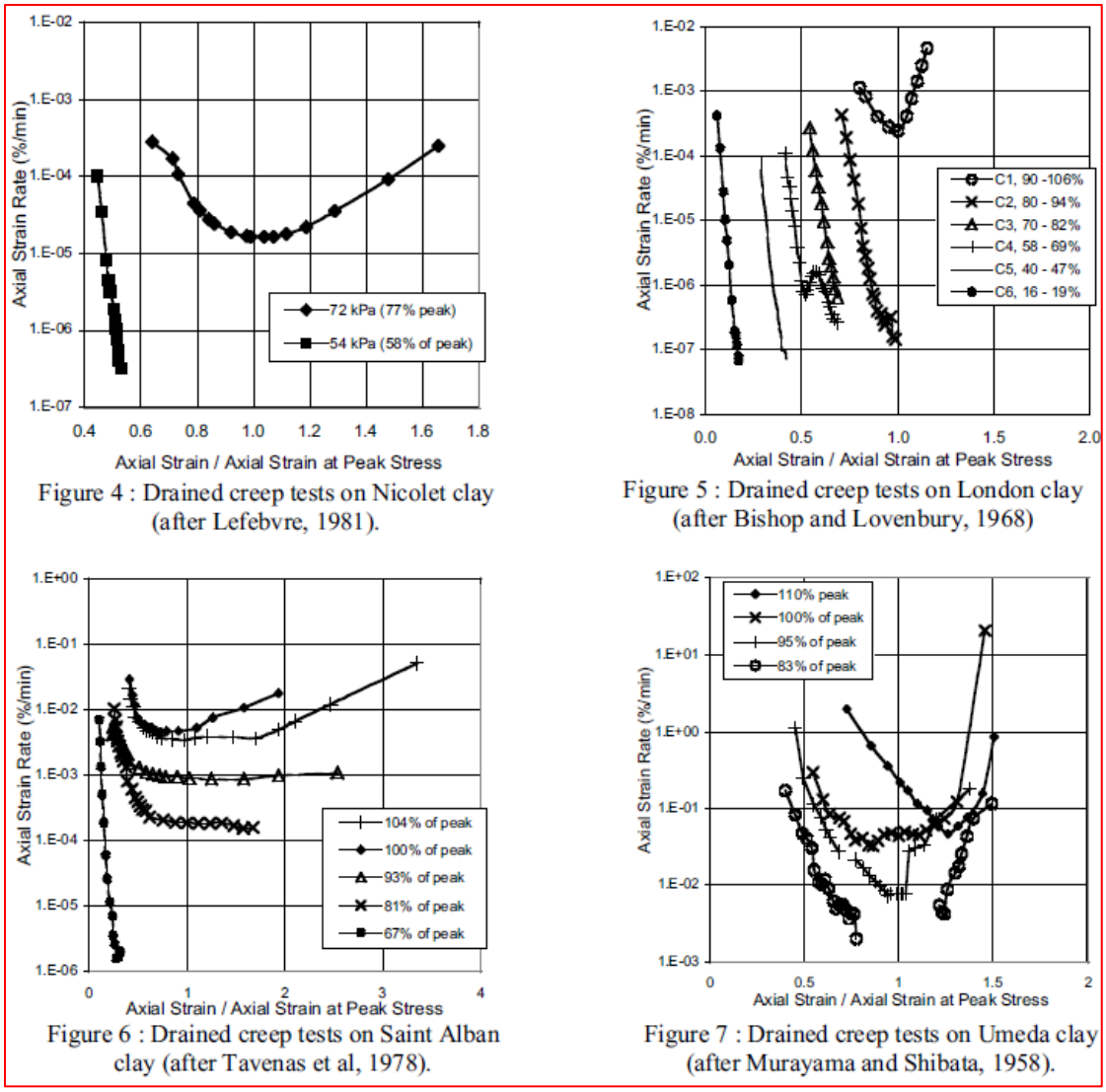

Figure 2-17. Model verified with data from literature (Hunter and Khalili, 2000)

2.4.4. Nelson and Thompson (1977)

Nelson and Thompson (1977) proposed a model based on two assumptions: 1), creep analysis can be based on the average shear stress reported by Skempton (1964, 1970); 2), creep rate can be represented by a power function of stress such that,

$$\dot{\varepsilon} = A \cdot \left(\frac{\tau}{\tau_r} \right)^n \tag{2-7}$$

If creep failure is brought about by an accumulation of plastic strains reaching a critical value, then time to creep failure (table 2-2) can be obtained by integrating, which yields,

$$\varepsilon_f = A \cdot \left(\frac{\tau}{\tau_r} \right)^n \cdot t_f \tag{2-8}$$

Where, $\dot{\varepsilon}$ is creep rate; τ is average applied stress; τ_r is average residual strength along the failure plane; ε_f is critical strain; t_f is time to creep failure; and *A* and *n* are material constants.

Table 2-2. Model verified with data from Skempton (1964, 1970) (Nelson and Thompson, 1977)

Location (1)	Date of failure (2)	Actual time to failure, in years (3)	Calculated[b] time to failure, in years (4)	Average Stress on Failure Surface		Average residual strength τ_r, in pounds per square foot (7)
				$\bar{\sigma}$, in pounds per square foot (5)	τ, in pounds per square foot (6)	
Northolt	1955	19	20	750	380	215
Kensal Green	1941	29	27	800	380	230
Sudbury Hill	1949	49	51	650	260	186

[a]Data from Skempton (26).

[b]Based on the equation $t_f = (0.00518)\left(\frac{\tau}{\tau_r}\right)^{-3.95}$.

Note: 1 psf = 47.9 N/m^2.

2.4.5. Singh and Mitchell (1968, 1969)

Singh and Mitchell (1968) proposed a general stress-strain-time model. The model was based on two assumptions: 1), linear relationship between strain rate and time in log-log scales (figure 2-18); 2), linear relationship between strain rate and stress in semi-log scales (figure 2-19).

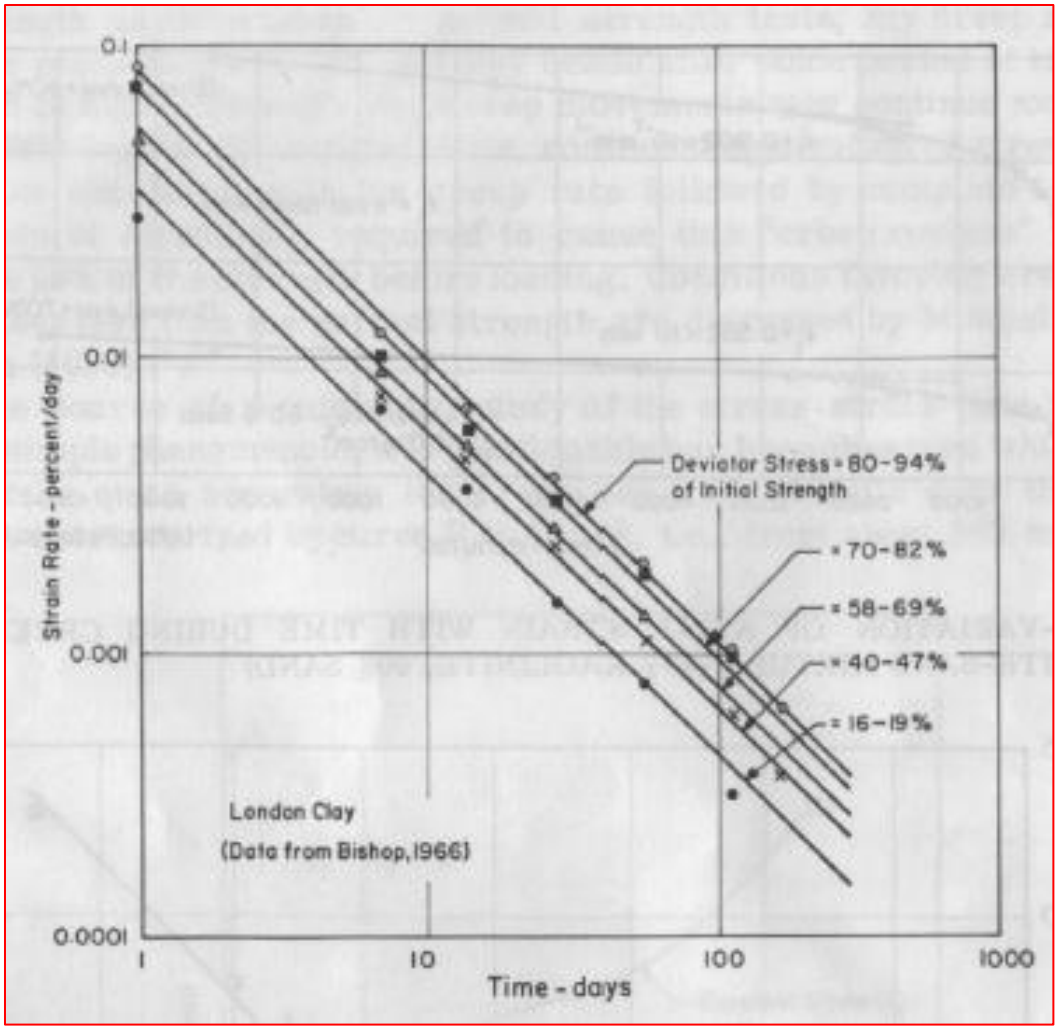

Figure 2-18. Relationship between strain rate and time (Singh and Mitchell, 1968)

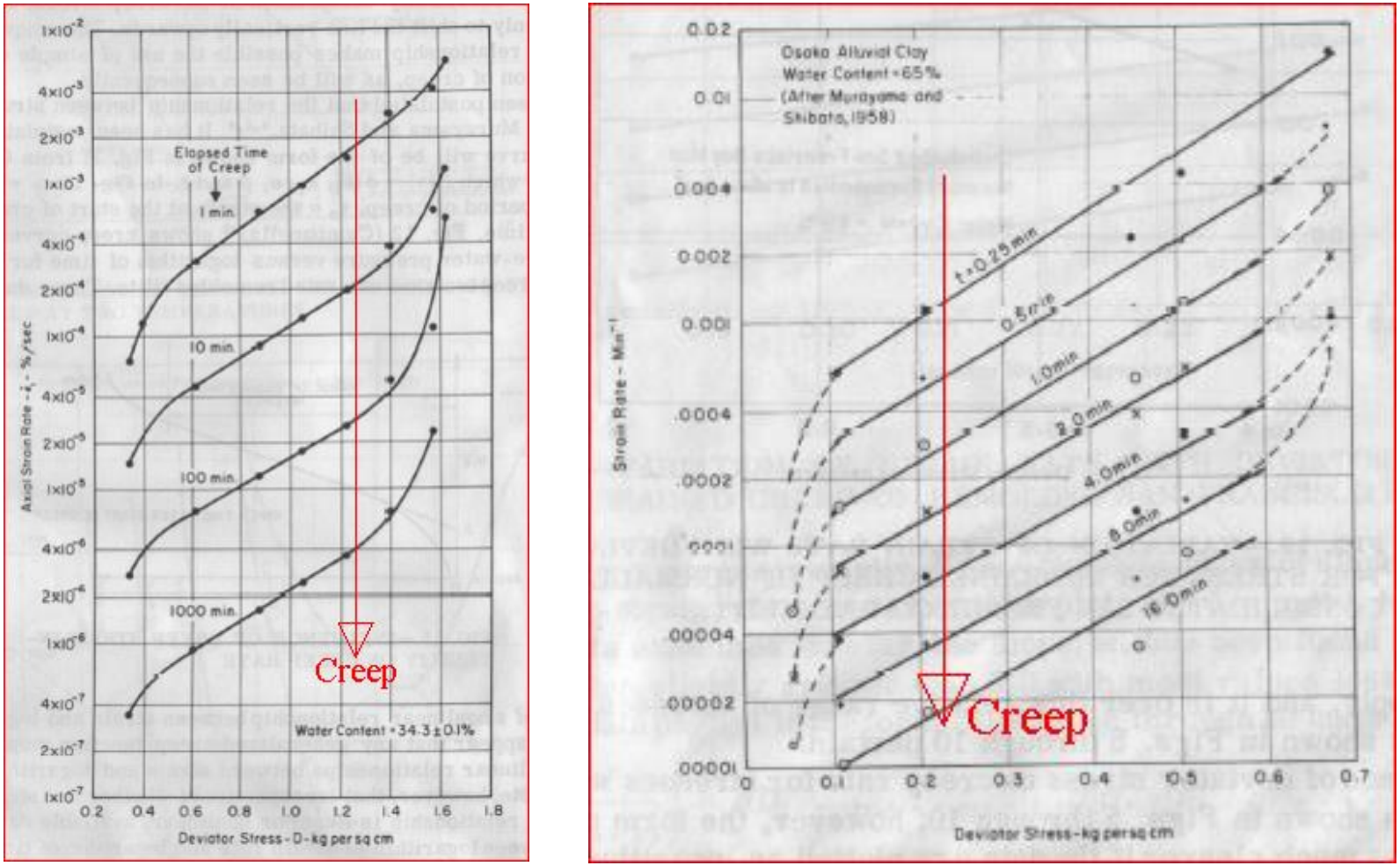

Figure 2-19. Relationship between strain rate and stress, after Singh and Mitchell (1968)

According to figure 2-18, it would have,

$$\log\left(\frac{\dot{\varepsilon}}{\dot{\varepsilon}_{(t_1,D)}}\right) = -m \cdot \log\left(\frac{t}{t_1}\right) \tag{2-9}$$

Where,

$\dot{\varepsilon}_{(t_1,D)}$: Reference strain rate at time t_1 and stress D;

$\dot{\varepsilon}$: Strain rate;

m: Slope.

According to figure 2-19, it would have,

$$\log\left(\frac{\dot{\varepsilon}}{\dot{\varepsilon}_{(t,D_0)}}\right) = \alpha \cdot D \tag{2-10}$$

Where,

α: Value of the slope of the mid-range linear portion;

$\dot{\varepsilon}_{(t,D_0)}$: Projected value of strain rate at D=0.

Combining equation 2-9 and equation 2-10, it would yield,

$$\dot{\varepsilon} = A \cdot e^{\alpha \cdot D} \cdot \left(\frac{t_1}{t}\right)^m \tag{2-11}$$

By integration,

$$\varepsilon = \begin{cases} \varepsilon_1 - \dfrac{A}{1-m} e^{\alpha \cdot D} + \dfrac{A}{1-m} e^{\alpha \cdot D} \cdot t^{1-m} \ (m \neq 1) \\ \varepsilon_1 + A \cdot e^{\alpha \cdot D} \cdot \log t \ (m = 1, t > 1) \end{cases} \tag{2-12}$$

Where, ε_1 is strain at time t=1; A is parameter.

Singh and Mitchell (1969) simplified the equation 2-12 into equation 2-13,

$$\varepsilon = c_1 + \frac{\dot{\varepsilon} \cdot t}{1-m} \tag{2-13}$$

Where, c_1 is constant.

Besides, Singh and Mitchell (1969) claimed that time to creep failure could be estimated with equation 2-14,

$$t_f = \frac{\left(\dot{\varepsilon} \cdot t\right)_f}{\dot{\varepsilon}} t_{rf} \tag{2-14}$$

Where, $\left(\dot{\varepsilon} \cdot t\right)_f$ is critical strain; t_f is time to creep failure; and $\dot{\varepsilon}$ is strain rate.

It should be pointed out both two assumptions made by Singh and Mitchell (1968) were not precisely correct. For 1st assumption, as mentioned before, Bishop (1969) stated that strain rate-time curve was not exactly linear in log-log scales (figure 2-7). For 2nd assumption, as admitted by Mitchell (1993), it was quite obvious that strain rate-stress curves were not linear in semi-log scales, and stress rate-stress curves at different stresses were not parallel (figure 2-19).

2.5. Summary

It is necessary to summarize studies by previous researchers,

- Two creep failure criteria are stress threshold and critical strain;
- Stress level and critical strain are implicit assumed to be estimated from conventional triaxial shear test;

- All current models estimate time to creep failure with critical strain divided by a constant strain rate;

However, outcome of this research will disagree with some views of previous researchers,

- Creep failure could happen at any stress level as long as duration is long enough, in other words, there is no stress threshold for creep failure. And the only creep failure criterion is critical strain;
- Peak stress (adopted to calculate stress level) and critical strain of triaxial UU creep test are estimated from those from conventional triaxial shear test being multiplied with a ratio, respectively. In most cases, ratios are not unit, while, previous researchers implicit assumed ratios equal to unit;
- It is not precisely to adopt a constant strain rate for estimating time to creep failure which includes both primary creep and secondary creep, while strain rate at primary creep keeps decreasing (still larger than strain rate at secondary creep);

3. POWER LAW MODEL

Briaud and Garland (1985) proposed a power law model to quantify the gain in undrained shear strength S_u with the decrease in time to failure t (i.e., rate of loading effect). The model was expressed as equation 3-1.

$$\frac{s_{u1}}{s_{u2}} = \left(\frac{t_2}{t_1}\right)^n \tag{3-1}$$

Where,

s_{u1} s_{u2}: Undrained shear strength measured with time to failure t_1 and t_2, respectively;

n: Viscous exponent.

The equation 3-1 was extended to the undrained capacity of piles in field, expressed as:

$$\frac{Q_{u1}}{Q_{u2}} = \left(\frac{t_2}{t_1}\right)^n \tag{3-2}$$

Where, Q_{u1} Q_{u2} are Ultimate pile capacity reached in a time to failure t_1 and t_2.

Data from 152 undrained laboratory tests on clay specimens were collected from the literature in order to find the range of values for the viscous exponent n (figure 3-1). Meanwhile, a total of 62 pile load tests were collected in which two identical piles had been subjected to two different rates of loading (figure 3-2). It was found the range of values and their average for pile load tests were similar to the ones obtained for the laboratory tests.

The variation of n with the reference undrained shear strength $s_{u(ref)}$ (time to failure=1h), water content *w*, plasticity index PI, liquidity index LI, and overconsolidation ratio OCR were shown in figure 3-3 to figure 3-7.

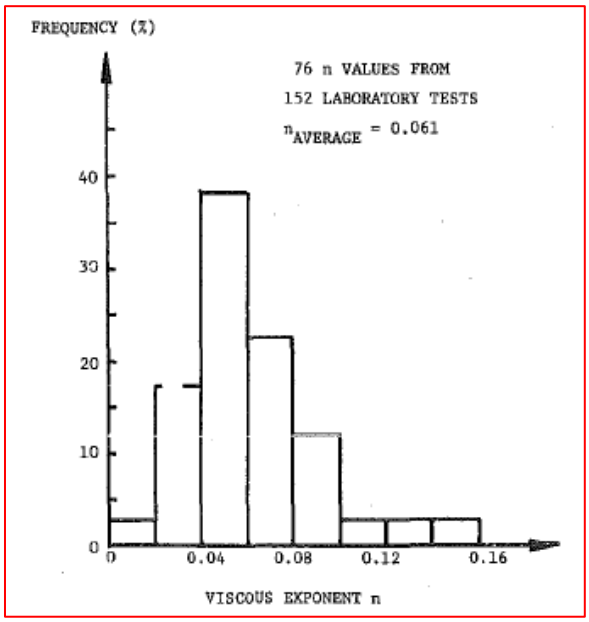

Figure 3-1. Frequency distribution of n values for 152 laboratory tests (Briaud and Garland, 1985)

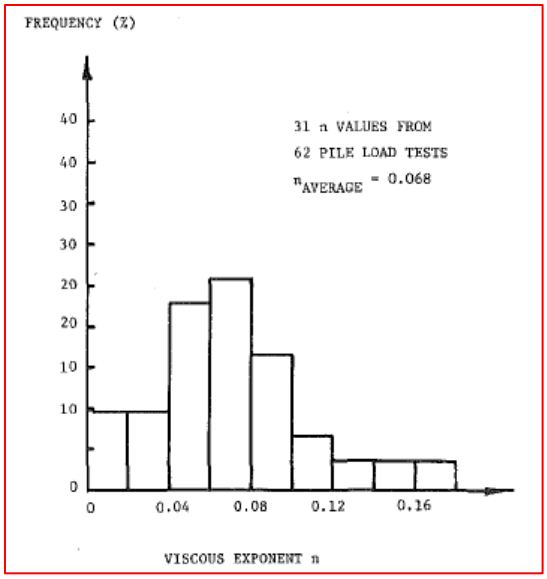

Figure 3-2. Frequency distribution of n values for 62 pile load tests (Briaud and Garland, 1985)

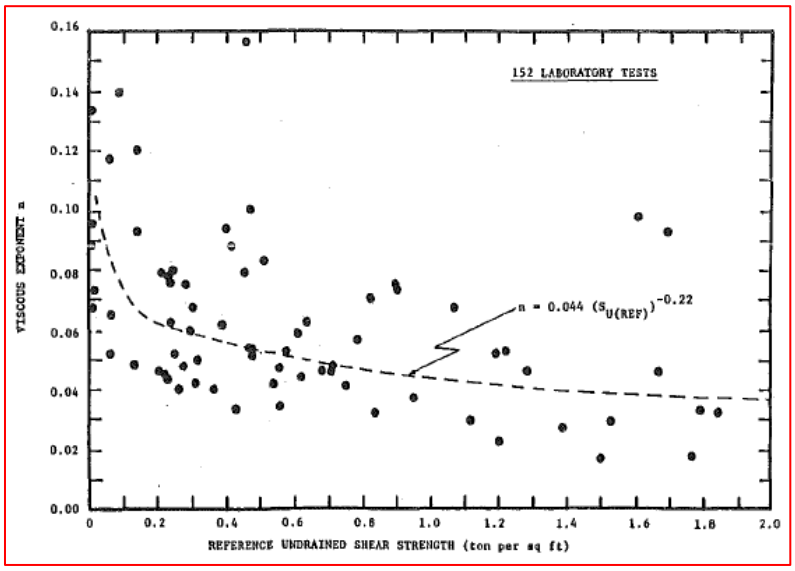

Figure 3-3. N value versus reference undrained shear strength (Briaud and Garland, 1985)

Note: 1tsf=95.8kPa

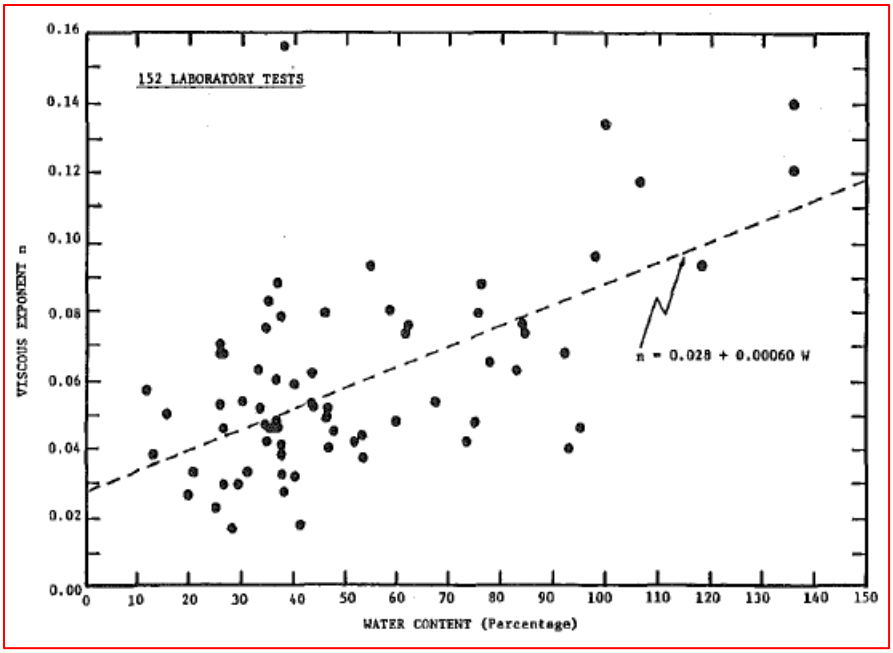

Figure 3-4. N value versus water content (Briaud and Garland, 1985)

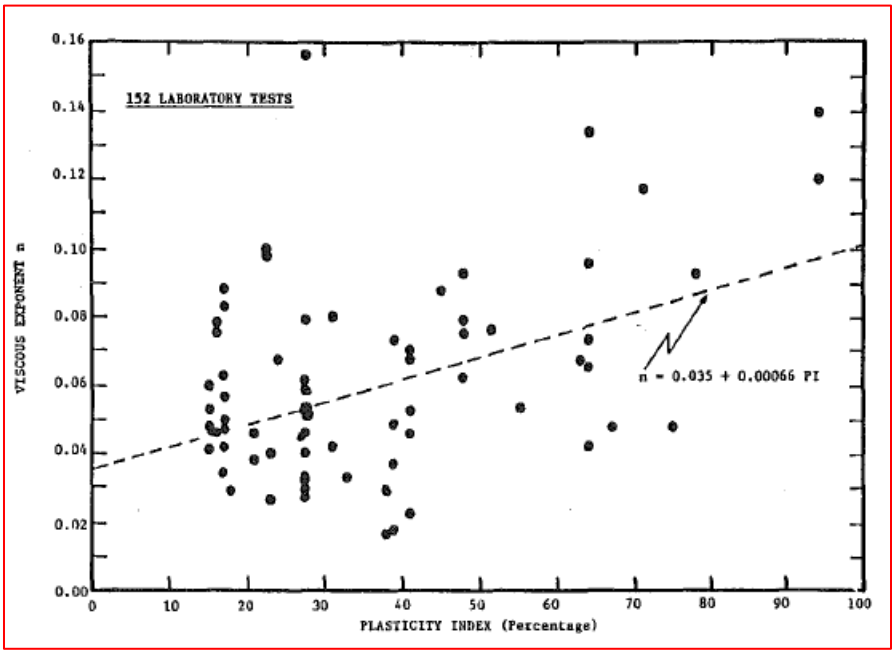

Figure 3-5. N value versus plasticity index (Briaud and Garland, 1985)

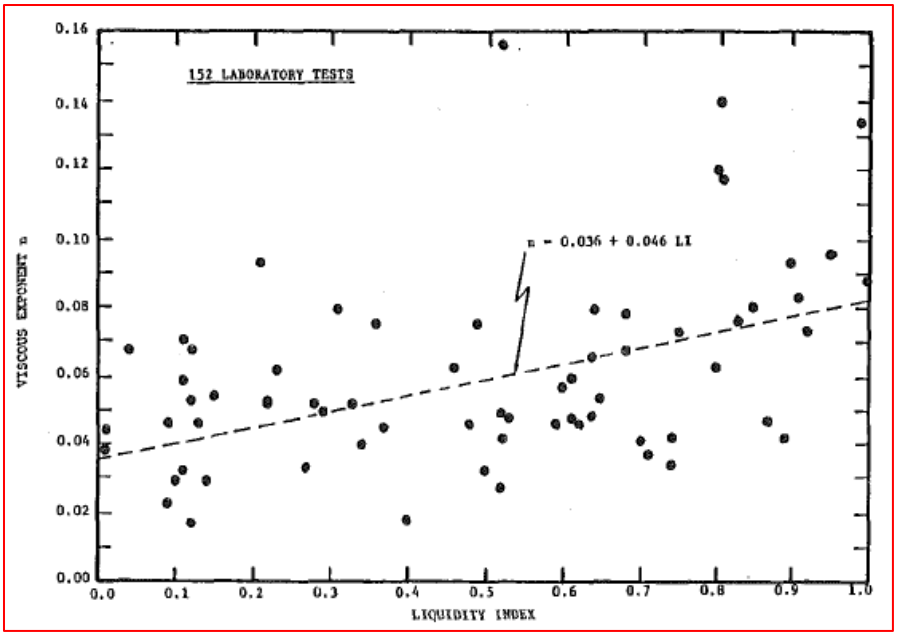

Figure 3-6. N value versus liquidity index (Briaud and Garland, 1985)

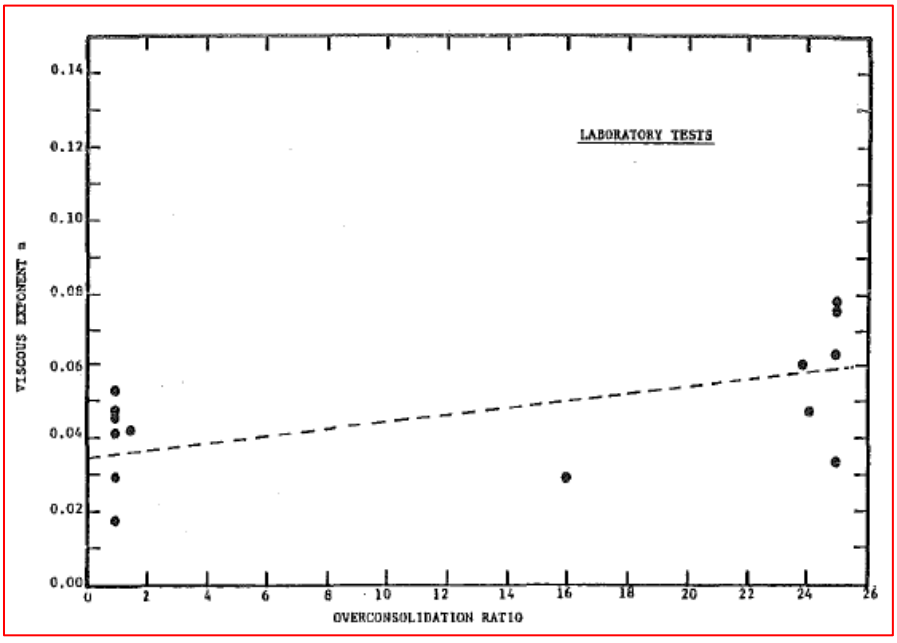

Figure 3-7. N vaule versus overconsoldiation ratio (Briaud and Garland, 1985)

Though there is no clear trend for n value correlated with soil properties listed above, it should be noted that it seems a higher n value will be obtained for a smaller undrain shear strength (figure 3-3). Besides, the data of n value versus plasticity index in figure 3-5 doesn't support the view in the GEC#7 that long-term deformation is simply associated with the plasticity index.

Kubena and Briaud (1989) mentioned in the report that n value from the equation 3-2 corresponds well to n value measured with the pressuremeter at that site. Briaud and Gibbens (1999) stated typical range of n value is 0.005~0.03 for sand and 0.02~0.08 for clay from the pressuremeter test (PMT). However, because the duration of creep test in PMT is 30 minutes, n value for clay from PMT is more likely to be n_{both} rather than n_{cr}, while n_{both} will be explained in detail in Chapter four.

Later, the power law model was extended to represent time dependent behavior of soils (Gibbens, 1995; Suroor, 1998), expressed as:

$$\frac{s}{s_1} = \left(\frac{t}{t_1} \right)^n \tag{3-3}$$

Where the deformation (movement, settlement, displacement, strain, etc.) s_1 is usually chosen to be the value of deformation s observed at time $t = 1\text{min}$ (after the beginning of a holding stress or sustained load) from the very beginning of the test (figure 3-8); and n is the viscous exponent.

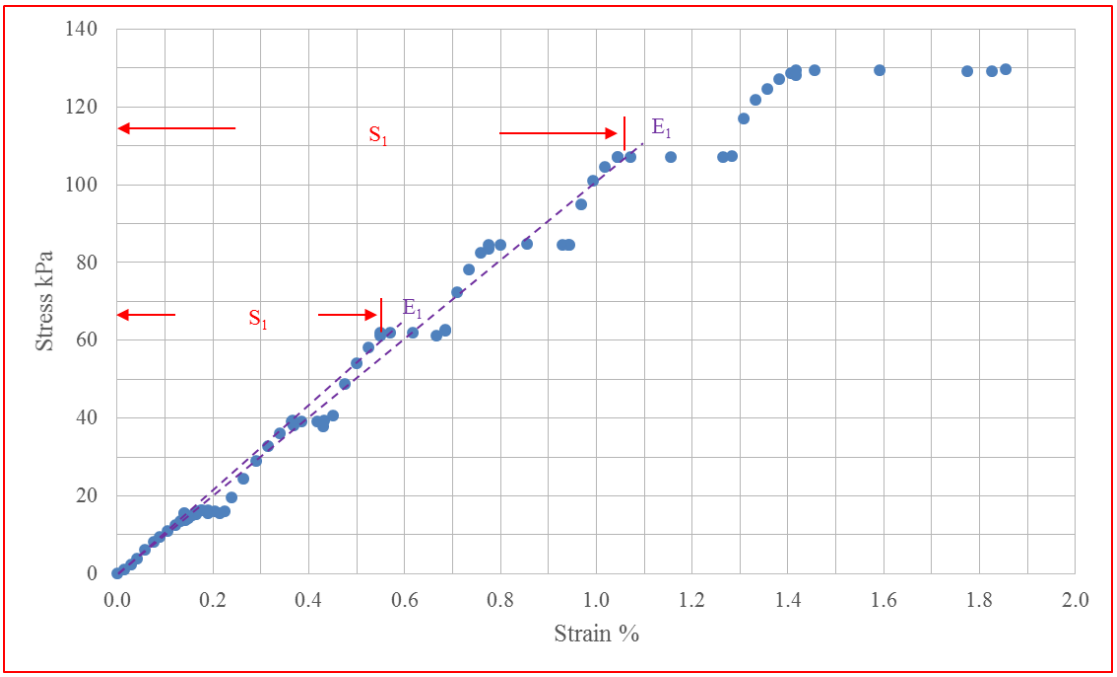

Figure 3-8. S_1 and E_1 adopted here

It is worth noting that s_1 could also be chosen as the deformation increment only at current stress level (figure 3-9). However, it is hard to apply in practice because s_1 is unknown until tests are conducted to obtain its value.

Meanwhile, the deformation s in equation 3-3 could be associated with the modulus E (figure 3-8). For one-dimensional (1D) consolidation test and 1D compression test presented in Chapter four and triaxial unconsolidated-undrained (UU) creep test in Chapter five, the conversion is shown below.

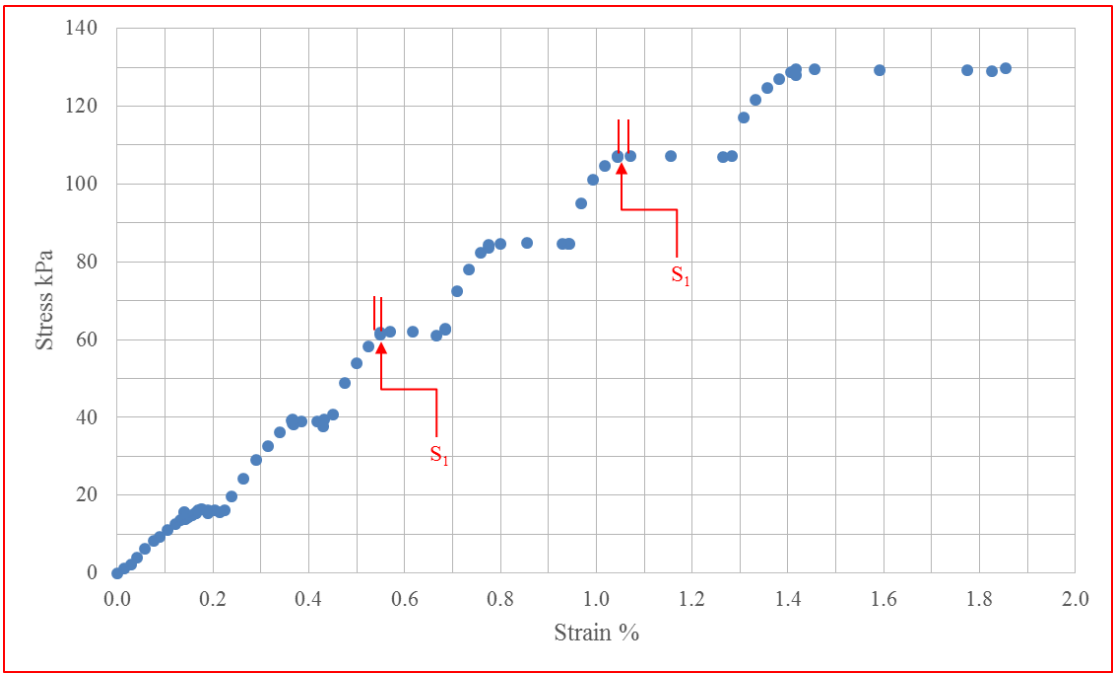

Figure 3-9. S_1 not adopted here

The Generalized Hooke's Law is described by the equations below:

$$\varepsilon_z = \frac{1}{E_z}\left[\sigma_z - \upsilon\left(\sigma_r + \sigma_\theta\right)\right]$$
$$\varepsilon_r = \frac{1}{E_r}\left[\sigma_r - \upsilon\left(\sigma_z + \sigma_\theta\right)\right] \quad (3\text{-}4)$$
$$\varepsilon_\theta = \frac{1}{E_\theta}\left[\sigma_\theta - \upsilon\left(\sigma_r + \sigma_z\right)\right]$$

Where,

$\sigma_z\ \sigma_r\ \sigma_\theta$: Vertical stress, radial stress, tangential stress;

$\varepsilon_z\ \varepsilon_r\ \varepsilon_\theta$: Vertical strain, radial strain, tangential strain;

$E_z\ E_r\ E_\theta$: Modulus associated with $\sigma_z\ \sigma_r\ \sigma_\theta$ and $\varepsilon_z\ \varepsilon_r\ \varepsilon_\theta$ respectively;

υ: Poisson's ratio, 0.48 for all 1D tests (i.e., 1D consolidation test and 1D compression test) and triaxial UU creep test on dry sand specimens; 0.35 for triaxial UU creep test on high PI clay specimens and low PI clay specimens.

It should be noted that the Generalized Hook's Law adopted here is just to clarify the linear contribution to strain by stress. It doesn't mean that the soil will be back to the original state (i.e., elastic material) after a loading-unloading cycle.

In 1D consolidation test and 1D compression test,

$$\begin{aligned} \varepsilon_r &= 0 \\ \varepsilon_\theta &= 0 \end{aligned} \tag{3-5}$$

The equation is derived,

$$\begin{aligned} \varepsilon_z &= \frac{\sigma_z}{E_z}\left(1-\frac{2\upsilon^2}{1-\upsilon}\right) \\ \sigma_\theta &= \sigma_r = \frac{\upsilon}{1-\upsilon}\sigma_z \end{aligned} \tag{3-6}$$

In triaxial UU creep test,

$$\begin{aligned} \sigma_r &= \gamma \cdot h = \rho \cdot g \cdot h \\ \sigma_\theta &= 0 \end{aligned} \tag{3-7}$$

The equation is derived,

$$\varepsilon_z = \frac{1}{E_z}\left[\sigma_z - \upsilon \cdot \gamma \cdot h\right] \tag{3-8}$$

Where,

γ: Unit weight;

ρ: Density;

g: Acceleration of Gravity;

h: Depth of samples (used for preparing specimens) in field.

When,

$$\varepsilon_z = \frac{s}{H} \tag{3-9}$$

Where,

H: Height of specimens, 1.9cm for all 1D tests and it varies for triaxial UU creep test;

s: Deformation.

Thus, the power law model equation 3-3 in 1D consolidation test, 1D compression test and triaxial UU creep test could be also expressed as follows:

$$\frac{s}{s_1} = \frac{E_1}{E} = \left(\frac{t}{t_1}\right)^n \tag{3-10}$$

Where,

E_1: Modulus E associated with s_1 at reference time t_1.

By plotting equation 3-10 in log-log scales, n value will be the slope if the curve is a straight line. In this case, n value could be back-calculated with as less as any two points on deformation/modulus-time curves.

4. LABORATORY TESTS – ONE-DIMENSIONAL (1D) CONSOLIDATION TEST AND 1D COMPRESSION TEST

4.1. Introduction

This chapter aims at demonstrating several points listed below:

- The power law model is feasible to represent time dependent behavior of soils in 1D consolidation test and 1D compression test;
- The power law model is capable of predicting long-term deformation in practice;
- Creep should be taken into account during the whole consolidation process.

It should be noted that the only difference between 1D consolidation test and 1D compression test is that the specimen is wrapped with several layers of plastic films to avoid drying during 1D compression test, while the specimen in 1D consolidation test is immersed into water.

4.2. Soil Properties

Three kinds of soils are adopted in 1D consolidation test and 1D compression test. They are high PI clay, low PI clay, and sand.

4.2.1. High PI Clay

High PI clay samples were taken with Shelby Tube sampling method from Texas A&M University riverside campus National Geotechnical Experimental Site (TAMU-NGES) (Briaud, 1997). The sampling (figure 4-1) was requested by following:

- BH1 ~ BH2, one sample every 0.6 m until the depth 5.5 m;

- N1 ~ N6, one sample every 0.6 m until 3m depth, then 4~4.6 m and 4.9~5.5 m;
- BH3 ~ BH4, one sample every 0.6 m until the depth 3 m;

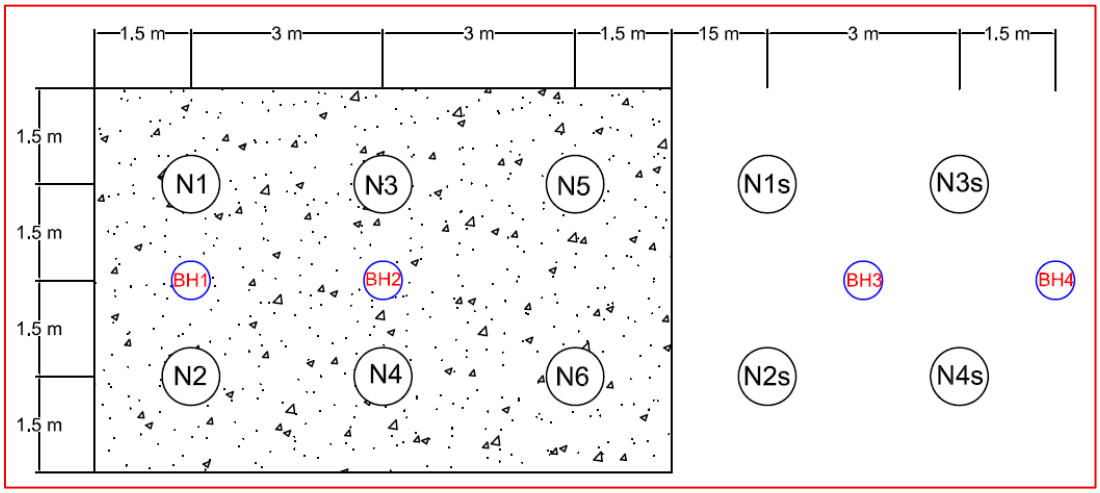

Figure 4-1. The layout of boreholes of high PI clay samples

The water content profile with depth is shown in figure 4-2. It should be noted that the depth of groundwater table is close to 6m. The unit weight profile with depth is shown in figure 4-3, which is essentially constant. The strength profile with depth is shown in figure 4-4. It is stiff clay, especially the layer at depth 2~3m which is very stiff. The Atterberg limits profile with depth is shown in figure 4-5. The plasticity index (PI) at any depth is larger than 15, which is classified as high PI clay according to GEC#7.

The degree of saturation is calculated based on the equation 4-1 with the assumption $G_s = 2.75$. The soil at any depth is saturated ($S_r \geq 85\%$) though it is above the groundwater table.

$$S_r = \frac{\omega}{\frac{\gamma_w(1+0.01\omega)}{\gamma} - \frac{1}{G_s}} \tag{4-1}$$

Where,

S_r: Degree of saturation;

ω: Water content;

γ: Unit weight;

γ_w: Unit weight of water;

G_s: Specific gravity of solid.

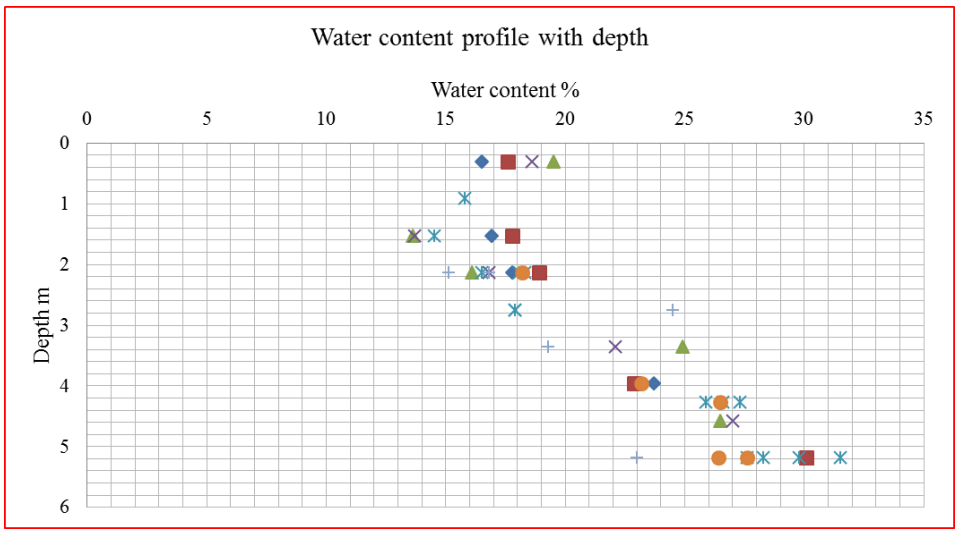

Figure 4-2. Water content profile with depth (high PI clay)

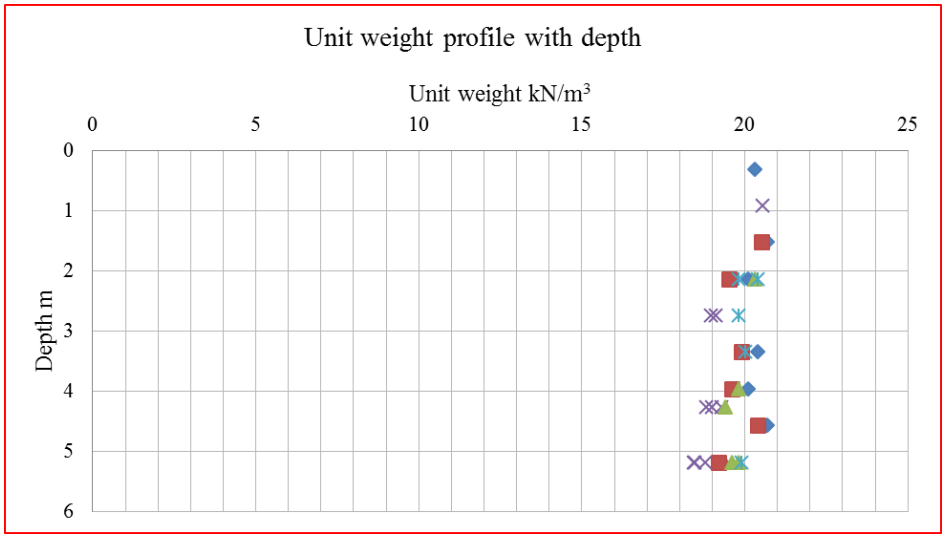

Figure 4-3. Unit weight profile with depth (high PI clay)

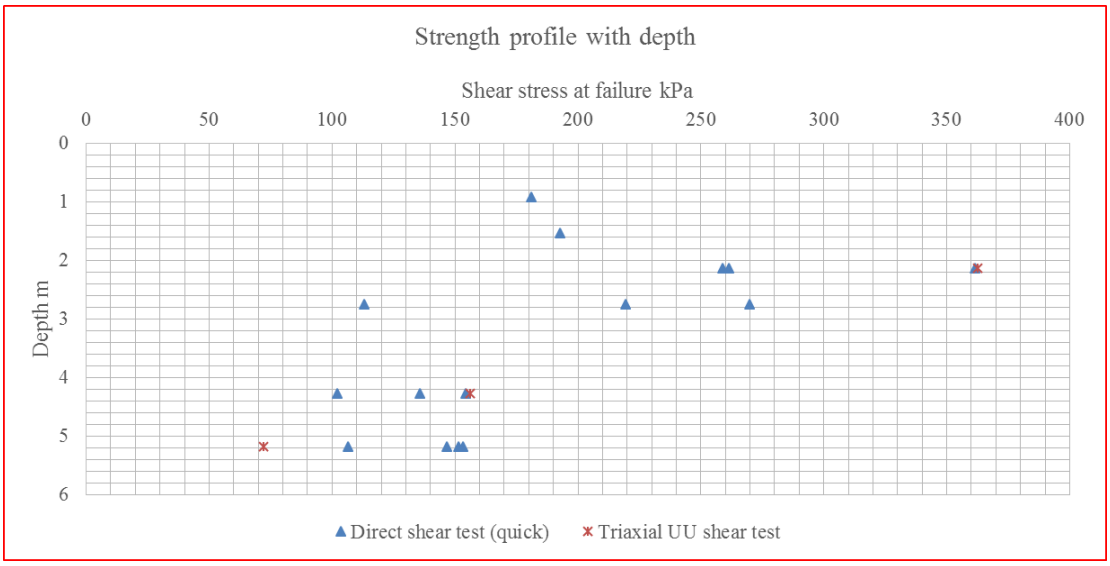

Figure 4-4. Strength profile with depth (high PI clay)

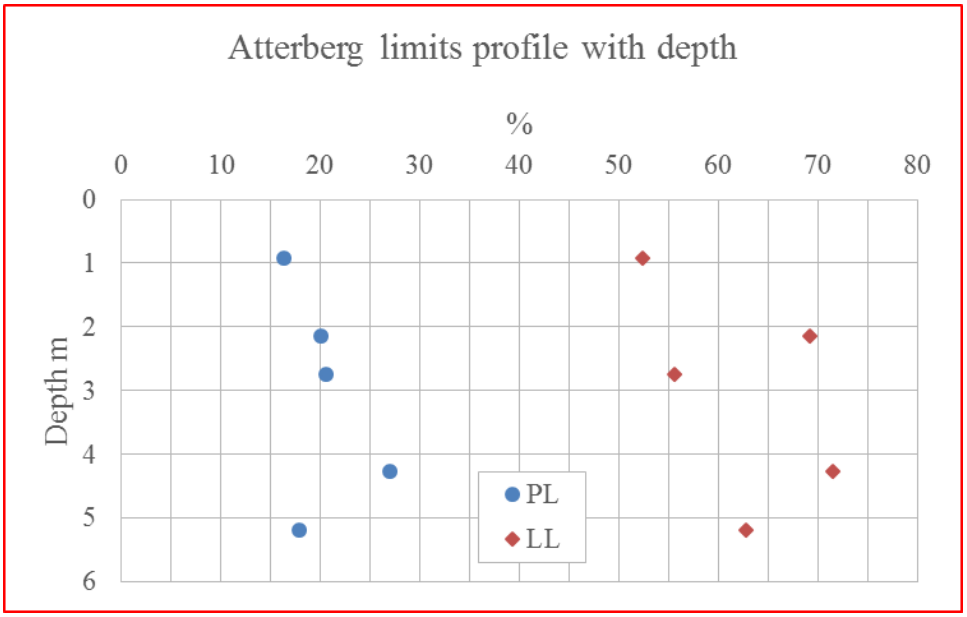

Figure 4-5. Atterberg limits profile with depth (high PI clay)

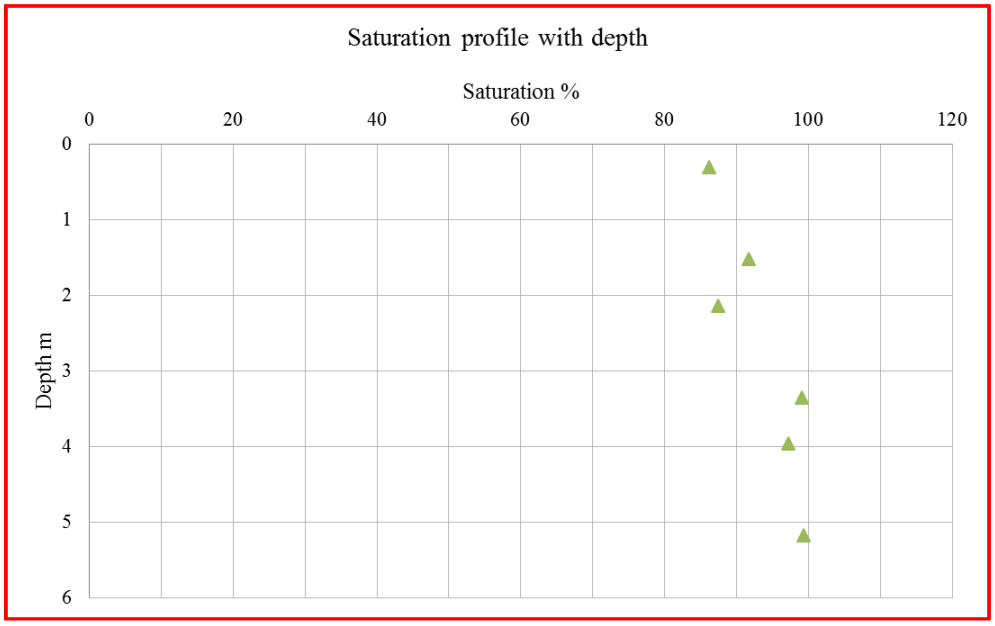

Figure 4-6. Degree of saturation profile with depth (high PI clay)

4.2.2. Low PI Clay

Low PI clay was porcelain clay, purchased from ARMADILIO CLAY & SUPPLIES, Inc.

- The water content was measured to be 20.1%;
- The strength from the mini vane shear test was 46.3kPa~54kPa (average 49.7kPa on six measurements);
- The PI was 13.8, and it was classified as low PI clay according to GEC#7.

4.2.3. Sand

Fine sand was supplied by Humboldt Mfg. Co. It was clean, dry, free-flowing uncemented sand with less than 1 percent variation in bulk density.

4.3. Loading Procedure

All 1D tests (i.e., 1D consolidation test and 1D compression test) follow ASTM D2435/D2435M – 11 (ASTM Standard, 2011). The dead weights applied during tests were: 5kg, 10kg, 20kg ... 160kg and 320kg, then 160kg, 80kg … 20kg, 10kg. The corresponding loading stresses were: 15.5kPa, 31.1kPa, 62.2kPa … 497.3kPa and 994.6kPa, then 497.3kPa, 248.7kPa … 62.2kPa, 31.1kPa. The duration of each loading stress was 24h.

It should be noted that the only exception is that the first dead weight for 1D compression test on dry sand is 10kg instead of 5kg.

4.4. Power Law Model

At each loading stress of 1D consolidation tests and 1D compression tests, the strain-time curve or modulus-time curve was plotted in log-log scales, and then the slope of curves would be the exponent n value in the power law model (equation 3-10). It was found that the curve was a straight line or two linear segments in the log-log scales, which depends on whether there is consolidation during the test or not. If there is consolidation the curve will consist of two linear segments (figure 4-7). If there is no consolidation the curve will be a straight line (figure 4-8).

In the former case (with consolidation, figure 4-7), the first linear segment corresponds to the primary consolidation, where the deformation includes two parts: deformation associated with excess pore pressure dissipation and deformation associated with creep. These two different parts of deformation need to be separated. The second linear segment corresponds to the secondary compression, where the deformation is only caused by creep. If it is assumed that the creep mechanism is the same during the primary consolidation and the secondary compression, then the deformation associated with excess pore pressure dissipation could be separated. The assumption will be verified in section 4.7 in detail.

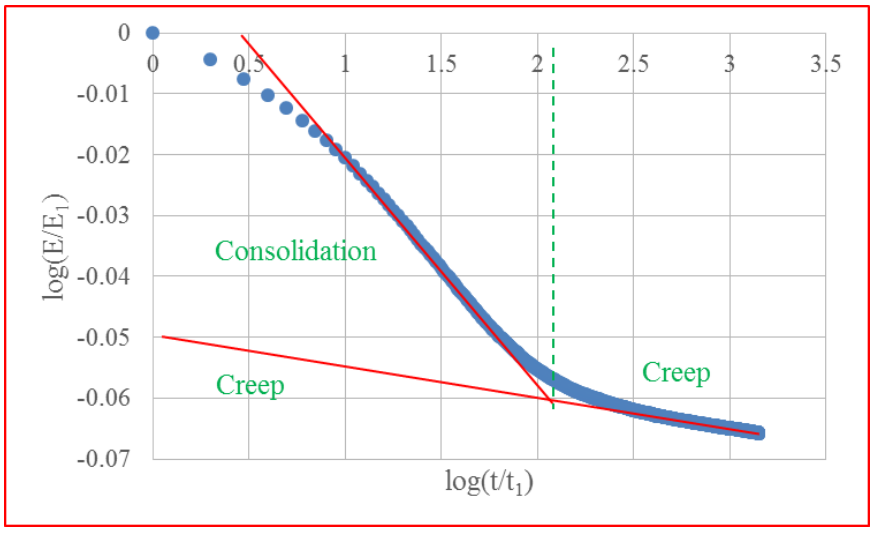

Figure 4-7. Modulus-time curve with consolidation

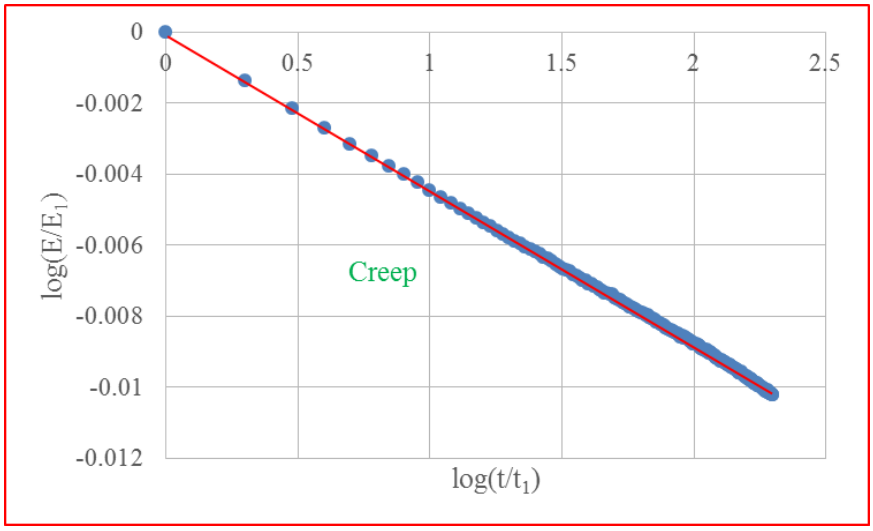

Figure 4-8. Modulus-time curve without consolidation

The slope of the first linear segment (primary consolidation) equals to n value including both consolidation and creep (n_{both}), while the slope of the second segment (secondary compression) equals to n value only including creep (n_{cr}). If the angle of slope for n_{both} is α, and the angle of slope for n_{cr} is β, the angle of slope for the n value corresponding to consolidation (n_{con}) during the primary consolidation will be $(\alpha - \beta)$, and the n value n_{con} can be calculated with the following equation 4-2.

$$n_{con} = \tan(\alpha - \beta) = \frac{\tan(\alpha) - \tan(\beta)}{1 + \tan(\alpha) * \tan(\beta)} = \frac{n_{both} - n_{cr}}{1 + n_{both} * n_{cr}} \quad (4\text{-}2)$$

In usual, $n_{both} < 0.1$ and $n_{cr} < n_{both}$. So, the equation 4-2 can be approximated:

$$n_{con} = \frac{n_{both} - n_{cr}}{1 + n_{both} * n_{cr}} \approx n_{both} - n_{cr} \quad (4\text{-}3)$$

In the latter case (without consolidation, figure 4-8), the slope of the straight line is n_{cr}, because there is no consolidation. And it is found that n_{cr} from both cases (with consolidation and without consolidation) is the same, which will be presented later in this chapter.

4.5. 1D Consolidation Test

1D consolidation test on high PI clay, low PI clay, and wet sand are described here.

4.5.1. High PI Clay

Test results of high PI clay specimen prepared from the sample at depth 4~4.6m from borehole N5 were used here for illustration.

At first, after specimens were immersed into the water, tests were carried out immediately. It was found that there was swelling at the low loading stresses (15.5kPa, 31.1kPa, and 62.2kPa), which impacted the shape of the modulus versus time curve when plotting in the log-log scales. After that, all specimens of new tests were allowed to swell for a few days under the stress 1.5kPa until it was stable. However, this swelling resulted in the disturbance (relaxation) in specimens and destroyed some soil structures. When tests were carried out after swelling, the loose zone of specimens caused by swelling were recompressed, which tremendously increased the value of s_1 than it should be at the low loading stresses (especially at the first loading stresses 15.5kPa), and further significantly reduced the value of n_{both}. It should be noted that s_1 is the value of deformation s observed at time $t = 1\text{min}$ (after the beginning of a holding stress or sustained load) from the very beginning of the test. So, s_1 used to calculate n values at any stress all include s_1 at the first loading stress, that is to say the swelling will have an impact on n values at any stress. However, the impact will be insignificant at high stresses. Modulus-time curves of 1D consolidation test on high PI clay are shown in figure 4-9 and figure 4-10. N value-stress curves of 1D consolidation on high PI clay are shown in figure 4-11. There are at least three interesting phenomena shown here:

- The modulus versus time curve consisted of two linear segments;
- n_{cr} is largely impacted by swelling;
- n_{con} is higher than n_{cr}, it shows consolidation is the dominant part in the primary consolidation.

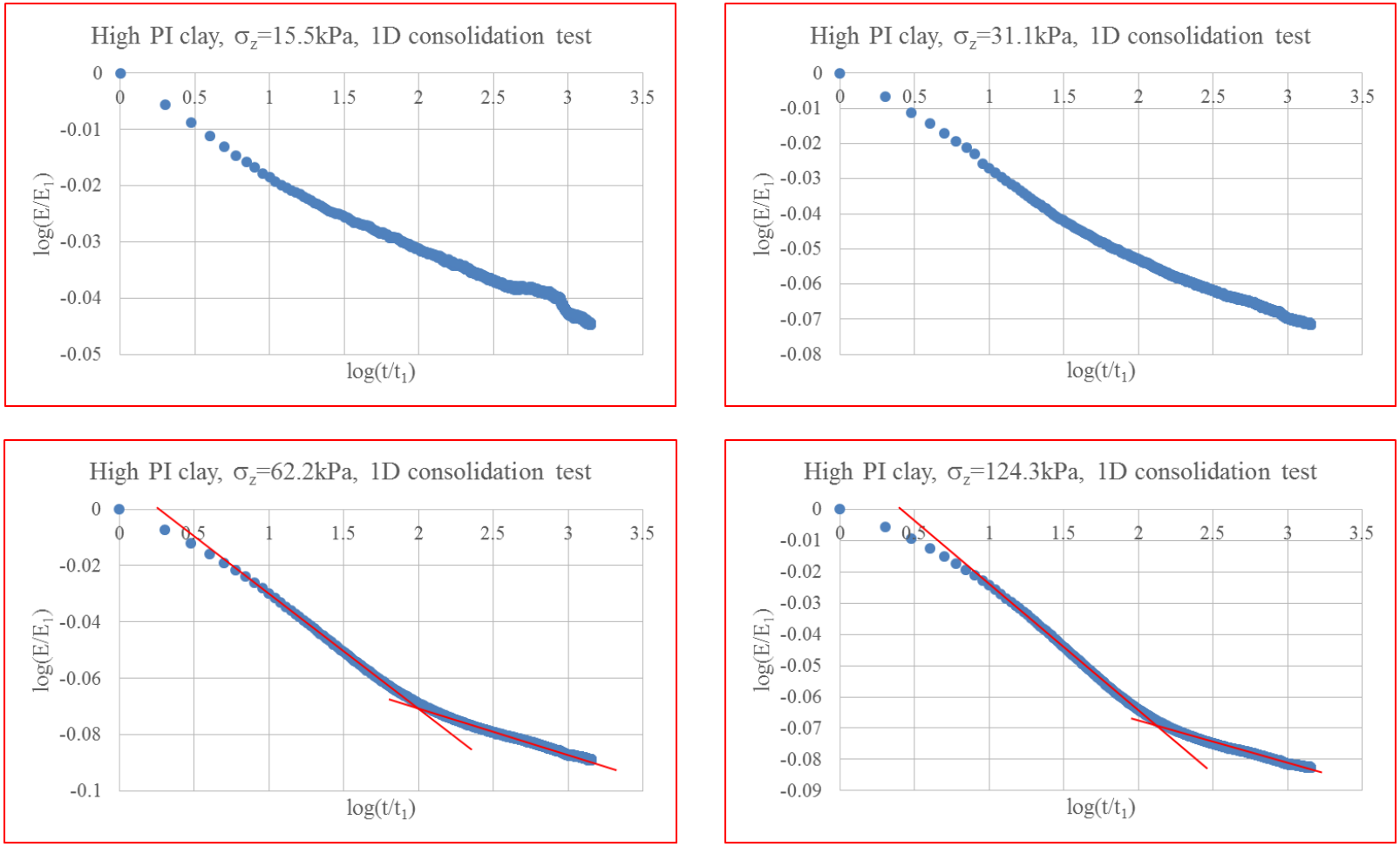

Figure 4-9. Modulus-time curves at any stress of high PI clay, 1D consolidation test

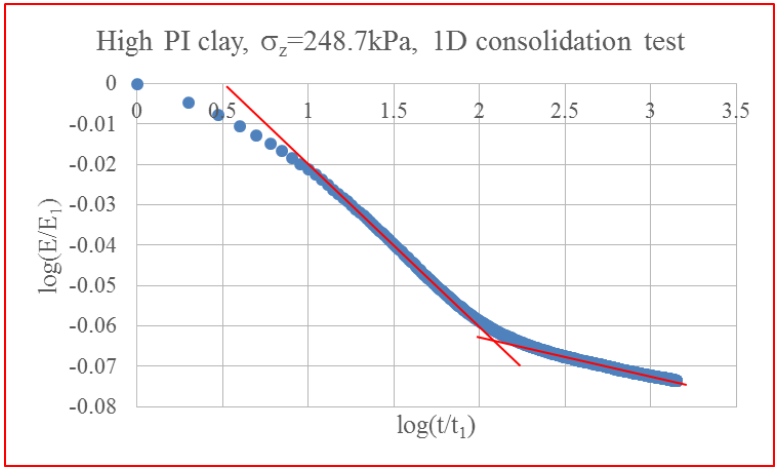

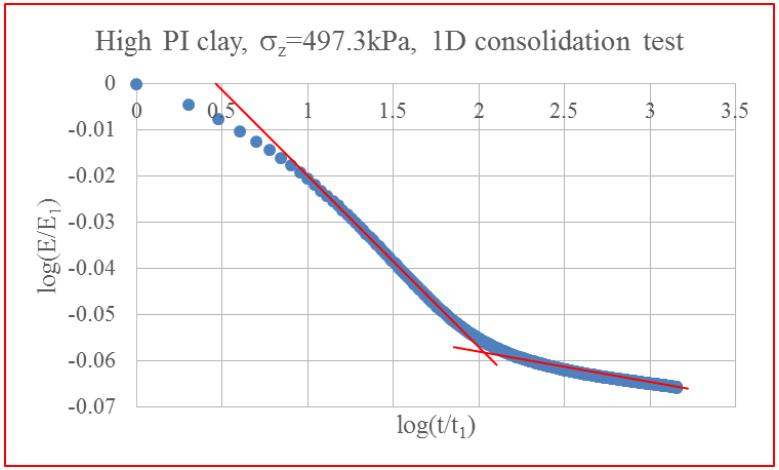

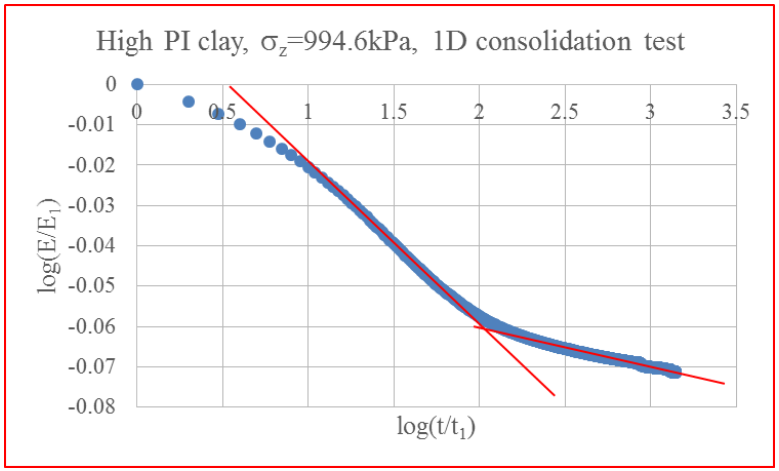

Figure 4-9 Continued

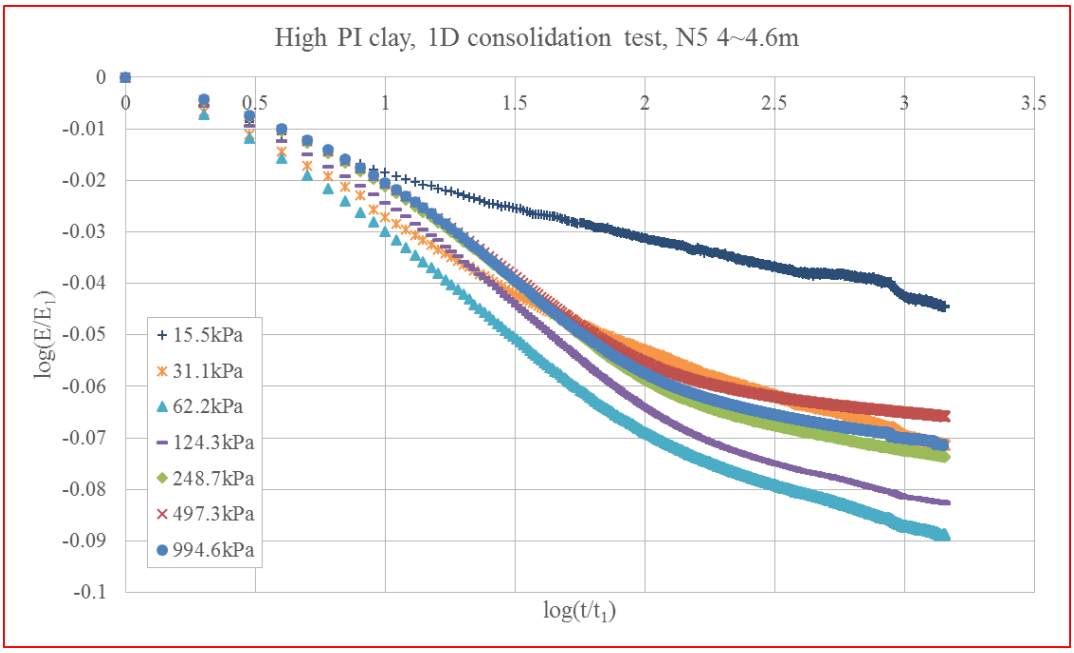

Figure 4-10. Modulus-time curves of high PI clay, 1D consolidation test

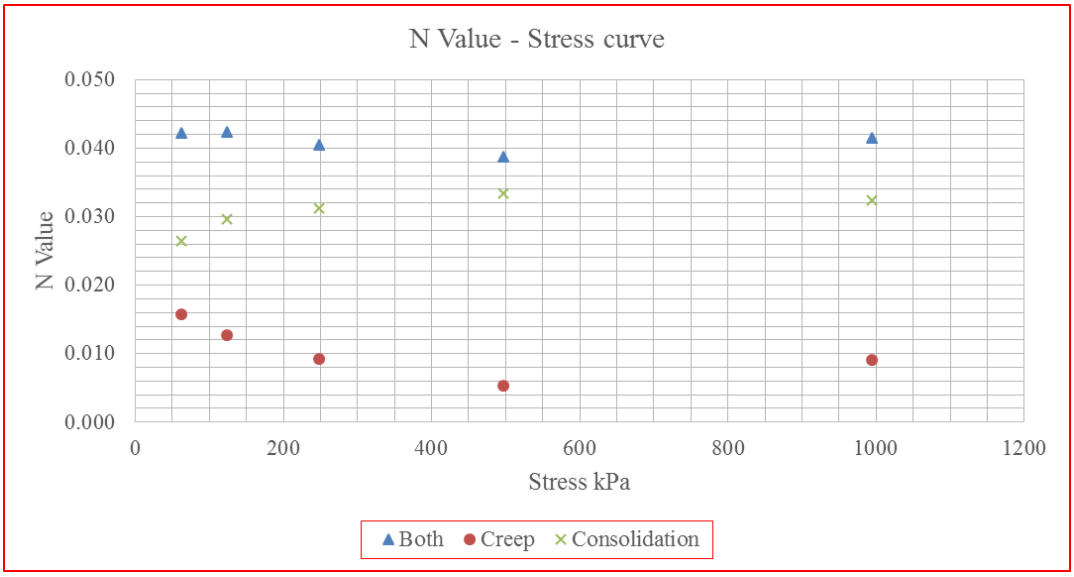

Figure 4-11. N value-stress curves of high PI clay, 1D consolidation test

4.5.2. Low PI Clay

Test results of one low PI clay specimen were used here for illustration.

Modulus-time curves of 1D consolidation test on low PI clay are shown in figure 4-12 and figure 4-13. N value-stress curves of 1D consolidation on low PI clay are shown in figure 4-14.

The three interesting phenomena were shown here:

- The modulus versus time curve consisted of two linear segments, which demonstrated the proposed power law model was able to describe the time dependent behavior of low PI clay in 1D consolidation test;
- Soil behavior is also impacted by swelling. Different with test results of high PI clay, n_{cr} is almost constant from 62.2kPa to 944.6kPa, while n_{both} is a little lower at loading stresses 62.2kPa and 124.3kPa;
- n_{con} is higher than n_{cr}, it shows consolidation is the dominant part in the primary consolidation.

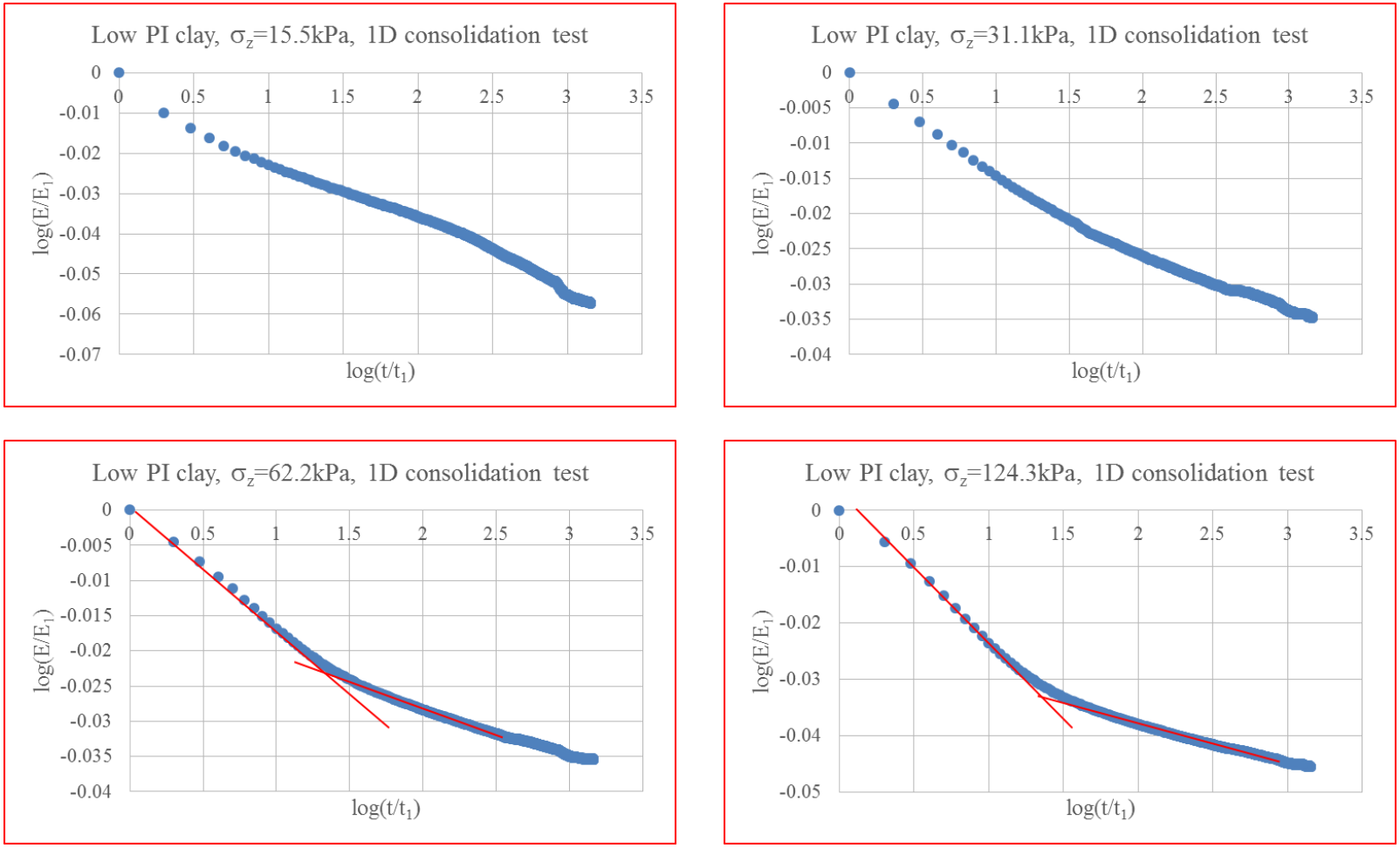

Figure 4-12. Modulus-time curves at any stress of low PI clay, 1D consolidation test

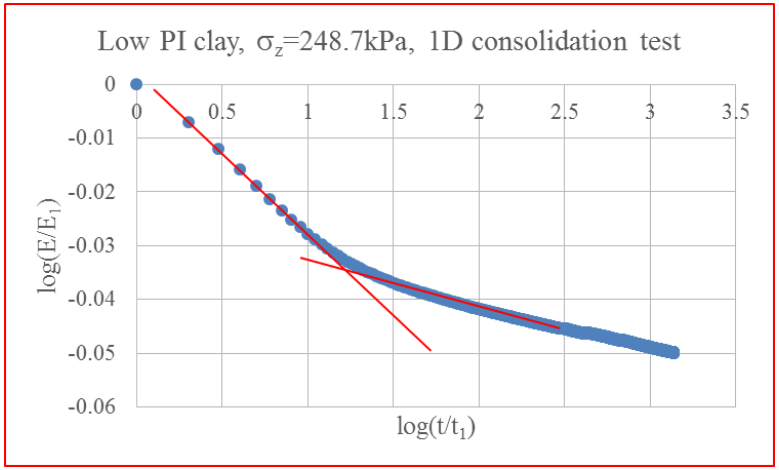

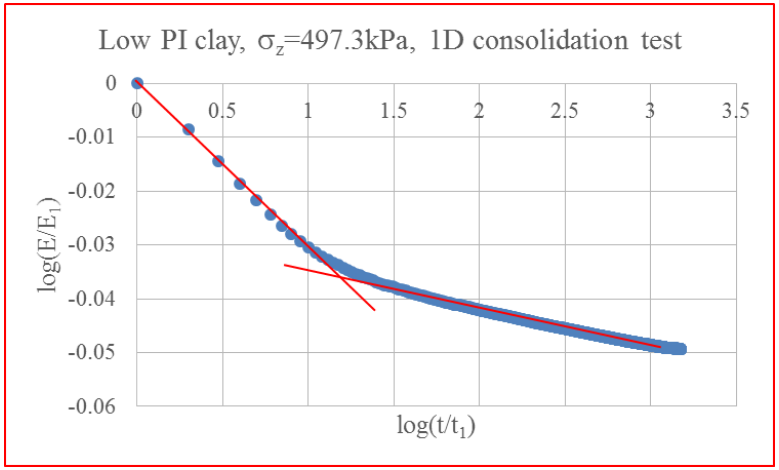

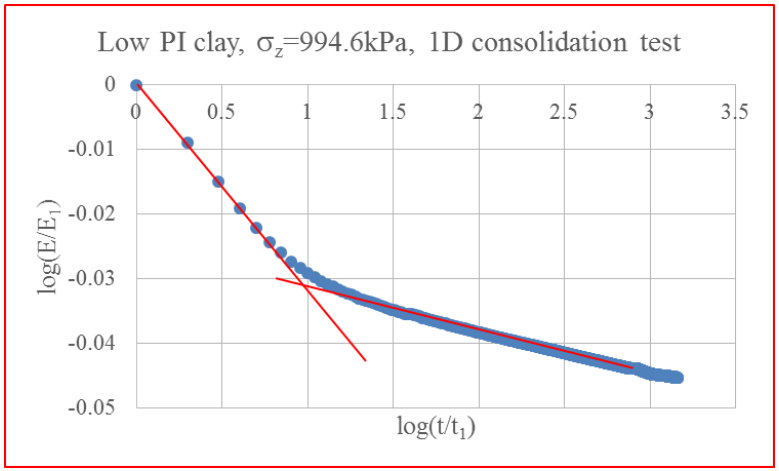

Figure 4-12 Continued

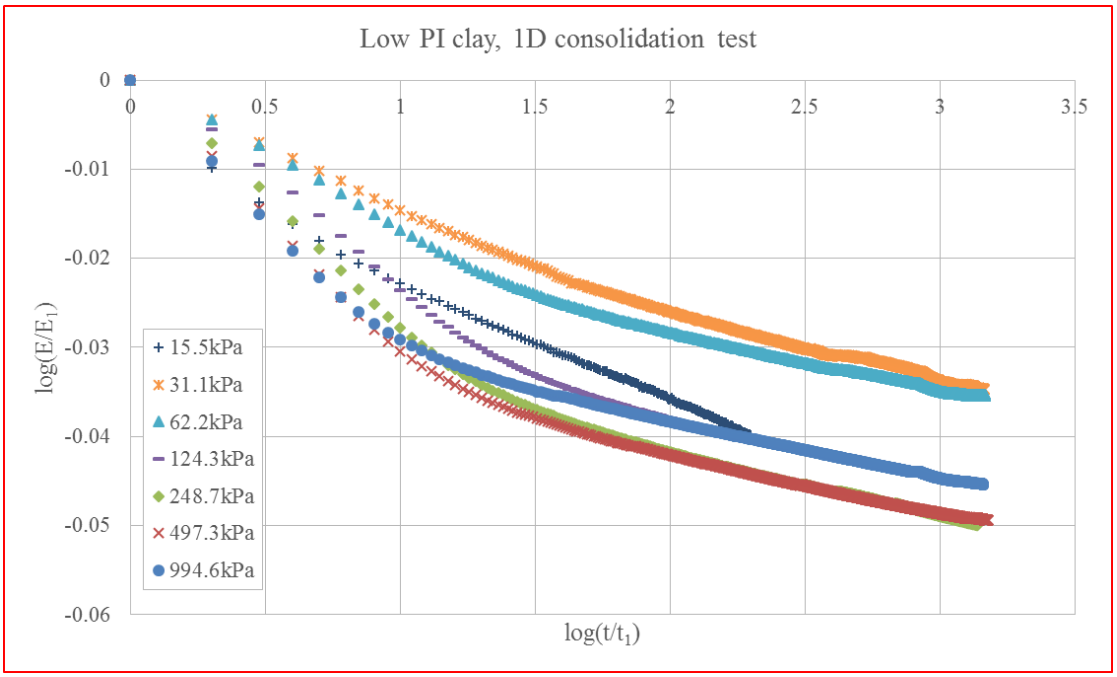

Figure 4-13. Modulus-time curves of low PI clay, 1D consolidation test

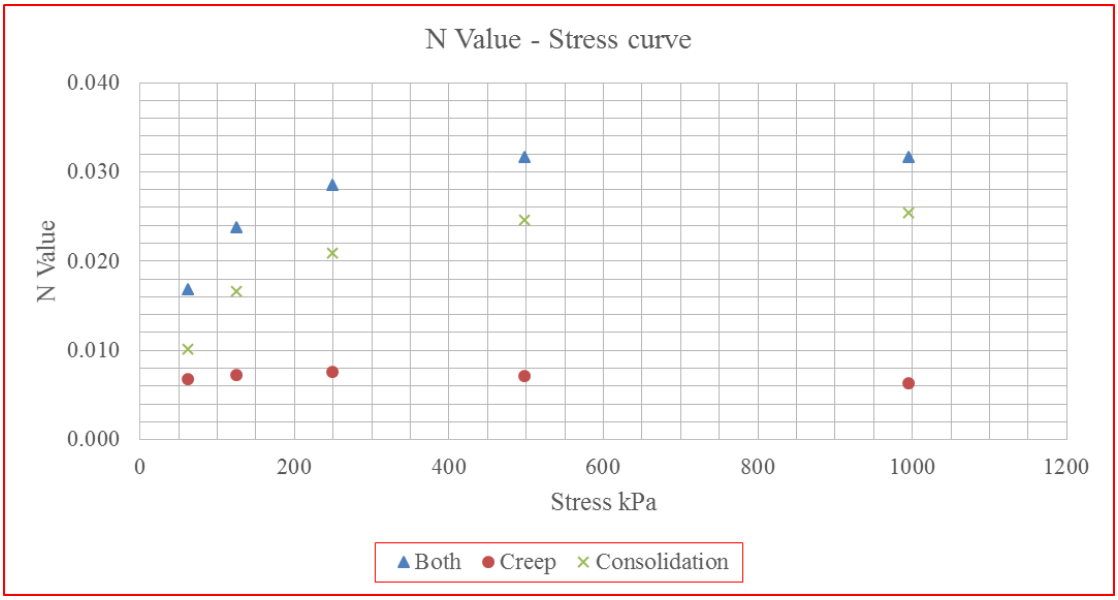

Figure 4-14. N value-stress curves of low PI clay, 1D consolidation test

4.5.3. Wet Sand

Test results of one wet sand specimen were used here for illustration.

It took only 2~3 seconds for wet sand to consolidate (figure 4-15), while the reference time t_1 was chosen to be equal to 1min. So, only data after 1min were plotted in modulus-time curves and the test data at every minute was extracted to process. Namely, a straight line would be shown when the power law model (equation 3-10) was plotted in log-log scales.

Modulus-time curves of 1D consolidation test on wet sand are shown in figure 4-16 and figure 4-17. N value-stress curves of 1D consolidation on wet sand are shown in figure 4-18.

The two interesting phenomena were shown here:

- The modulus versus time curve is a straight line, no matter the loading stress is low or high, which demonstrated the proposed power law model was able to describe the time dependent behavior of wet sand in 1D consolidation test;
- n_{cr} is constant (i.e., independent) during all the loading stresses.

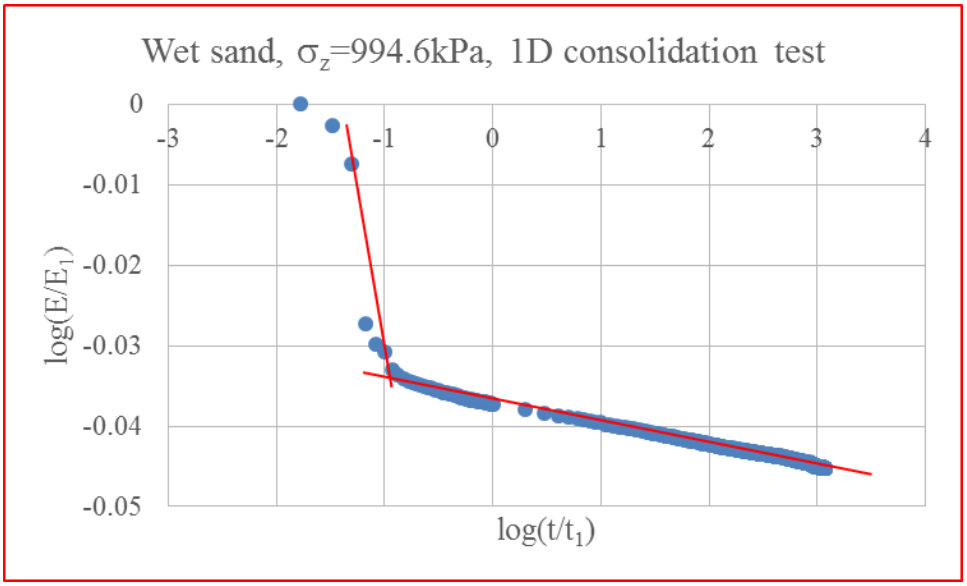

Figure 4-15. Modulus-time curve of wet sand showing consolidation, 1D consolidation test

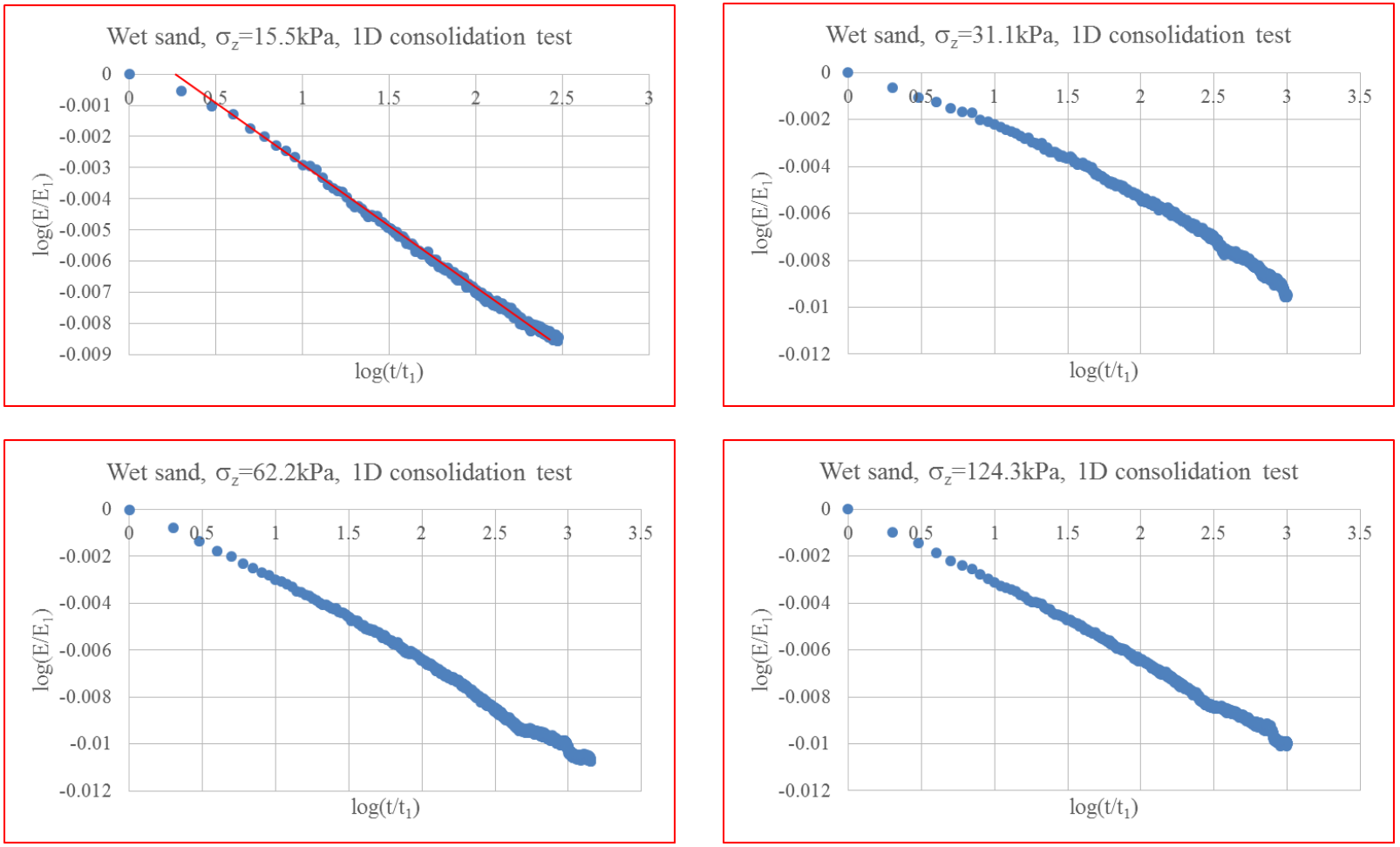

Figure 4-16. Modulus-time curves at any stress of wet sand, 1D consolidation test

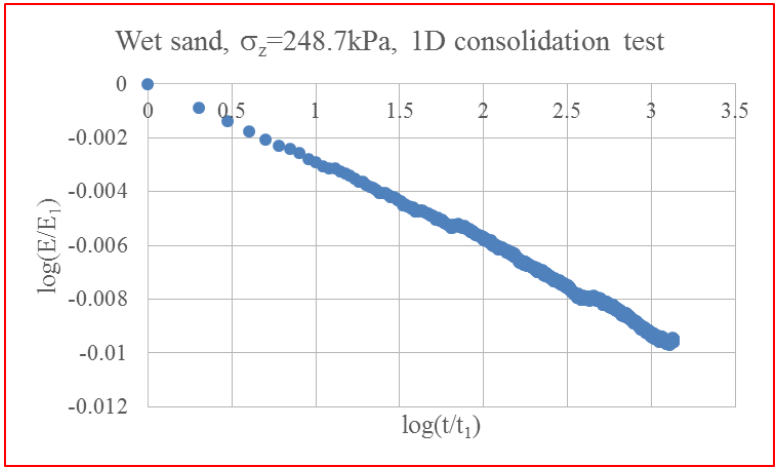

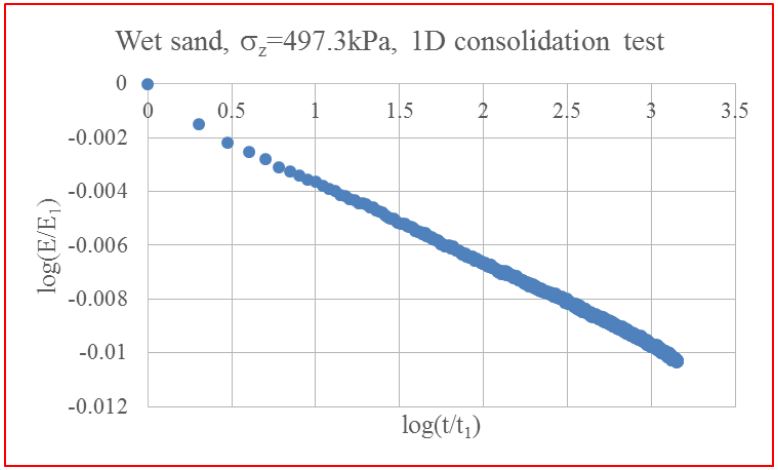

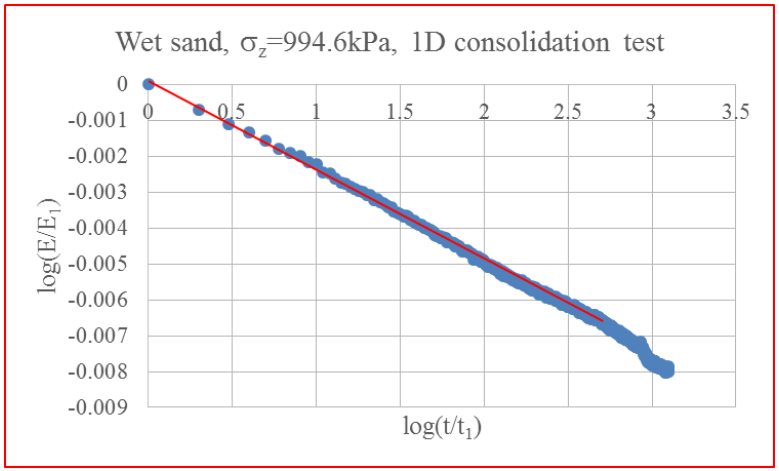

Figure 4-16 Continued

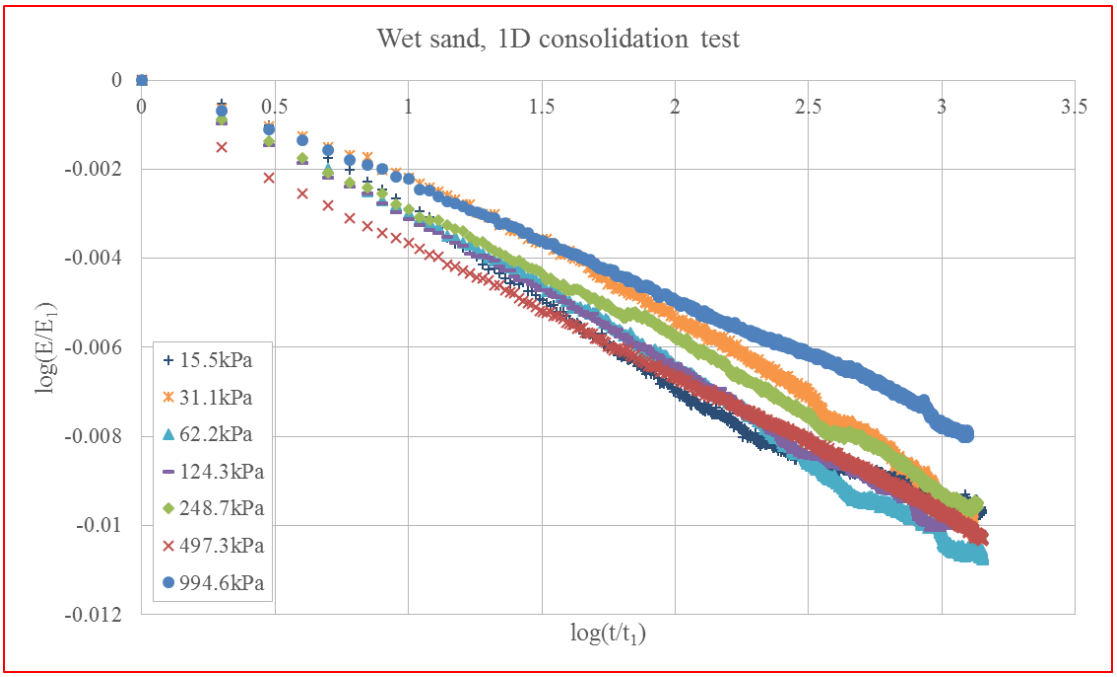

Figure 4-17. Modulus-time curves of wet sand, 1D consolidation test

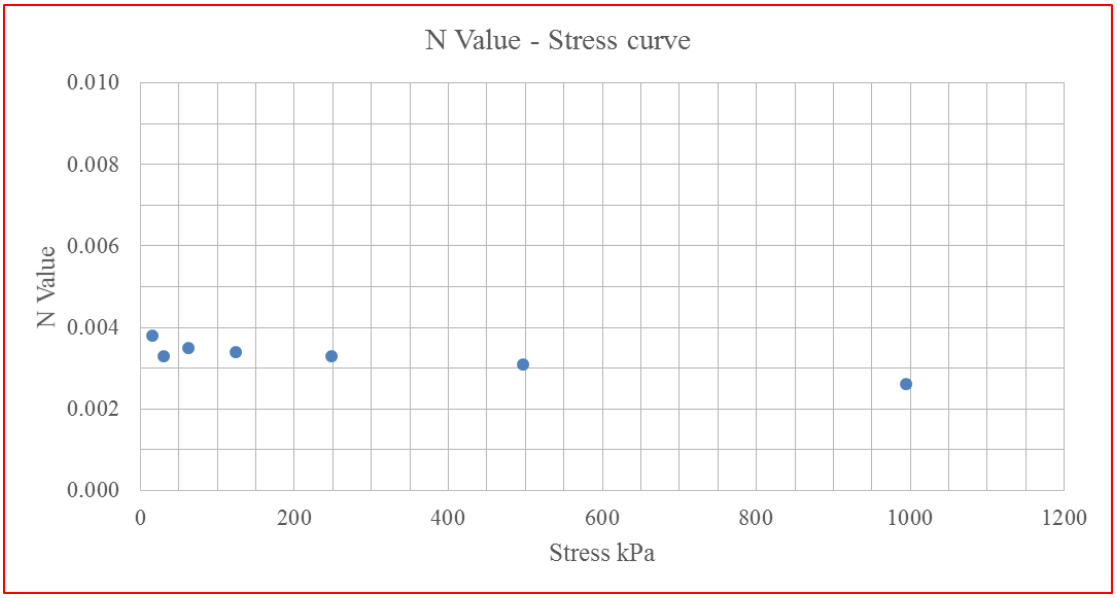

Figure 4-18. N value-stress curve of wet sand, 1D consolidation test

4.6. 1D Compression Test

1D compression test on high PI clay, low PI clay, and dry sand are described here. To remind, the specimen during 1D compression test is wrapped with several layers of plastic films to avoid drying rather than being immersed into water.

4.6.1. High PI Clay

Test results of high PI clay specimen prepared from the sample at depth 4.9~5.5m from borehole N4 were used here for illustration.

Modulus-time curves of 1D compression test on high PI clay are shown in figure 4-19 and figure 4-20. N value-stress curves of 1D compression on high PI clay are shown in figure 4-21.

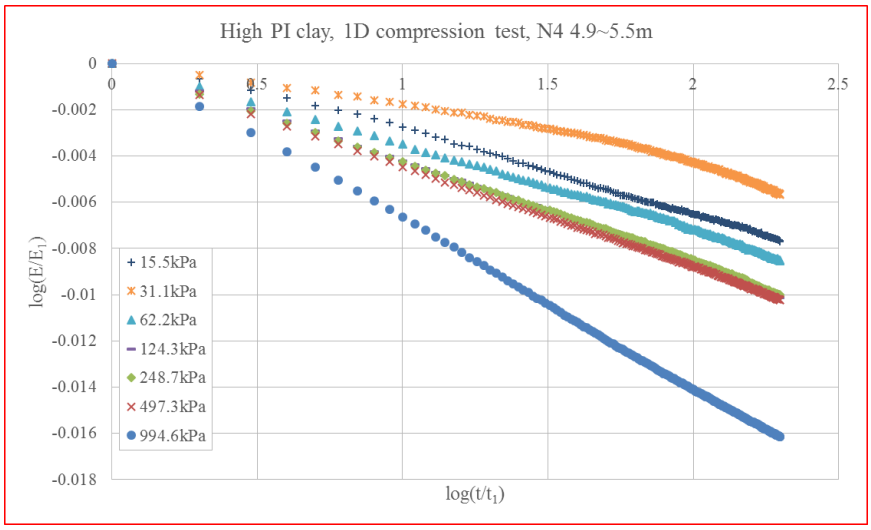

Figure 4-19. Modulus-time curves of high PI clay, 1D compression test

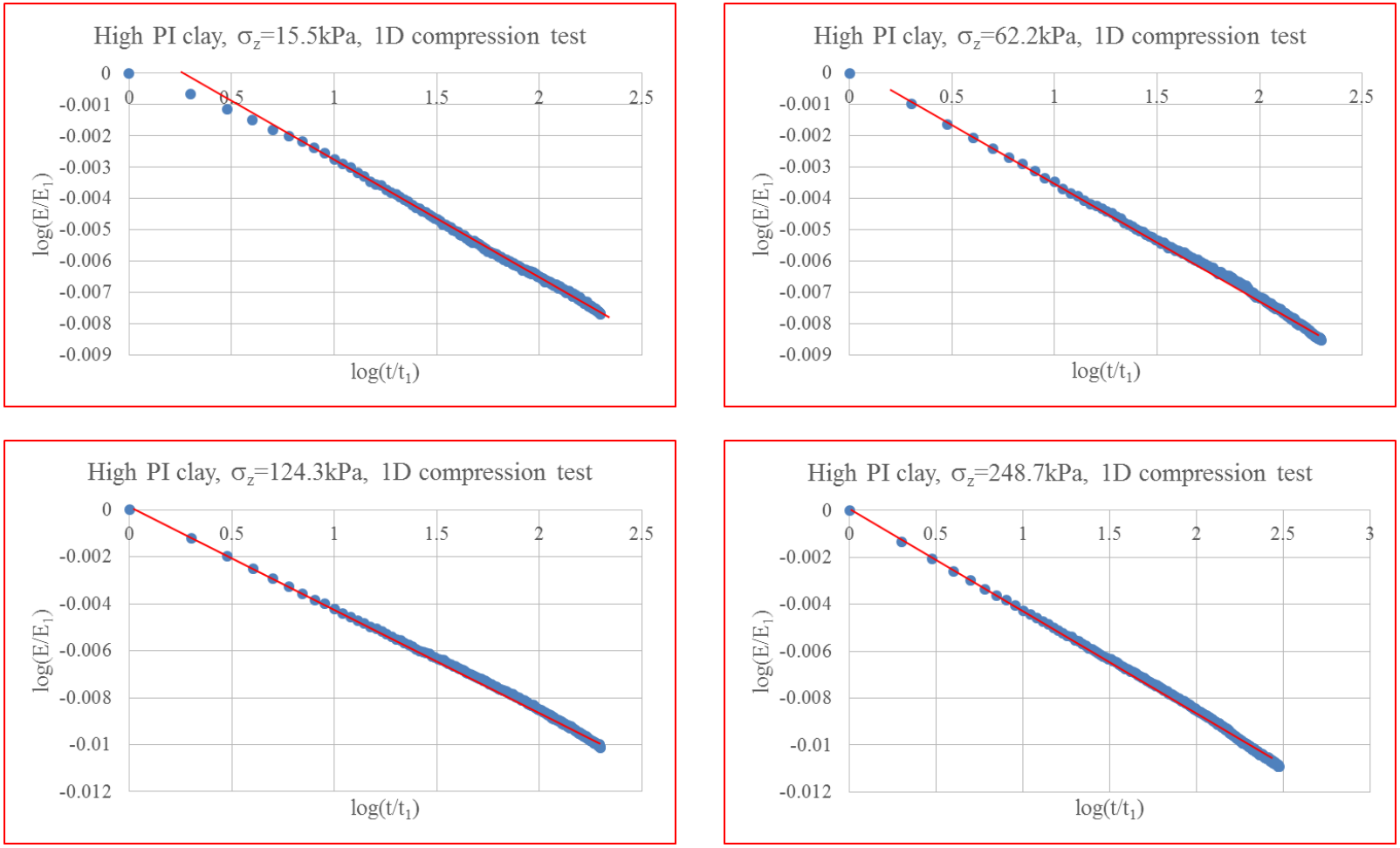

Figure 4-20. Modulus-time curves at any stress of high PI clay, 1D compression test

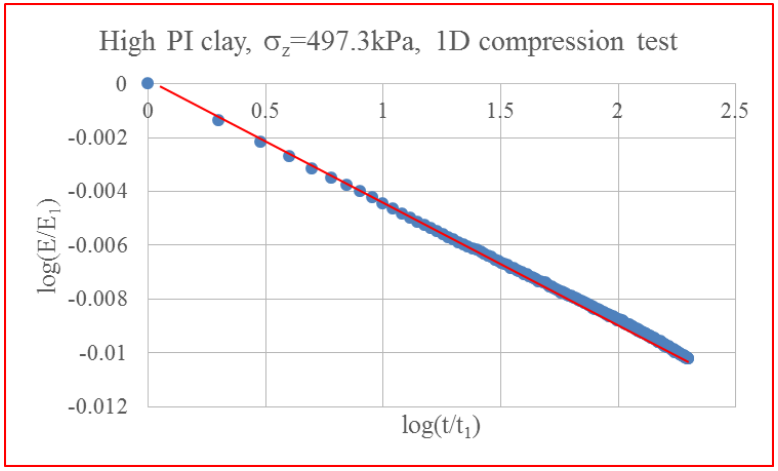

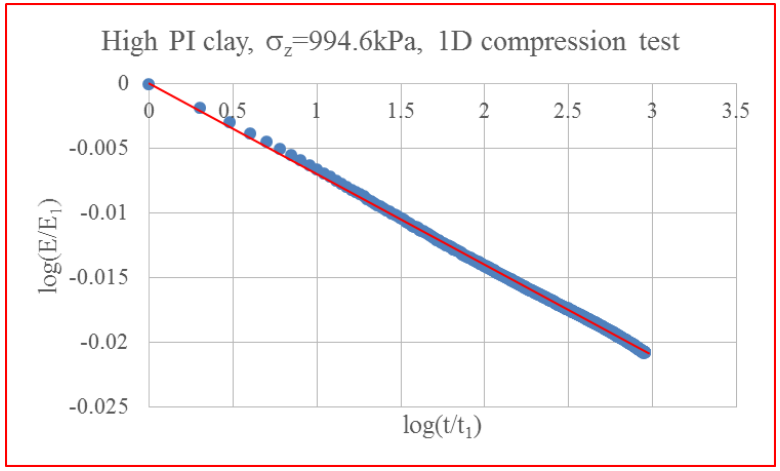

Figure 4-20 Continued

The two interesting phenomena were shown here:

- The modulus versus time curve is a straight line, no matter the loading stress is low or high, which demonstrated the proposed power law model was able to describe the time dependent behavior of high PI clay in 1D compression test;
- n_{cr} is essentially constant during all the loading stresses.

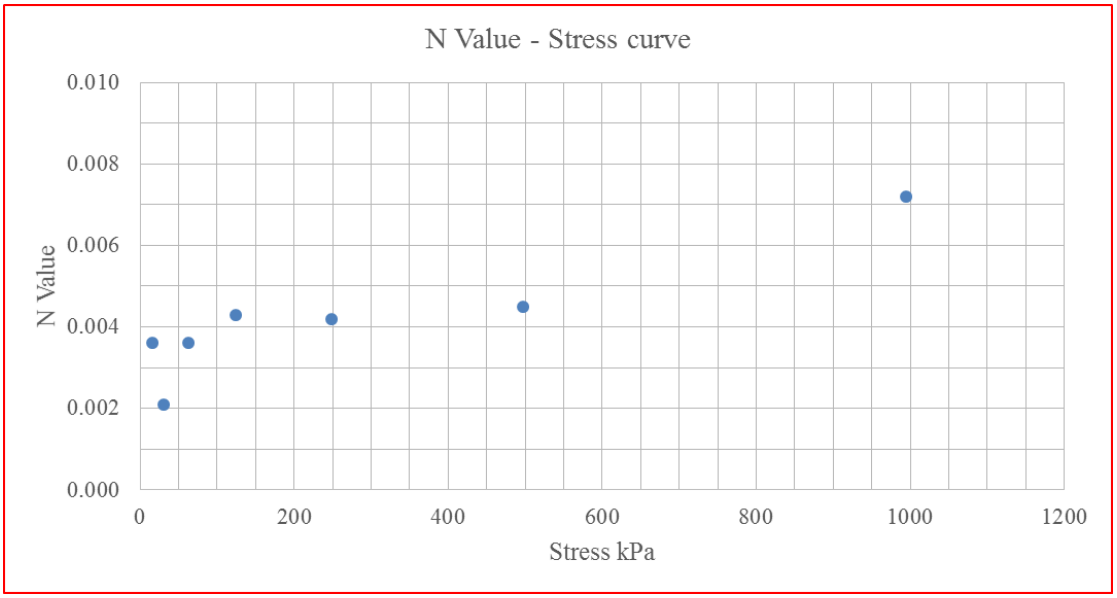

Figure 4-21. N value-stress curve of high PI clay, 1D compression test

4.6.2. Low PI Clay

Test results of one low PI clay specimen were used here for illustration.

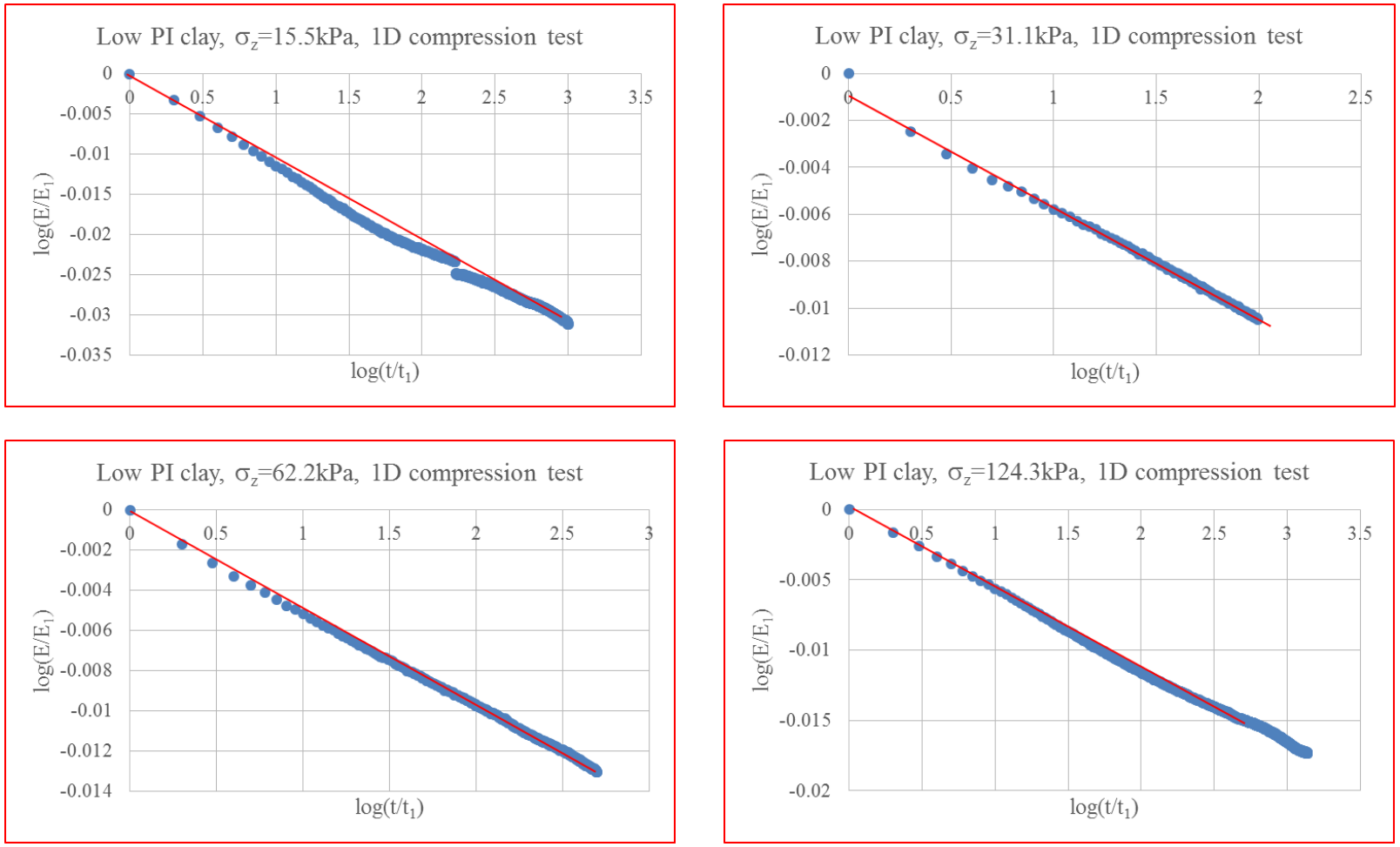

Figure 4-22. Modulus-time curves at any stress of low PI clay, 1D compression test

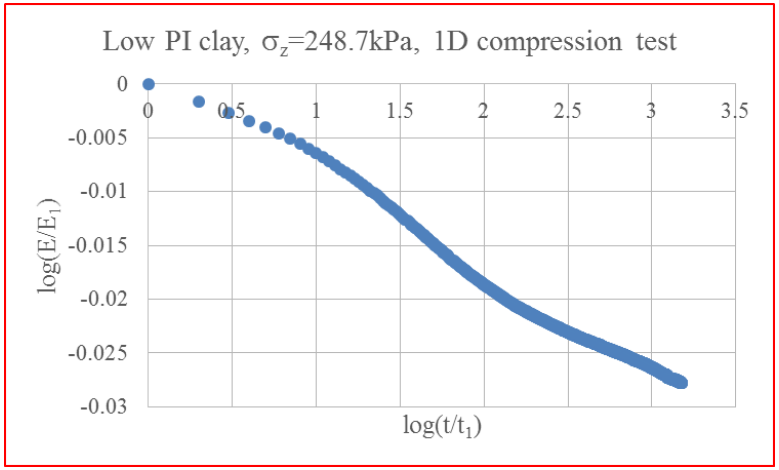

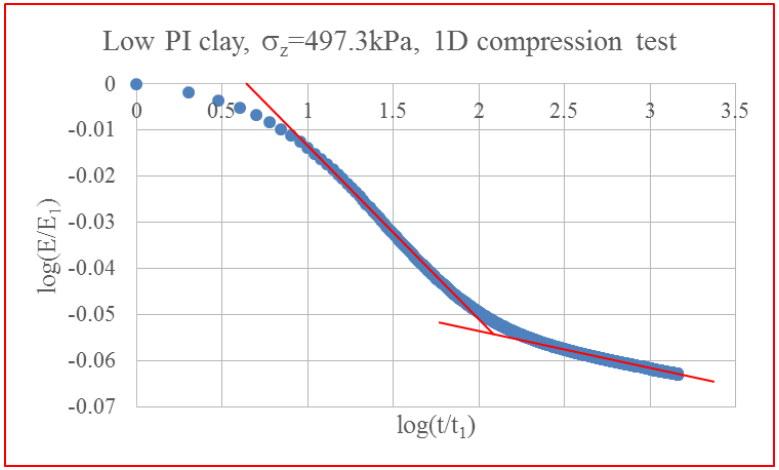

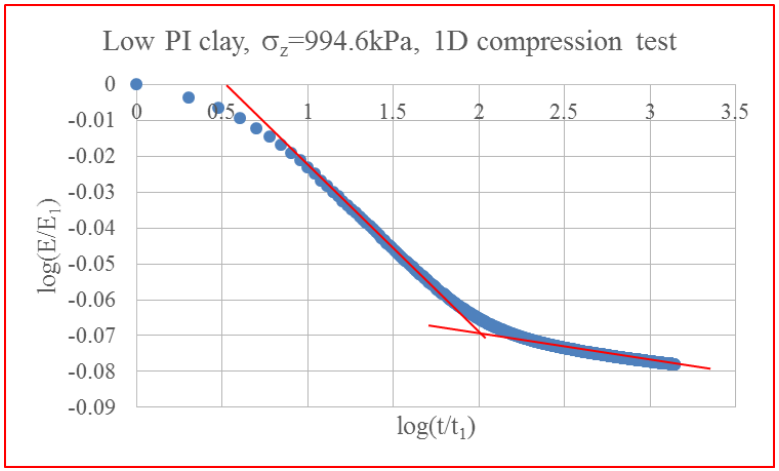

Figure 4-22 Continued

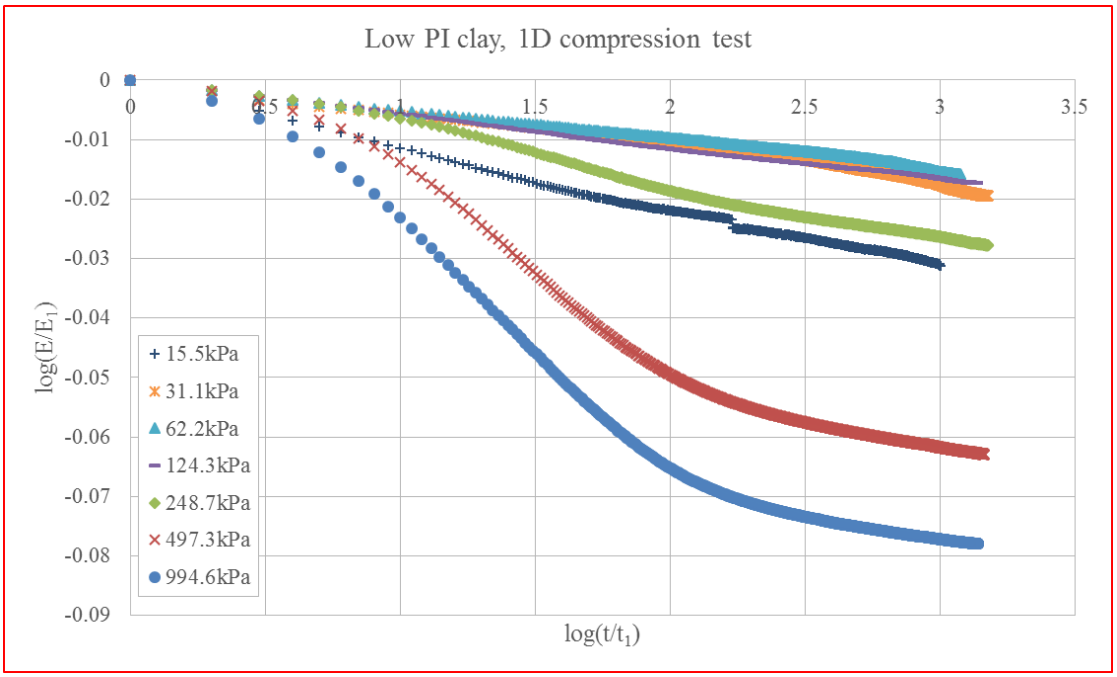

Figure 4-23. Modulus-time curves of low PI clay, 1D compression test

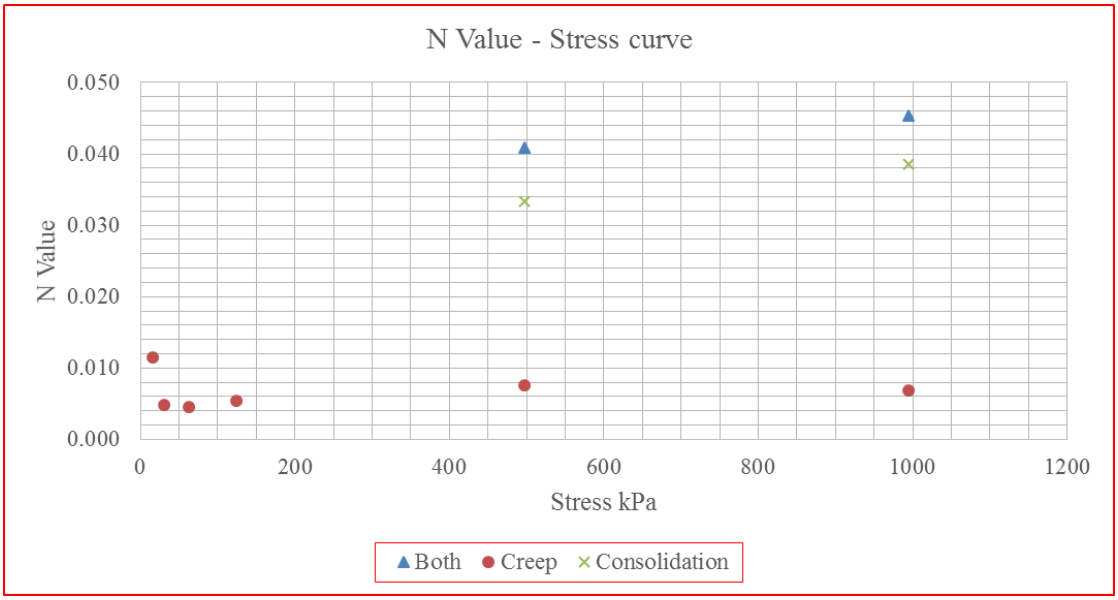

Figure 4-24. N value-stress curves of low PI clay, 1D compression test

An interesting phenomenon is that the modulus-time curve of low PI clay in 1D compression test is a straight line (creep) below 124.3kPa, but it switches to consist of two linear segments (with consolidation) over 497.3kPa (figure 4-22).

Modulus-time curves of 1D compression test on low PI clay are shown in figure 4-22 and figure 4-23. N value-stress curves of 1D compression on high PI clay are shown in figure 4-24.

The two interesting phenomena were shown here:

- The modulus versus time curve is a straight line or two linear segments, which demonstrated the proposed power law model was able to describe the time dependent behavior of low PI clay in 1D compression test;
- n_{cr} is in virtually constant during all the loading stresses.

4.6.3. Dry Sand

Test results of one dry sand specimen were used here for illustration.

Modulus-time curves of 1D compression test on dry sand are shown in figure 4-25 and figure 4-26. N value-stress curves of 1D consolidation on dry sand are shown in figure 4-27.

The two interesting phenomena were shown here:

- The modulus versus time curve is a straight line, no matter the loading stress is low or high, which demonstrated the proposed power law model was able to describe the time dependent behavior of dry sand in 1D compression test;
- n_{cr} is independent of loading stresses.

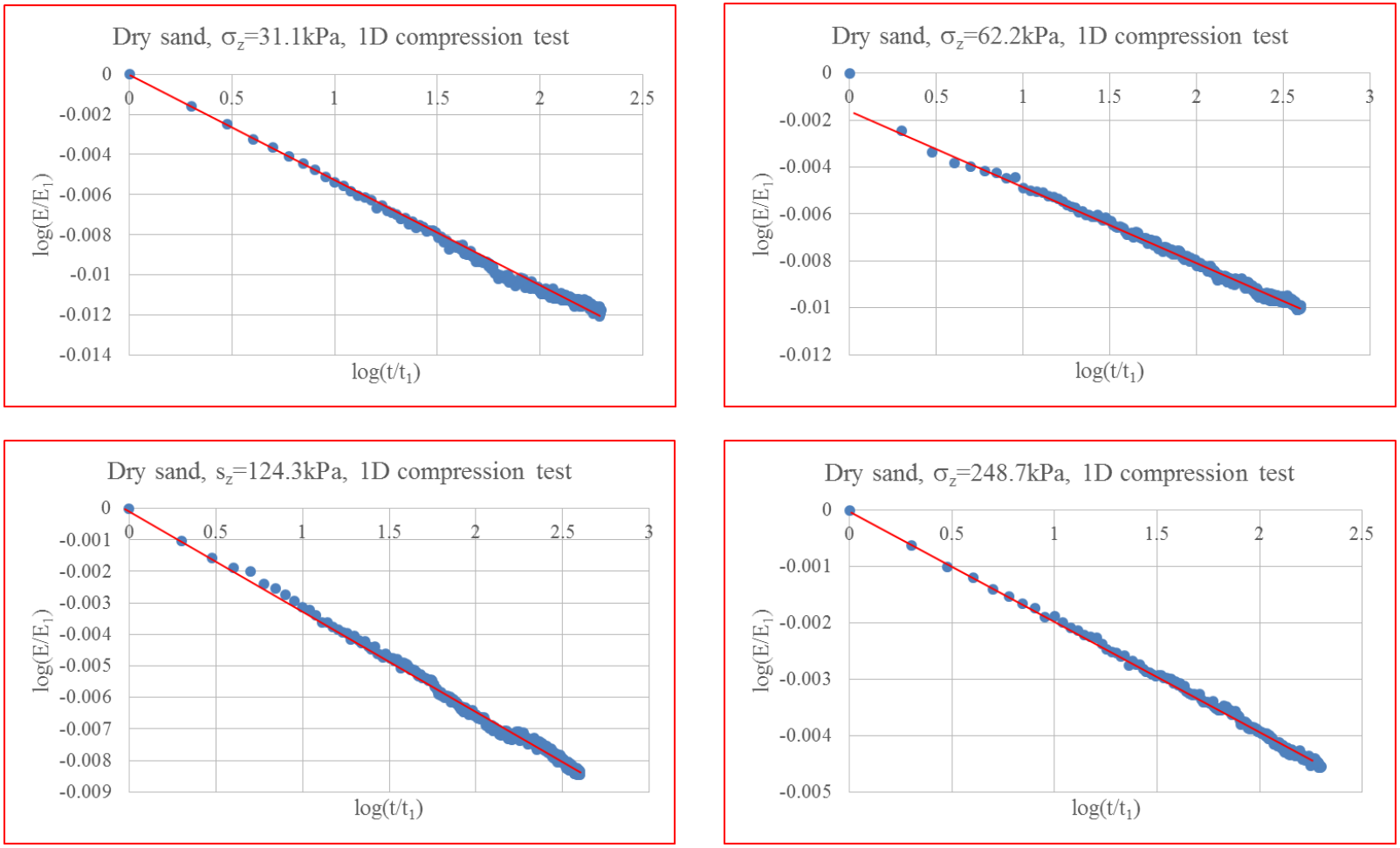

Figure 4-25. Modulus-time curves at any stress of dry sand, 1D compression test

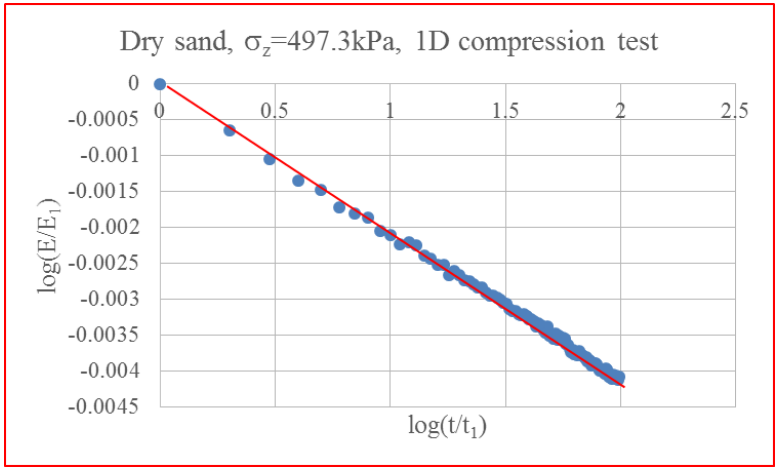

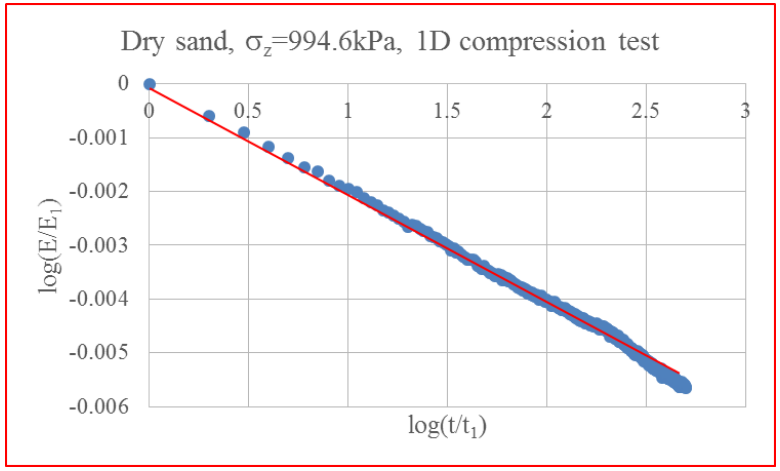

Figure 4-25 Continued

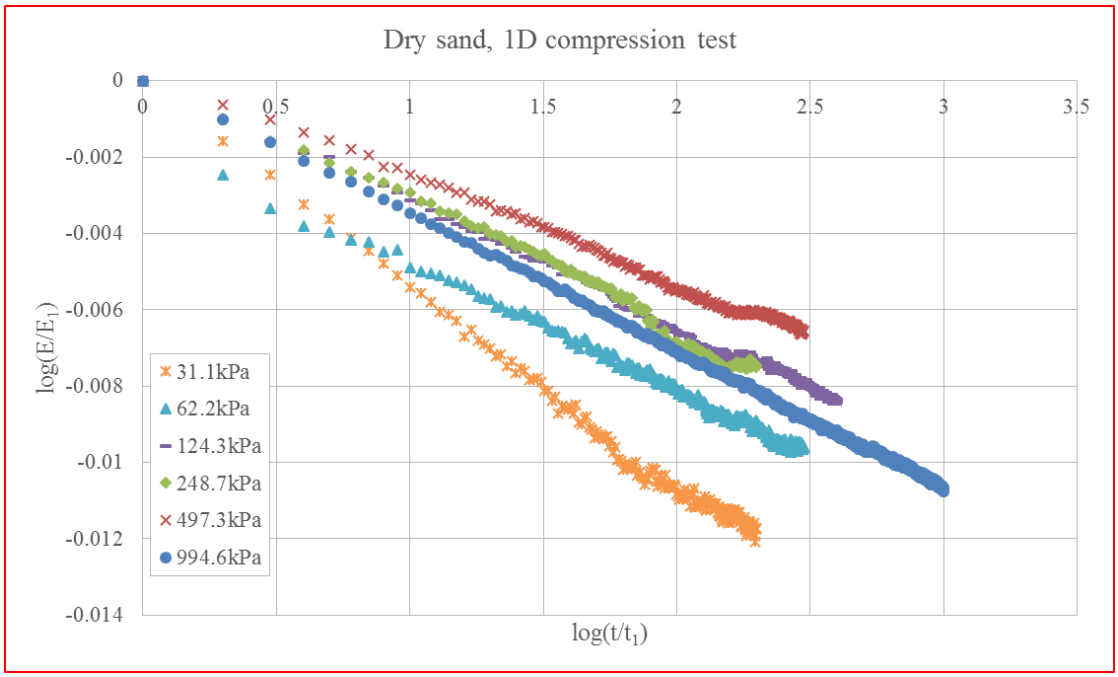

Figure 4-26. Modulus-time curves of dry sand, 1D compression test

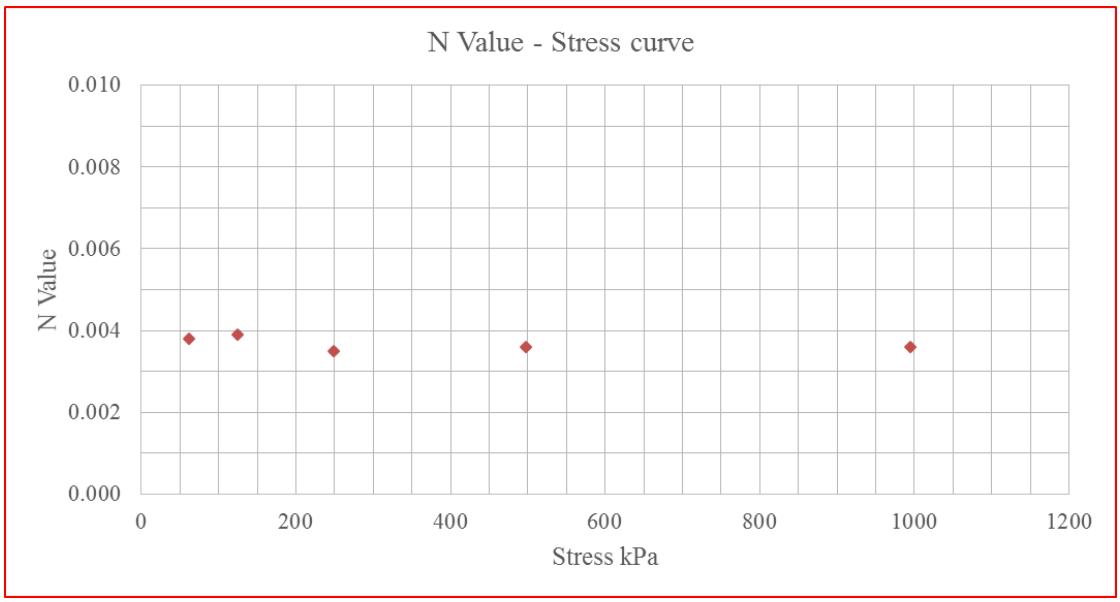

Figure 4-27. N value-stress curves of dry sand, 1D compression test

4.7. Discussion

N_{cr} from 1D consolidation test and n_{cr} from 1D compression test on three soils are compared in figure 4-28 to figure 4-30. It is worth noting that N_{cr} is very close, if not the same, in both 1D tests. The exception is n value of high PI clay from 1D consolidation test which is highly impacted by the swelling as explained before. For another test results of high PI clay (named "test 2" in figure 4-28) from 1D consolidation, n value is closer to that from 1D compression test, though it is also impacted by swelling.

The "same" N_{cr} from both 1D tests gives the support to extend the second linear segment on figure 4-7 to separate deformation caused by creep from deformation caused by excess pore pressure dissipation (see details in section 4.4). It also demonstrate that deformation caused by creep should be taken into account during the whole consolidation process rather than only the secondary compression.

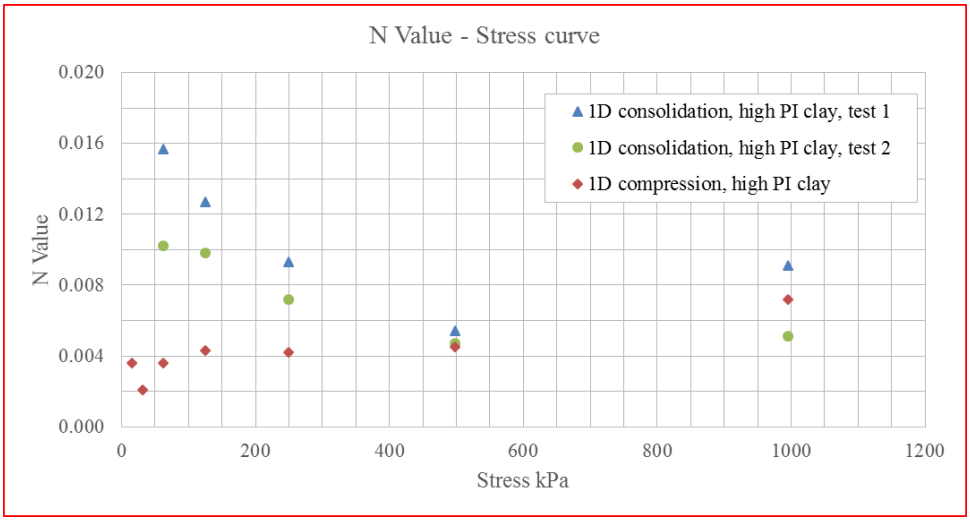

Figure 4-28. N_{cr} from 1D consolidation versus N_{cr} from 1D compression, high PI clay

Another tricky thing should be mentioned here is that the definition of creep is deformation under constant effective stress, while effective stress is increasing during the primary consolidation. The way to separate n_{cr} from n_{both} seems to be in conflict with the definition of creep. However, from figure 4-28 to figure 4-30, it is found that n value is independent of stress level, which S_1 in the power law model is dependent of stress level (i.e., the higher stress level, the higher S_1). Therefore, n_{cr} could be separated from n_{both}.

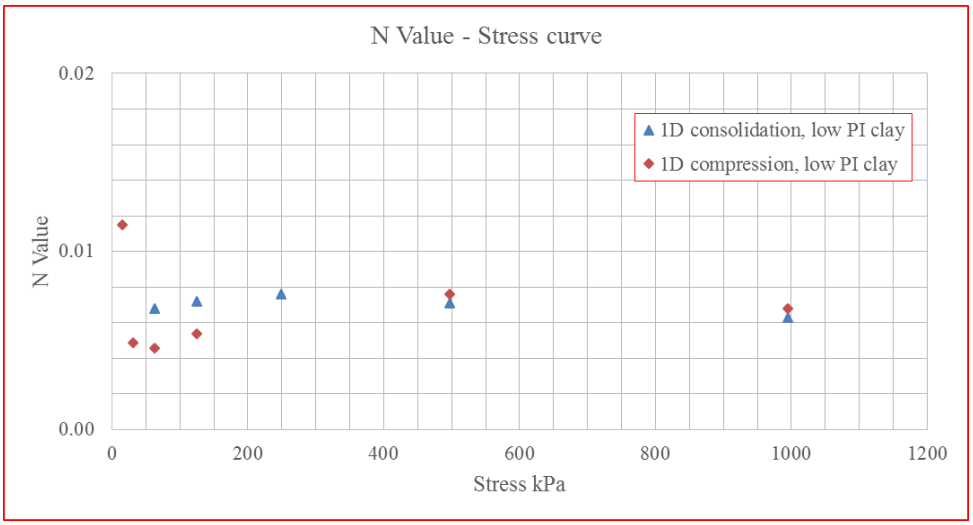

Figure 4-29. N_{cr} from 1D consolidation versus N_{cr} from 1D compression, low PI clay

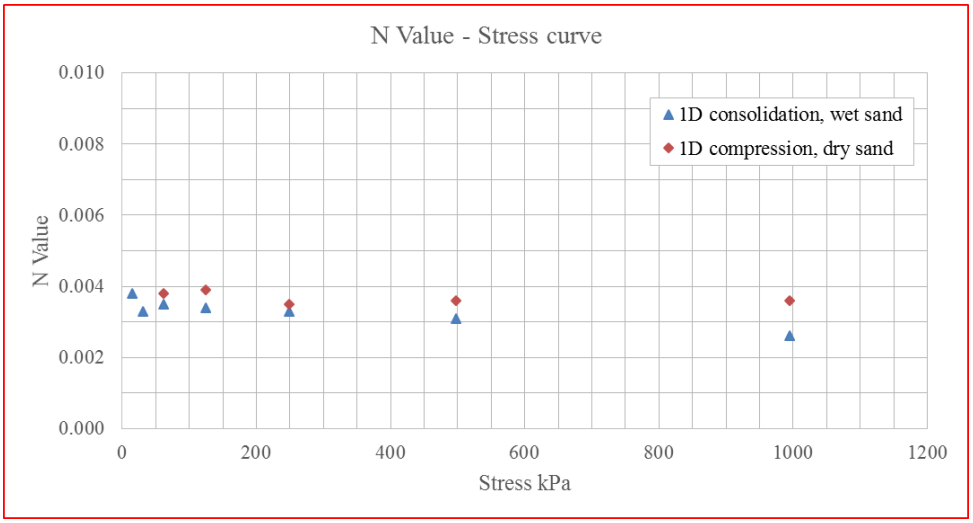

Figure 4-30. N_{cr} from 1D consolidation versus N_{cr} from 1D compression, sand

For cases that include both creep and consolidation, the N_{cr}/N_{con}-stress curve is plotted in figure 4-31. It shows a significant contribution to deformation is made by creep at low stresses, even though consolidation is the dominant part in the primary consolidation.

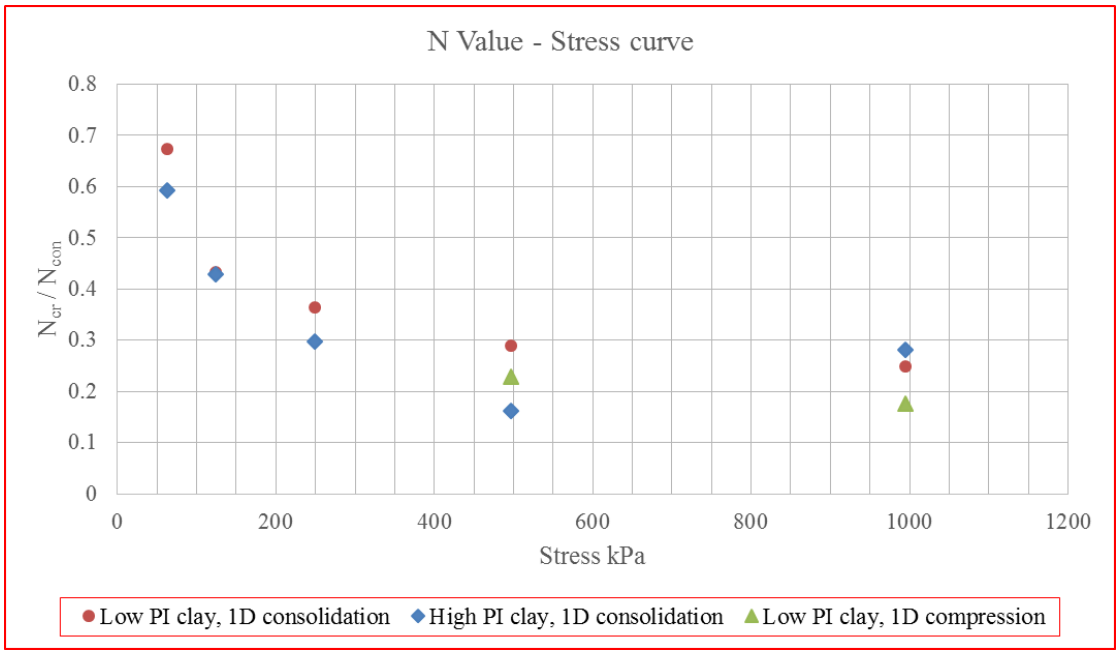

Figure 4-31. N_{cr}/N_{con} versus stress curves in both 1D tests

4.8. Prediction

To rebuild or predict the deformation in lab and in field, the time corresponding to the end to primary consolidation t_{eop} is in need. It is the time at the intersection by extrapolating two linear segments (figure 4-32). And it is found that the value of t_{eop} is very close to, if not same to, the value of t_{eop} gotten from semi-log of strain-time curve (figure 4-33), which follows the ASTM D2435/D2435M - 11.

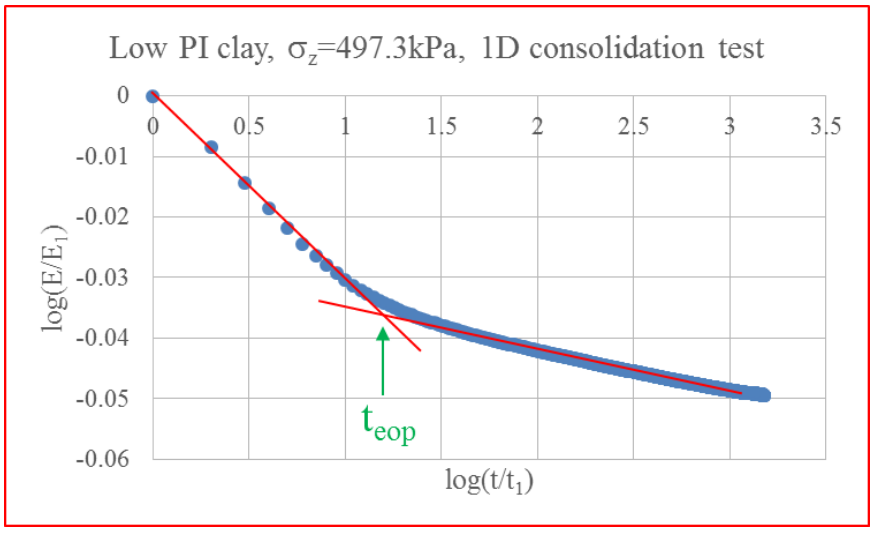

Figure 4-32. t_{eop} from power law model

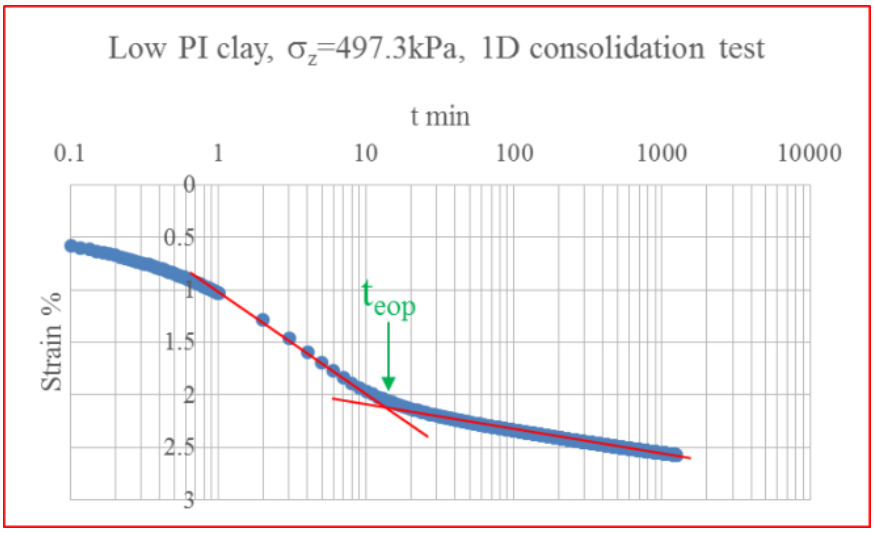

Figure 4-33. t_{eop} from ASTM standard

4.8.1. Laboratory Prediction

Given s_1 (or E_1), n_{both}, n_{cr}, and t_{eop}, the strain-time curve of any loading stress in the lab can be rebuilt with equation 4-4, and compared to the original measured data.

$$\frac{s}{s_1} = \left(\frac{t}{t_1}\right)^{n_{both}} \qquad t \le t_{eop}$$
$$\frac{s}{s_1} = \left(\frac{t}{t_{eop}}\right)^{n_{cr}} \left(\frac{t_{eop}}{t_1}\right)^{n_{both}} \qquad t \ge t_{eop} \tag{4-4}$$

The measured versus rebuilt strain-time curves of high PI clay, low PI clay and wet sand in 1D consolidation test are plotted in the left of figure 4-34; the measured versus rebuilt strain-time curves of high PI clay, low PI clay and dry sand in 1D compression test are plotted in the right of figure 4-34. The rebuilt data are in excellent agreement with the measured data, which demonstrates the proposed power law model is feasible to represent time dependent behavior of soils in 1D consolidation test and 1D compression test.

4.8.2. Field Prediction – Fictitious Example

A fictitious example is presented to illustrate the prediction of field deformation by the proposed power law model, also compared to the prediction of field deformation by the conventional method.

The thickness of a soil layer in the field is 1.9m (100 times the thickness in 1D consolidation test), and the soil is assumed to be exactly identical to the low PI clay in this research. The above and below layer of the analyzed soil layer are both permeable.

The soil is subject to a stress increment from 248.7kPa to 497.3kPa. The long-term deformation of the soil in the field is predicted with the conventional method and power law model, respectively.

Conventional method

The final increment of settlement (also strain) because of the stress increment from 248.7kPa to 497.3kPa is calculated with equation 4-5:

$$\Delta\varepsilon = \frac{e_1 - e_2}{1 + e_0}$$
$$\Delta H_{field} = \frac{e_1 - e_2}{1 + e_0} H_{field} \quad (4\text{-}5)$$

Where,

e_1 e_2: Void ratio corresponding to 248.7kPa and 497.3kPa, respectively, obtained from e-logP curve based on 1D consolidation test in the laboratory;

e_0: Initial void ratio, obtained from e-logP curve based on 1D consolidation test in the laboratory;

H_{field}: Thickness of soil layer in the field, 1.9m herein;

ΔH_{field}: Final increment of settlement;

$\Delta\varepsilon$: Final increment of strain.

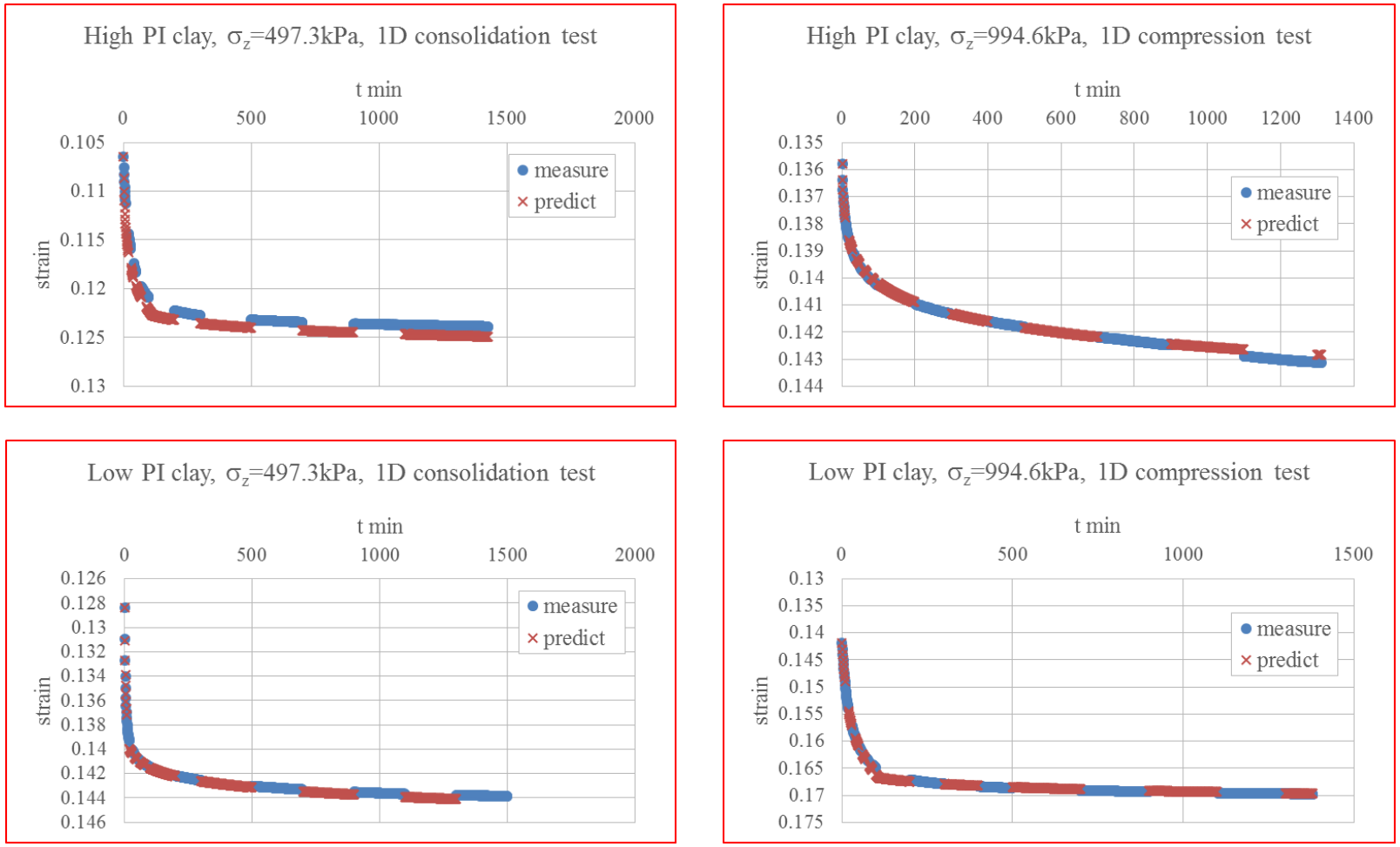

Figure 4-34. Rebuilt strain-time curves with power law model versus measured strain-time curves

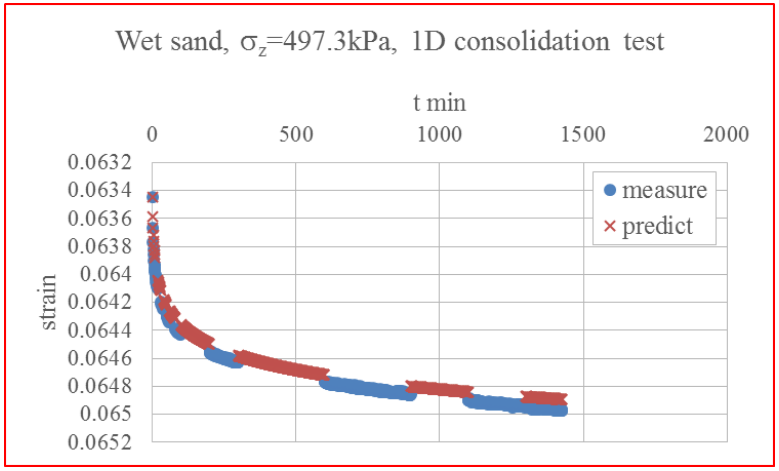

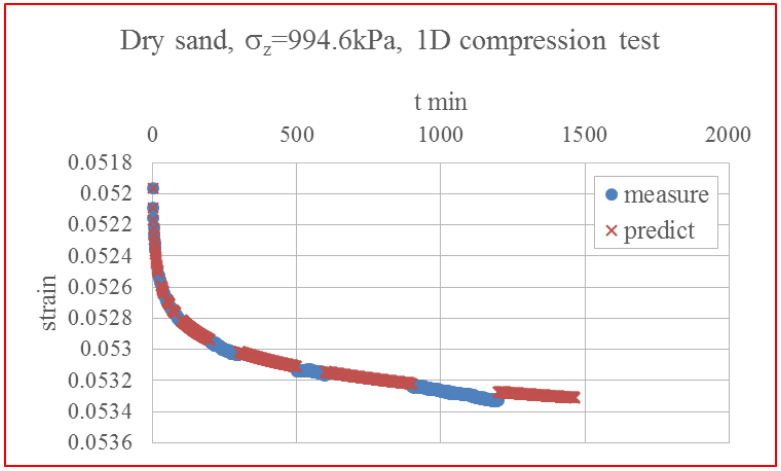

Figure 4-34 Continued

The average degree of consolidation in the soil layer is approximated with the equation 4-6, when the value is no less than 30%:

$$\bar{U} = 1 - \frac{8}{\pi^2} \exp\left(-\frac{\pi^2}{4} \frac{c_v \cdot t}{H_{field}^2} \right) \quad (4\text{-}6)$$

Where,

$\bar{U}$: Average degree of consolidation;

H_{field} : Length of drainage path in the field, which is half of thickness of soil layer in the field, 0.95m in this example;

c_v : Coefficient of consolidation, obtained from strain-time (semi-log scales) curve based on 1D consolidation test in the laboratory.

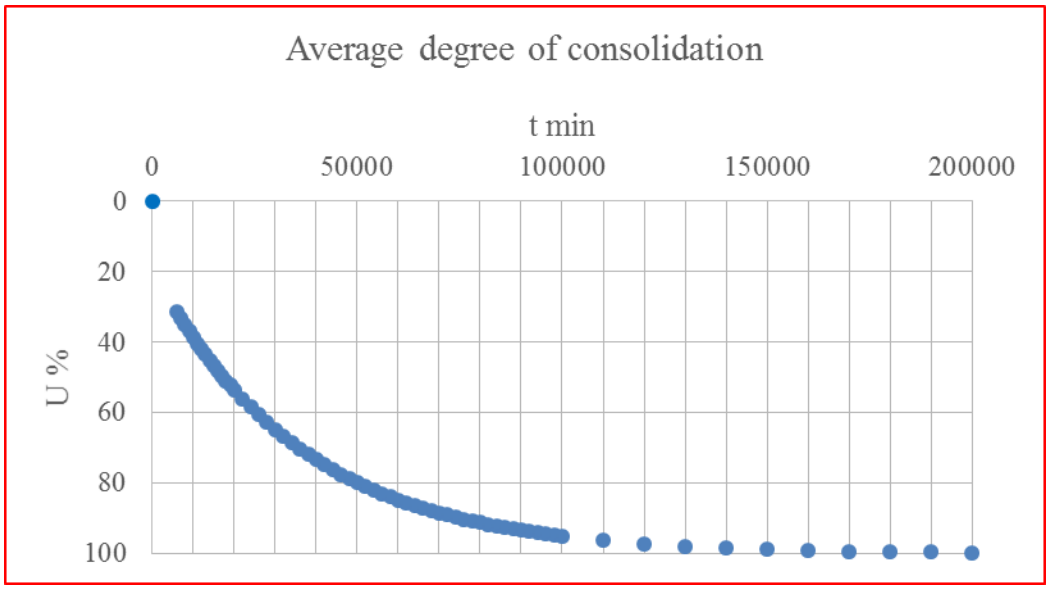

Figure 4-35. Average degree of consolidation with time

Combining equation 4-6 (figure 4-35) and equation 4-5, will yield the long-term deformation prediction by the conventional method (figure 4-36).

Power law model

The long-term deformation in the field is forecasted in a similar way as the prediction in the lab, given $(E_1)_{field}$ (or $(s_1)_{field}$), $(n_{both})_{field}$, $(n_{cr})_{field}$, and $(t_{eop})_{field}$.

While,

$$\frac{(t_{eop})_{field}}{(t_{eop})_{lab}} = \frac{\frac{(T_v)_{field} \cdot H_{field}^2}{(c_v)_{field}}}{\frac{(T_v)_{lab} \cdot H_{lab}^2}{(c_v)_{lab}}} = \left(\frac{H_{field}}{H_{lab}}\right)^2 \cdot \frac{(c_v)_{lab}}{(c_v)_{field}} \cdot \frac{(T_v)_{field}}{(T_v)_{lab}} = K \cdot \left(\frac{H_{field}}{H_{lab}}\right)^2 \quad (4\text{-}7)$$

In this example,

$$\frac{(t_{eop})_{field}}{(t_{eop})_{lab}} = K \cdot \left(\frac{H_{field}}{H_{lab}}\right)^2 = 1 \cdot \left(\frac{1.9\,\mathrm{m}/2}{1.9cm/2}\right)^2 = 10000 \quad (4\text{-}8)$$

Where,

$(t_{eop})_{lab}$: Time corresponding to the end to primary consolidation in the laboratory;

$(t_{eop})_{field}$: Time corresponding to the end to primary consolidation in the field;

H_{field}: Length of drainage path in the field, which is half of thickness of soil layer in the field, 0.95m in this example;

H_{lab}: Length of drainage path in the laboratory, which is half of thickness of specimen in 1D consolidation test, i.e., 0.95cm.

As can be seen in the power law model, n value is largely related with E_1 and t_1. $(E_1)_{field}$ is to be chosen randomly by the engineering designer to forecast the long-term deformation. However, if $(E_1)_{field}$ is assumed to be equal to $(E_1)_{lab}$, in this case, it will have,

$$\left(t_1\right)_{field} = \left(t_1\right)_{lab} \cdot \frac{\left(t_{eop}\right)_{field}}{\left(t_{eop}\right)_{lab}} = 10000\,\text{min} \approx 1\,\text{w} \tag{4-9}$$

That is, $(E_1)_{field}$ is no longer corresponding to t=1min in the field, instead, it corresponds to the value calculated with the equation 4-9.

Assuming:

$$\begin{aligned} \left(n_{both}\right)_{field} &= \left(n_{both}\right)_{lab} \\ \left(n_{cr}\right)_{field} &= \left(n_{cr}\right)_{lab} \end{aligned} \tag{4-10}$$

The long-term deformation prediction in the field (figure 4-36) is readily obtained by multiplying the x-axis of long-term deformation prediction in the lab (figure 4-34) with the factor $(t_{eop})_{field}/(t_{eop})_{lab}$.

The agreement between the prediction based on conventional method and that based on power law model is very good in figure 4-36, which demonstrates the proposed power law model is feasible to apply in the practice.

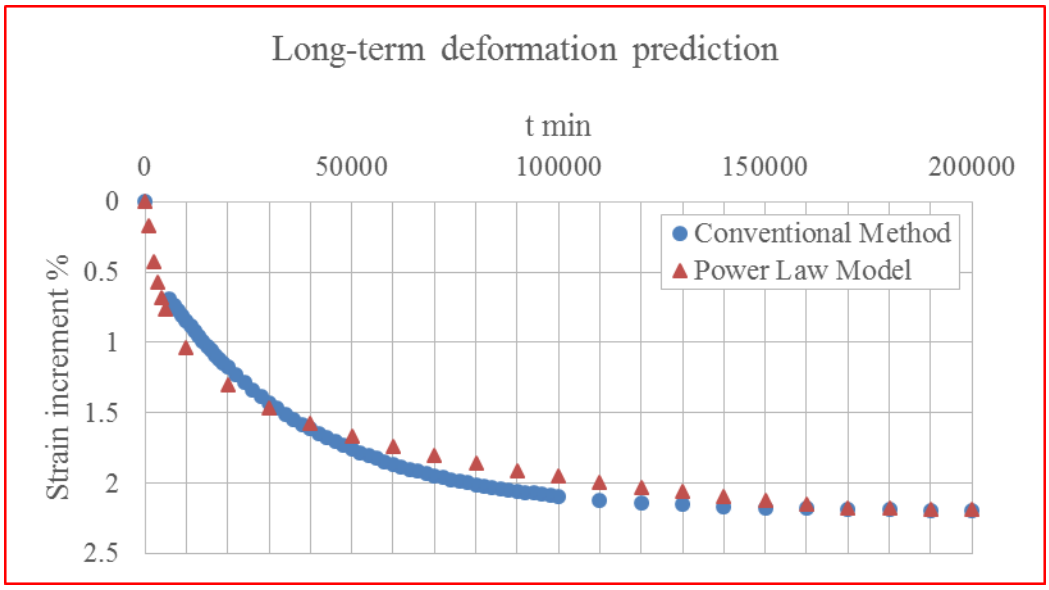

Figure 4-36. Long-term deformation prediction in practice

4.8.3. Field Prediction – San Jacinto Monument

The San Jacinto monument was built on November 1936 and the settlement of the monument has been recorded since then. The data is adopted here to verify the application of proposed power law model in practice. More details of San Jacinto monument could be found from Briaud et al. (2007, 2015).

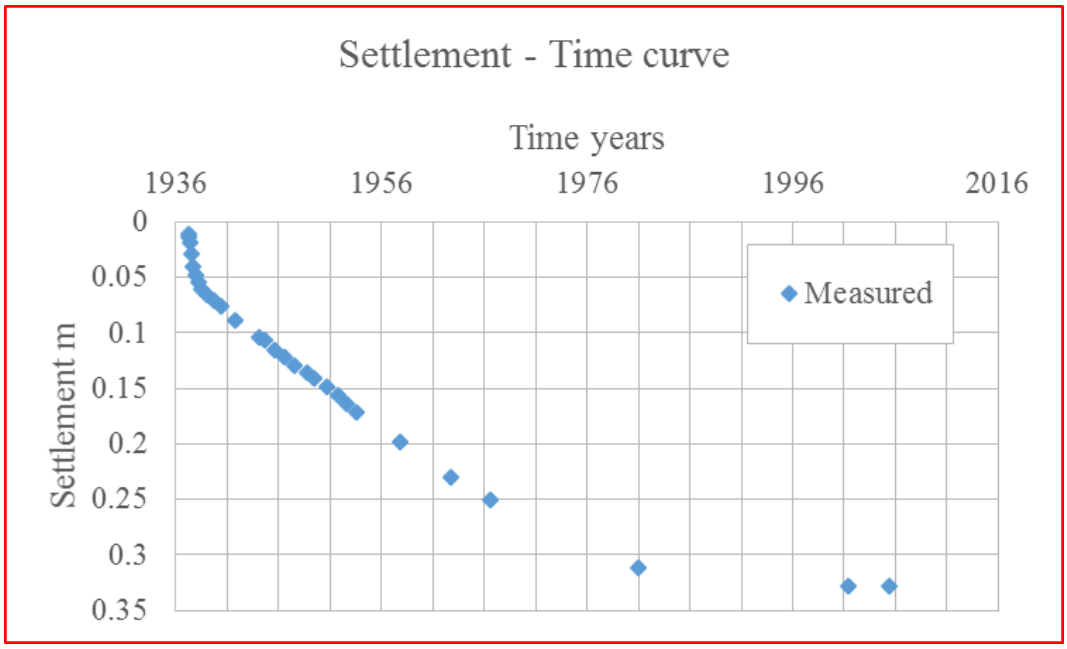

Figure 4-37. Measured settlement of San Jacinto monument, after Briaud et al. (2007)

The measured settlement of San Jacinto monument is plotted in figure 4-37, and the date of these measurements is tabulated in table 4-1. It should be pointed out that unfortunately, so few points are recorded after 1953, specifically around 1977.

If the first measurement (i.e., corresponding to date February 10, 1937, bold red marked in table 4-1) is taken as s_1 in power law model, the measured settlement-time curve will be as shown in figure 4-38. The curve is consisted of four linear segments, and there are reasons for inconsistence among slopes of all linear segments. The first linear segment is corresponding to the phase of construction, which lasts from November 1936 to November 1937, and the net pressure on soil keeps increasing (figure 4-39). Because the stress is not constant, a new s_1 is taken at the date corresponding to end of

construction (bold green marked in table 4-1), though it just shifts the origin of axes from the beginning of first linear segment to the end of first linear segment, while slopes (i.e., n value) of the remaining linear segments won't change.

Table 4-1. Date to measure settlement of San Jacinto Monument

	Date	Time (yr)	Note
1936	11/10/36	0	1 year constrution
1937	**2/10/37**	**0.25**	
1937	3/17/37	0.35	
1937	5/05/37	0.47	
1937	6/05/37	0.6	
1937	8/13/37	0.76	
1937	**11/03/37**	**0.98**	
1938	2/11/38	1.25	
1938	5/20/38	1.53	
1938	11/21/38	2	
1939	9/07/39	2.83	
1940	5/11/40	3.5	
1941	8/18/41	4.77	Groundwater depletion 1941~1977
1943	12/28/43	7.13	
1944	8/01/44	7.73	
1945	7/11/45	8.67	
1946	6/27/46	9.63	
1947	6/19/47	10.61	
1948	9/02/48	11.81	
1949	5/31/49	12.56	
1950	9/04/50	13.82	
1951	9/03/51	14.82	
1952	7/15/52	15.68	
1953	6/04/53	16.57	
1957	9/06/57	20.82	
1962	8/28/62	25.8	
1966	7/15/66	29.59	
1980	11/05/80	43.99	
2001	5/01/01	64	
2005	5/01/05	68.25	

Briaud et al. (2015) claimed that the inconsistence of slopes (i.e., n value) is caused by groundwater level, however, data is missing from 1936 to 1964 to support the view (figure 4-40). With continuous searching, groundwater level from 1990 to 2008 (figure 4-41) is found in the report published by Konikow (2013). The groundwater level is steadily lowering down, which is in excellent agreement with the trend of settlement (figure 4-38).

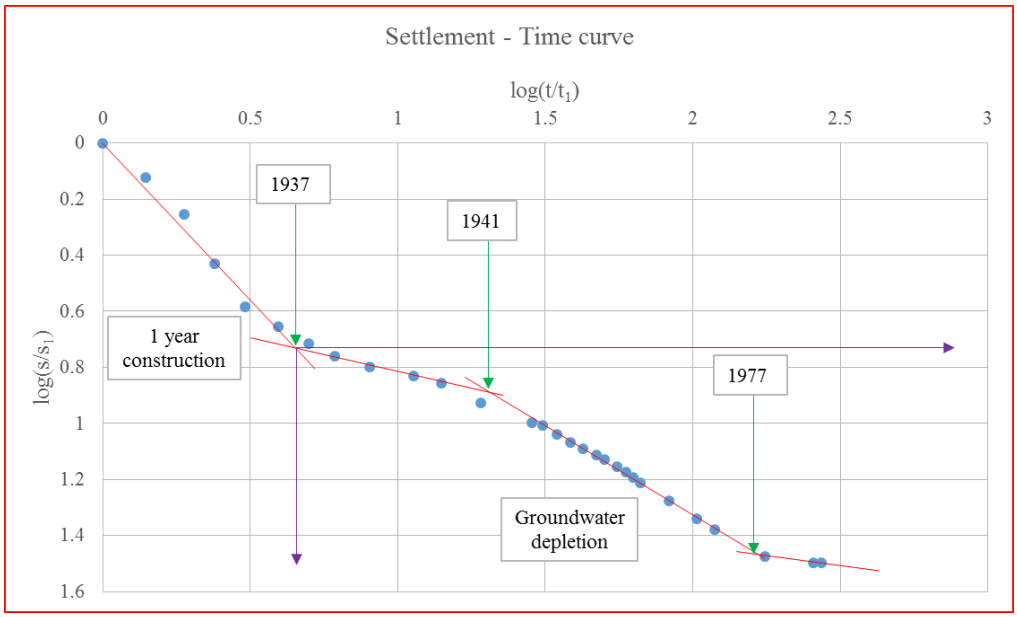

Figure 4-38. Settlement-time curve (log-log scales) of San Jacinto monument

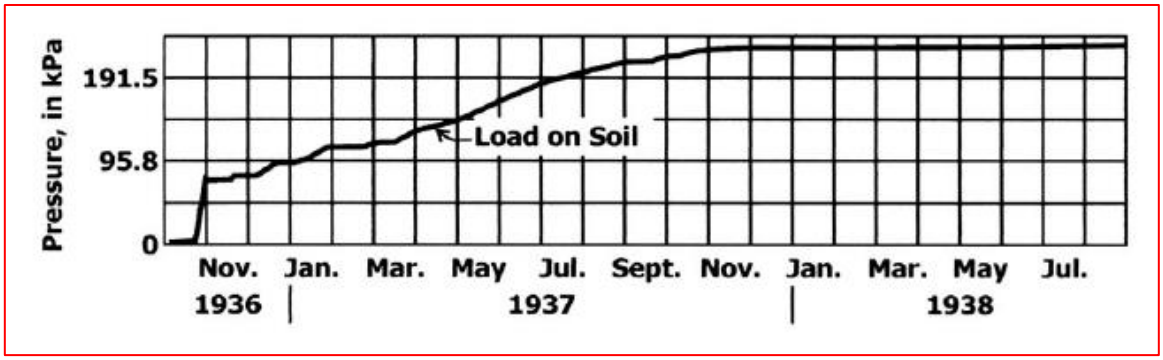

Figure 4-39. Increase in net pressure during construction (Briaud et al., 2007)

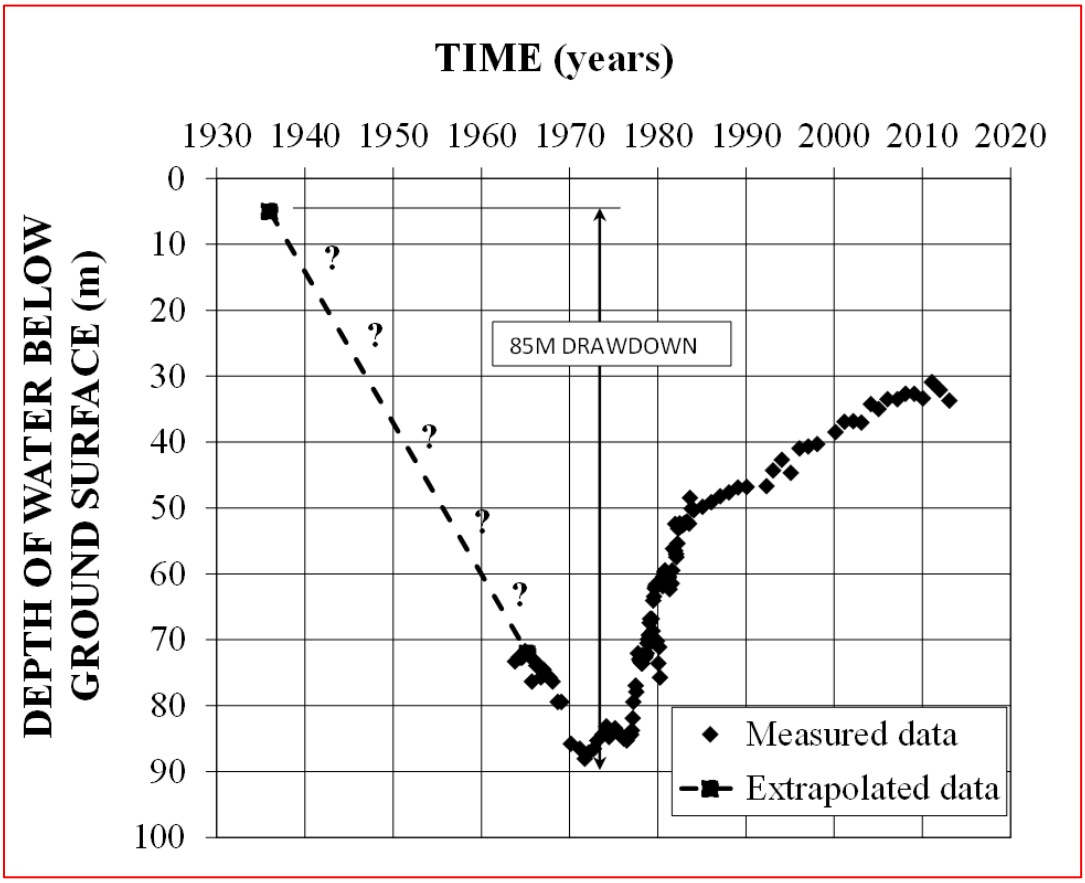

Figure 4-40. Groundwater level (Briaud et al., 2015)

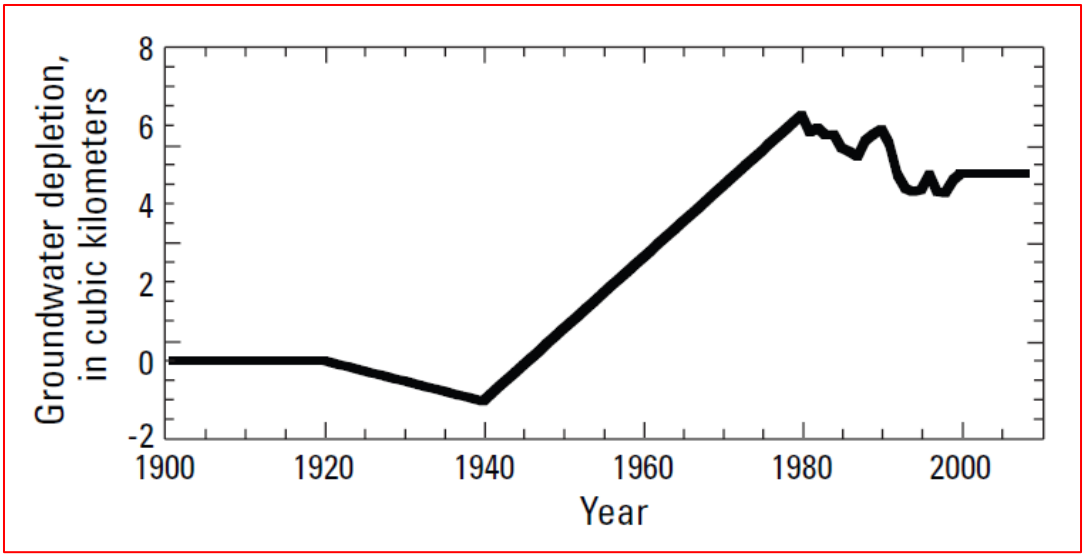

Figure 4-41. Cumulative groundwater depletion in Houston area (Konikow, 2013)

N value is readily obtained from 1937 to 2005 (figure 4-42 to figure 4-44), and the settlement-time curve is easily predicted with power law model in figure 4-45. The agreement is excellent, which demonstrates the proposed power law model is feasible to predict the long-term deformation in practice.

Two points should be noted: a), n value is corresponding to primary consolidation (i.e., n_{both}) because on one hand as long as groundwater keeps lowering down, the primary consolidation won't end, on the other hand it will take more than 50 years for primary consolidation (rough estimation) when groundwater level is stabilized; b), only two or three recorded data is available after 1977, thus, n value is not accurately acquired. It is though that n value from 1937~1944 will be close to n value from 1977~2005, which could be verified if more data is collected.

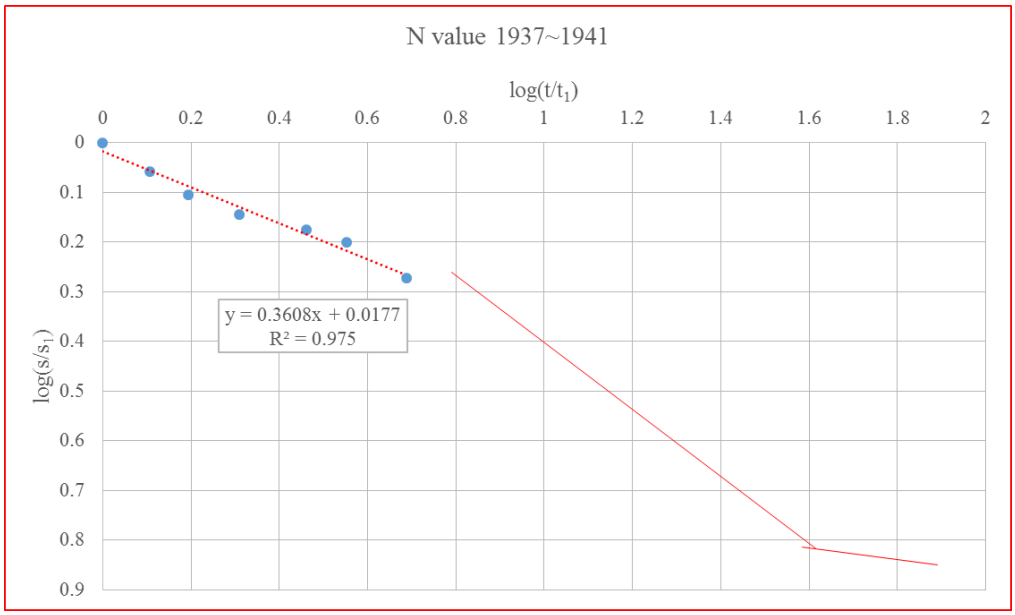

Figure 4-42. N value, 1937~1941, San Jacinto monument

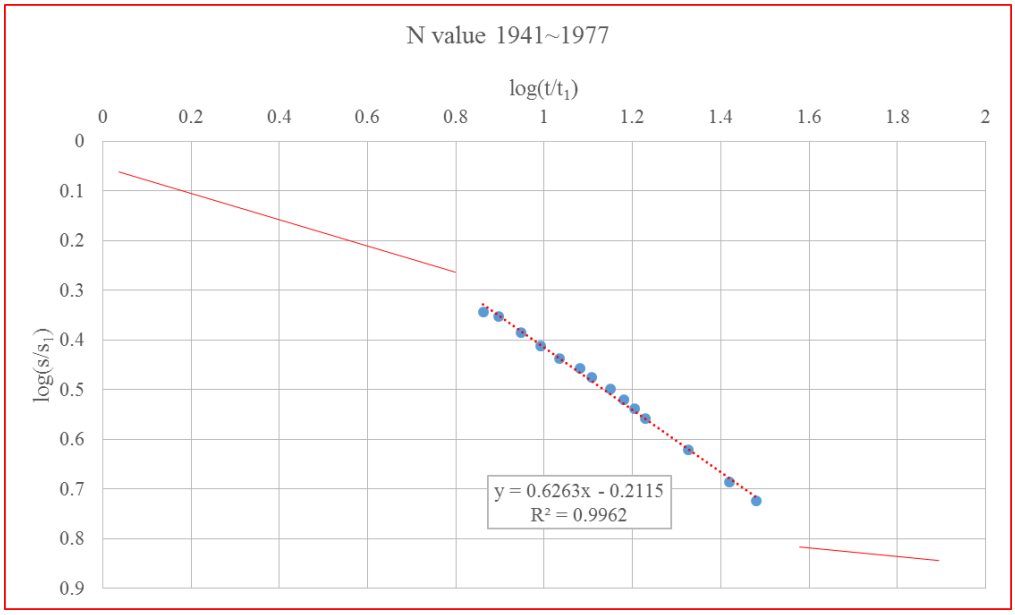

Figure 4-43. N value, 1941~1977, San Jacinto monument

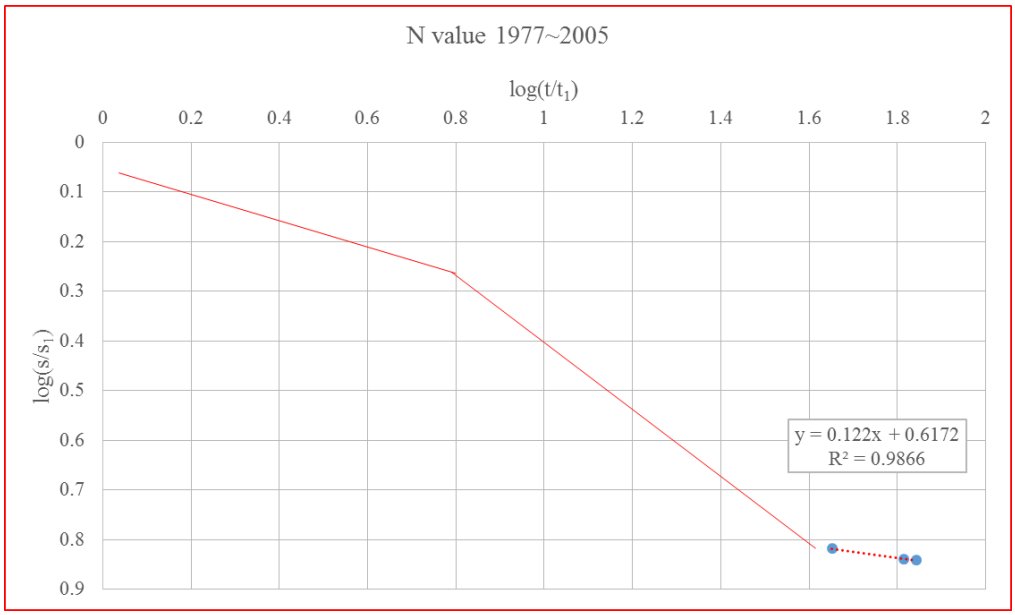

Figure 4-44. N value, 1977~2005, San Jacinto monument

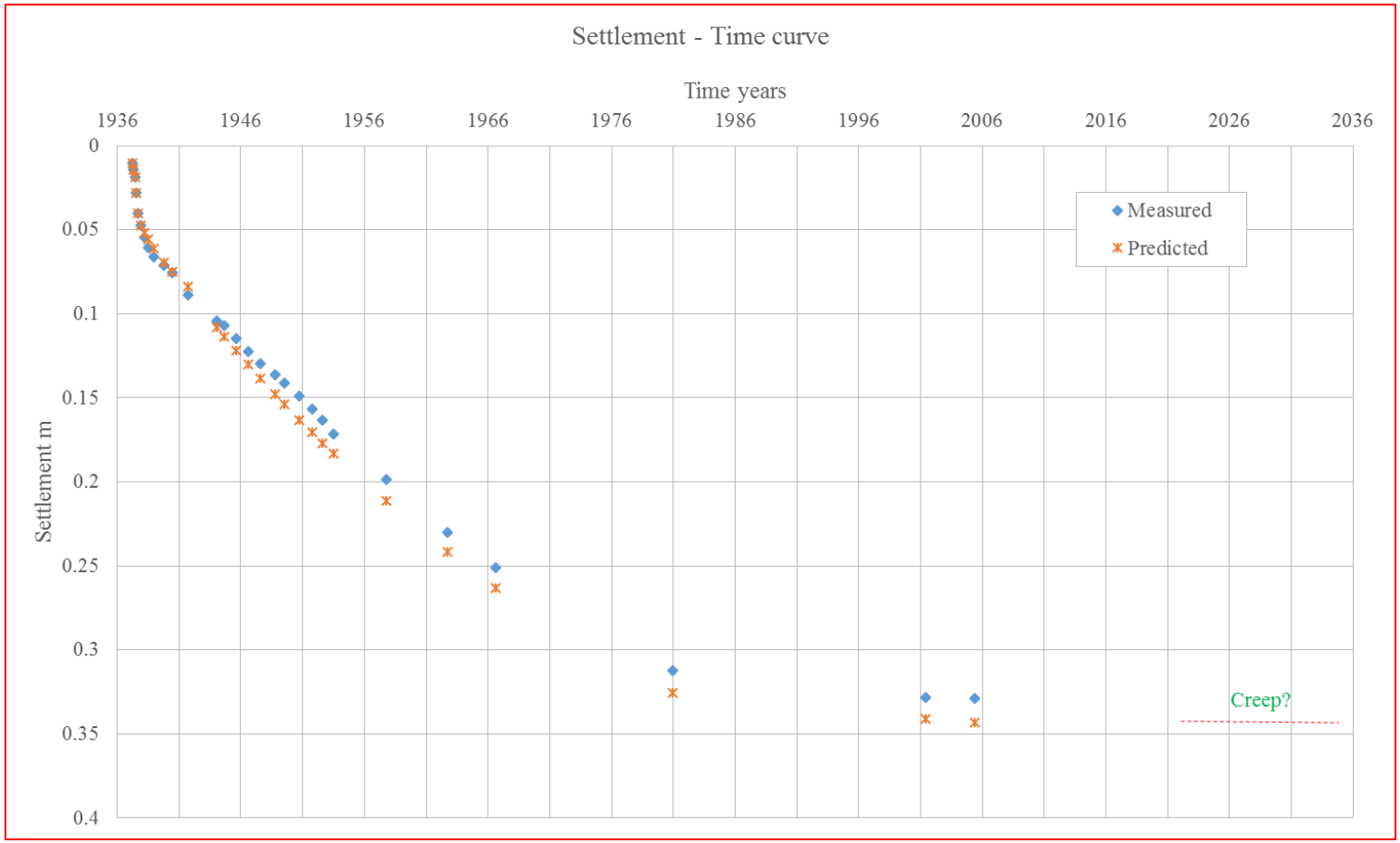

Figure 4-45. Measured settlement versus predicted settlement, San Jacinto monument

A boring was performed in 2007 by Fugro near the monument to a depth of 78 m. 1D consolidation tests were conducted on samples from depth 5.2m to 60m. Because the width of the monument is 37.8m, strain-time curves on samples from two depths (38m and 60m) are chosen to be analyzed (figure 4-46 and figure 4-47). It should be noted that t_1 is equal to 0.1min (6sec) instead of 1min. Strain-time curves still consist of two linear segments as described before. Because most stresses for the test on sample from 38m were sustained less than 1h, the second linear segment (i.e., creep only) is not quite clear on figure 4-46.

N value-stress curves are plotted in figure 4-48. The nboth is a little smaller than that on figure 4-44. Two possible reasons are: a), stress conditions at the site has been changing these years because of groundwater depletion; b), stress conditions at the site are not exactly close to those in 1D consolidation test.

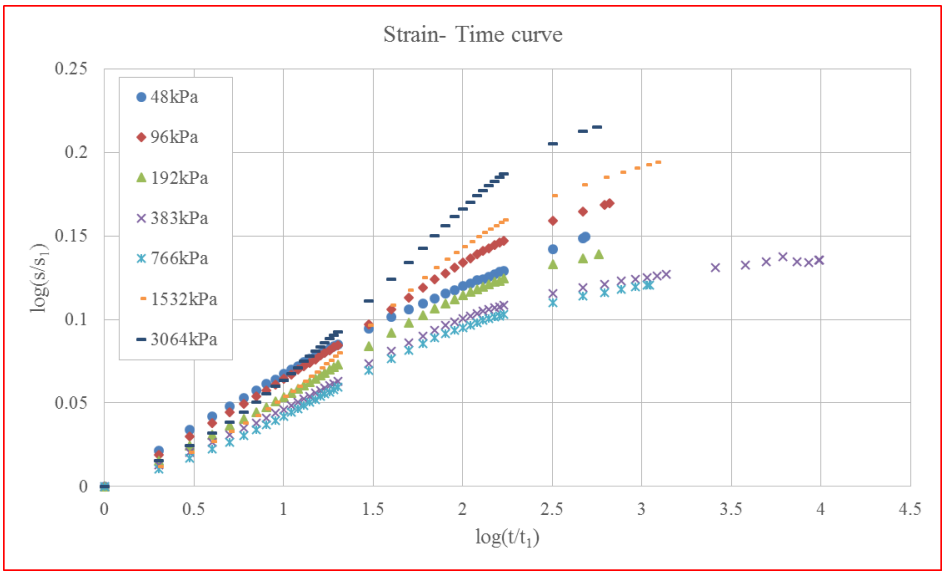

Figure 4-46. Strain-time curves on sample from depth 38m, 1D consolidation test, San Jacinto monument (Note: t_1=0.1min)

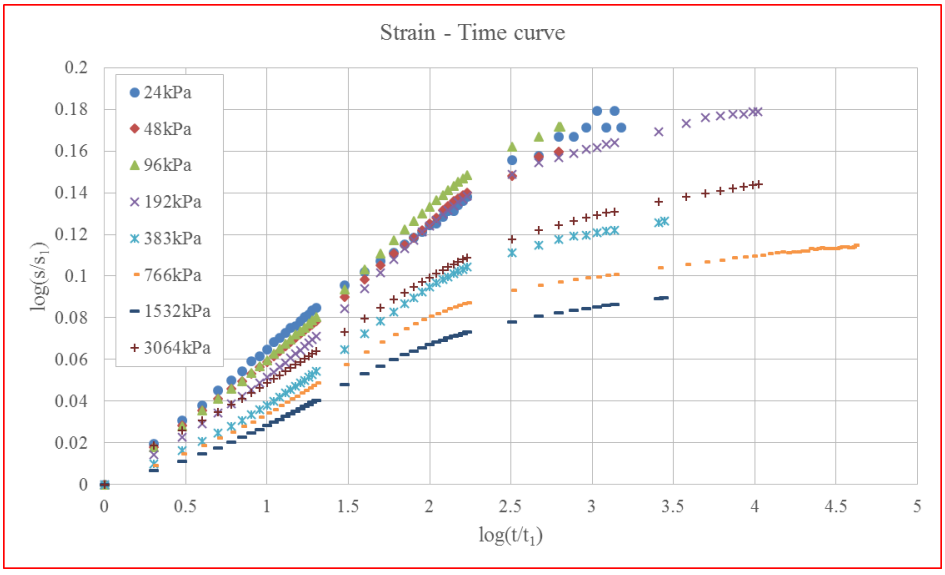

Figure 4-47. Strain-time curves on sample from depth 60m, 1D consolidation test, San Jacinto monument (Note: t_1=0.1min)

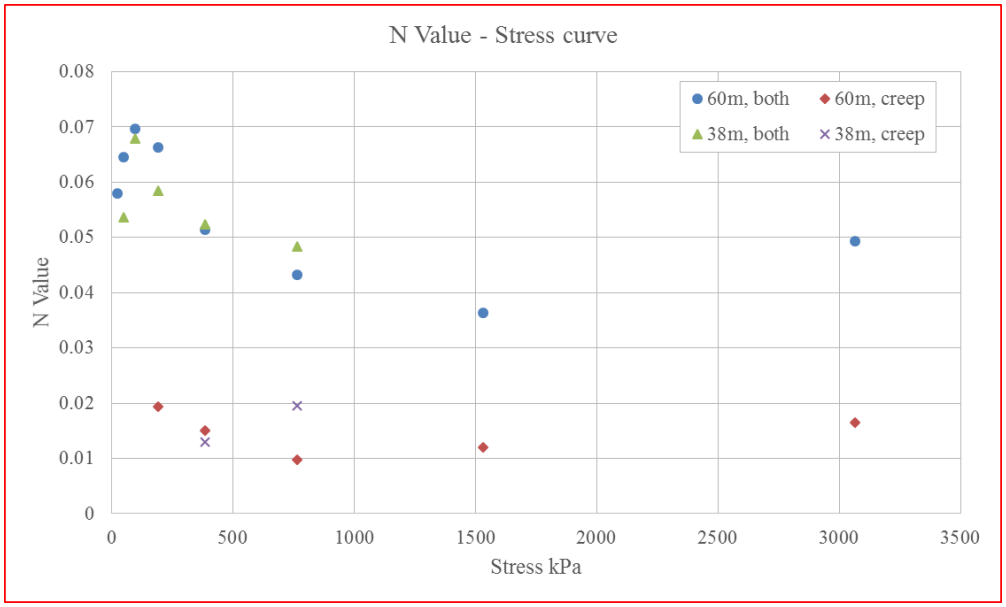

Figure 4-48. N value-stress curves, 1D consolidation test, San Jacinto monument

4.9. Conclusion

In this chapter the proposed power law model was applied to 1D consolidation test (on high PI clay, low PI clay and wet sand) and 1D compression test (on high PI clay, low PI clay, and dry sand). Several findings are made below:

- By plotting in log-log scales, the time dependent behavior of soils (strain-time curves or modulus-time curves) will be two linear segments if there is consolidation during the test or a straight line if there is no consolidation during the test. The slope of the line or linear segment will be the exponent n value in the model. For the former case (with consolidation), the slope of the

second linear segment will be n_{cr}. For the latter case (without consolidation), the slope of the line is also n_{cr}.

- It is found that for the same soil, n_{cr} from 1D consolidation is close to n_{cr} from 1D compression test. This gives a strong support to extend the second linear segment of figure 4-7 to separate deformation caused by creep from deformation caused by excess pore pressure dissipation during primary consolidation. The separation is obtained with equation 4-2 or equation 4-3. It should be noted this separation is reasonable because n_{cr} is essentially independent of stress level, though effective stress is increasing during primary consolidation. In final, it also demonstrate that deformation caused by creep should be taken into account during the whole consolidation process rather than only the secondary compression.
- n_{con} is higher than n_{cr}, which proves consolidation is the dominant part in the primary consolidation. However, the ratio of N_{cr}/N_{con} shows that a significant contribution to deformation is made by creep at low stresses;
- The long-term deformation in the lab is rebuilt and the long-term deformation in the field (fictitious example and San Jacinto monument) is predicted with the proposed power law model. The rebuilt data in the laboratory is in excellent agreement with the measured data, while the forecasted data in the field for fictitious example is in very good agreement with the prediction based on the conventional method and the forecasted data for San Jacinto

monument is in excellent agreement with recorded data, which demonstrate the proposed power law model in this paper is not only feasible to describe the time dependent behavior of soils in one-dimensional consolidation test and one-dimensional compression test in the laboratory, but also capable of prediction the long-term deformation in the practice.

5. LABORATORY TESTS - TRIAXIAL UNCONSOLIDATED-UNDRAINED (UU) CREEP TEST

5.1. Introduction

This chapter aims at demonstrating several points listed below:

- The power law model is feasible to represent time dependent behavior of soils (including creep failure) in triaxial creep test;
- Estimate the peak stress with normalization curve when creep failure exists;
- Predict time to creep failure with normalization curve and n value-stress level curve;
- Reduce creep deformation by prestressing.

5.2. Soil Properties

Three kinds of soils are adopted in triaxial creep test. They are high PI clay, low PI clay, and sand. Details of soil properties are presented in section 4.2.

It should be noted that because high PI clay and low PI clay are close to full saturation, triaxial UU creep test is conducted so that deformation will only be caused by creep (i.e., without consolidation).

5.3. Loading Procedure

The applied confining stress during triaxial UU shear test and triaxial (UU) creep test for high PI clay was assumed equal to stress by gravity (equation 5-1).

$$\sigma_3 = \sigma_r = \gamma \cdot h \tag{5-1}$$

Where γ is unit weight (figure 4-3); h is depth of specimen and $\sigma_3(\sigma_r)$ is applied confining stress.

The confining pressure is chosen to be 55.2kPa and 103.4kPa for low PI clay, and 55.2kPa, 82.7kPa, 110.3kPa and 165.5kPa for dry sand. These chosen values are close to the range of values applied on high PI clay.

The general test procedure of triaxial (UU) creep test (ASTM Standard, 2007) is as follows:

a), after the specimen and the test machine are all set, test starts;

b), the loading part is strain control (constant strain rate), after the first chosen stress (or load) is reached, it switches to stress control (or load control) to allow specimens to creep;

c), in usual, after creep for 24 h (sometimes longer), switching back to strain control to loading, after the next chosen stress is arrived, switching to stress control again;

d), repeating step c, until the specimen fails at some loading part (loading from one chosen stress to the next chosen stress) or at the part of holding the constant chosen stress (i.e., creep failure), test ends.

Connecting the ending points (24h) under each holding stress provides a curve called “1 day creep curve”. In similar, connecting the starting points under each holding stresses provides a curve called “0 minute creep curve”. Casagrande and Wilson (1951) had demonstrated that “0 minute creep curve” is unique for a given constant strain rate

of a given soil. The critical part during triaxial UU creep test is that, when switching from stress control to strain control, the stress increment should be enough to back from "1 day creep curve" to "0 minute creep curve" to avoid the impact of previous holding stress on creep behavior of current holding stress. The minimum stress increment was found to be a little larger than 20kPa. The stress increasing from 120.4kPa to 133.4kPa in figure 5-1 is not large enough which results in the creep deformation at 133.4kPa is impacted by the creep deformation at previous stress (i.e., 120.4kPa).

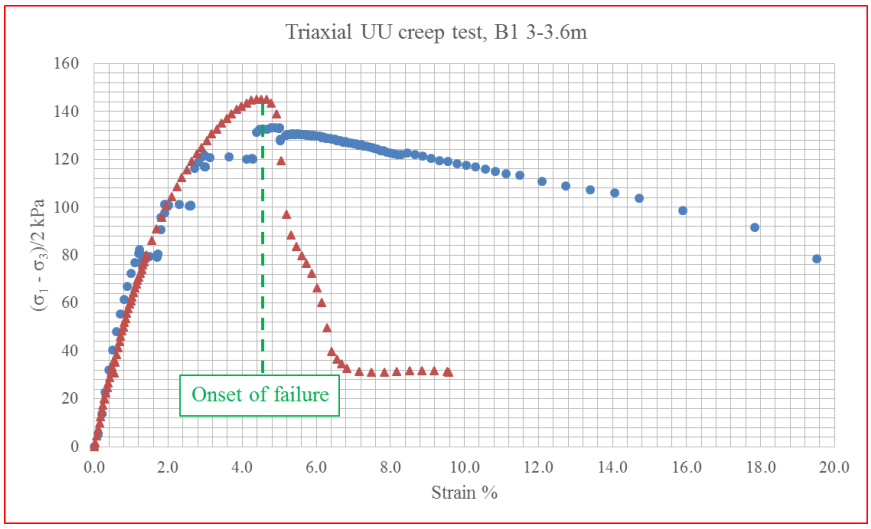

Figure 5-1. Minimum stress increment to avoid the influence of previous stress on deformation under current stress

5.4. Triaxial UU Creep Test on High PI Clay

The procedure of this research is presented in the following order: first, triaxial UU creep tests are carried out to provide the data for the proposed power law model, specially the range of n value; second, the stress-strain curves of triaxial UU shear tests are normalized for estimating the peak stress and its corresponding strain of triaxial UU creep test in the third step; third, the criterion of creep failure is analyzed; fourth, estimating the time and possibility for creep failure with the proposed power law model; fifth, an example is provided to further demonstrate the model; sixth, prestressing is proposed to reduce creep deformation.

5.4.1. Test Results

Triaxial UU creep tests on samples at different depths from different boreholes are selected here for illustration.

Triaxial UU creep test on sample at depth 1.8~2.4m, borehole N1

The stress-strain curve of triaxial UU creep test on specimen prepared from sample from borehole N1 at depth 1.8~2.4m was plotted in figure 5-2. The strain-time curves under all holding stresses were plotted in figure 5-3 and figure 5-4. At the last holding stress (221.8kPa), the sample couldn't maintain the applied stress (i.e., creep failure). The n value is acquired by plotting the model (equation 3-10) in log-log scales (figure 5-5).

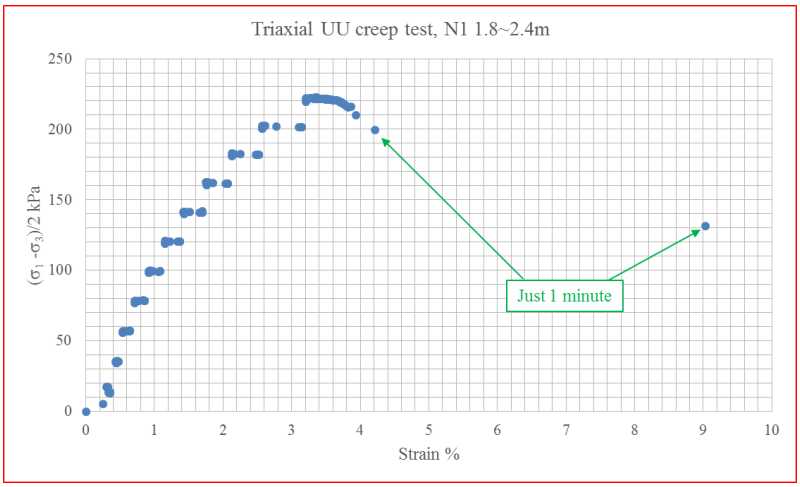

Figure 5-2. Stress-strain curve, N1 1.8~2.4m, high PI clay, triaxial creep test

Two points should be noted: a), the nonlinear part at the beginning (20~30 minutes) is due to the (lagging) adjustment of the test apparatus switching from strain control to stress control (figure 5-6); b), there is seating problem at the first two stresses (figure 5-5) which impacts the shape of the curve.

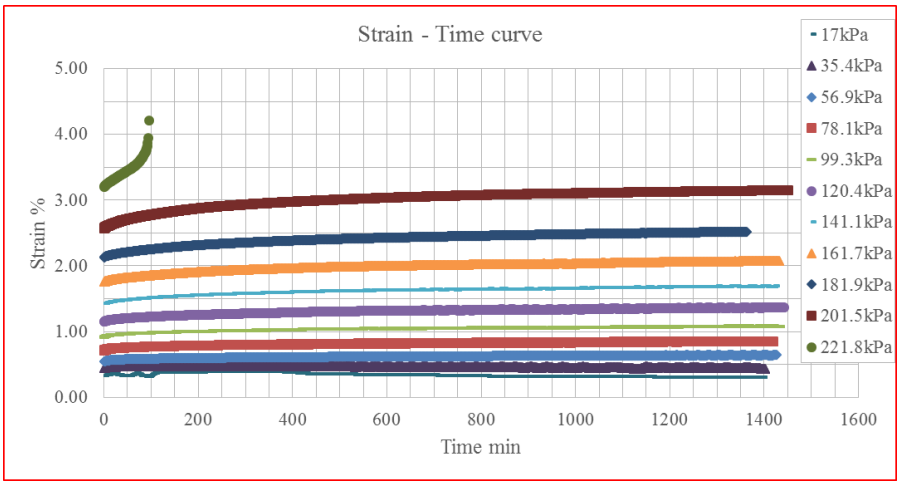

Figure 5-3. Strain-time curves, N1 1.8~2.4m, high PI clay, triaxial creep test

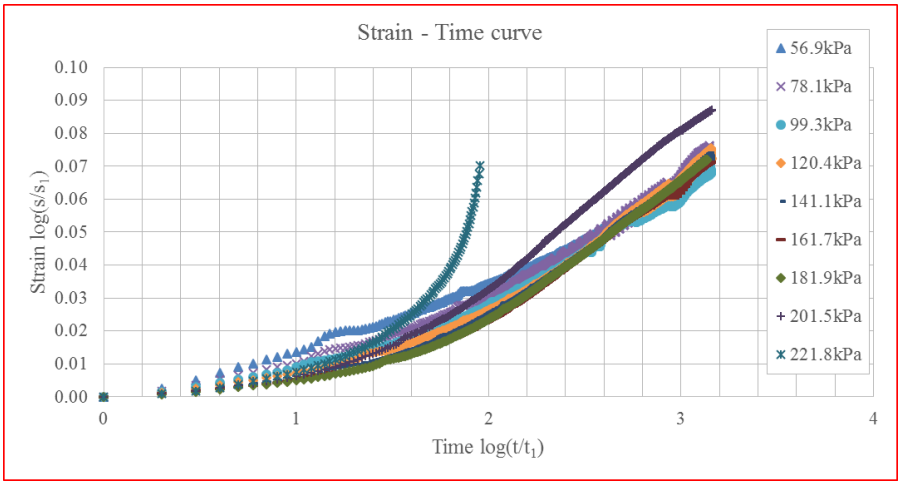

Figure 5-4. Strain-time curves (log-log scales), N1 1.8~2.4m, high PI clay, triaxial creep test

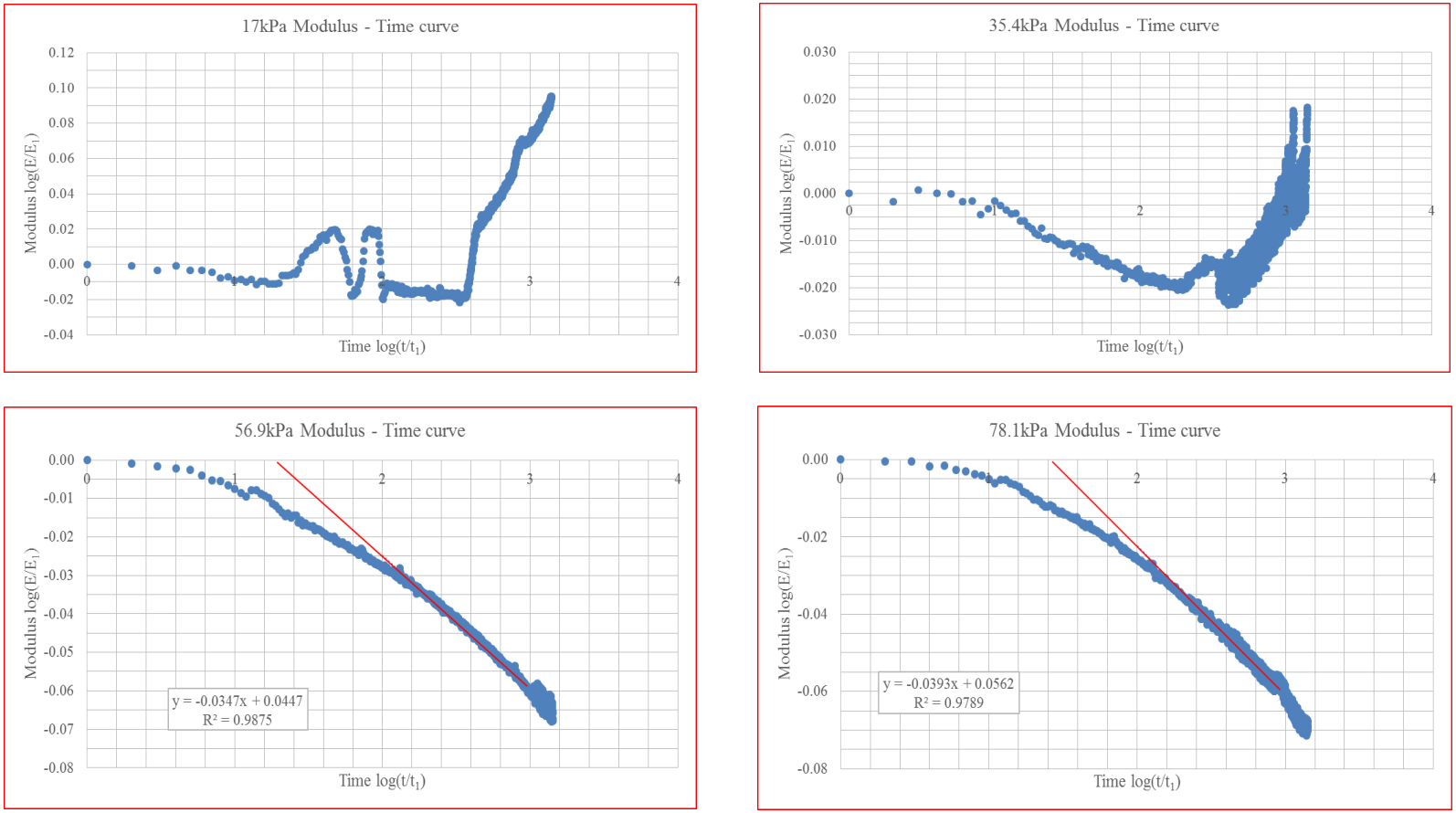

Figure 5-5. Modulus-time curves at any stress, N1 1.8~2.4m, high PI clay, triaxial creep test

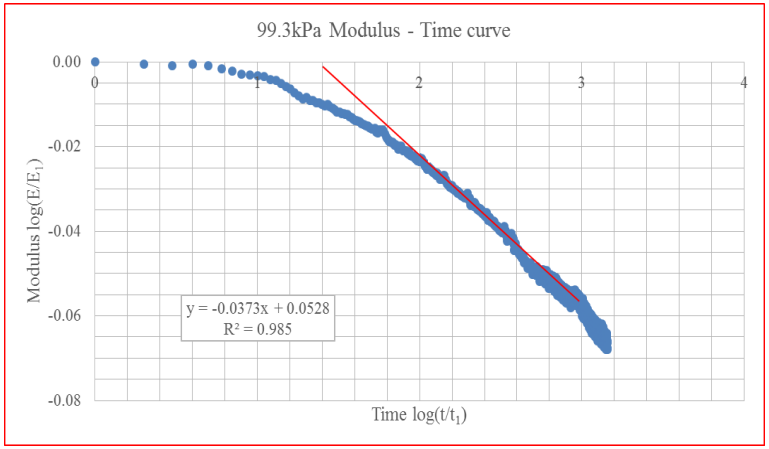

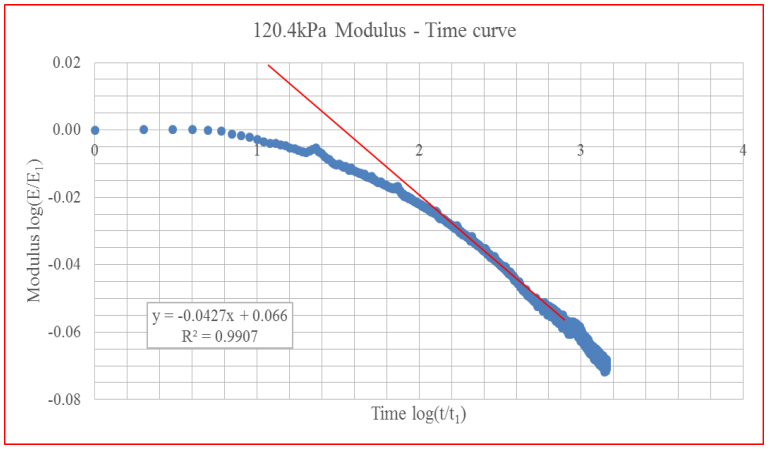

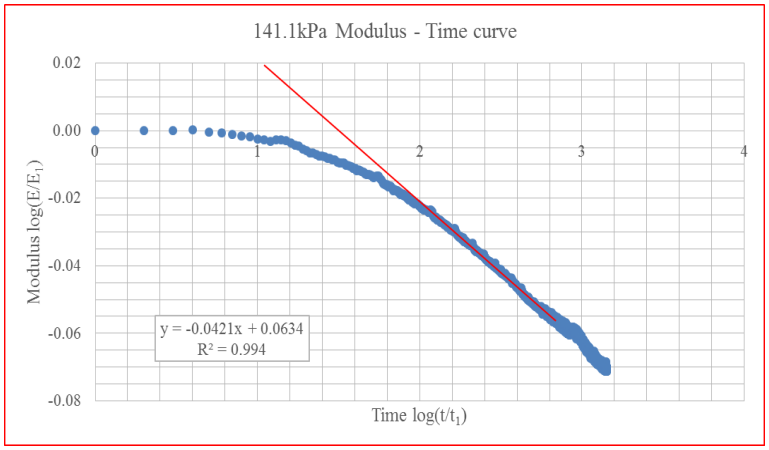

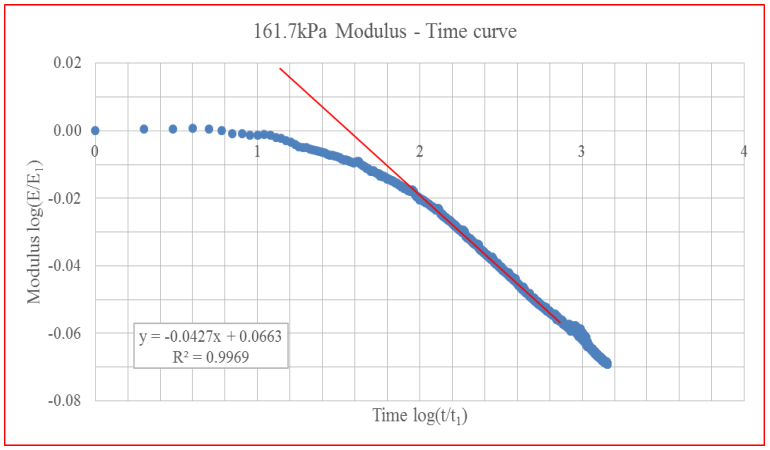

Figure 5-5 Continued

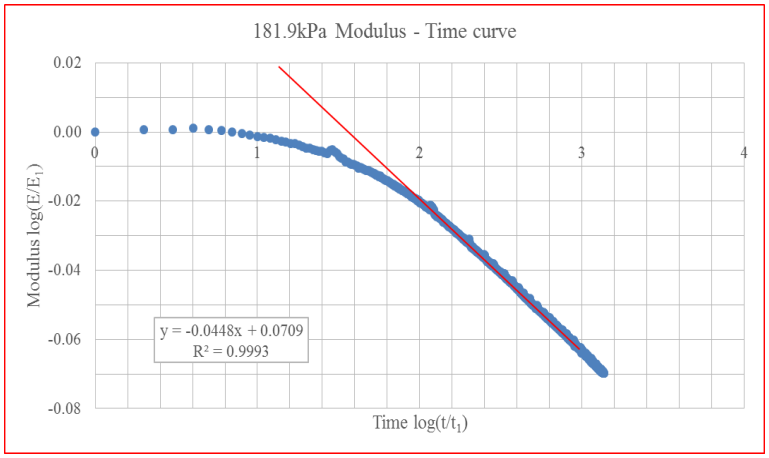

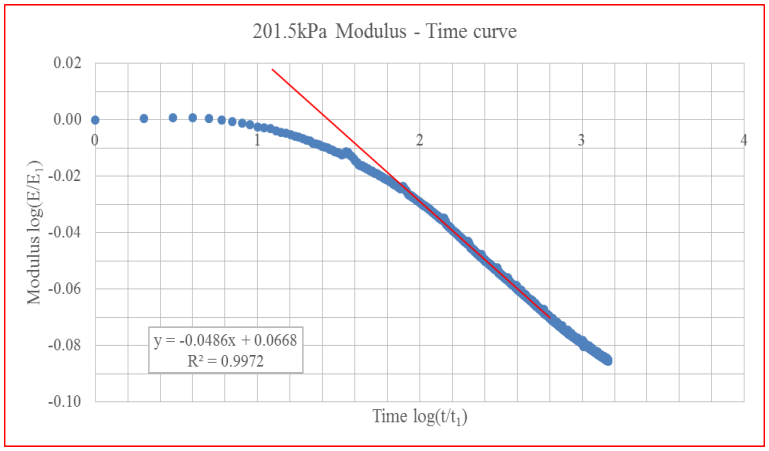

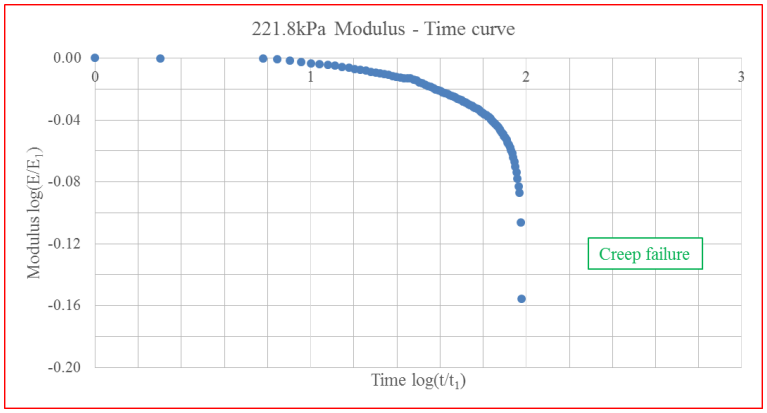

Figure 5-5 Continued

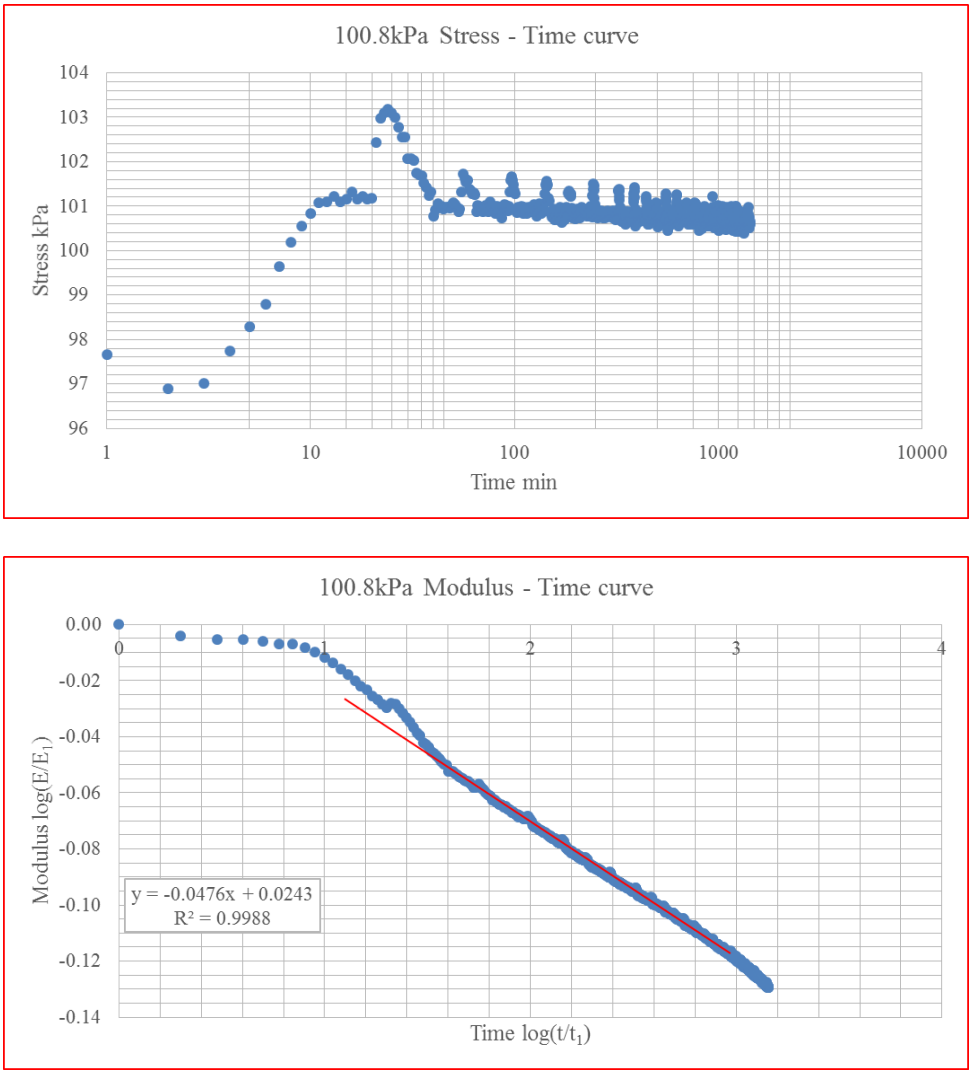

Figure 5-6. Lagging adjustment when switching from strain control to stress control

Triaxial UU creep test on sample at depth 2.4~3m, borehole N3

The stress-strain curve of triaxial UU creep test on specimen prepared from sample from borehole N3 at depth 2.4~3m was plotted in figure 5-7. The strain-time curves under all holding stresses were plotted in figure 5-8 and figure 5-9. At the last holding

stress (148.2kPa), the sample couldn't maintain the applied stress (i.e., creep failure). The n value is acquired by plotting the model (equation 3-10) in log-log scales (figure 5-10). Still, two problems (lagging and seating) exist.

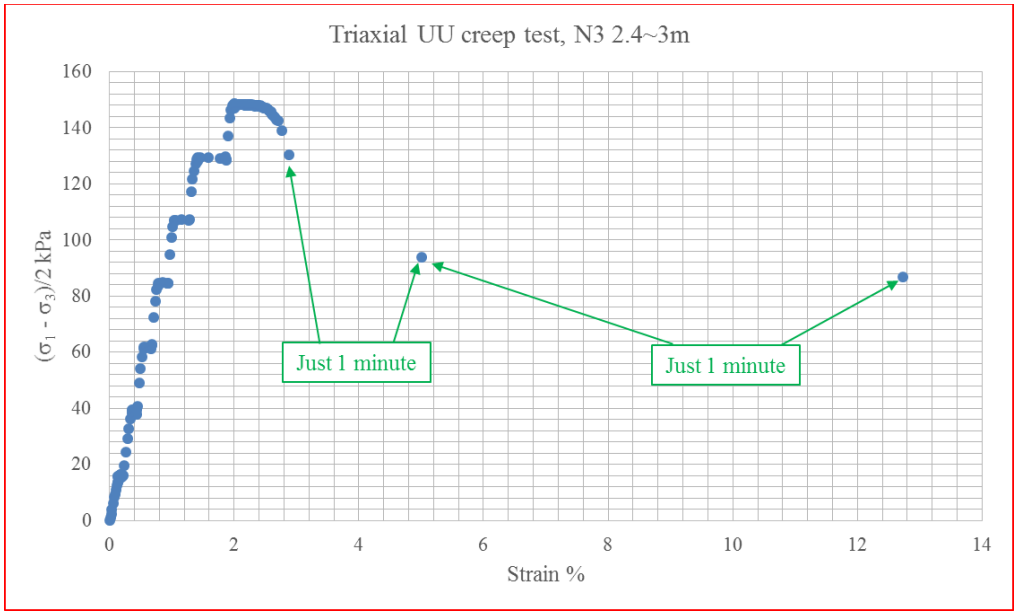

Figure 5-7. Stress-strain curve, N3 2.4~3m, high PI clay, triaxial creep test

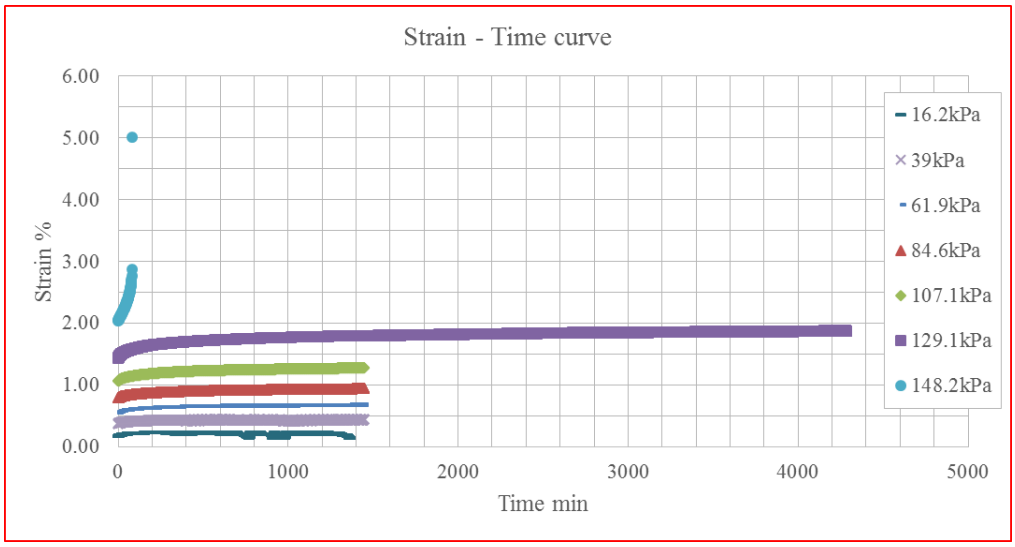

Figure 5-8. Strain-time curves, N3 2.4~3m, high PI clay, triaxial creep test

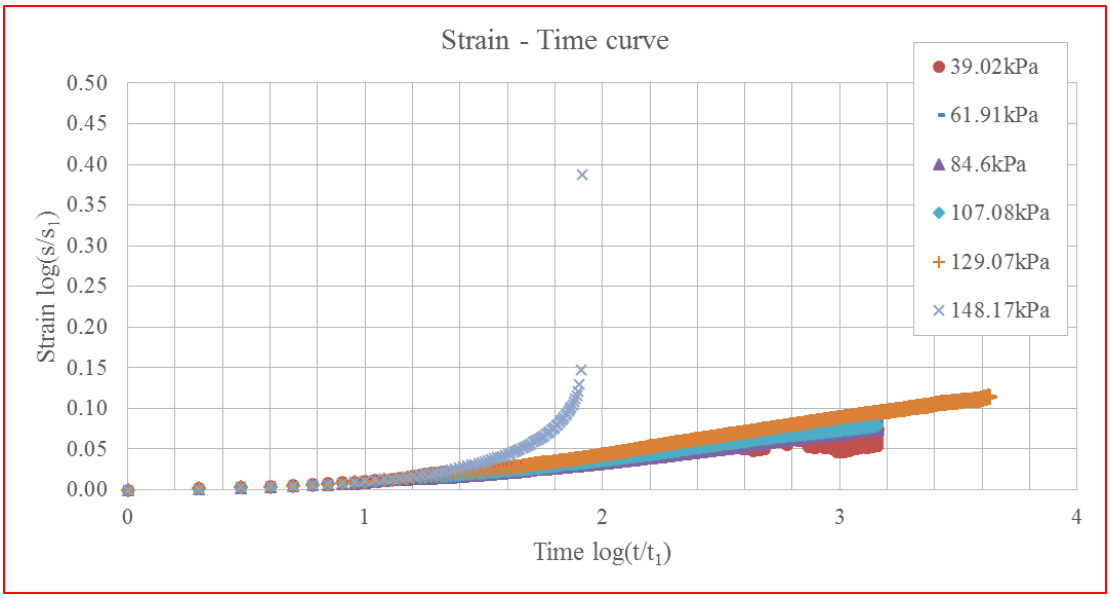

Figure 5-9. Strain-time curves (log-log scales), N3 2.4~3m, high PI clay, triaxial creep test

Triaxial UU creep test on sample at depth 3~3.6m, borehole B1

The stress-strain curve of triaxial UU creep test on specimen prepared from sample from borehole B1 at depth 3~3.6m was plotted in figure 5-11. The strain-time curves under all holding stresses were plotted in figure 5-12 and figure 5-13. At the last holding stress (133.4kPa), the sample couldn't maintain the applied stress (i.e., creep failure). As mentioned before, the stress increment at the last step from 120.4kPa to 133.4kPa is not larger enough to bring the curve back to "0 minute creep curve". The n value is acquired by plotting the model (equation 3-10) in log-log scales (figure 5-14).

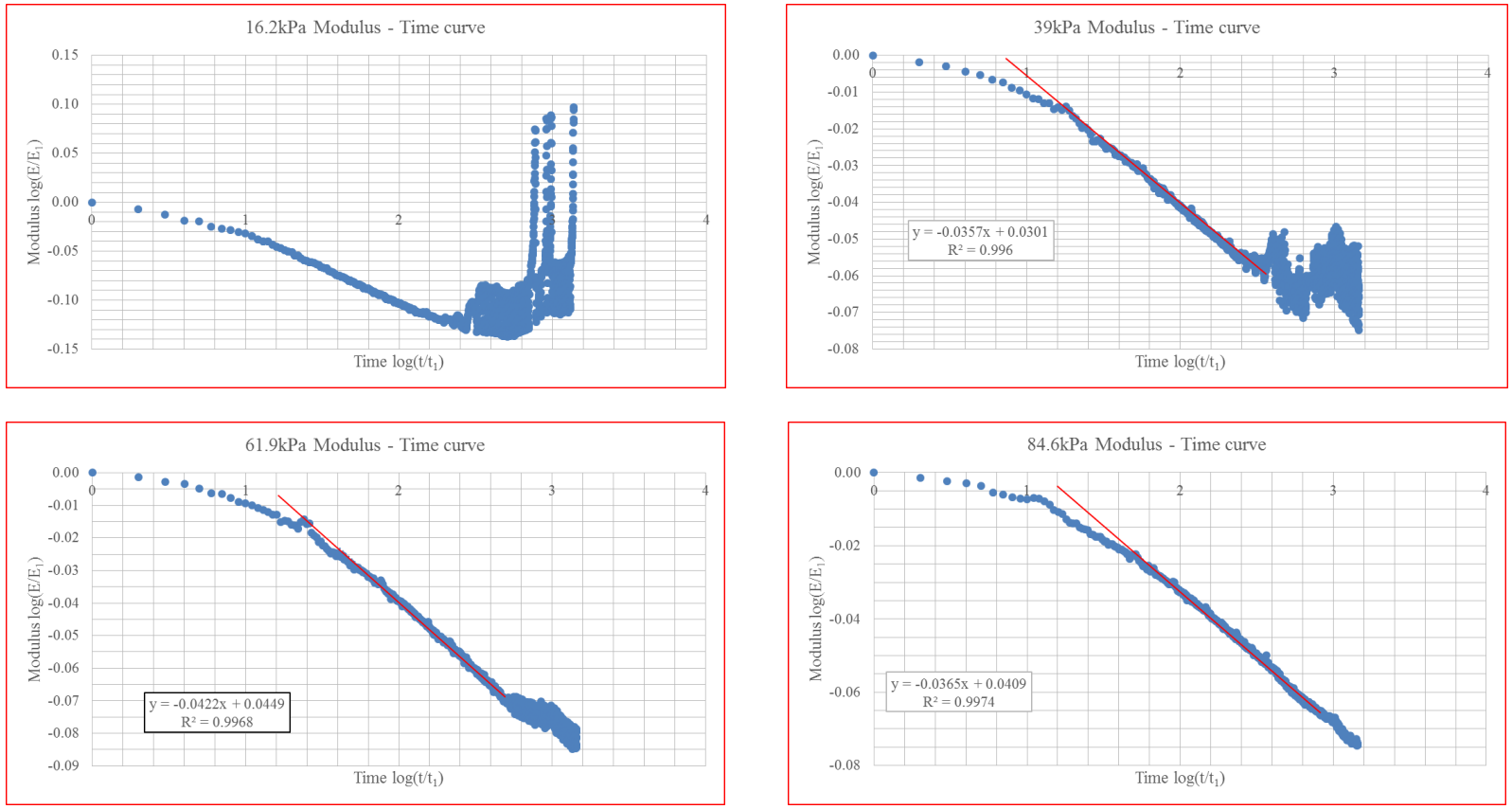

Figure 5-10. Modulus-time curves at any stress, N3 2.4~3m, high PI clay, triaxial creep test

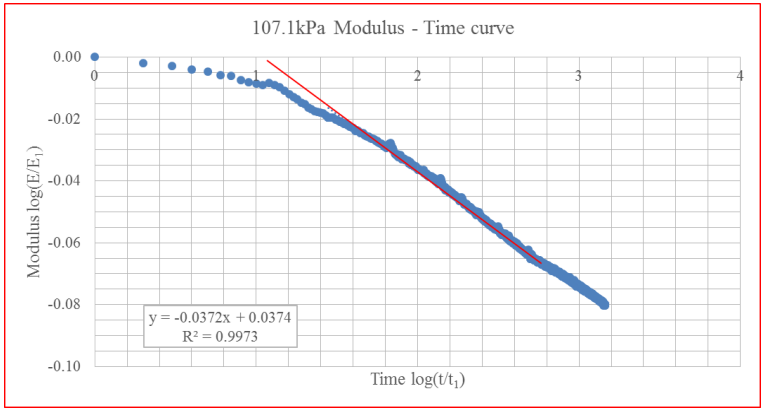

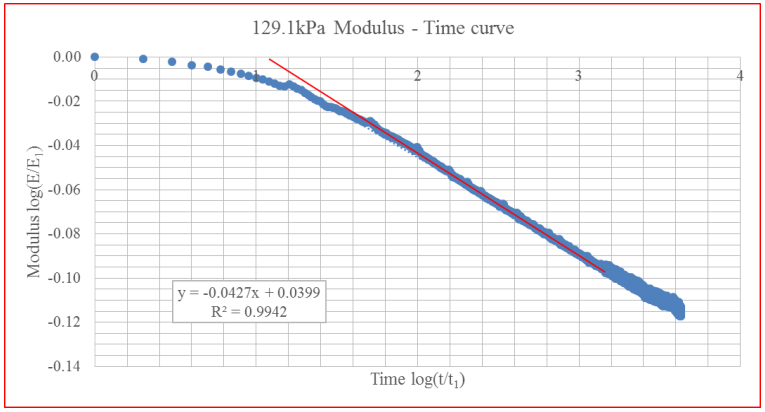

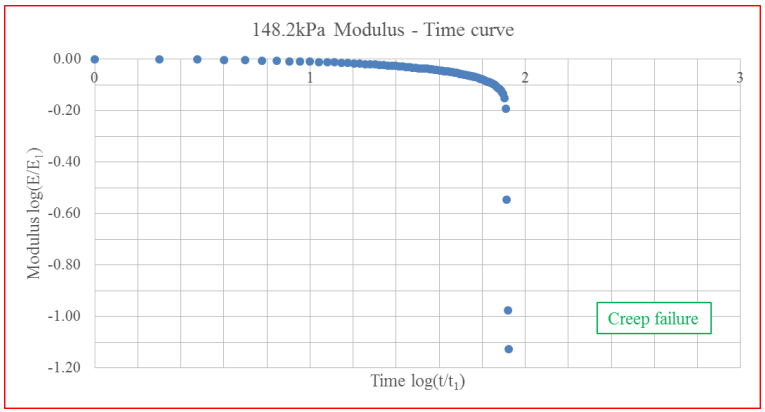

Figure 5-10 Continued

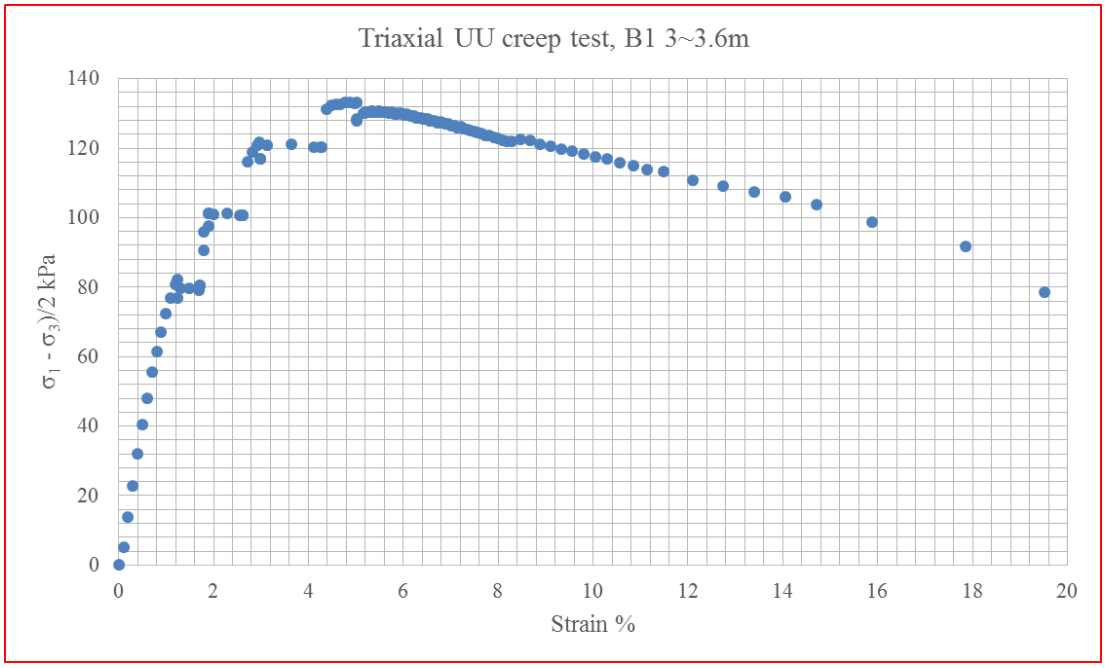

Figure 5-11. Stress-strain curve, B1 3~3.6m, high PI clay, triaxial creep test

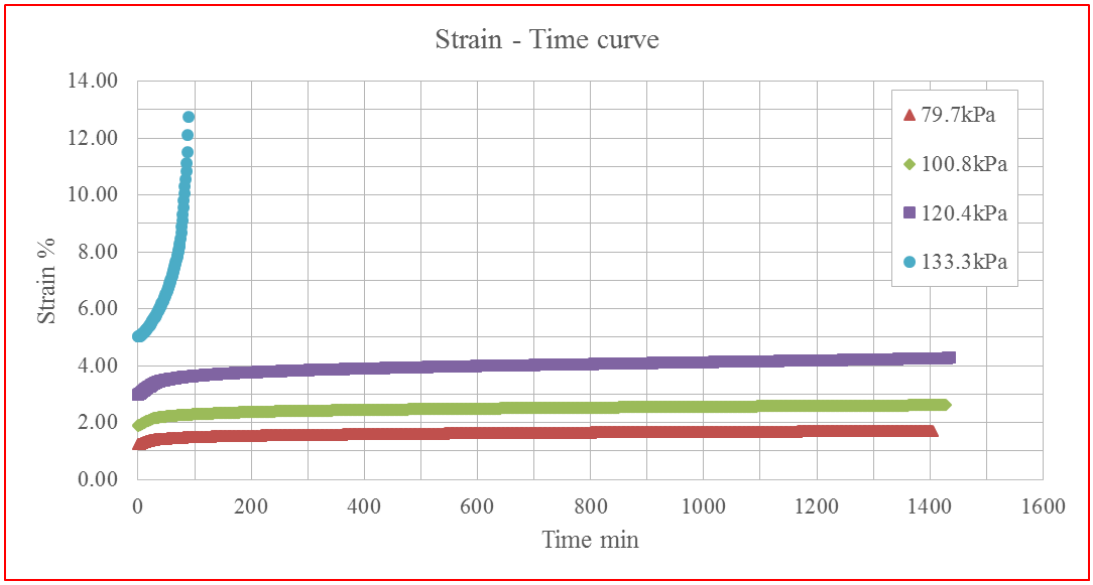

Figure 5-12. Strain-time curves, B1 3~3.6m, high PI clay, triaxial creep test

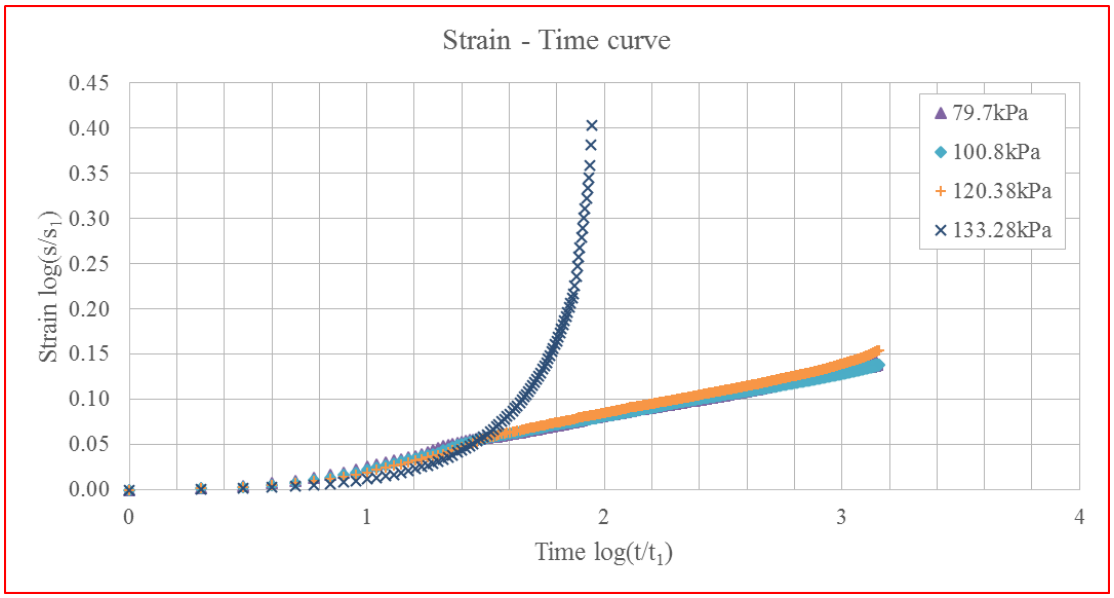

Figure 5-13. Strain-time curves (log-log scales), B1 3~3.6m, high PI clay, triaxial creep test

Triaxial UU creep test on sample at depth 1.8~2.4m, borehole N6

The stress-strain curve of triaxial UU creep test on specimen prepared from sample from borehole N6 at depth 1.8~2.4m was plotted in figure 5-15. The strain-time curves under all holding stresses were plotted in figure 5-16. The last holding stress (256.8kPa) was sustained eight weeks, however, creep failure didn't happen. The n value is acquired by plotting the model (equation 3-10) in log-log scales (figure 5-17 and figure 5-18).

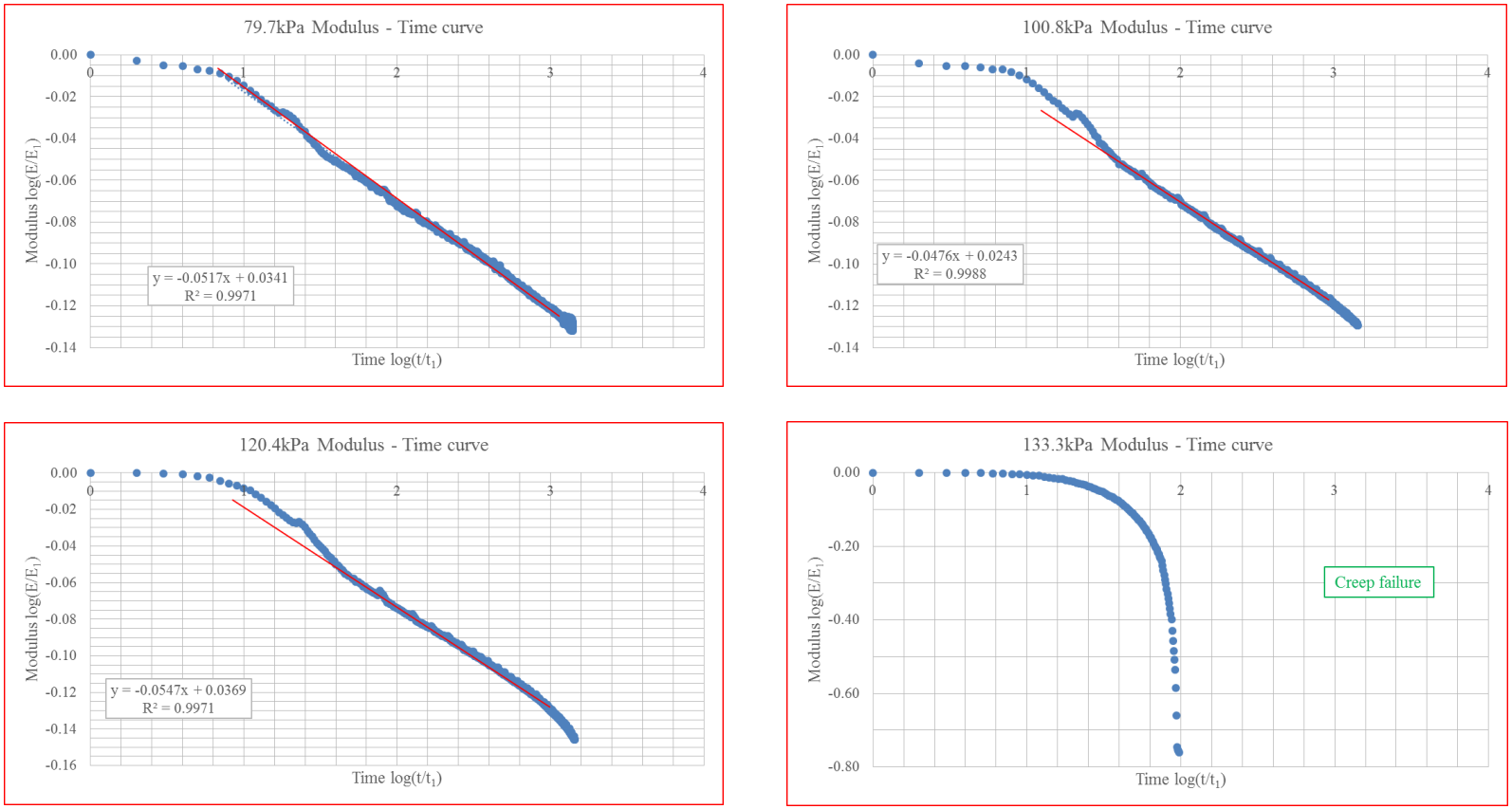

Figure 5-14. Modulus-time curves at any stress, B1 3~3.6m, high PI clay, triaxial creep test

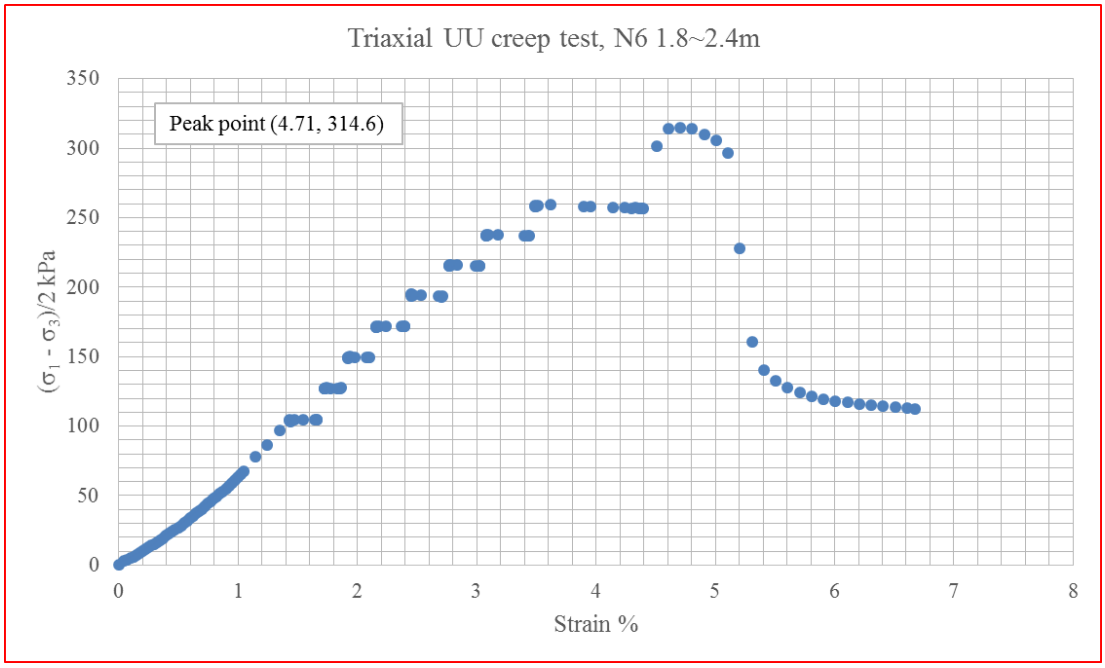

Figure 5-15. Stress-strain curve, N6 1.8~2.4m, high PI clay, triaxial creep test

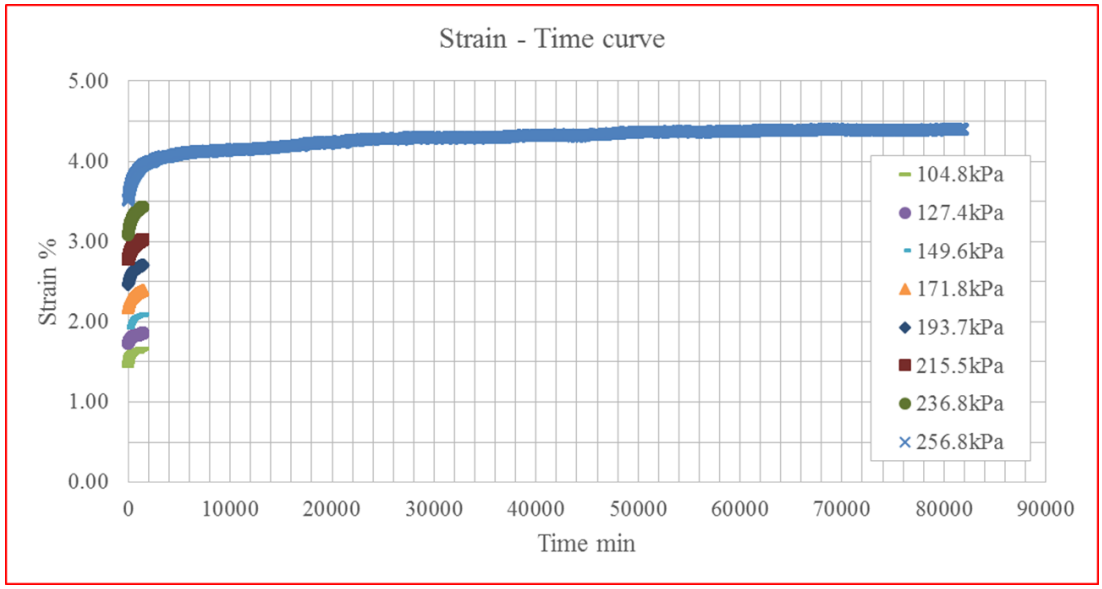

Figure 5-16. Strain-time curves, N6 1.8~2.4m, high PI clay, triaxial creep test

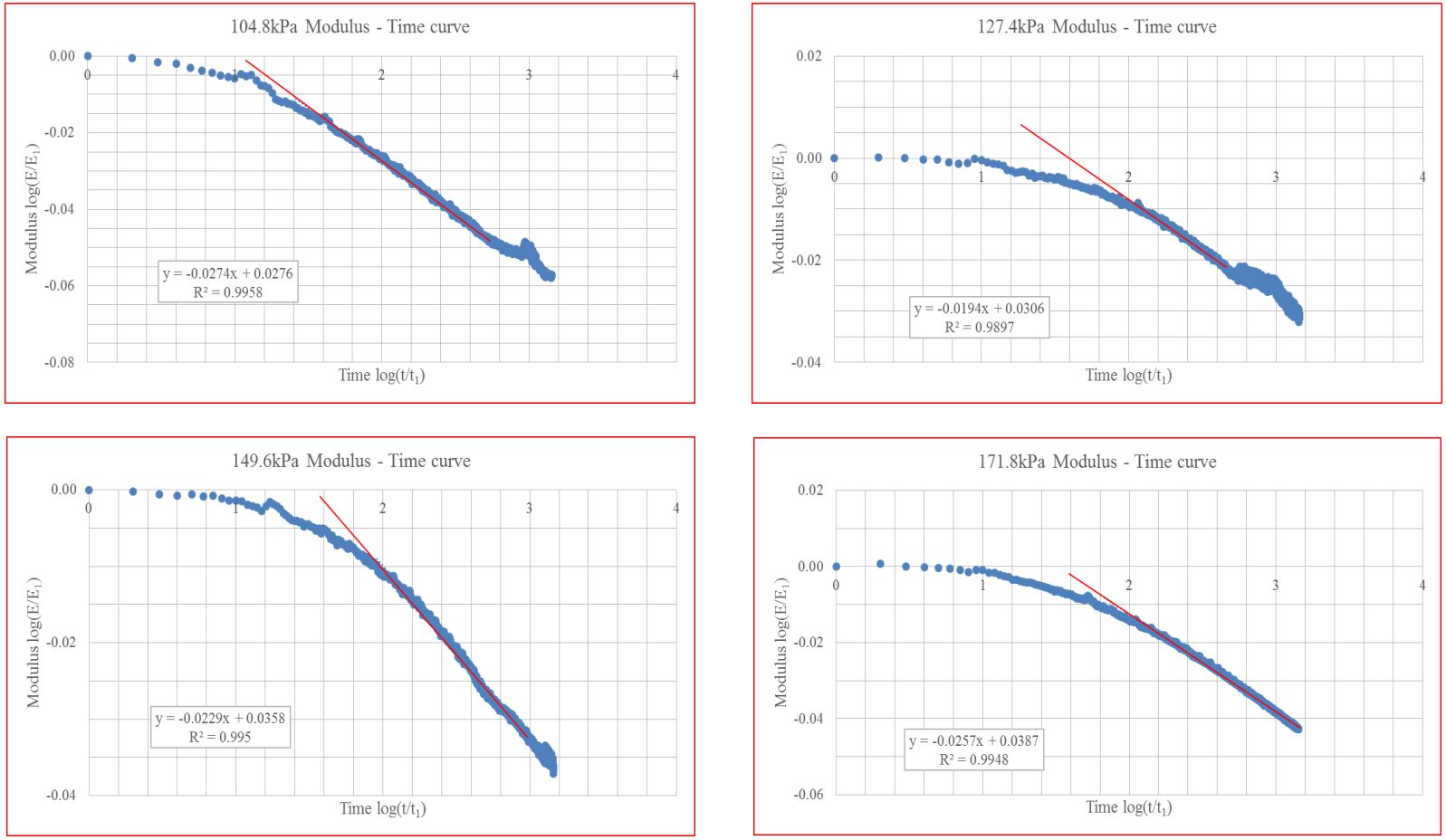

Figure 5-17. Modulus-time curves at any stress, N6 1.8~2.4m, high PI clay, triaxial creep test

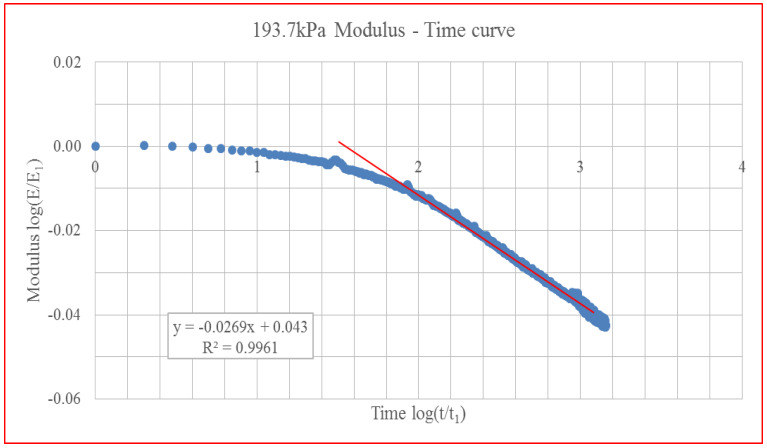

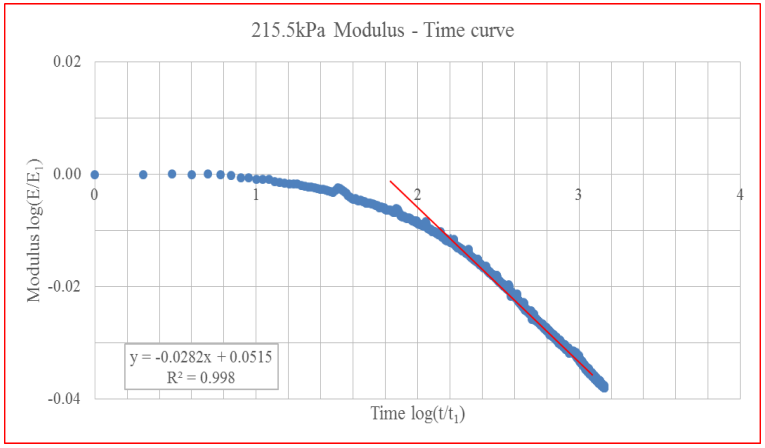

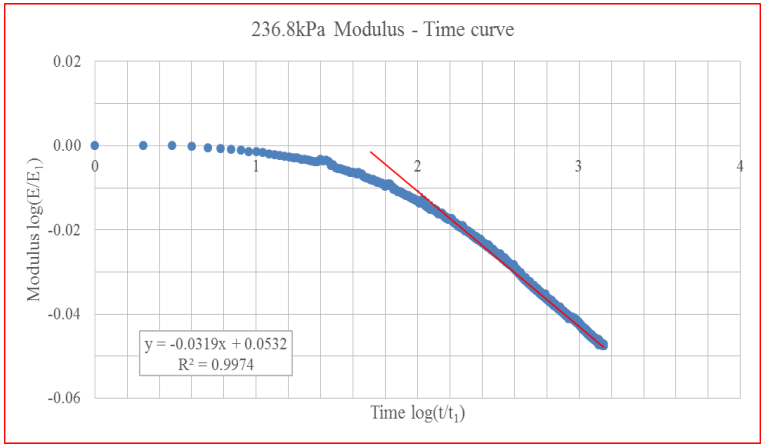

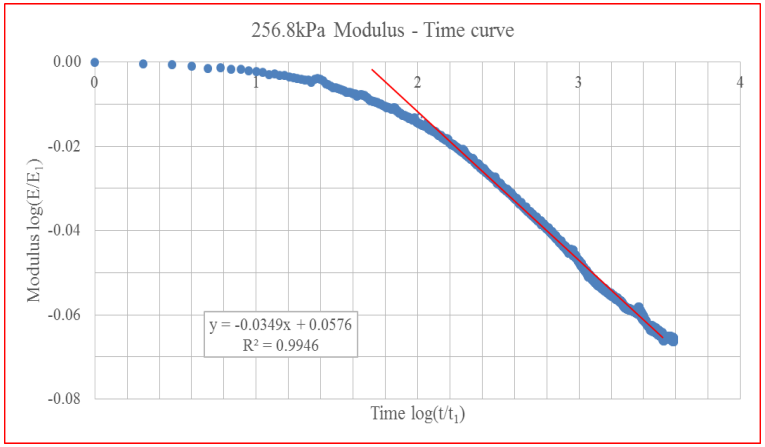

Figure 5-17 Continued

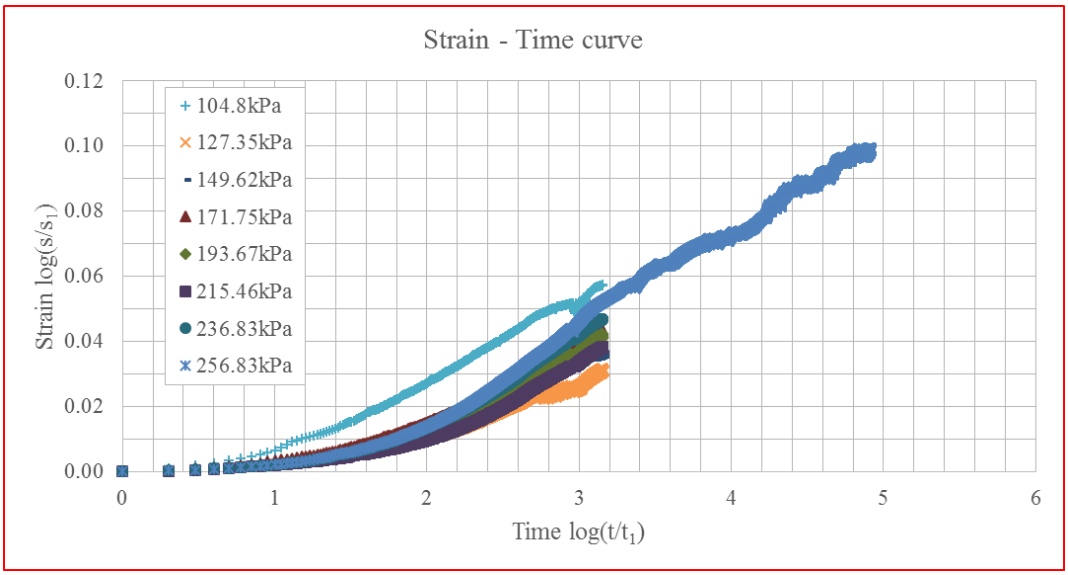

Figure 5-18. Strain-time curves (log-log scales), N6 1.8~2.4m, high PI clay, triaxial creep test

5.4.2. Normalization Curve

As holding stresses are different between tests on different specimens, they are normalized with peak stress to be compared. However, peak stress is unknown when creep failure happens. Previous researchers took the peak stress from conventional triaxial shear test (It is kind of right, but not exactly!). It is based on an implicit assumption that conventional triaxial shear test can be compared to triaxial creep test.

For a given soil, stress-strain curves of conventional triaxial shear test may vary quite a lot, which are plotted on the left side of figure 5-19. However, after normalized by the peak stress and its corresponding strain, it is found that there is a quite unique curve (not exactly unique) that is capable of representing stress-strain behavior until the

peak stress (right side of figure 5-19). Soil on the top row in figure 5-19 is high PI clay in this dissertation; soil on the middle row in figure 5-19 is also high PI clay from Beaumont, TX; soil on the bottom row in figure 5-19 is low PI clay, data from Suroor (1998).

Because of the existence of normalization curve, it is readily to estimate peak stress of triaxial creep test. The critical point is to adjust stress-strain curve of conventional triaxial shear test until the pre-peak part fitting well with the "0 minute creep curve" of triaxial creep test.

In figure 5-20, the stress-strain curve of triaxial UU creep test on sample from borehole N1 at depth 1.8~2.4m fits with the stress-strain curve of triaxial UU shear test on specimen from borehole N2 at depth 1.8~2.4m, while the x-scale of the curve of triaxial UU shear test times 1 (i.e., no adjustment) and the y-scale of the curve of triaxial UU shear test times 0.63. The estimated peak stress will be 228.3kPa and its corresponding strain will be 3.41%. The ratio of holding stress (221.8kPa) for creep failure over estimated peak stress will be 97%.

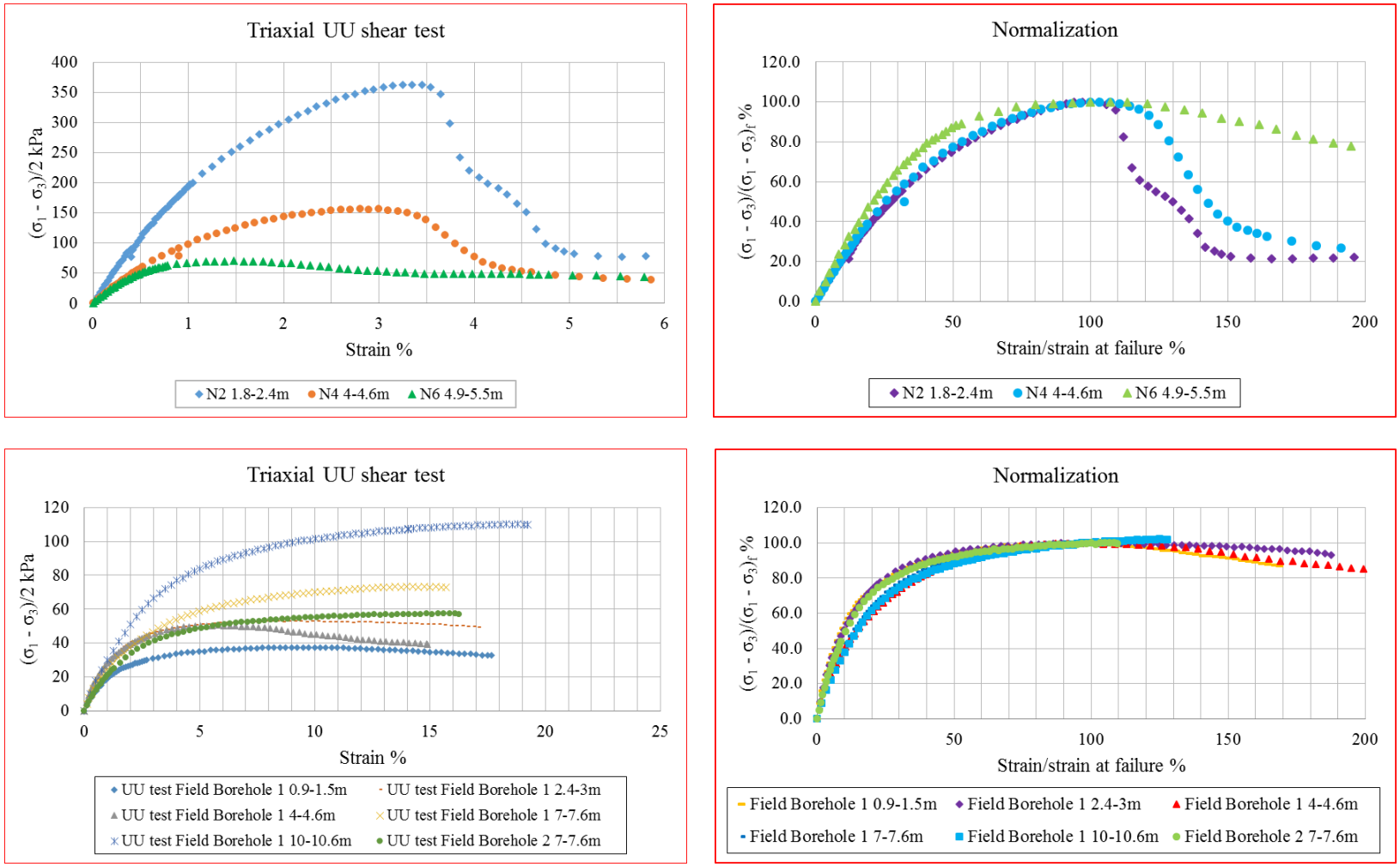

Figure 5-19. Stress-strain curves before and after normalization

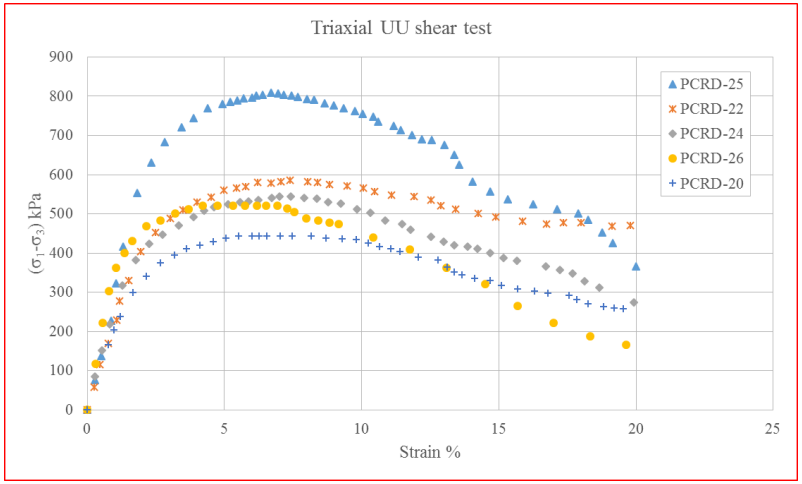

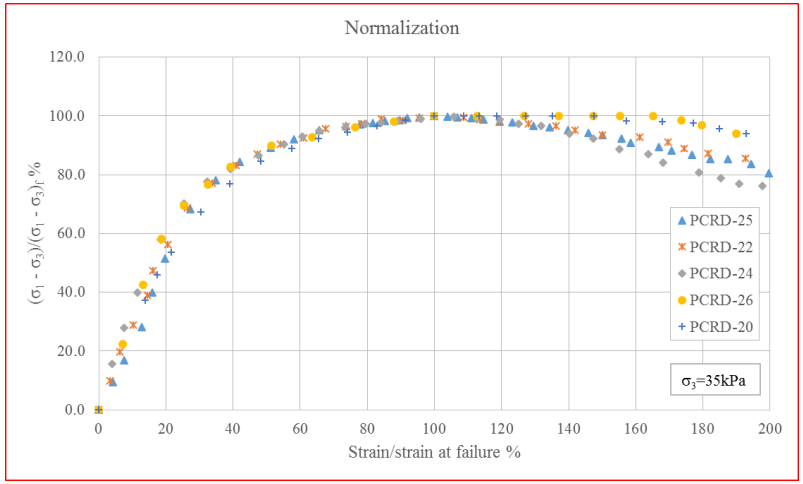

Figure 5-19 Continued

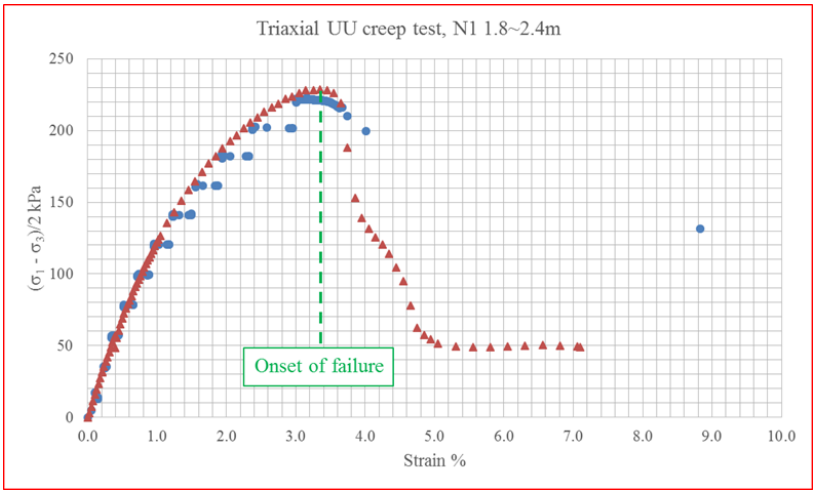

Figure 5-20. Estimating peak stress and its corresponding strain with normalization curve, N1 1.8~2.4m

In figure 5-21, the stress-strain curve of triaxial UU creep test on sample from borehole N3 at depth 2.4~3m fits with the stress-strain curve of triaxial UU shear test on specimen from borehole N2 at depth 1.8~2.4m, while the x-scale of the curve of triaxial UU shear test times 0.74 and the y-scale of the curve of triaxial UU shear test times 0.44. The estimated peak stress will be 159.6kPa and its corresponding strain will be 2.47%. The ratio of holding stress (148.2kPa) for creep failure over estimated peak stress will be 93%.

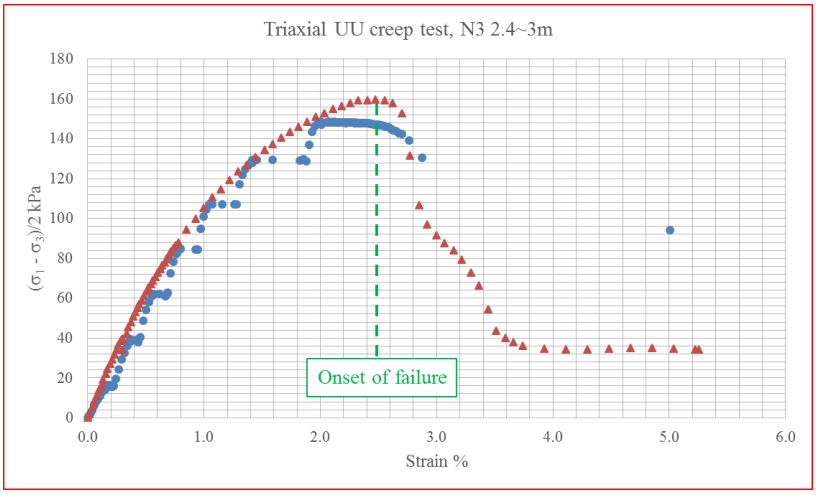

Figure 5-21. Estimating peak stress and its corresponding strain with normalization curve, N3 2.4~3m

In figure 5-22, the stress-strain curve of triaxial UU creep test on sample from borehole B1 at depth 3~3.6m fits with the stress-strain curve of triaxial UU shear test on specimen from borehole N2 at depth 1.8~2.4m, while the x-scale of the curve of triaxial UU shear test times 1.35 and the y-scale of the curve of triaxial UU shear test times 0.4. The estimated peak stress will be 144.8kPa and its corresponding strain will be 4.24%. The ratio of holding stress (133.3kPa) for creep failure over estimated peak stress will be 92%.

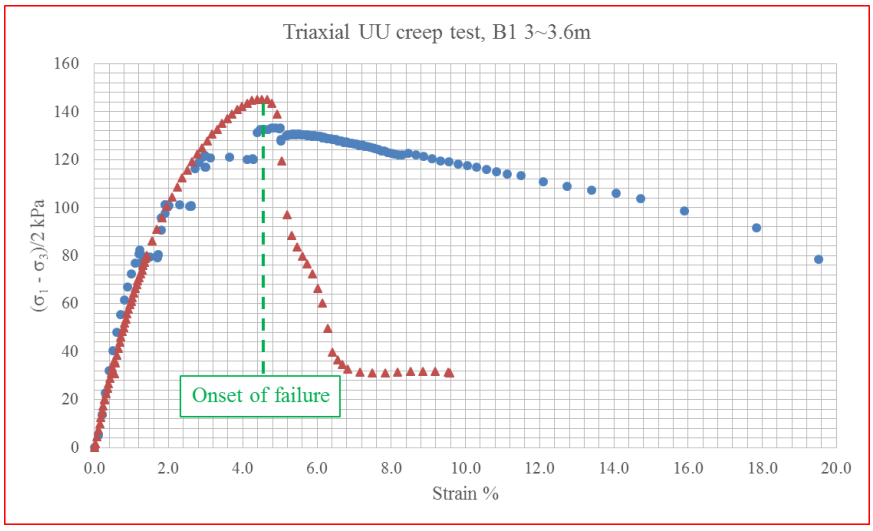

Figure 5-22. Estimating peak stress and its corresponding strain with normalization curve, B1 3~3.6m

It should be noted that stress (y-axis) and strain (x-axis) of conventional triaxial shear test will be multiplied with a ratio, respectively. In most cases, ratios are not unit. It is different from views of previous researchers which just directly took the value from conventional triaxial shear test (i.e., ratios equal to unit).

Besides, it is likely that the criterion of creep failure is to reach the critical strain, namely, strain corresponding to the estimated peak stress, which is verified by strain-time curves and fitting curves (figure 5-3 and figure 5-20, figure 5-8 and figure 5-21, figure 5-12 and figure 5-22) on specimens from three samples with different depths. Again, this critical strain will be obtained by multiplying the strain corresponding to peak stress from conventional triaxial shear test with a ratio, while previous researchers implicitly assumed this ratio was unit.

5.4.3. N Value – Stress Level Curve

After the estimated peak stress is acquired with the normalization curve, n value-stress level curve could be plotted (figure 5-23). Though n value varied from triaxial creep tests on different specimens, it is in virtually independent of stress level. To remind, the same founding was made in 1D tests.

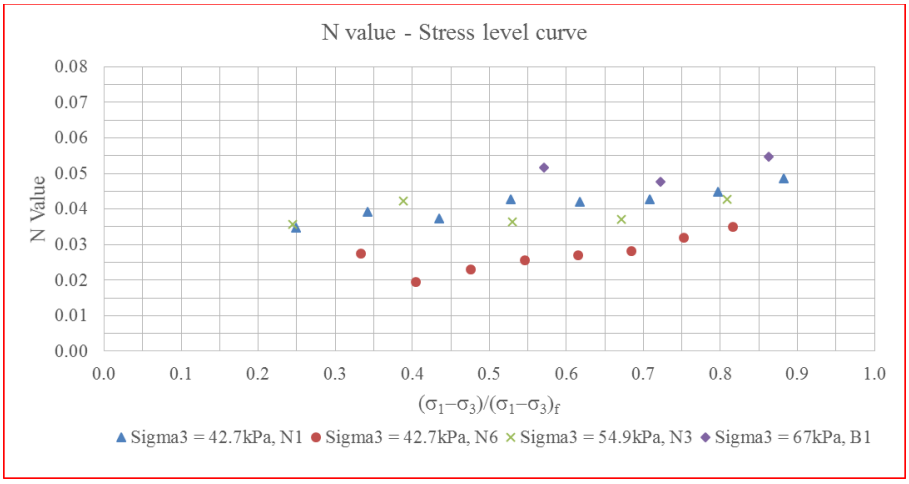

Figure 5-23. N value-stress level curve, high PI clay, triaxial creep test

5.4.4. Time to Creep Failure

Since the criterion of creep failure during triaxial UU creep test is critical strain for creep failure is exceeded, the minimum time to creep failure can be estimated with equation 5-2.

$$\frac{s_f}{s_0} \approx \frac{s_f}{s_1} = \left(\frac{t_f}{t_1}\right)^n \tag{5-2}$$

It is reasonable to approximate s_1 to s_0 because of the lagging adjustment of the test apparatus switching from strain control to stress control.

According to the normalization curve,

$$\frac{s_0}{s_f} = f\left(\frac{(\sigma_1 - \sigma_3)}{(\sigma_1 - \sigma_3)_f}\right) \tag{5-3}$$

Where,

s_0: Strain at the start point of creep ($t = 0\,\text{min}$);

s_f: Strain corresponding to onset of creep failure;

t_f: Time to creep failure;

$(\sigma_1 - \sigma_3)_f$: Estimated peak stress;

$(\sigma_1 - \sigma_3)$: Holding stress;

$\frac{(\sigma_1 - \sigma_3)}{(\sigma_1 - \sigma_3)_f}$: Stress level;

$f(\cdot)$: Function that represents the normalization curve.

In this case, the time to creep failure at any holding stress will depend on the n value, but also, to an important extent, on the stress level. The time to creep failure at any holding stress can be readily estimated for a given specific soil (figure 5-24), as long as the normalization curve (figure 5-19) and the n value versus stress level curves (figure 5-23) are acquired.

Creep failure can happen at any stress level as long as enough time is given. For duration of interest of engineering (50 years for example), the prerequisite for creep

failure is at a high stress level (>80% in this case) with a high n value (>0.04 in this case). Otherwise, it will take time longer than duration of interest of engineering for creep failure to happen. For TxDOT's design approach (stress level 33%) and most engineering design (stress level 50%), it will take more than 200 years for creep failure to happen. However, it will be a little arbitrary to draw the conclusion that deformation by creep will be negligible based on it.

Except the possibility of creep failure, long-term deformation is also a concern for engineers. Again, the value can be readily calculated given normalization curve, n value-stress level curve, stress level, and duration of interest of engineer (figure 5-25). Long-term deformation in figure 5-25 is expressed in terms of strain normalized by strain at failure, however, it can be converted into settlement/displacement, which will be presented in the chapter focusing on field test. At this moment, it will be convincing to draw the conclusion that long-term deformation by creep will be negligible for TxDOT's design approach.

It is worth to point out that there is a stress threshold for a selected time for creep failure, as plotted in figure 5-26. For example, the stress (or load) threshold for creep failure at 50yr with n value equal to 0.04 will be 76% of peak stress (or ultimate load).

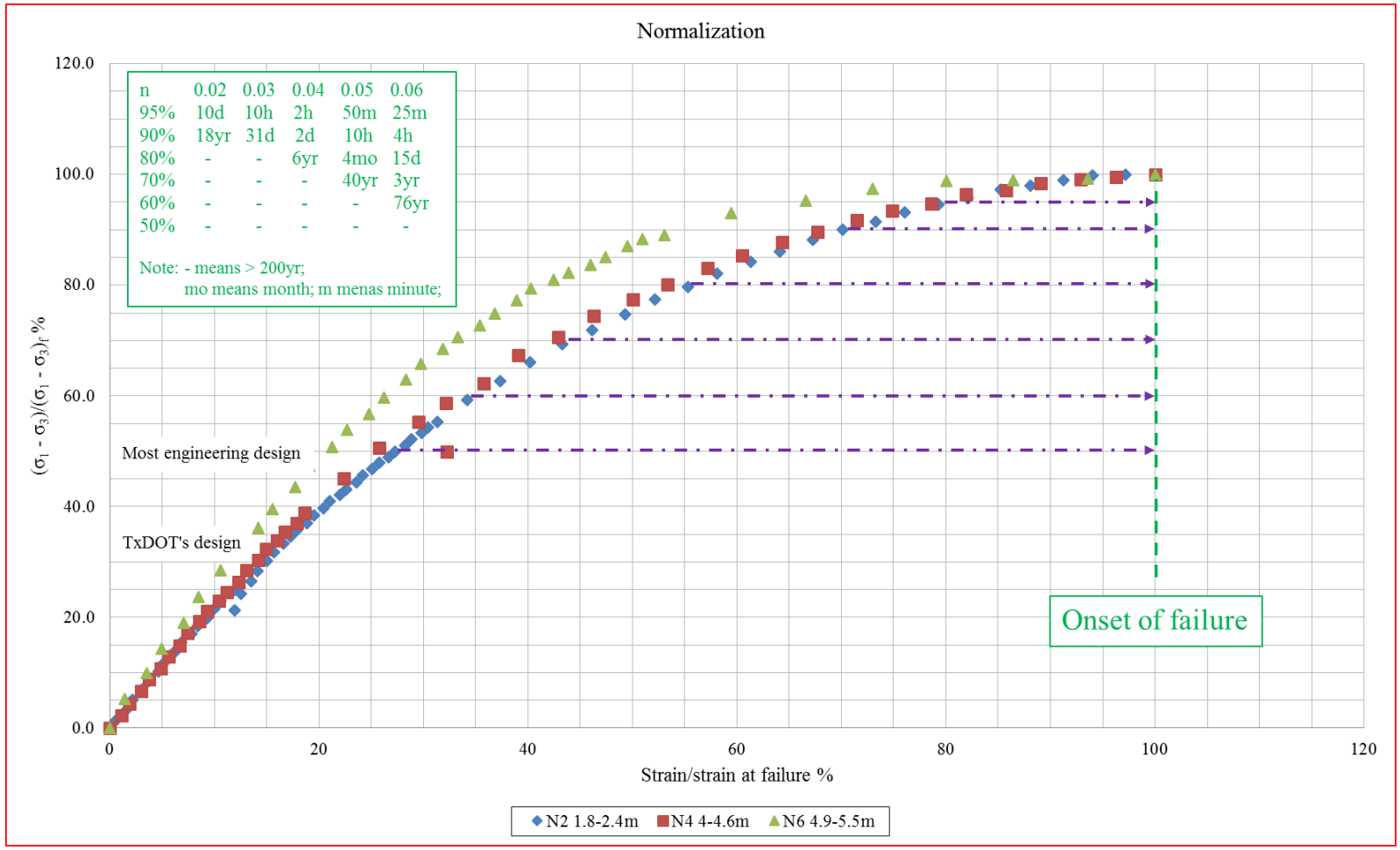

Figure 5-24. Forecasting the time to creep failure at any stress level with normalization curve and n value-stress level curve

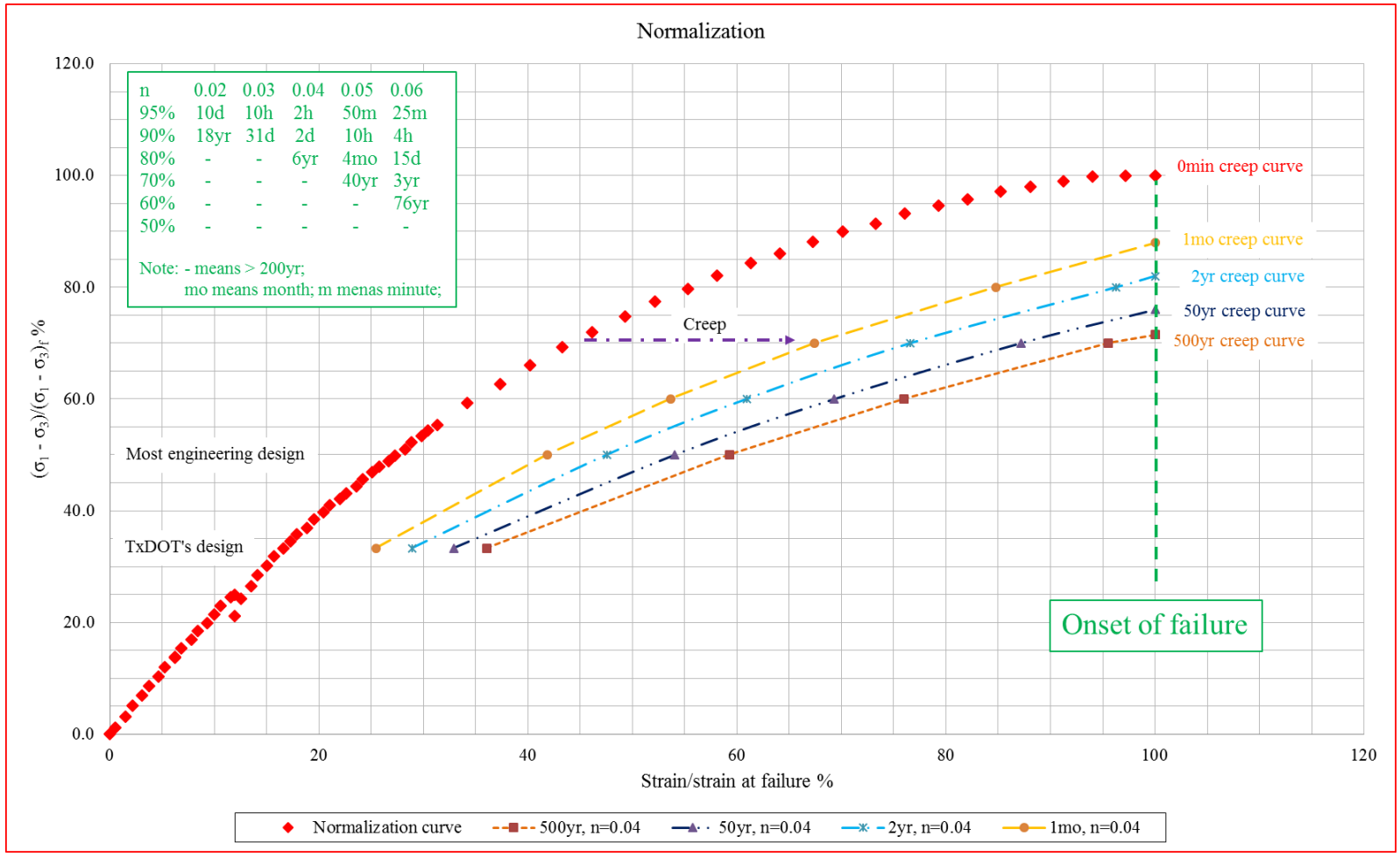

Figure 5-25. Long-term deformation predicted with normalization curve and n value-stress level curve

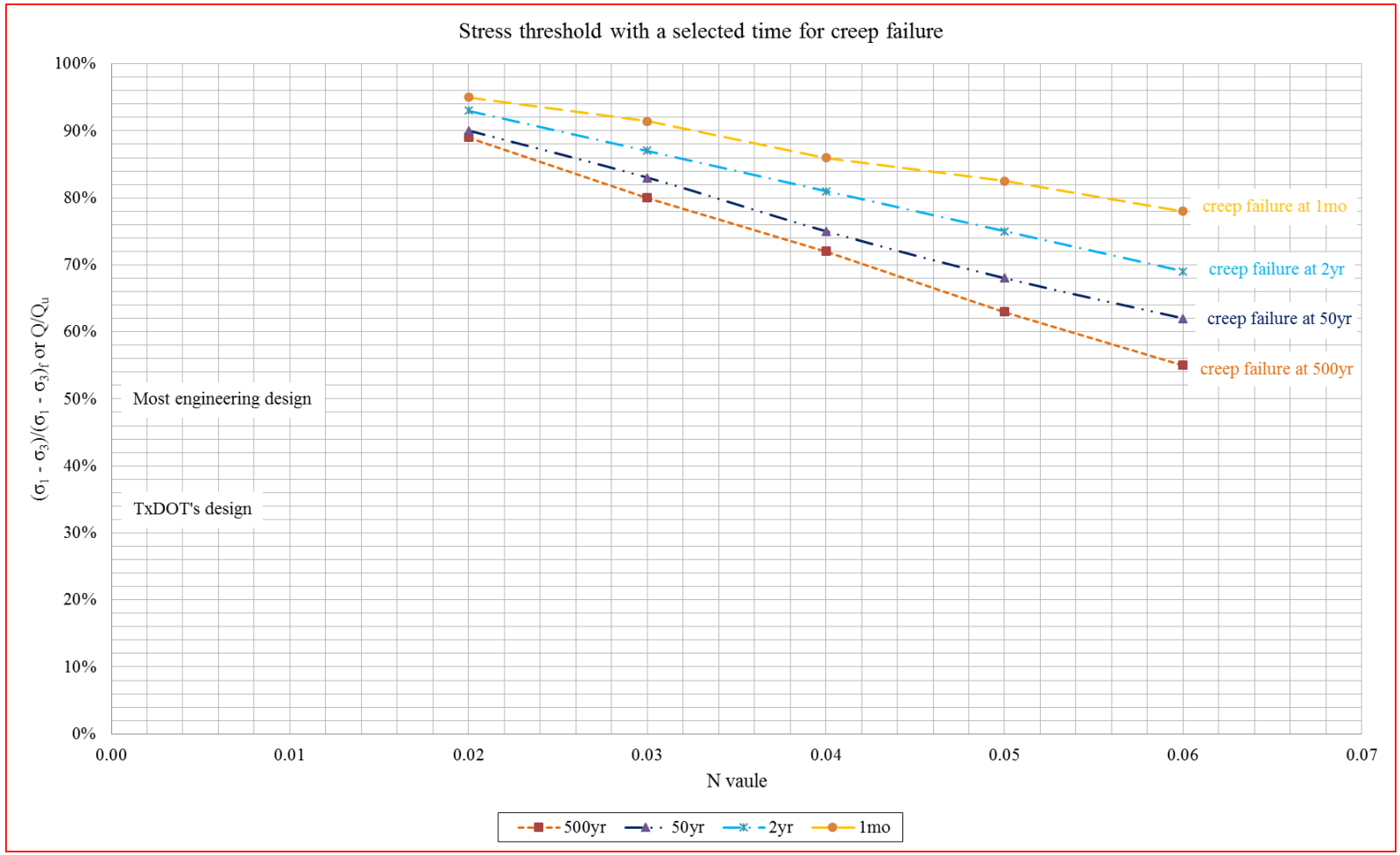

Figure 5-26. Stress threshold with a selected time for creep failure

Triaxial UU creep test on sample at depth 4.9~5.5m, borehole B1

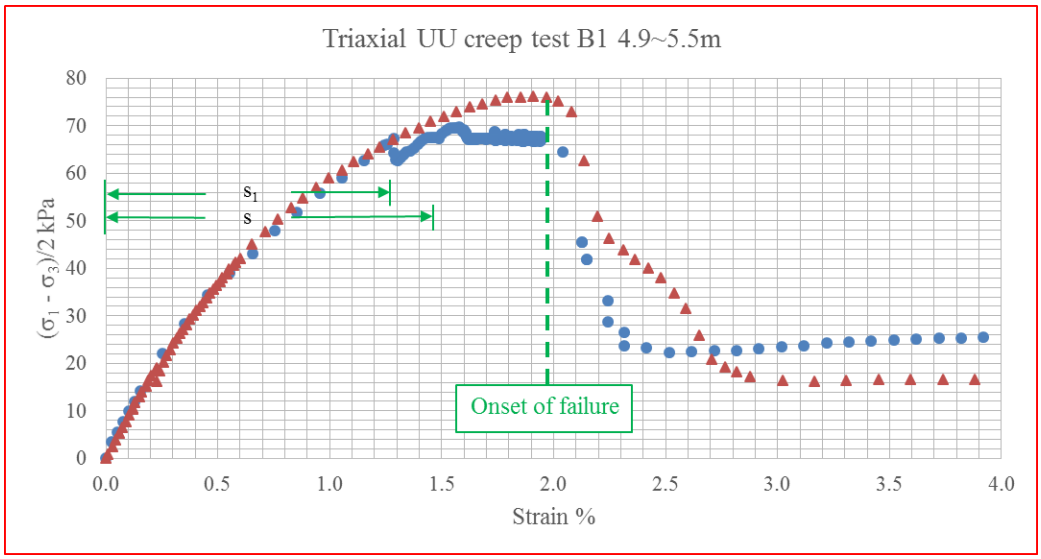

Figure 5-27. Creep failure at stress level 89.2% with 1 day duration of triaxial creep test, B1 4.9~5.5m

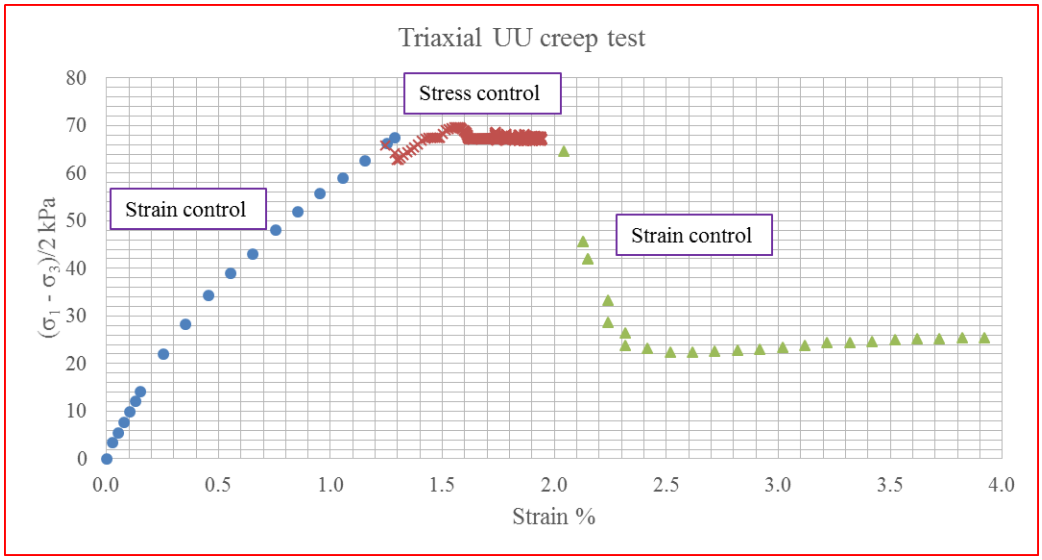

Figure 5-28. Stress-strain curve (including post-peak) of triaxial creep test, B1 4.9~5.5m

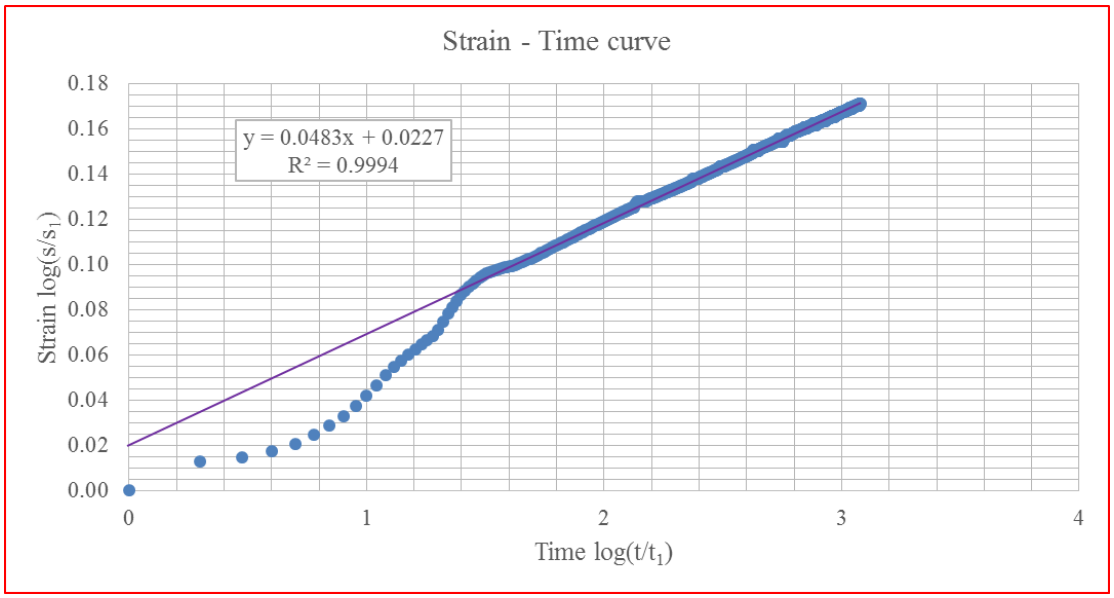

Figure 5-29. Strain-time curve (log-log scales), B1 4.9~5.5m, high PI clay, triaxial creep test

One more triaxial creep test was carried out to further demonstrate the previously analysis. The holding stress is 68kPa, and the estimated peak stress is 76.2kPa (figure 5-27), stress level is 89.2%. The duration of holding stress is 1 day, and the critical strain is reached (creep failure). At this time, switching back to strain control from stress control so that complete stress-strain curve including the post-peak curve is achieved (figure 5-28). The n value is 0.0483 by plotting the strain-time curve in log-log scales (figure 5-29).

5.4.5. Prestressing

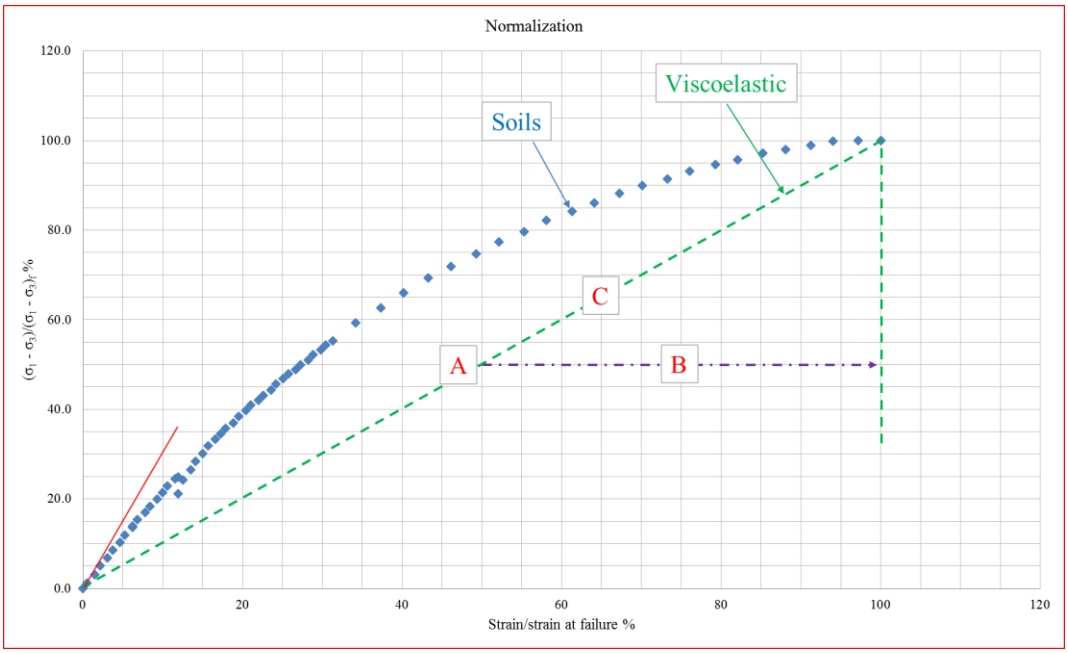

Figure 5-30. Creep behavior with/without prestressing for viscoelastic material

It is thought deformation caused by creep will significantly reduce by prestressing. For a viscoelastic material, considering two different loading protocols (figure 5-30):

Protocol one: loading to point A, then creep to point B;

Protocol two: loading to point C, then immediately unloading to point A, followed by creep to point B;

It is believed (also verified by test data) that creep behavior will be the same.

Thus, according to GEC#7 (FHWA, 2003), the design load is half of ultimate load. If prestressing with 20%, 40% and 50% higher than design load, then unloading to design load (figure 5-31), creep behavior after point C, point E and point G will be same

to behavior creep from point A without prestressing. It should be noted that it is based on the same s_1 (deformation at 1min after point A) used in the power law model regardless of prestressing or no prestressing.

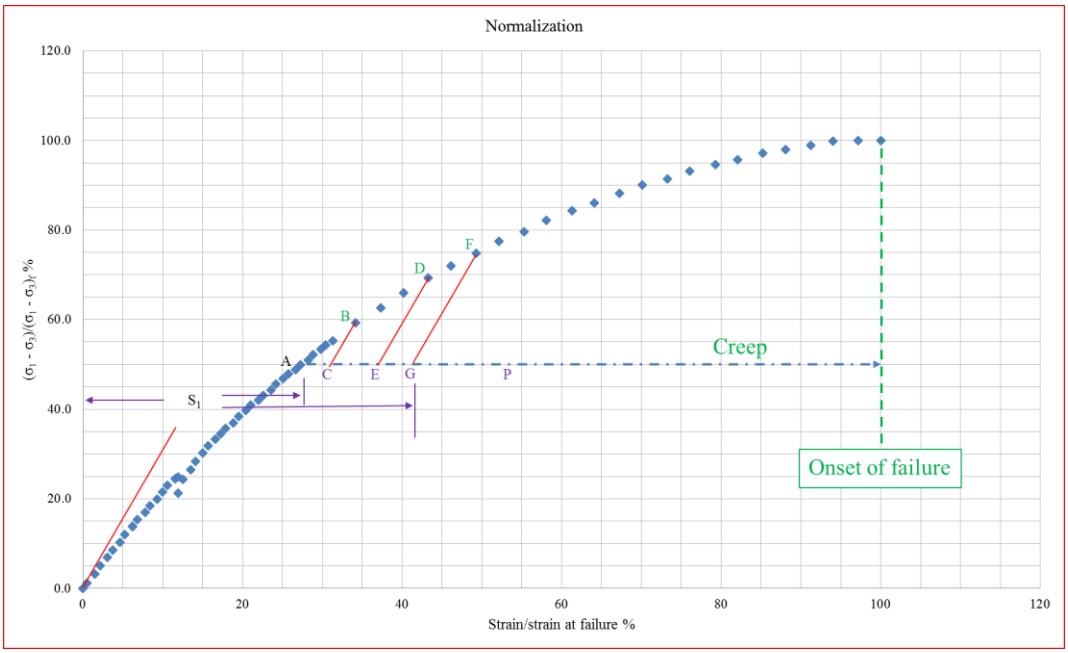

Figure 5-31. Creep behavior with prestress for high PI clay

However, there is another s_1 for the case of prestressing, for example, deformation at 1min after point G with prestressing ratio 50%. N value based on the latter s_1 has a relationship with n value based on the former s_1.

$$\frac{s_P}{(s_1)_A} = \left(\frac{t_p}{t_1}\right)^{n_A}$$
$$\frac{s_{G'}}{(s_1)_A} = \left(\frac{t_{G'}}{t_1}\right)^{n_A} \quad (5\text{-}4)$$
$$\frac{s_P}{(s_1)_G} = \left(\frac{t_p - t_{G'}}{t_1}\right)^{n_G}$$
$$s_{G'} = (s_1)_G$$

Where,

s_P: Deformation at prediction time t_p;

$s_{G'}$: Deformation at 1min after point G, also used as $(s_1)_G$;

$(s_1)_A$: Deformation at 1min after point A;

t_p: Prediction time, duration of interest of engineering;

t_1: Reference time, 1min after point A or point G;

$t_{G'}$: Reference time (1min), adding time from point A to point G, which is saved (skipped) by prestressing;

n_A: N valued based on $(s_1)_A$, deformation at 1min after point A;

n_G: N valued based on $(s_1)_G$, deformation at 1min after point A.

It will yield:

$$n_G = n_A \frac{\log\left(\frac{t_P}{t_{G'}}\right)}{\log\left(\frac{t_p - t_{G'}}{t_1}\right)} \quad (5\text{-}5)$$

It says that n_G will be largely related to n_A, $t_{G'}$ (i.e., prestressing ratio) and t_p (i.e., duration of interest of engineering). On one hand, if prestressing ratio is too small that $t_{G'}$ is slightly larger than t_1, n_G will be close to n_A with a large t_p. On the other hand, if prestressing ratio is pretty high that $t_{G'}$ (for instance, 2yr) is tremendously larger than t_1, n_G will be close to zero with a t_p slightly larger than $t_{G'}$ (for instance, 2yr plus 1d).

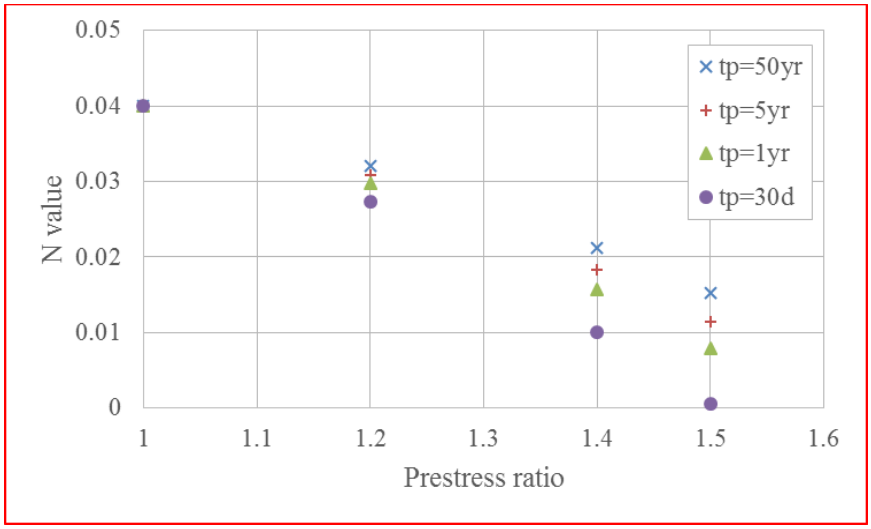

Figure 5-32. n_G versus $t_{G'}$ (prestressing ratio) and t_p (duration of interest of engineering)

For n_A equal to 0.04, with prestressing ratio 50%, after duration of 50yr, n_G is only 0.015 (figure 5-32). It should be noted that n_G is not constant, in general, it increases with t_p, while decreasing with $t_{G'}$.

$t_{G'}$ with two different prestressing ratio (50% and 20%) is calculated in table 5-1 and table 5-2 for the range of n_A. The criterion of creep failure in GEC#7 (FHWA, 2003, 2015) is creep movement less than 1mm between 1min and 10min readings (i.e., 1mm/per log cycle). The third column to the ninth column is strain (normalized by strain corresponding to peak stress) after 1 log cycle (i.e., reading between 1min and 10min) to 7 log cycle (i.e., reading between 1min and 200yr). As mentioned earlier, strain/per log cycle can be converted into movement/per log cycle to be compared to GEC#7, which will be presented in the chapter focusing on field test.

Table 5-1. $t_{G'}$ with prestressing ratio 50%

N value	AG, time	After G, strain difference/log cycle						
		10min	100min	1w	10w	2yr	20yr	200yr
		1 log cycle	2 log cycle	3 log cycle	4 log cycle	5 log cycle	6 log cycle	7 log cycle
0.02	>200yr	4.937E-11	5.431E-10	5.48E-09	5.485E-08	5.486E-07	5.484E-06	5.468E-05
0.03	2.5yr	8.482E-08	9.329E-07	9.411E-06	9.388E-05	0.0009092	0.0070644	0.0275107
0.04	27d	3.827E-06	4.204E-05	0.0004196	0.0037999	0.0215642	0.05792	0.1025536
0.05	3.3d	3.953E-05	0.0004309	0.0040007	0.0242168	0.0692314	0.1268423	0.1924645
0.06	0.8d	0.0001934	0.0020531	0.0157896	0.060247	0.1270674	0.2065552	0.2981557

Table 5-2. $t_{G'}$ with prestressing ratio 20%

N value	AC, time	After C, strain difference/log cycle						
		10min	100min	1w	10w	2yr	20yr	200yr
		1 log cycle	2 log cycle	3 log cycle	4 log cycle	5 log cycle	6 log cycle	7 log cycle
0.02	850min	6.498E-05	0.0006804	0.0048341	0.0161346	0.0309602	0.0469281	0.0636971
0.03	90min	0.0008779	0.0069147	0.0239277	0.0469221	0.0722927	0.0995599	0.1287861
0.04	29min	0.0032485	0.0185345	0.0469219	0.0808972	0.1185092	0.1597898	0.2050575
0.05	15min	0.0070472	0.0322639	0.0716583	0.1179448	0.1701309	0.2287131	0.2944466
0.06	9.5min	0.0117847	0.047002	0.098027	0.1583671	0.2278581	0.3076688	0.3993066

5.5. Triaxial UU Creep Test on Low PI Clay

5.5.1. Test Results

Test results of one low PI clay specimen were used here for illustration.

The stress-strain curve of triaxial UU creep test on low PI clay specimen was plotted in figure 5-33. Actually, the test is constant load control instead of constant stress control, so when the strain is quite large (10% for example), stress during the creep seems to drop down in figure 5-33. The strain-time curves under all holding stresses were plotted in figure 5-34 and figure 5-35. Creep failure didn't happen, and n value-stress level curve of two tests was plotted in figure 5-36. The n value is acquired by plotting the model (equation 3-10) in log-log scales (figure 5-37).

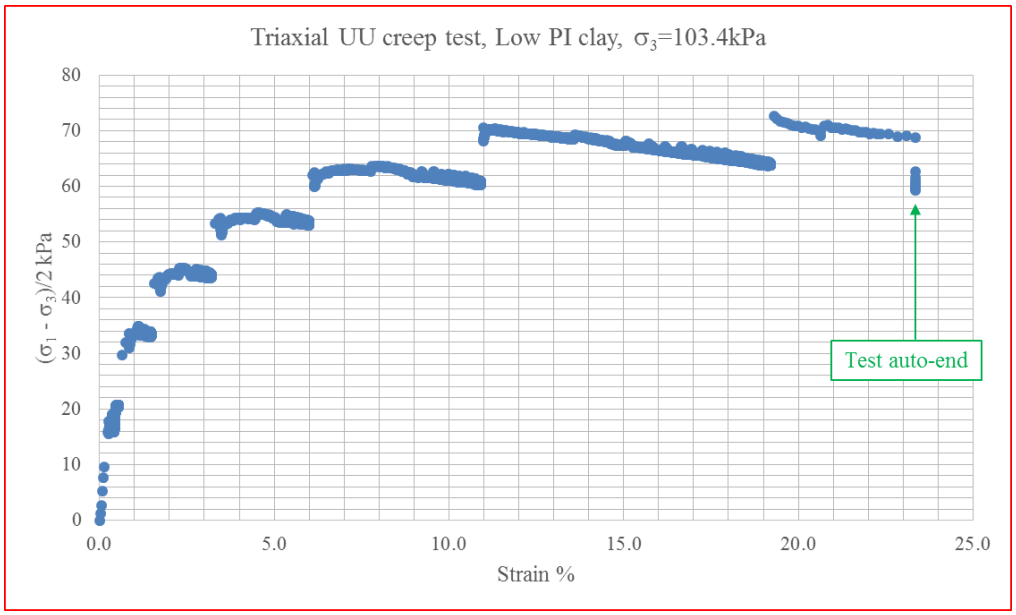

Figure 5-33. Stress-strain curve, σ_3=103.4kPa, low PI clay, triaxial creep test

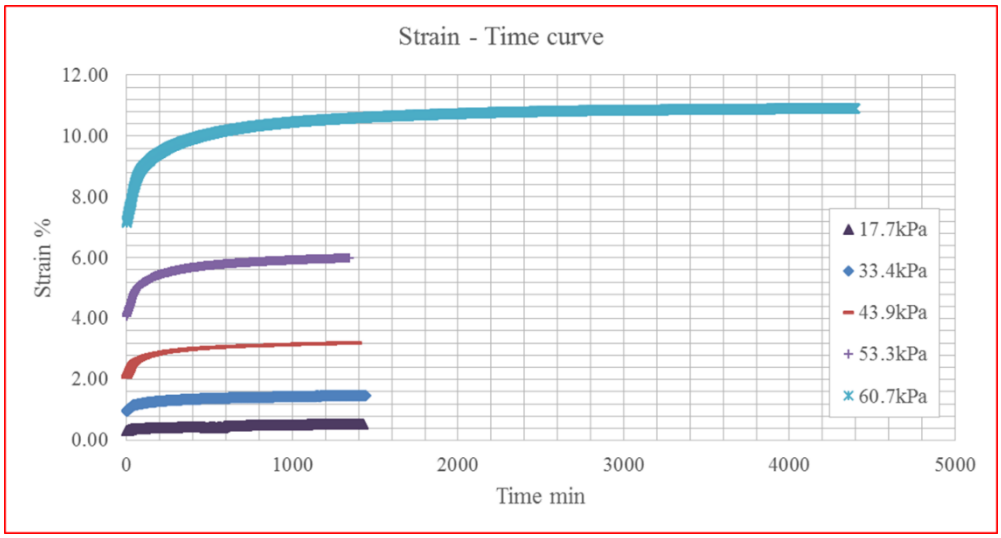

Figure 5-34. Strain-time curves, σ_3=103.4kPa, low PI clay, triaxial creep test

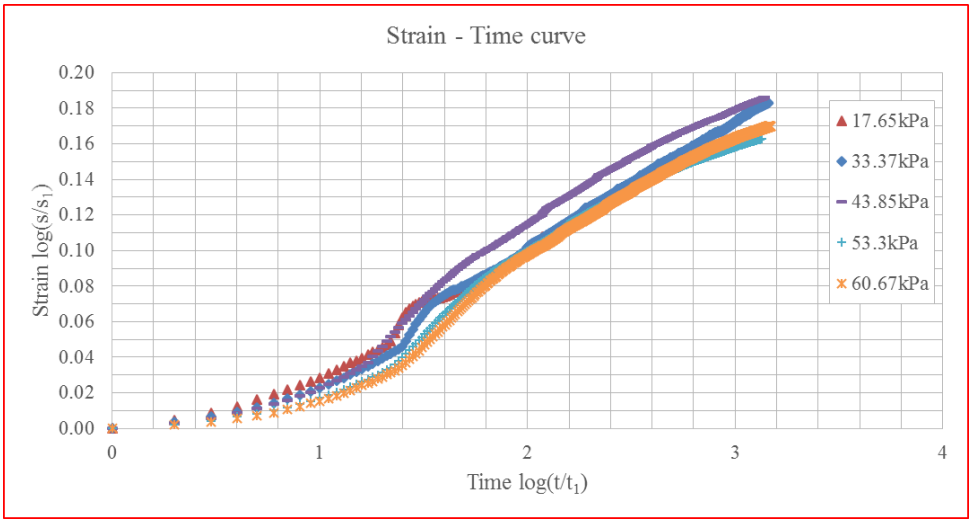

Figure 5-35. Strain-time curves (log-log scales), σ_3=103.4kPa, low PI clay, triaxial creep test

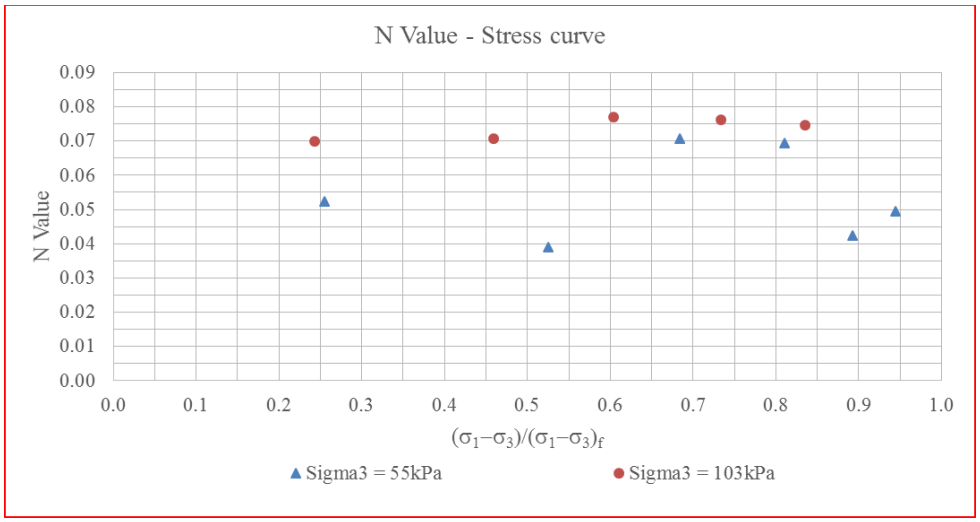

Figure 5-36. N value-stress level curve, low PI clay, triaxial creep test

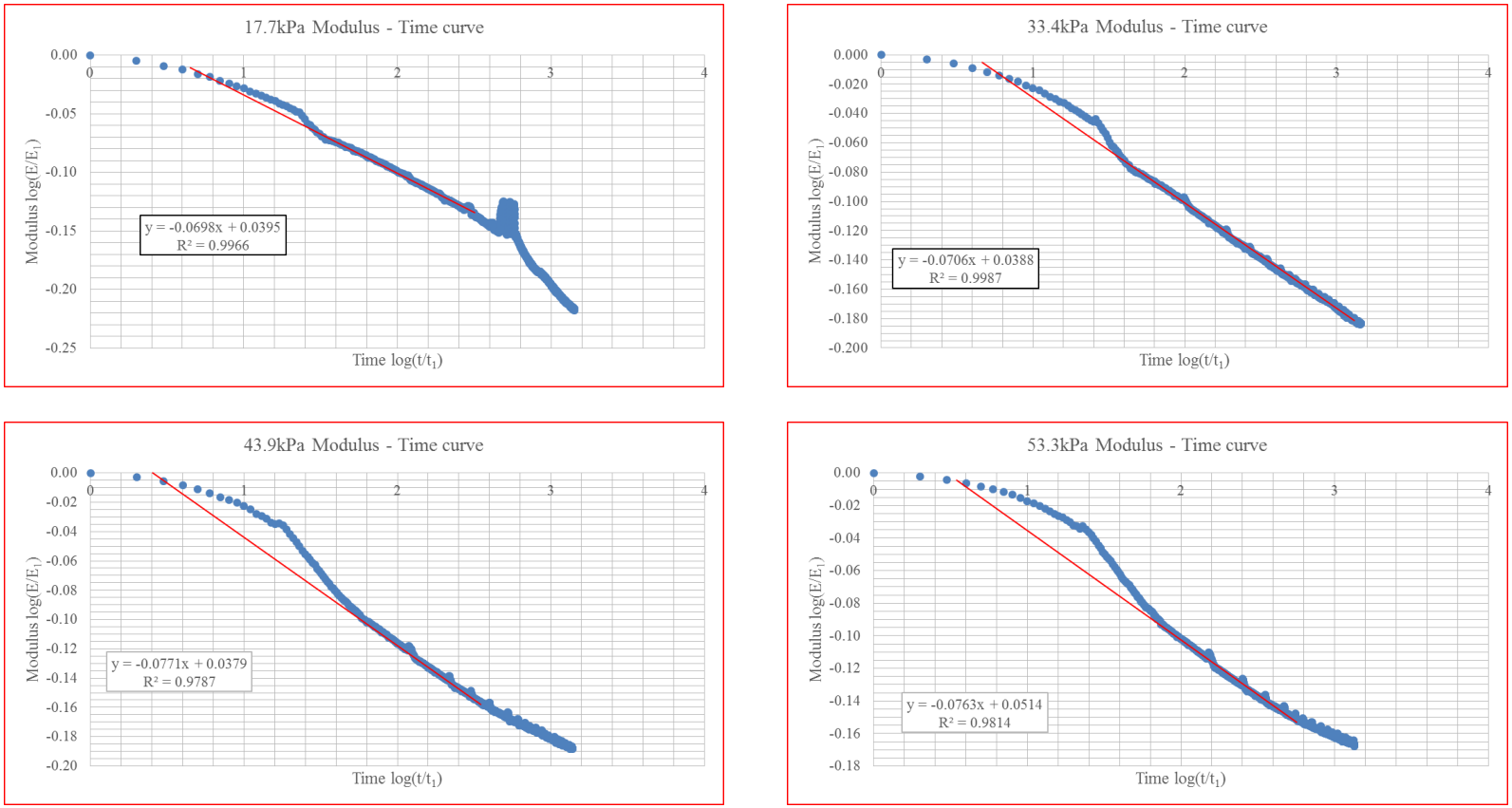

Figure 5-37. Modulus-time curves at any stress, σ_3=103.4kPa, low PI clay, triaxial creep test

5.5.2. Prestressing

Test results of one low PI clay specimen were used here for illustration.

The stress-strain curve of triaxial creep test on low PI clay specimen with prestressing was plotted in figure 5-38. In total there are four prestressing (figure 5-39 and table 5-3). Because the prestressing ratio is so small (5% and 10%), saved time (i.e., $t_{G'}$ minus reference time) is also small. To note, t_p is 1d plus saved time.

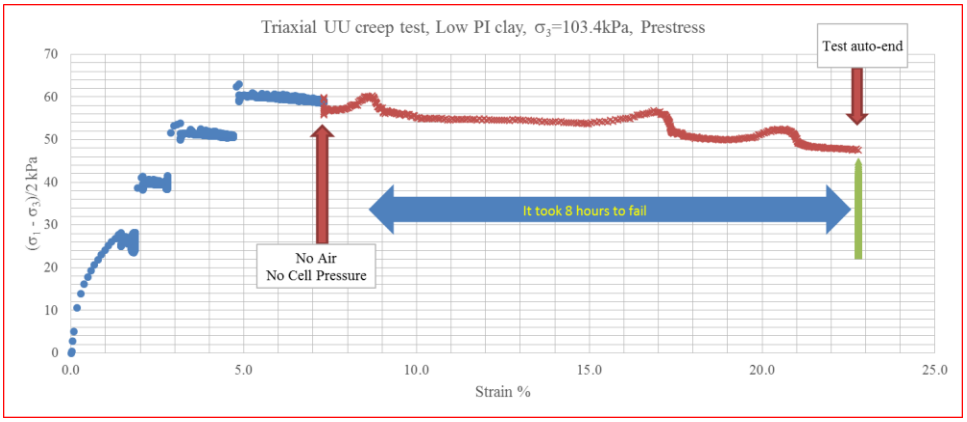

Figure 5-38. Stress-strain curve, σ_3=103.4kPa, low PI clay, triaxial creep test, prestressing

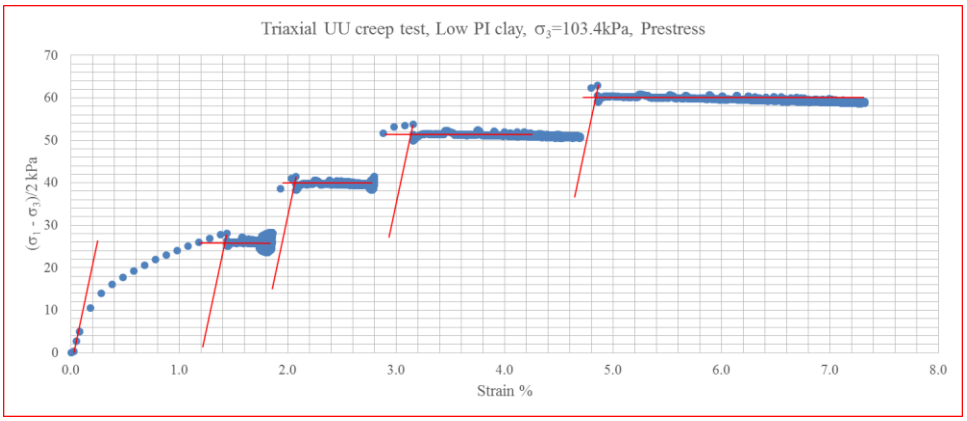

Figure 5-39. Low PI clay, triaxial creep test, prestressing

Table 5-3. Prestressing ratio and time saved

Prestress kPa	Holding stress kPa	Stree level	Time min
28.2	25.9	109	47
41.4	39.6	105	4
53.8	50.8	106	5
63	60	105	2

As mentioned in section 5.4.5, creep behavior after prestressing has two s_1, strain-time curves of s_1 two are plotted in figure 5-40, where s_1 of the curve named "original" is deformation at 1min after point G (see figure 5-31), and s_1 of the curve named "revised" is deformation at 1min after point A (see figure 5-31). It is worth noting that strain-time curve at 25.9kPa on the top left corner of figure 5-31, the shape of revised curve is curving to another direction. It is because the time saved (47min) is larger than

the lagging adjustment time of the test apparatus (20~30min) that the curve is collapsing in the x-axis.

N value-stress level curves are plotted in figure 5-41. There are two n values, namely, n_A and n_G (see equation 5-5 and figure 5-31). It should be noted that n_A (named "revised" in figure 5-41) with prestressing is close to, if not same to, n_A without prestressing (figure 5-36). It supports the idea that creep behavior after point G with prestressing and without prestressing (figure 5-30) will be the same if the same s_1 is chosen (i.e., deformation at 1min after point A).

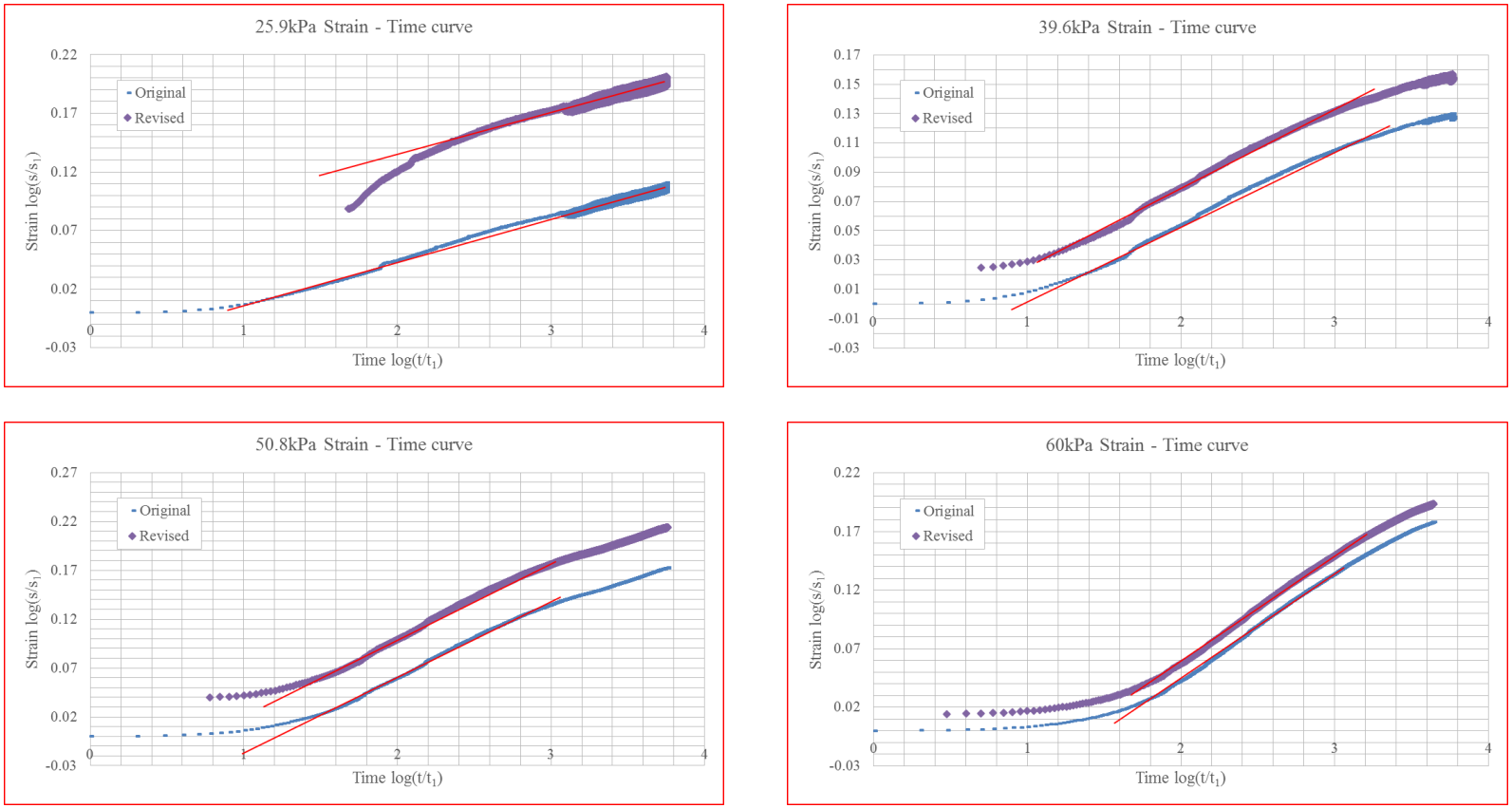

Figure 5-40. Strain-time curves with two s_1, low PI clay, triaxial creep test, prestressing

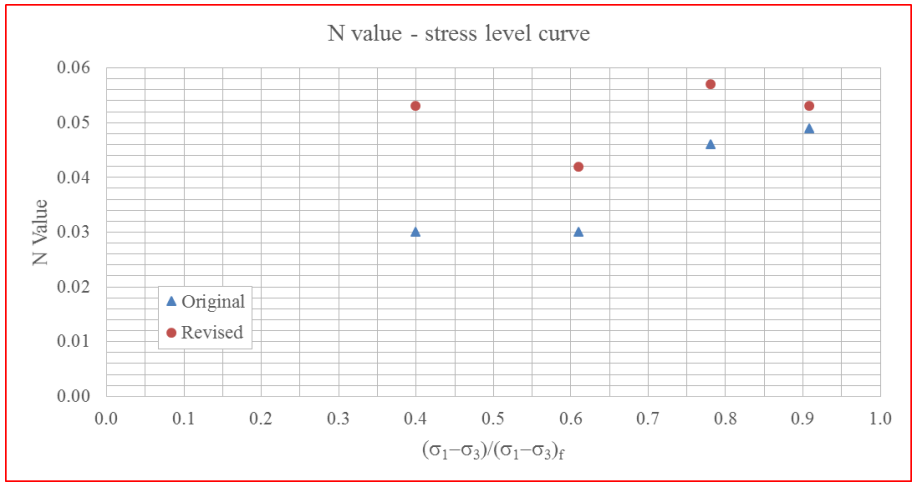

Figure 5-41. N value-stress level curve, low PI clay, triaxial creep test, prestressing

5.6. Triaxial Creep Test on Dry Sand

5.6.1. Test Results

The stress-strain curve of triaxial creep test on dry clay specimen was plotted in figure 5-42. The strain suddenly increased from 2% to 4.8% at 174.6kPa. This increase released the strain energy which resulted in a much lower n value than usual. Besides, similar to prestressing, there are two n values by choosing two different s_1: one is deformation at 1min after 4.8% while the other is deformation at 1min after 4.8% minus the increase from 2% to 4.8%.

The strain-time curves under all holding stresses were plotted in figure 5-43 and figure 5-44. It should be noted s_1 is chosen at deformation at 1min after 4.8% minus the increase from 2% to 4.8% is chosen to plot strain-time curves at 174.6kPa and 198.5kPa in figure 5-44. N value-stress level curve is plotted in figure 5-45. The n value is

acquired by plotting the model (equation 3-10) in log-log scales (figure 5-46 and figure 5-47).

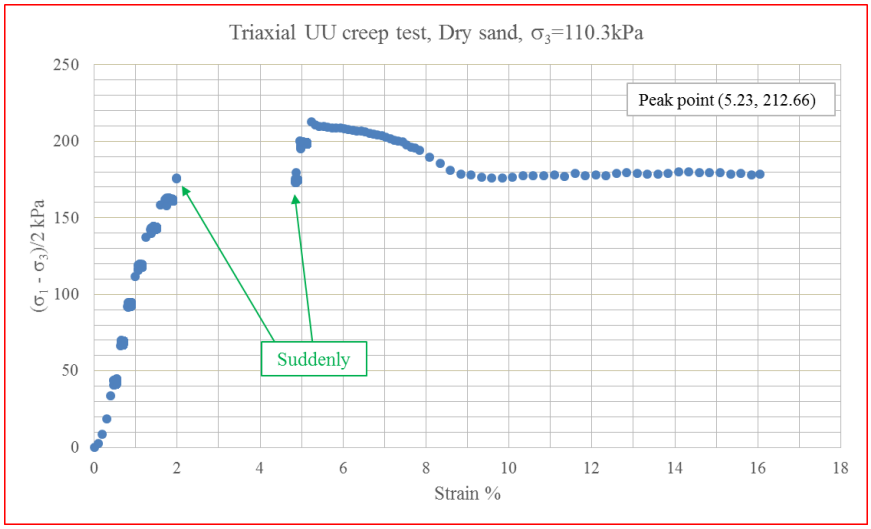

Figure 5-42. Stress-strain curve, σ_3=110.3kPa, dry sand, triaxial creep test

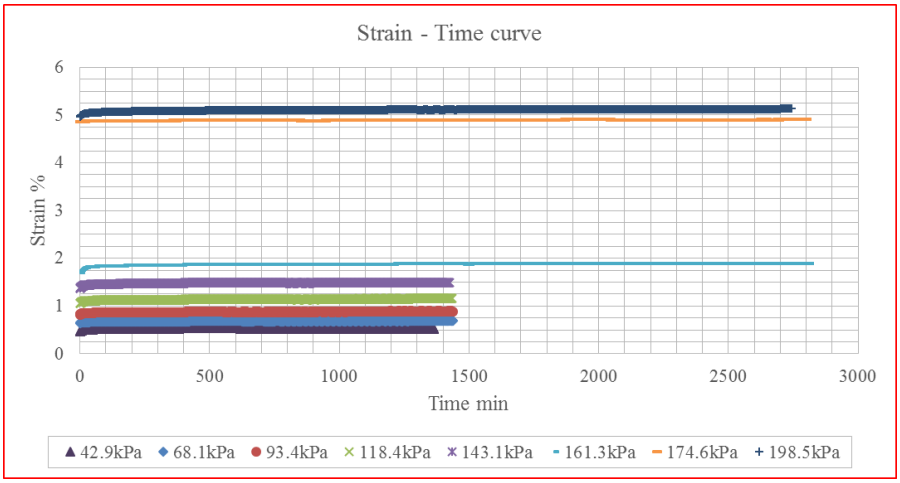

Figure 5-43. Strain-time curves, σ_3=110.3kPa, dry sand, triaxial creep test

Strain-time curve in left side of figure 5-46 is based on s_1 deformation at 1min after 4.8% (named "original" in figure 5-45), while right side of figure 5-47 is based on s_1 deformation at 1min after 4.8% minus the increase from 2% to 4.8% (named "revised" in figure 5-45). It is found that the release of strain energy mainly impact the current stress level, while n value at higher stress level recovers to normal range.

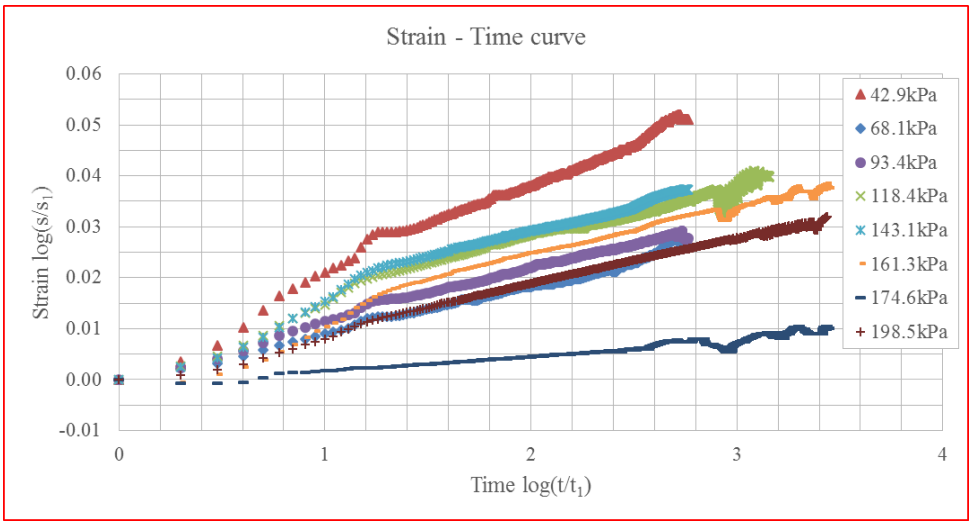

Figure 5-44. Strain-time curves (log-log scales), σ_3=110.3kPa, dry sand, triaxial creep test

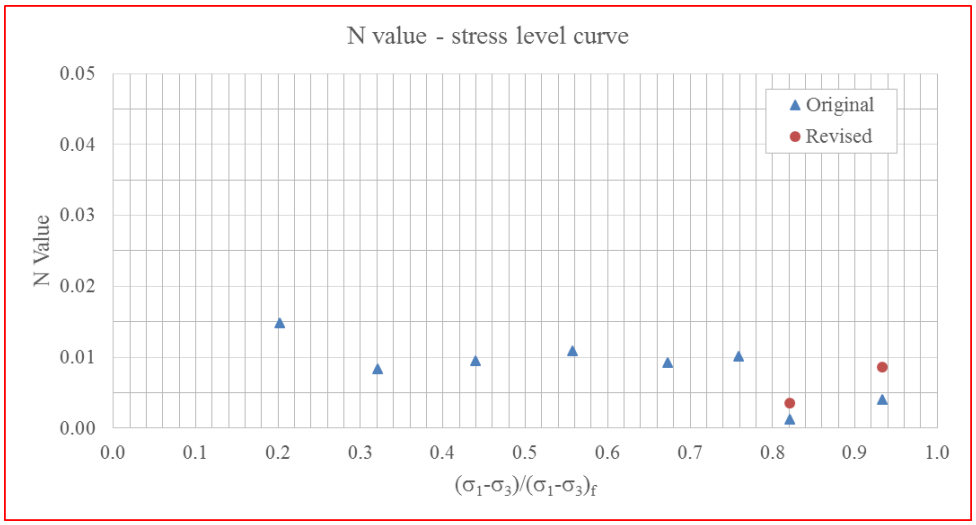

Figure 5-45. N value-stress level curve, dry sand, triaxial creep test

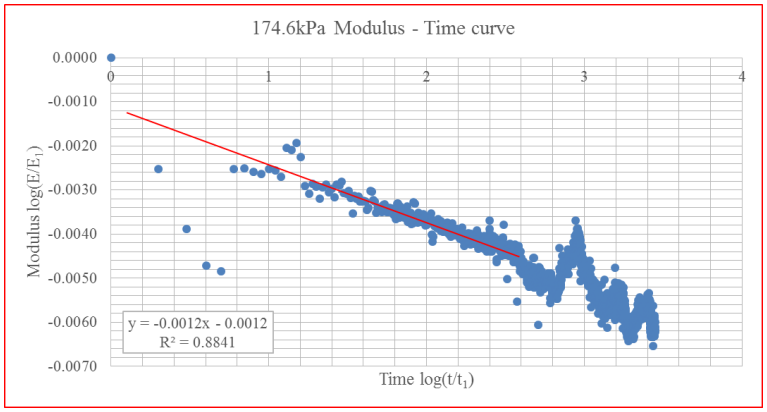

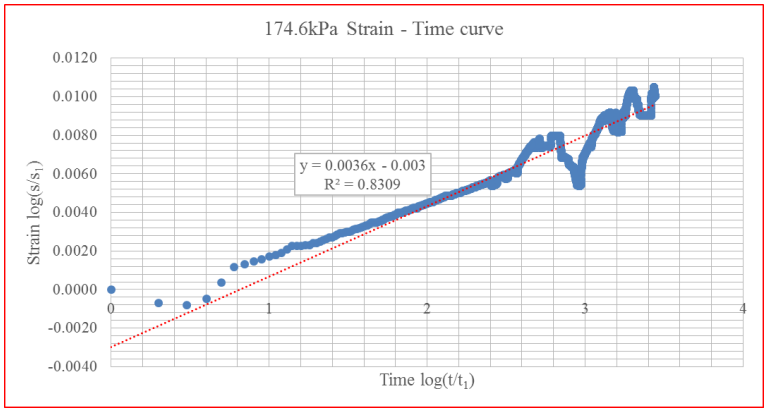

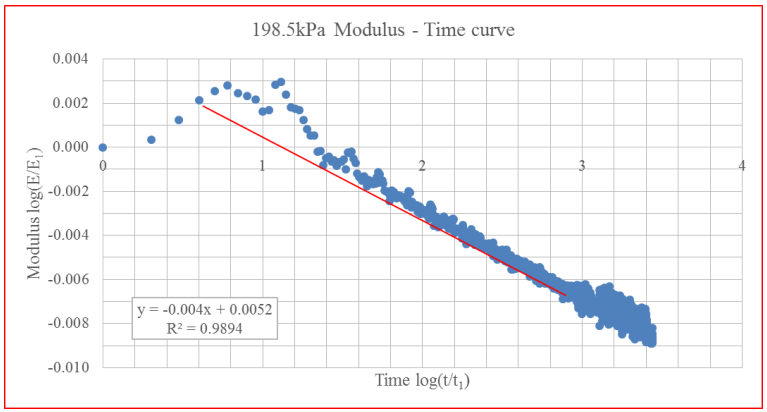

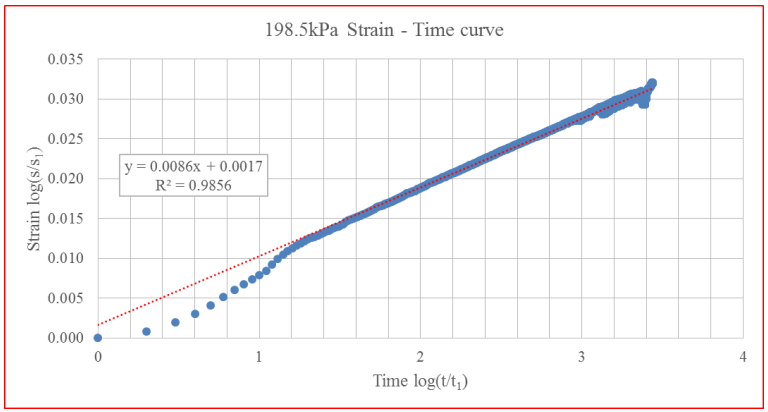

Figure 5-46. N value at 174.6kPa and 198.5kPa with two different s_1

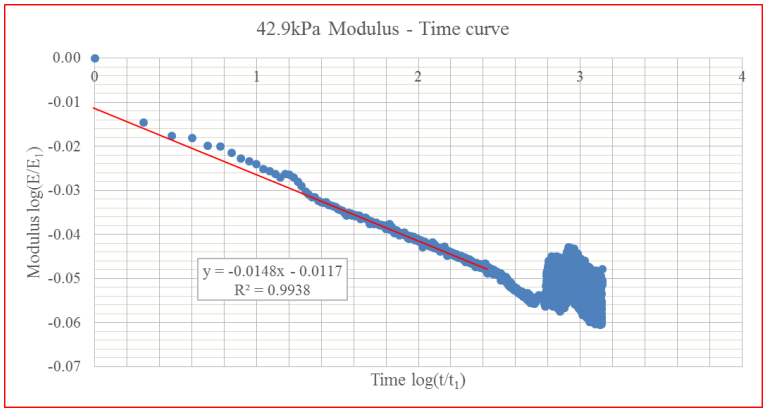

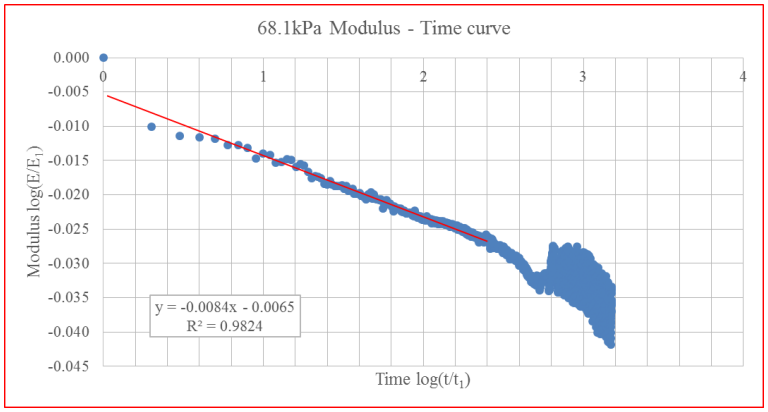

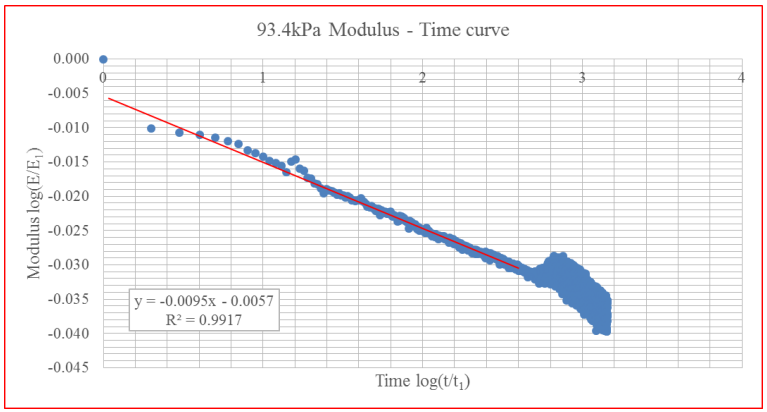

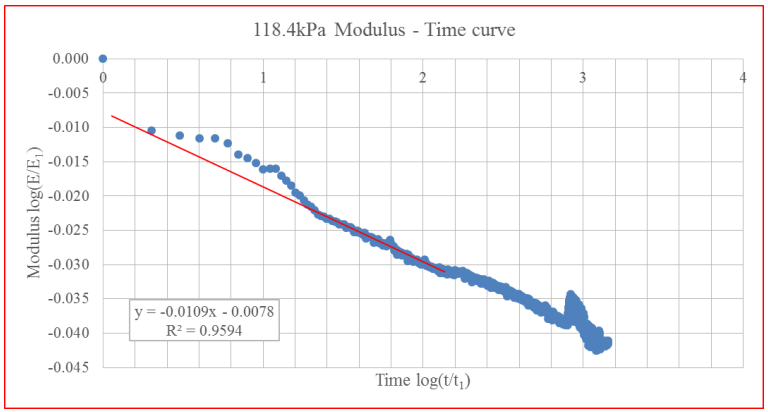

Figure 5-47. Modulus-time curves at any stress, σ_3=110.3kPa, dry sand, triaxial creep test

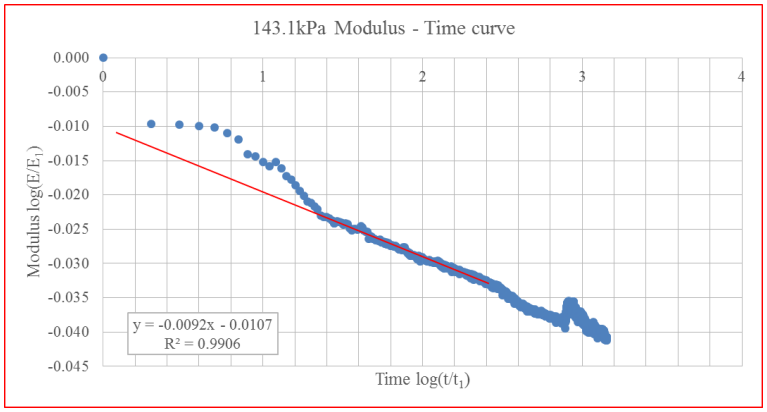

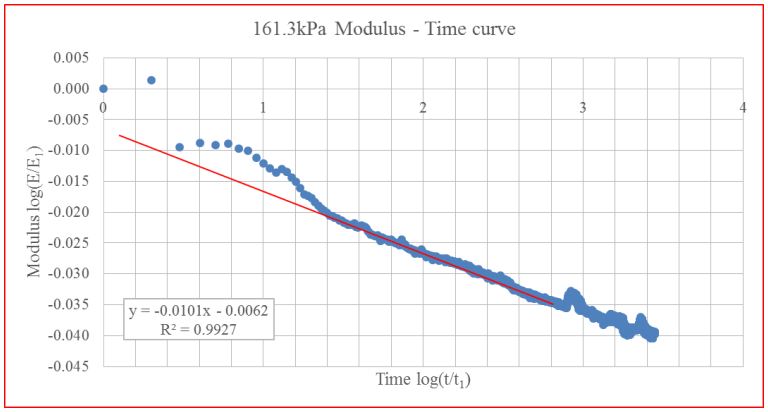

Figure 5-47 Continued

N value from four triaxial creep tests on dry sand are plotted in figure 5-48. The range is 0.005~0.02 with average 0.01.

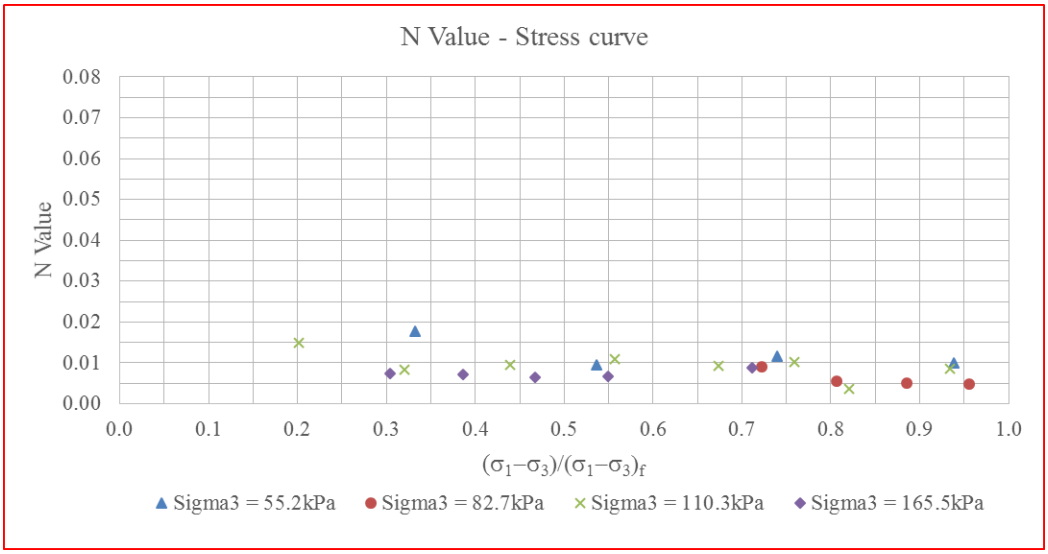

Figure 5-48. N value-stress level curve, dry sand, triaxial creep test

5.6.2. Prestressing

Test results of one dry sand specimen were used here for illustration.

The stress-strain curve of triaxial creep test on dry sand specimen with prestressing was plotted in figure 5-49. In total there are two prestressing (figure 5-50). The loading protocol is loading to 60.1kPa then unloading to 51.3kPa (i.e., prestressing) followed by loading back to 60kPa (holding 1d), then continues loading to 80.7kPa then unloading to 72.1kPa (i.e., prestressing) followed by loading back to 80.7kPa (holding 1d). However,

saved time of the first prestressing is 4mo, and saved time of the second prestressing is 5yr. Because of $t_p - t_{G'}$ is just 1d, deformation caused by creep at low stress level is so small that is not caught by the test apparatus (left side of figure 5-51).

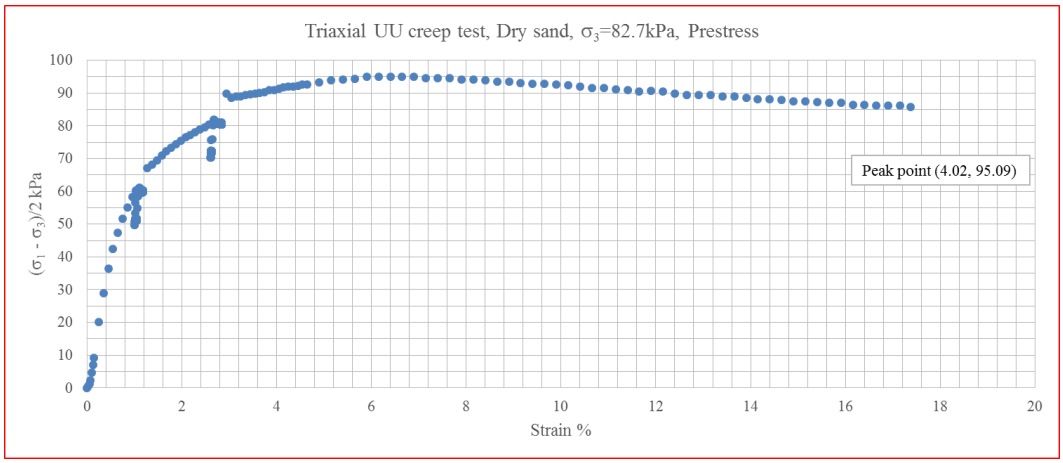

Figure 5-49. Stress-strain curve, σ_3=82.7kPa, dry sand, triaxial creep test, prestressing

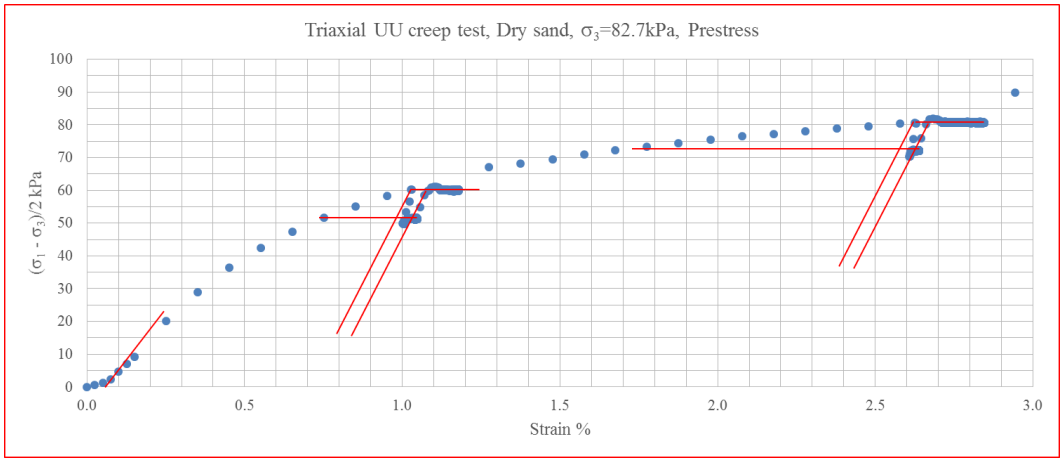

Figure 5-50. Dry sand, triaxial creep test, prestressing

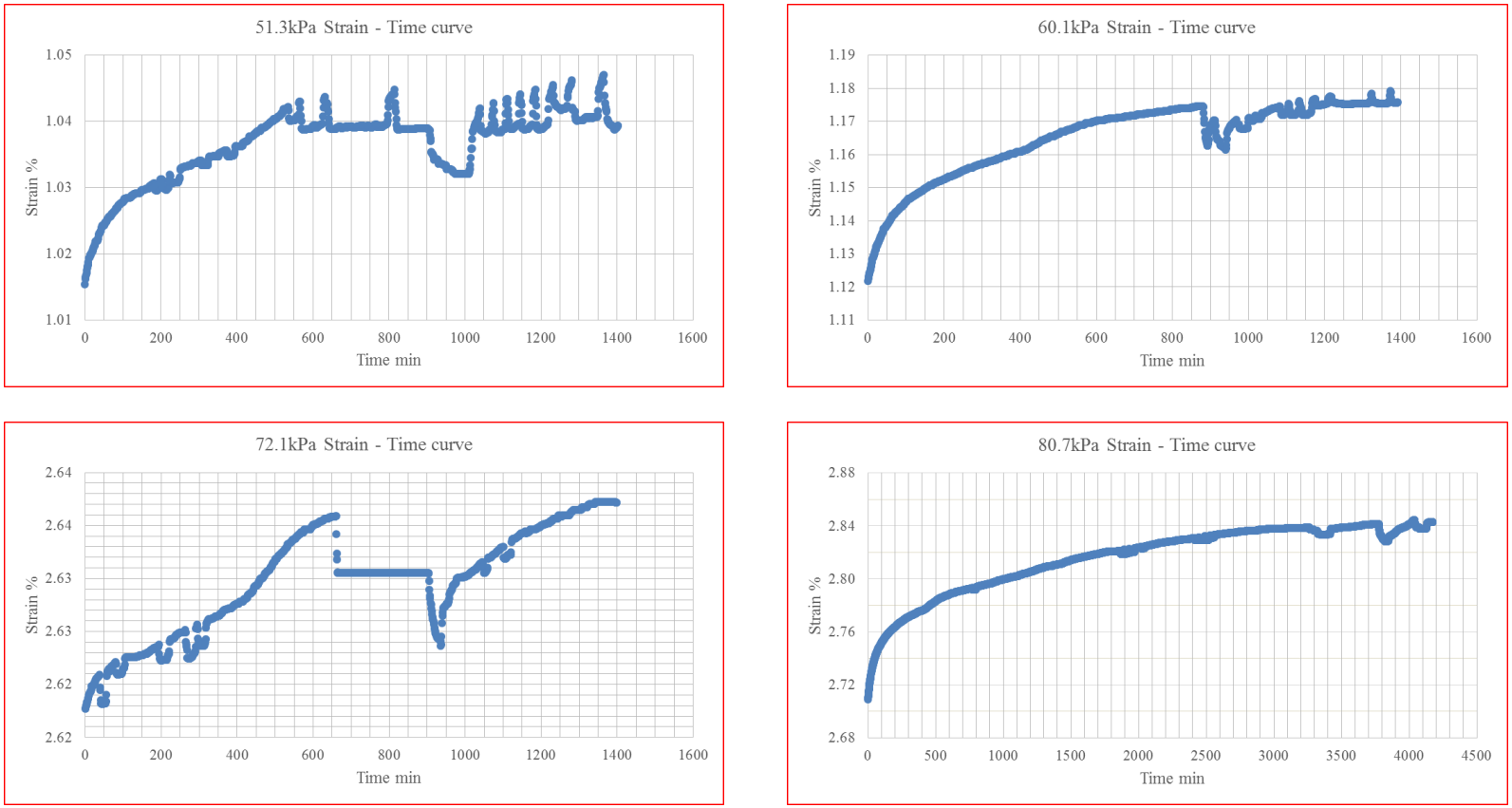

Figure 5-51. Strain-time curve, dry sand, triaxial creep test, prestressing

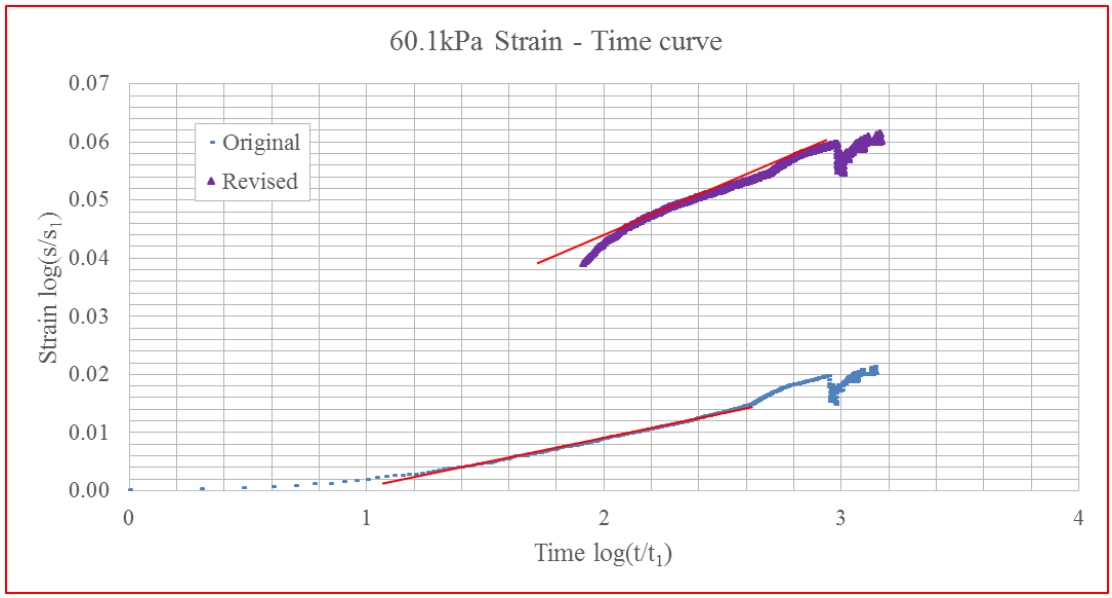

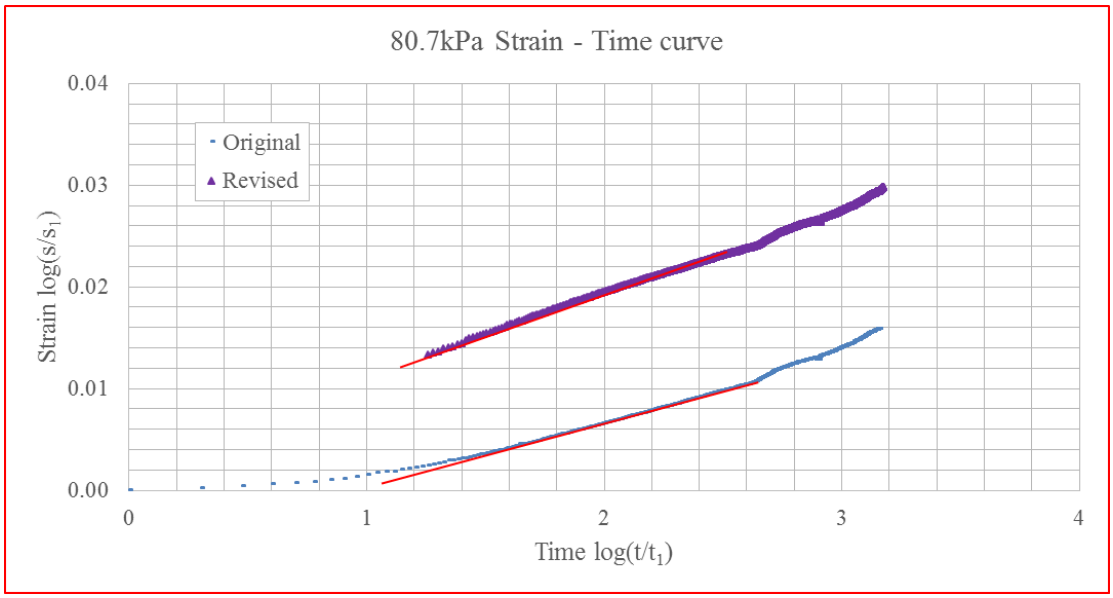

Figure 5-52. Strain-time curve at high stress level, two different s_1

When it loads back to high stress level, creep behavior is recovered. However, part of strain energy is released during this unload-reload cycle, there will be two s_1 here,

thus, two n values (figure 5-52 and figure 5-53). The first s_1 is associated with the first time loading to high stress level, the second s_1 is associated with the second time loading to high stress level. Between these two loading, there is one unload-reload cycle and creep at low stress level (though it is negligible). Again, n value based on the first is close to, if not same to, the range of n value (figure 5-48) without impact from this unload-reload cycle. The impact of unload-reload cycle on n value will be studied in detail in the chapter of field test.

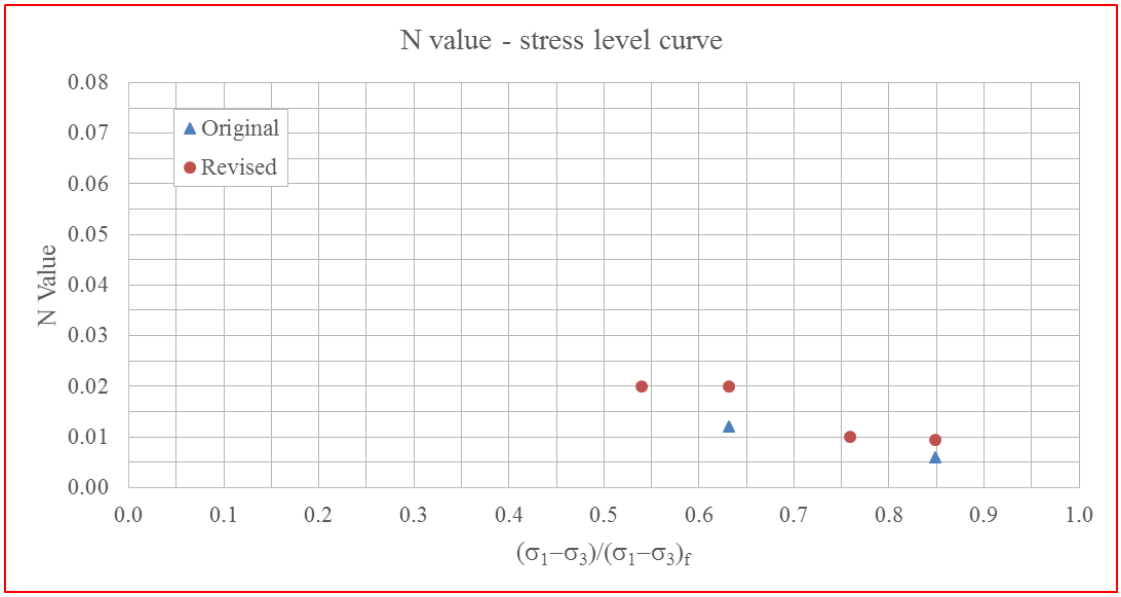

Figure 5-53. N value-stress level curve

5.7. Triaxial Creep Test versus 1D Test

By comparing n value from triaxial creep tests in Chapter five with n value from 1D tests in Chapter four, it is found that n_{cr} from triaxial creep tests is much larger than that from 1D tests. The difference may be caused by the different confining boundary between triaxial tests and 1D tests. Strain in triaxial tests is more due to deviatoric stress, while strain in 1D tests is more due to hydrostatic stress.

5.8. Conclusion

In this chapter the proposed power law model was applied to triaxial creep test on high PI clay, low PI clay and dry sand. Several findings are made below:

- The proposed power law model is feasible to represent time dependent behavior in triaxial creep test, while modulus-time curve (or strain-time curve) will be a straight line and slope of the line is n value, exponent in the model;
- It is found that there is a quite unique curve (named “normalization curve”) to describe stress-strain curve until the peak stress for a given soil. It can be used to estimate peak stress in triaxial creep test when creep failure happens that results in the peak stress is unknown. It should be noted that estimated peak stress is obtained by multiplying peak stress from conventional triaxial shear test by a ratio, and in most cases this ratio is not equal to unit which previous researchers implicitly assumed it to be unit;

- N value at different holding stresses could be compared by normalizing holding stresses over estimated peak stress, and n value-stress level curve is plotted. It is found that n value is in virtually independent of stress level;
- Not only the possibility of creep failure at any stress level could be predicted based on normalization curve and n value-stress level curve, but also creep curve after any duration (50yr creep curve for example) at any stress level could be forecasted. It should be noted the criterion of creep failure is to exceed critical strain, namely, strain corresponding to estimated peak stress (again, critical strain is obtain by strain corresponding to peak stress from conventional triaxial shear test multiplying a ratio). Meanwhile, creep failure can happen at any stress level as long as enough time is given, which means there is no stress threshold. However, the time of interest of engineering maybe 100yr in maximum, there will be a stress level corresponding to this duration;
- It is found that one way to reduce long-term deformation caused by creep is prestressing. N value with prestressing and without prestressing (n_A) will be the same if the same s_1 is chosen (s_1 corresponding to the first time to reach current stress level). For the case with prestressing, there will be another s_1, corresponding to the second time to reach current stress level. N value (n_G) based on the latter s_1 will be largely decided by prestressing ratio ($t_{G'}$) and duration interest of engineering (t_p). Besides, n_G is not constant (n_A is

constant), in general, it increases with t_p, while decreasing with $t_{G'}$. For n_A equal to 0.04, with prestressing ratio 50%, after duration of 50yr, n_G is only 0.015.

6. DATA FROM LITERATURE

6.1. Introduction

This chapter aims at demonstrating proposed power law model is a generalized model by applying it to data from literature.

6.2. Philibert (1976) and Lefebvre (1981)

Lefebvre (1981) published some creep tests conducted by his student Philibert (1976) on clay of Eastern Canada. Details of these tests are presented in the master's thesis of Philibert, though it is French.

6.2.1. Normalization Curve

The clay of Eastern Canada is overconsolidated clay with preconsolidation pressure from 110kPa to 160kPa for borehole samples and block samples at depth 4.4m~5.6m. It should be noted that all conventional triaxial consolidated-drained (CD) shear test and triaxial creep test are carried out on samples at the depth range. Plasticity limit is 25% and liquidity limit is 65%, so the PI is 40 (i.e., high PI clay).

Conventional triaxial CD shear test are carried out to obtain stress-strain curves (figure 6-1). It is a very brittle clay with strain corresponding to peak stress equal to 1% at most cases. It is interesting that confining pressure (5kPa~40kPa) is much smaller whether compared to preconsolidation pressure (110kPa~160kPa) or $\gamma \cdot h$ (90kPa~110kPa), where γ is unit weight which can be assumed to 20kN/m^3, and h is depth of samples. The reason for choosing these confining pressure is unknown.

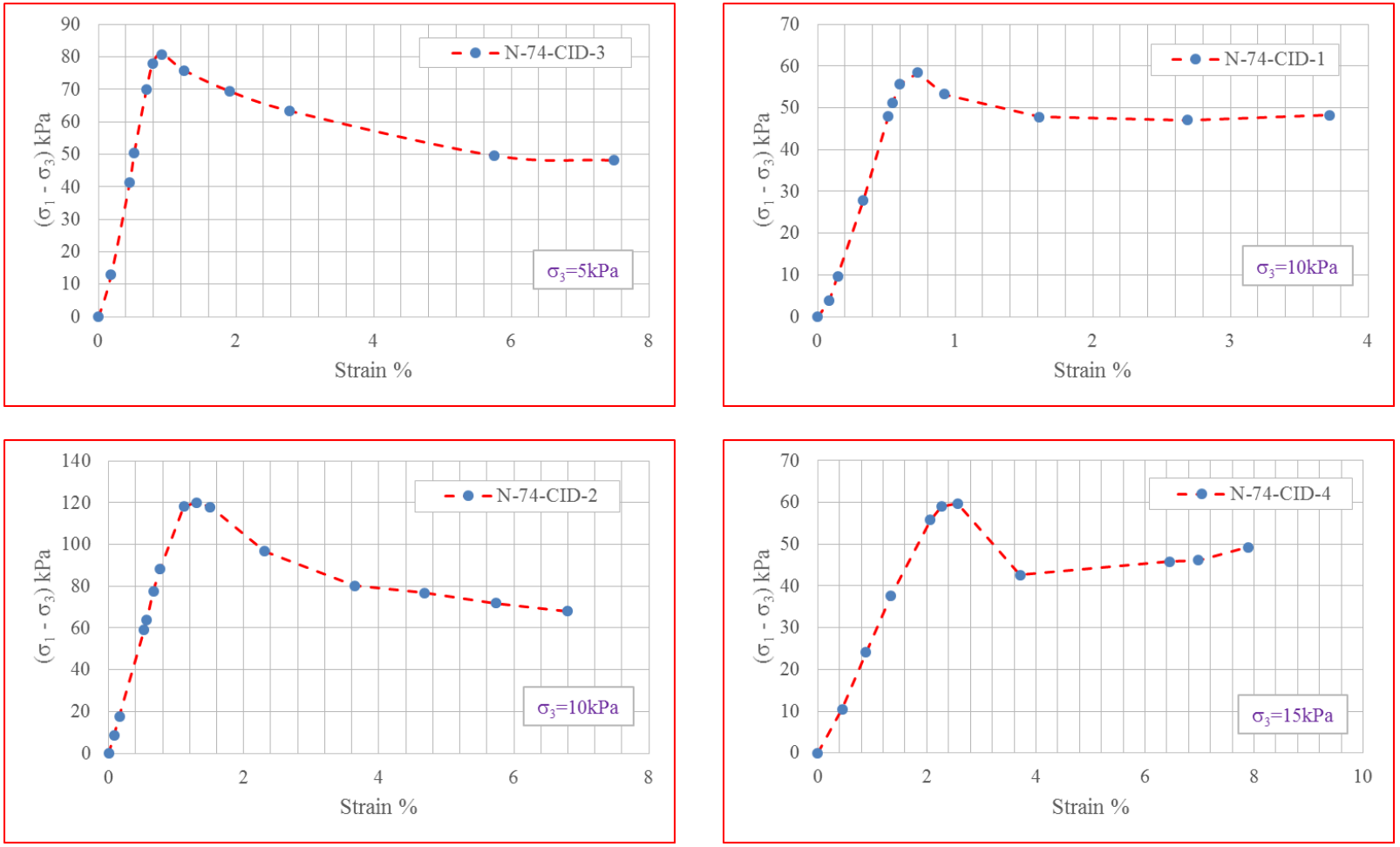

Figure 6-1. Stress-strain curves of clay of Eastern Canada, after Philibert (1976)

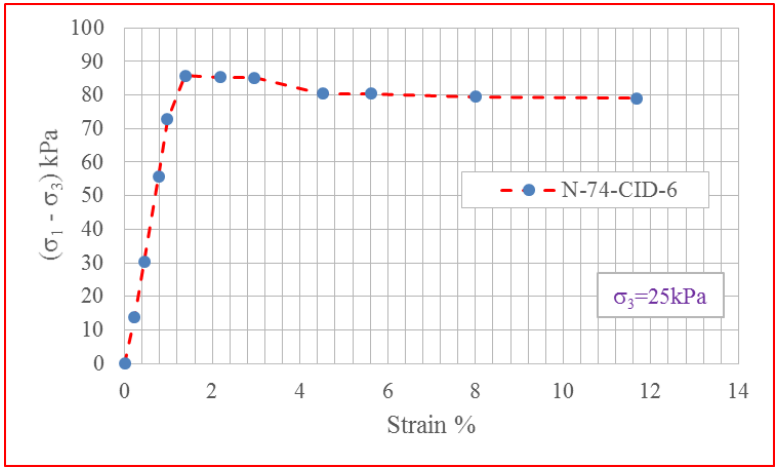

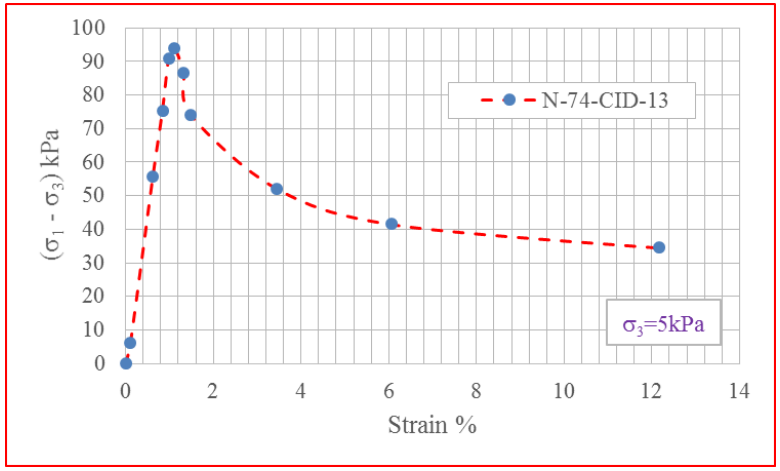

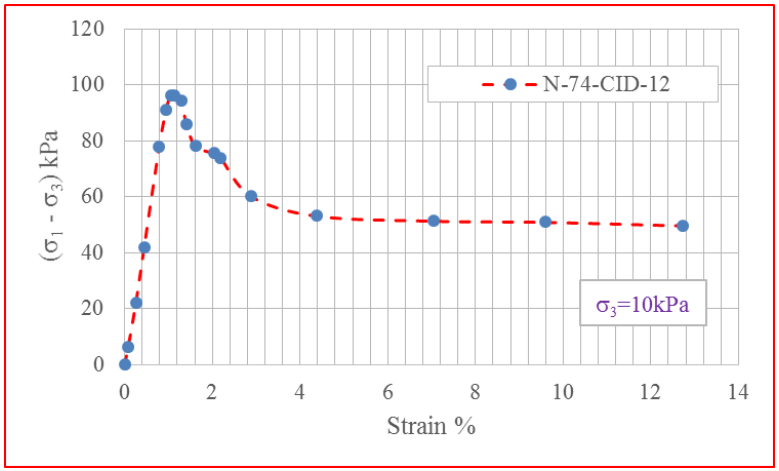

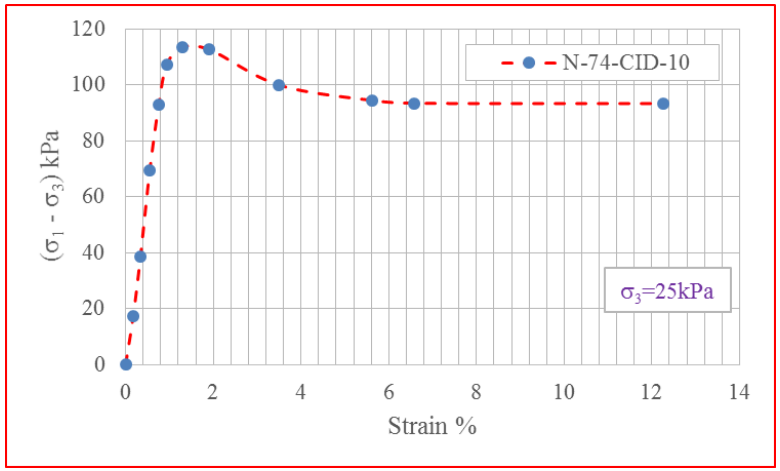

Figure 6-1 Continued

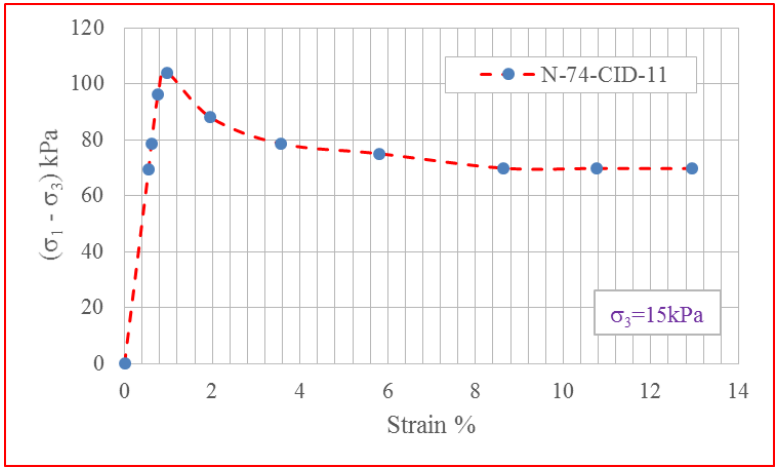

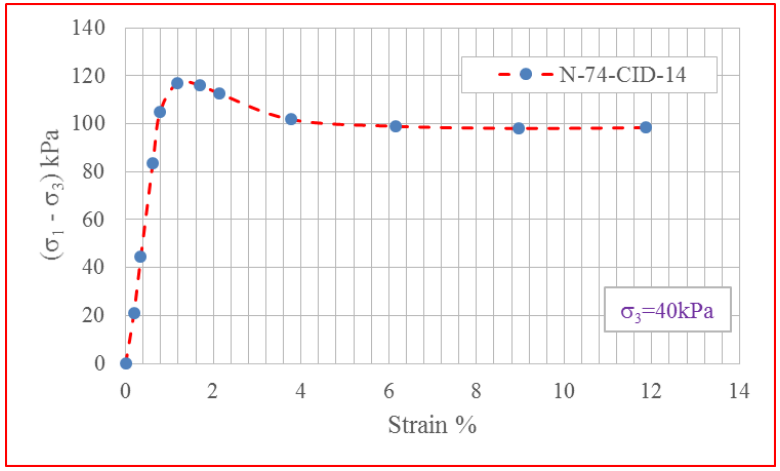

Figure 6-1 Continued

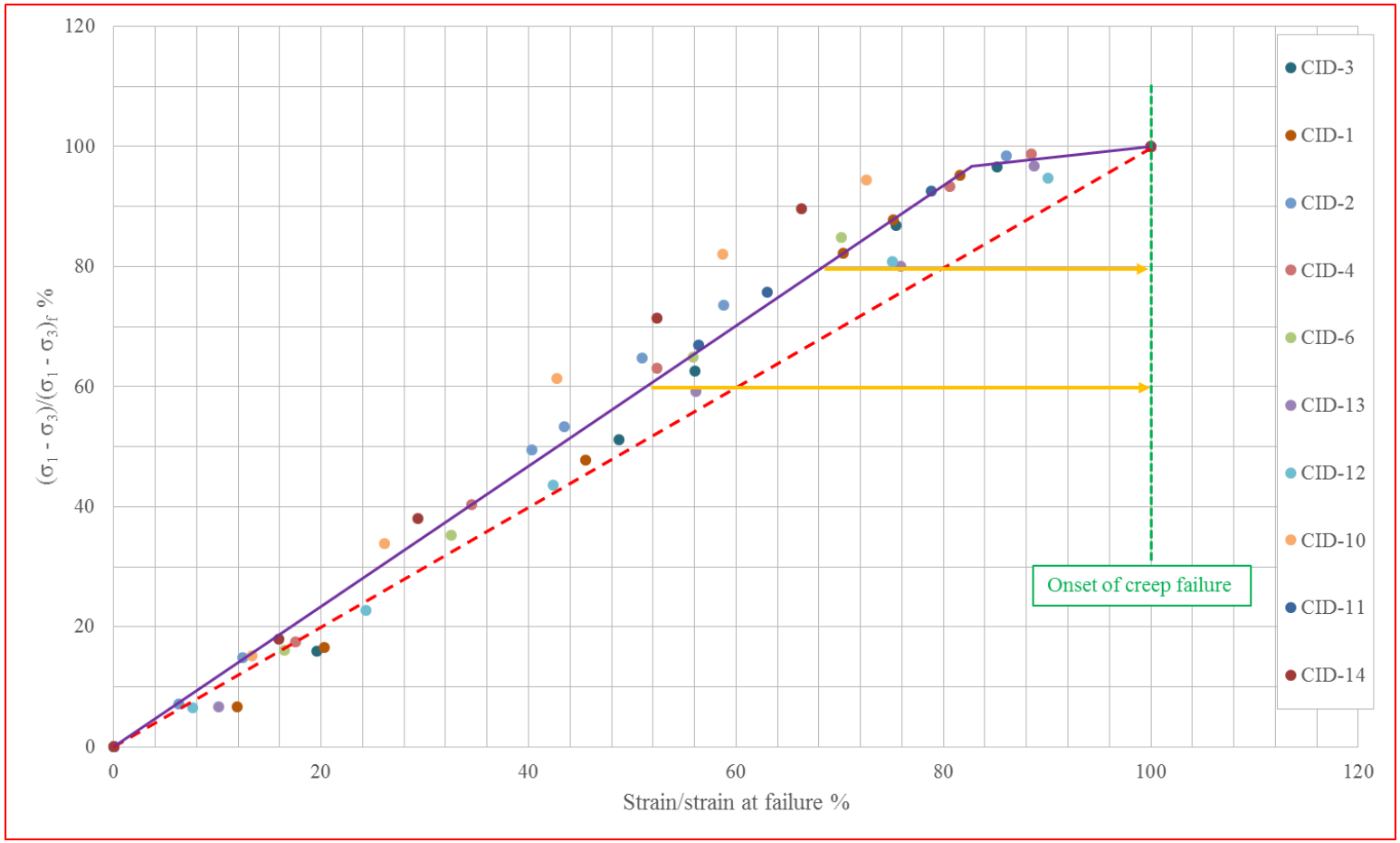

Figure 6-2. Normalization curve of clay of Eastern Canada, after Philibert (1976)

Similar to section 5.4.2, normalization curve of this clay is acquired by normalizing the pre-peak part of stress-strain curve with peak stress and its corresponding strain (figure 6-2). The average curve of these a little scattered data is taken as normalization curve to predict the possibility of creep failure at any stress level.

6.2.2. Creep Test

In total eight triaxial creep test are carried out by Philibert (1976). Four of them are carried out at stress level 60% and the other four at stress level 80%. The maximum duration of creep test is three months. Creep failure happens at stress level 80% during all tests, while creep failure doesn't happen at stress level 60% during three (out of four) tests. Creep failure at stress level 60% of one test is strange, which will be explained below.

Creep tests are plotted in figure 6-3. Tests with stress level at 60% are at left side and tests with stress level at 80% are at right side. The author defined "post-peak strength" corresponding to 8% strain on stress-strain curves of conventional triaxial CD shear test, and drew the conclusion that creep failure would happen when stress level was higher than post-peak strength (i.e., post-peak strength is stress threshold for creep failure). However, creep test labelled "N-75-CIDF-34" had already denied the conclusion.

It is worth noting that it is "load increment test" rather than "strain rate test" for creep test. Perhaps limited to knowledge at that time, load increment test conducted by the author is ruining the creep test. The load increment is not constant (decreasing as

shown in figure 6-3) and the duration of each load is also not constant. As mentioned earlier, “0 minute creep curve” with constant strain rate test is unique, while “0 minute creep curve” with constant load increment test is not unique. However, it could be compared (or fitting) if the duration of each load with constant load increment test is kept the same (An example will be given in the chapter of field test). The impact of this not well organized loading protocol will be studied in the chapter of field test. It is because of the loading protocol that creep failure happens at creep test labelled “N-75-CIDF-36” with stress level 60%.

Besides, as mentioned earlier, when comparing creep test to conventional triaxial shear test, x-axis and y-axis will be multiplied with a ratio respectively to fit the “0 minute creep curve” of creep test to pre-peak curve of conventional triaxial shear test. Except two creep tests at bottom row of figure 6-3, the remaining six creep tests are fitting with the normalization curve (figure 6-4). One argument is that creep failure happens at creep test labelled “N-75-CIDF-30” with stress level 60%, and strain-time curve (figure 6-5) and strain-time curve at log-log scales (figure 6-6) both support it. However, Philibert (1976) didn’t take it as creep failure.

Thus, creep failure happens during six of eight creep tests. Only two n values are obtained in figure 6-6. No data about creep tests labelled “N-75-CIDF-33” and “N-75-CIDF-37” are provide by Philibert (1976), so there are no strain-time curves about these two tests. It should be pointed out that t_1 in figure 6-6 is not equal to 1min. Because data is digitized from figures, t_1 is chosen to make sure the error as little as possible. However,

n value is independent of the chosen of t_1, as long as it is a straight line in log-log scales of strain-time curves.

With these two n values (i.e., 0.035 and 0.047) and the normalization curve (figure 6-2), the same procedure described in subsection 5.4.4 could be repeated here, which could estimate the time to creep failure, predict long-term deformation after a special duration of engineering interest, and draw the stress threshold of creep failure with a selected time.

Regarding the creep test performed by Philibert (1976), the time to creep failure at two stress levels (80% and 60%) is necessary to be estimated. The time to creep failure with stress level 80% based power law model is 0.4d~34d, and the time to creep failure with stress level 60% will be 3m~430yr. It is a range, which is resulted by the variation of two n values obtained. However, the test data falls in these ranges, which demonstrates that the proposed power law model is feasible to data from others.

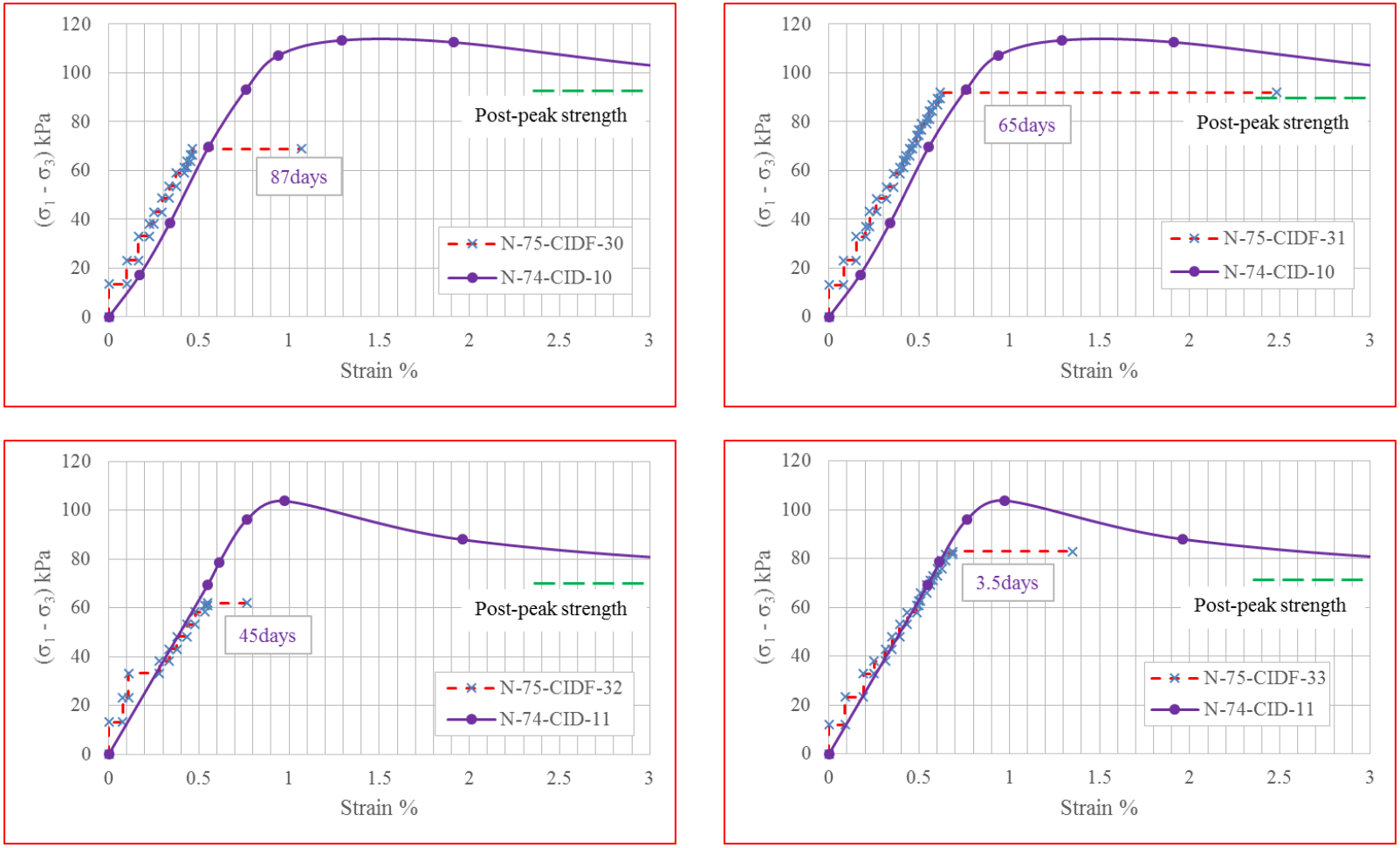

Figure 6-3. Creep test on clay of Eastern Canada, after Philibert (1976)

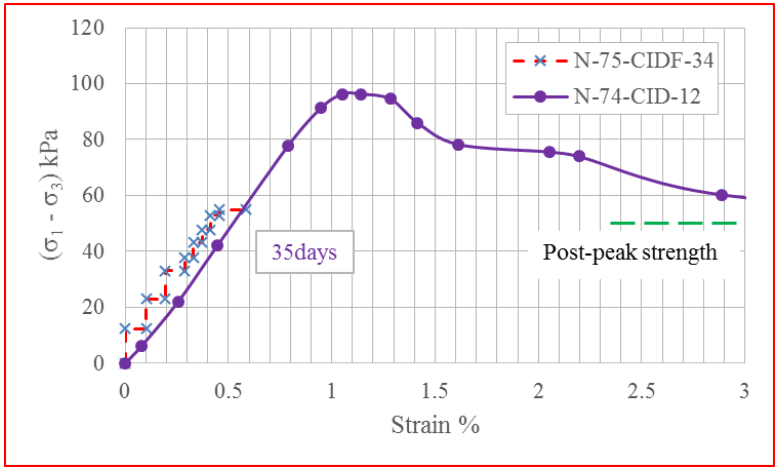

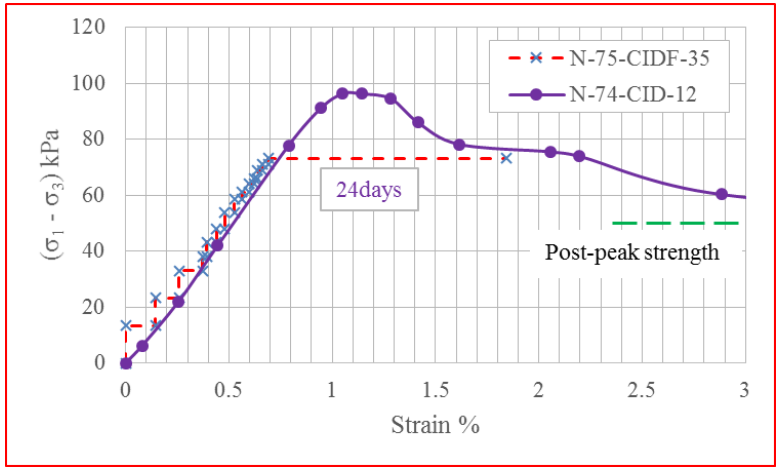

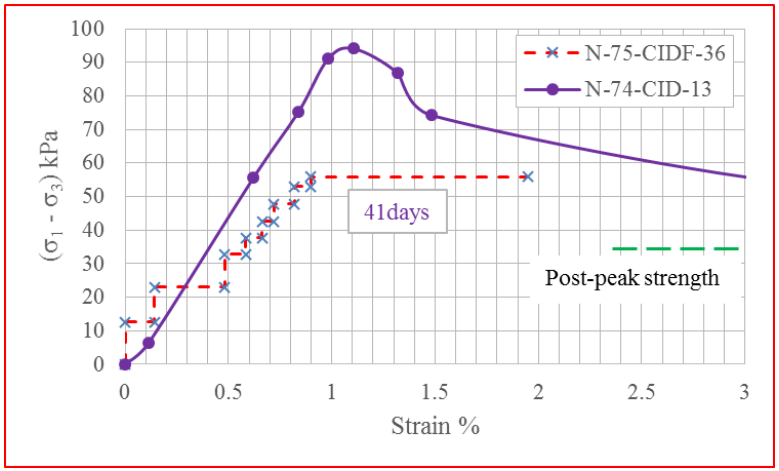

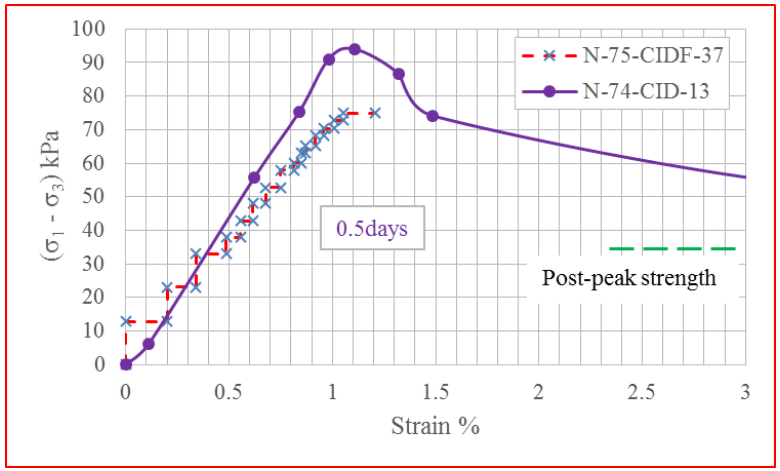

Figure 6-3 Continued

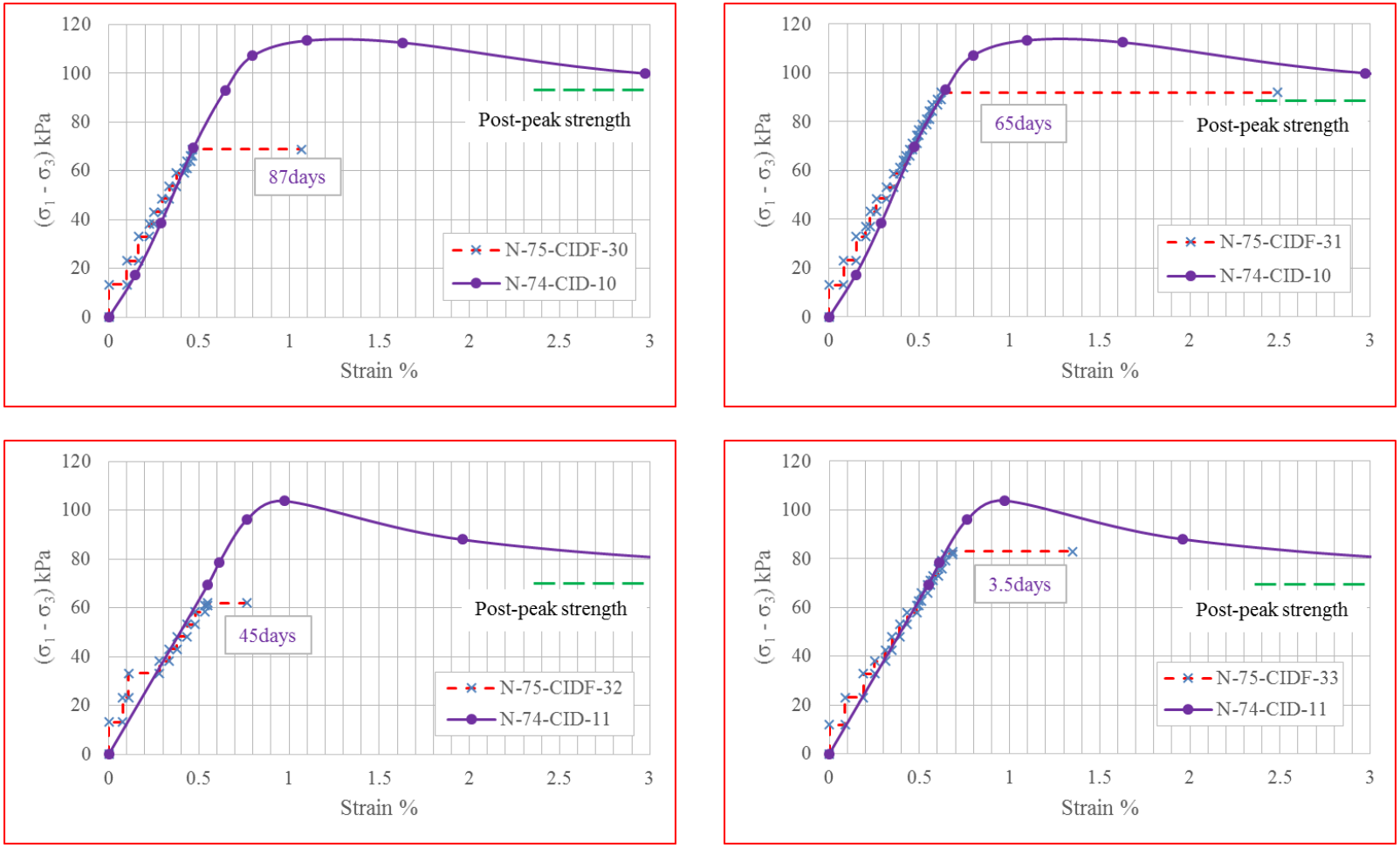

Figure 6-4. Creep test curve fitting with normalization curve, after Philibert (1976)

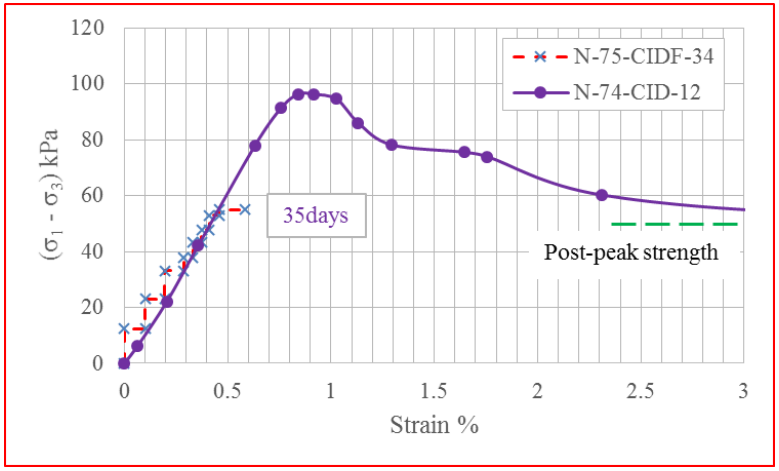

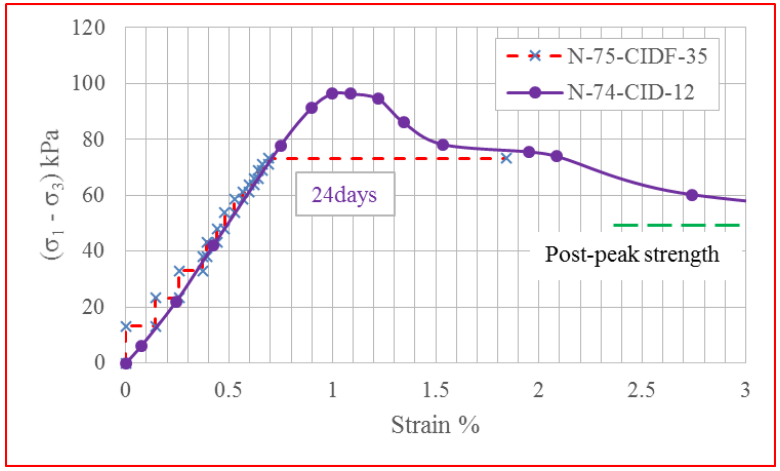

Figure 6-4 Continued

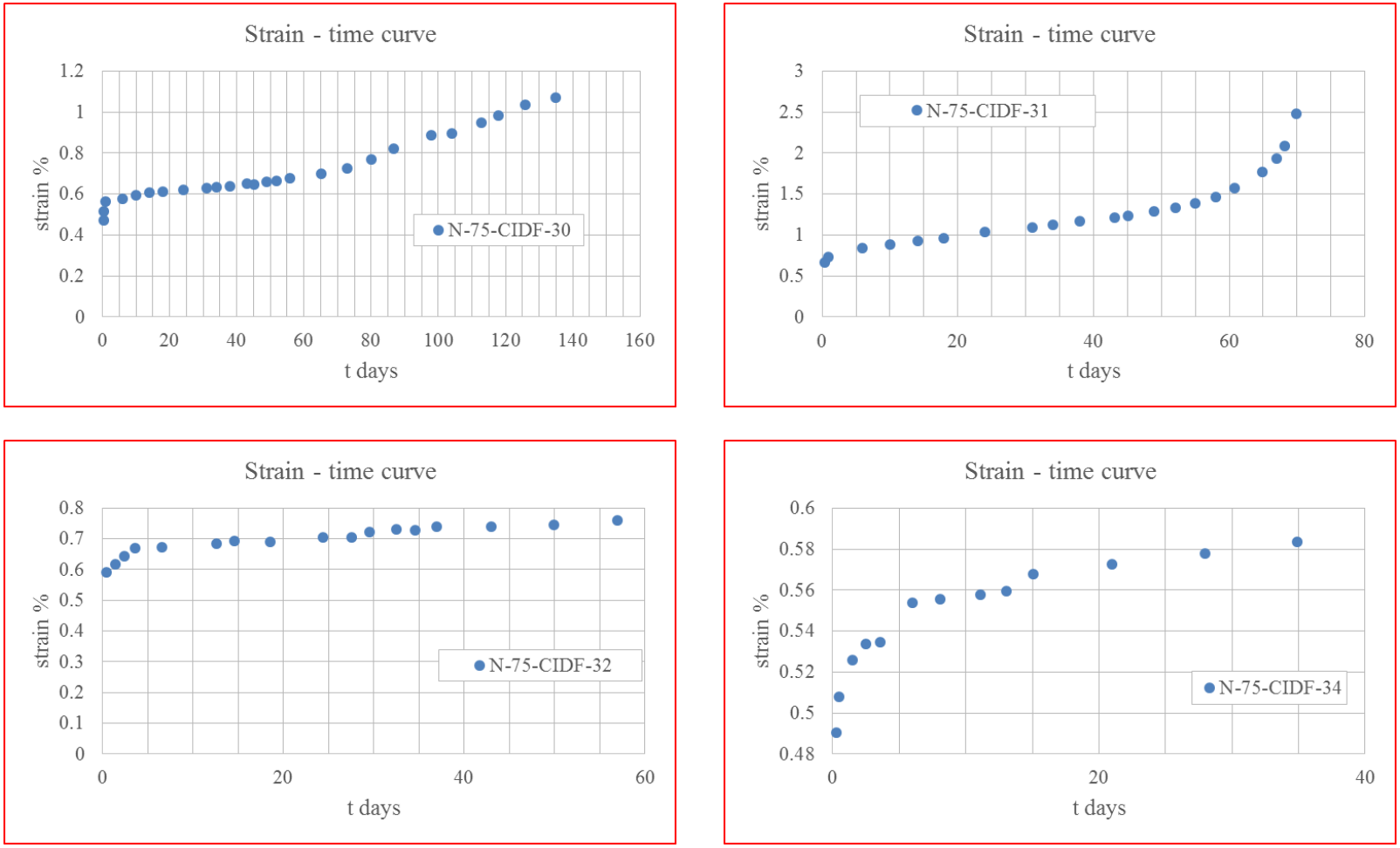

Figure 6-5. Strain-time curves, after Philibert (1996)

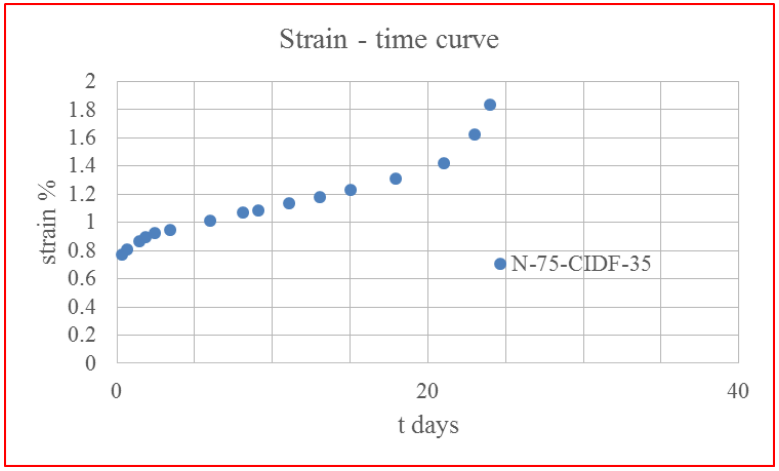

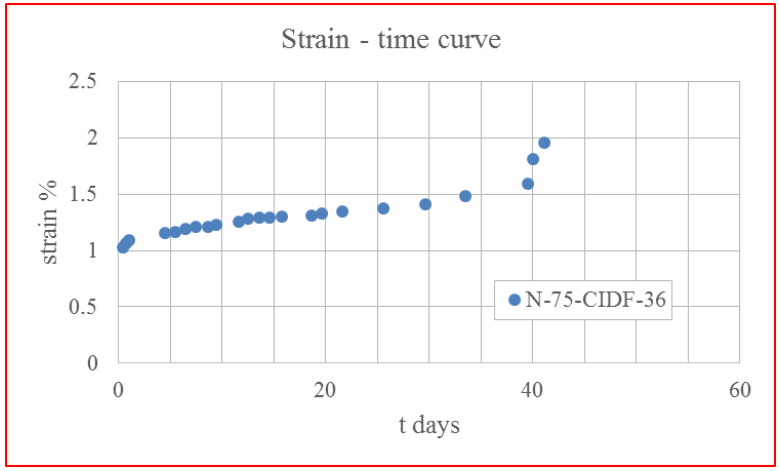

Figure 6-5 Continued

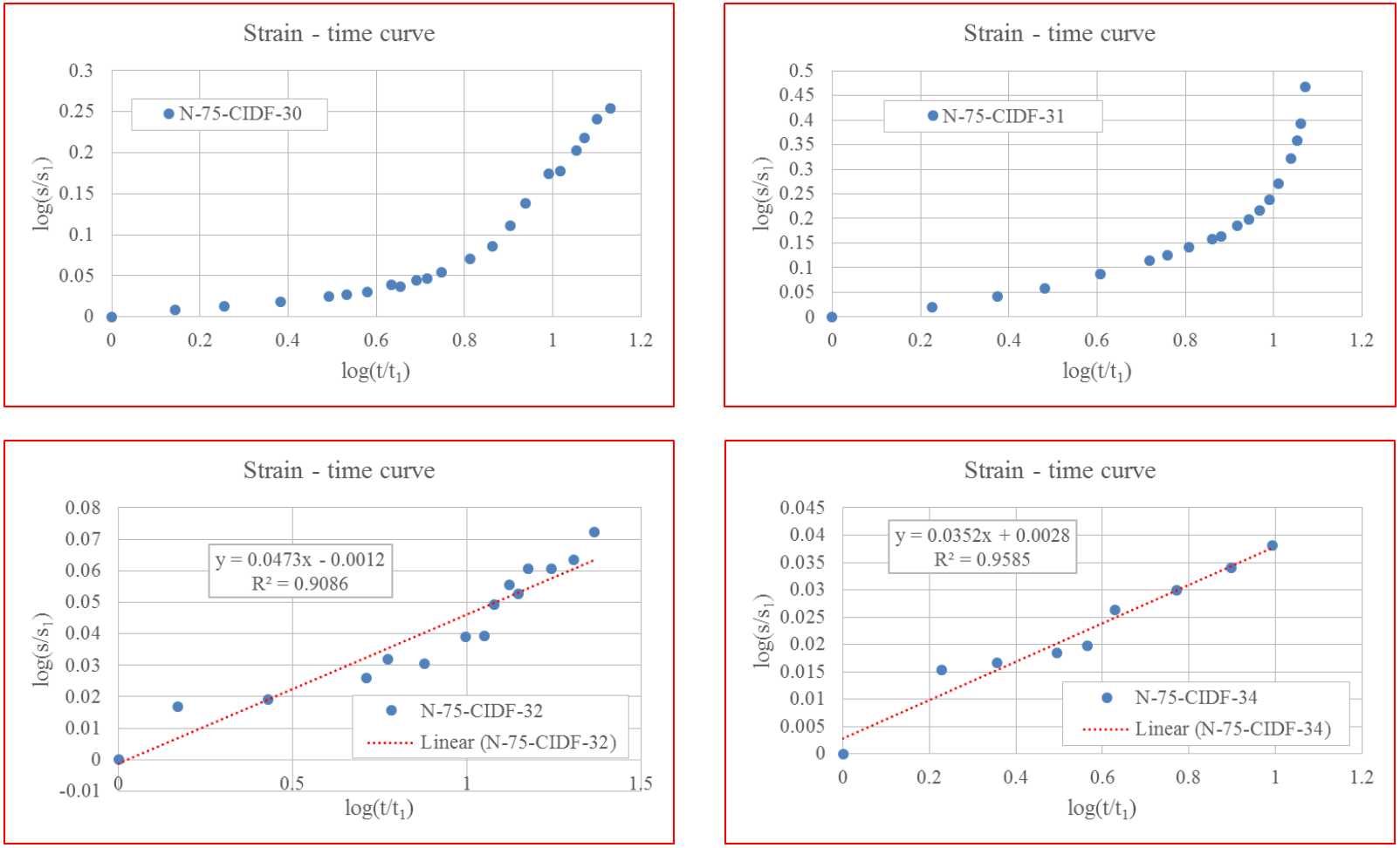

Figure 6-6. Strain-time curves (log-log scales), after Philibert (1996)

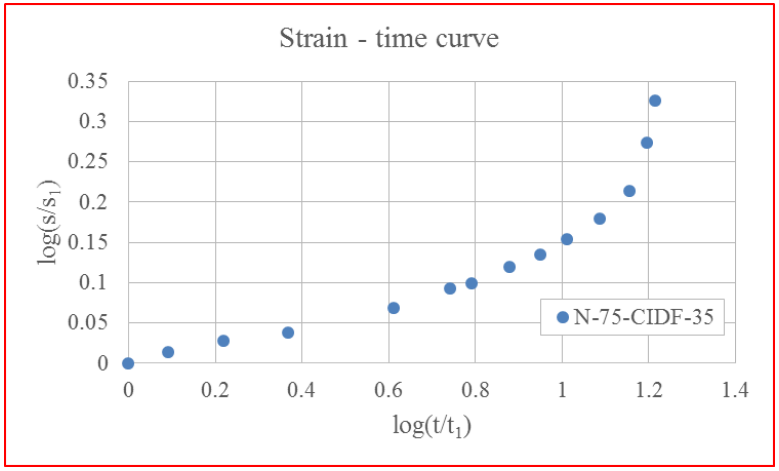

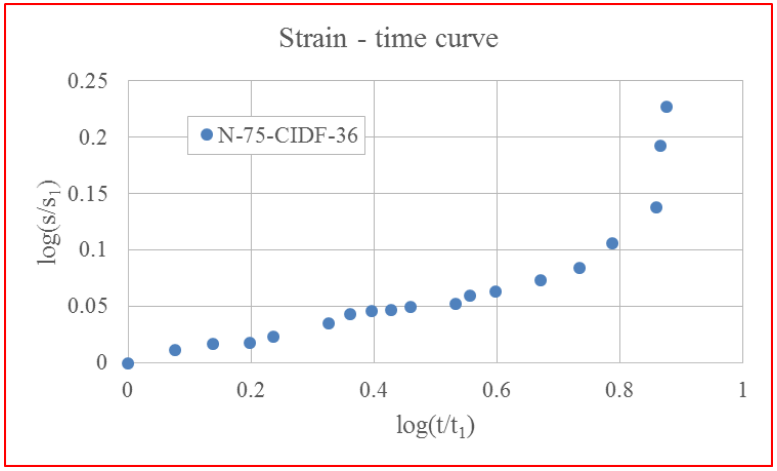

Figure 6-6 Continued

6.3. Bishop (1966, 1969) and Skempton (1964, 1970, 1977)

Bishop (1966, 1969) performed triaxial creep test on six specimens up to 3.5yr. One soil adopted in the test is London clay with plasticity limit 29% and liquidity limit 76% (i.e., PI=47, high PI clay). It should be noted creep tests with different stress level are performed on different specimens rather than on the same one specimen (like those in Chapter five). There is one figure in Bishop (1969) presenting strain-time curve of creep test on London clay, thus, n value could be obtained (figure 6-7 and figure 6-8). N value is pretty constant. However, there is only stress-strain curve of conventional triaxial CD shear test available to draw the normalization curve (figure 6-9). Thus, the estimation as follows is pretty rough.

Little information about three cutting slopes failure presented by Skempton (1964, 1970, 1977). However, it is London clay, thus, it is assumed that n value and stress-strain curve from data of Bishop could be applied to data of Skempton.

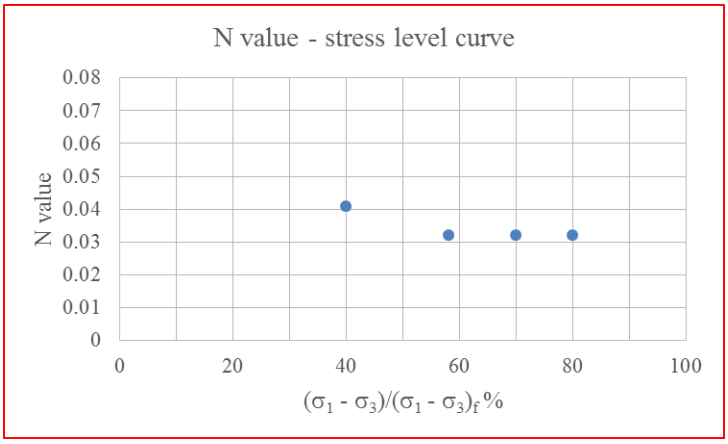

Figure 6-7. N value-stress level curve, London clay, after Bishop (1969)

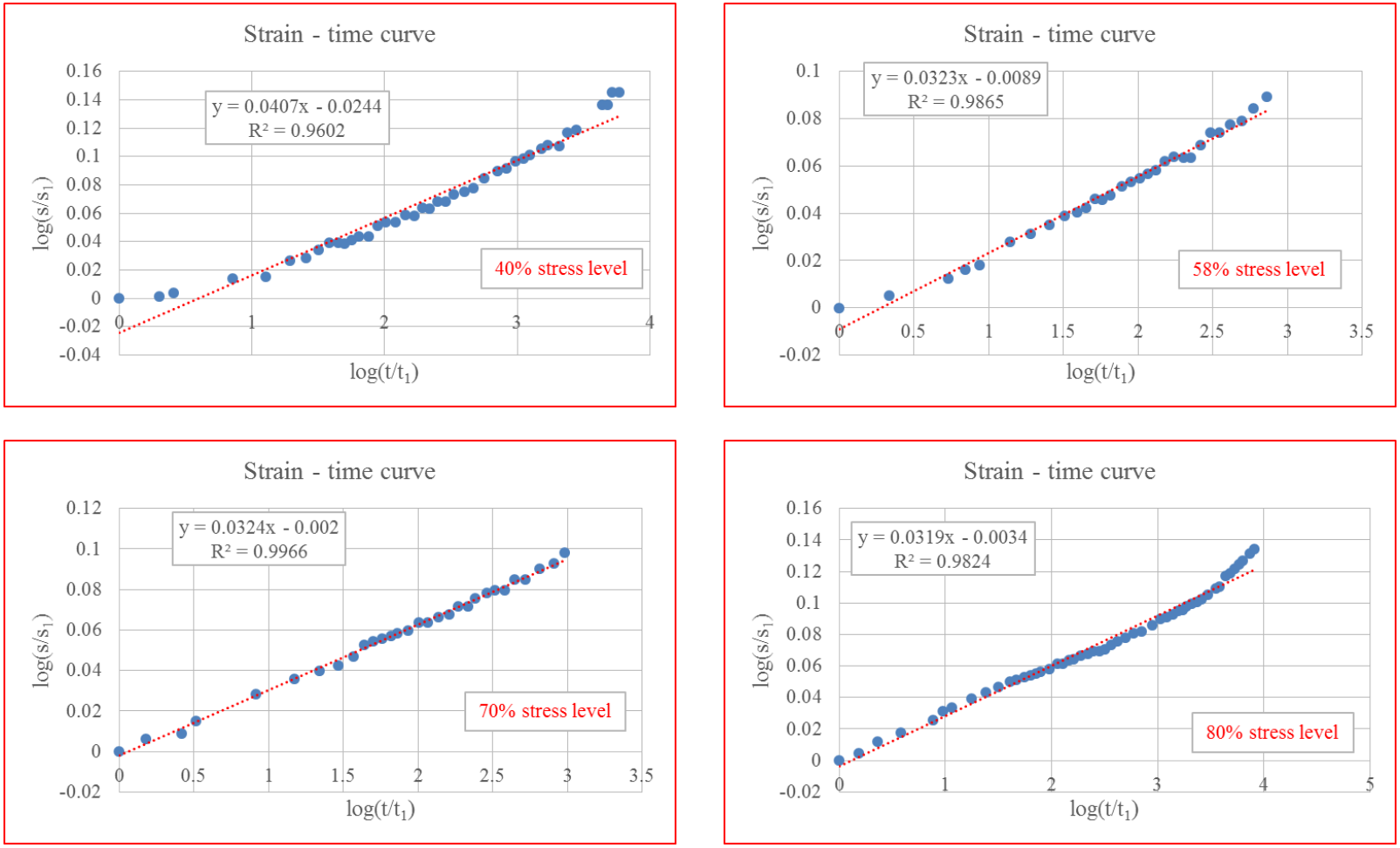

Figure 6-8. Strain-time curves (log-log scales), London clay, after Bishop (1969)

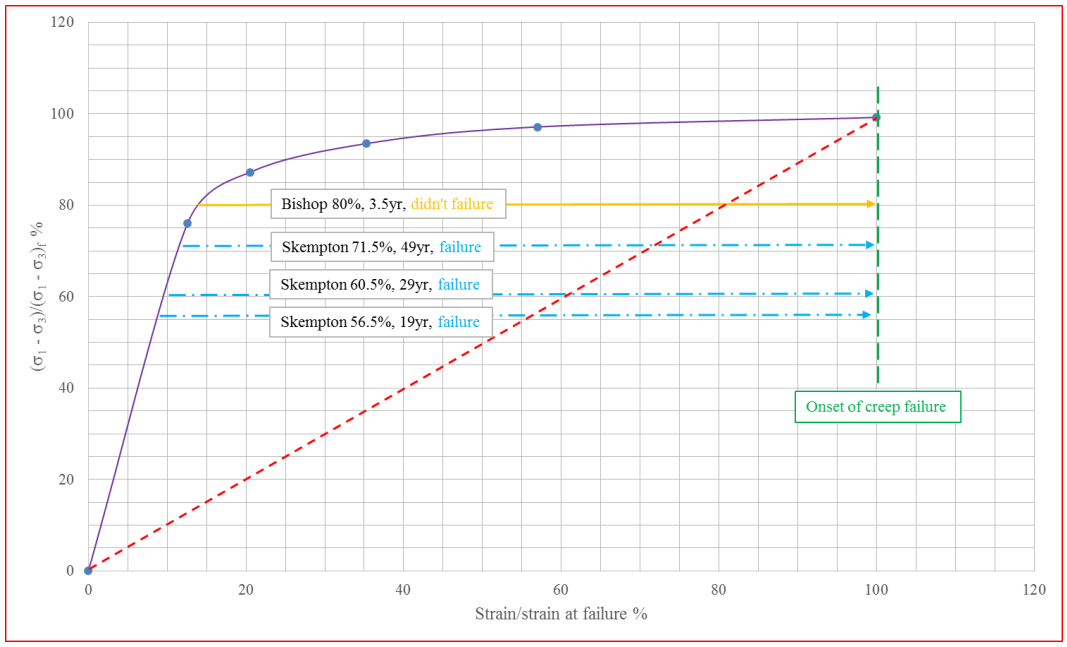

Figure 6-9. Normalization curve, London clay, after Bishop (1969)

Nelson (1977) provided stress level for data of Skempton, as shown in figure 6-9. It will take more than 200yr for London clay to creep failure with normalization curve (figure 6-9) and n value-stress level curve (figure 6-7). However, three cutting slopes failed in less than 200yr, it agrees with the view by Skempton (1970) and Dr. Suklje comment on Bishop (1967) that failure of three cutting slopes is caused by combination with creep failure and progressive failure.

6.4. Conclusion

In this chapter the proposed power law model was applied to data from literature. Several previous findings are again made here:

- Plotting strain-time curves in log-log scales, it will be a straight line and slope of the line is n value, exponent in the model;
- N value is independent of stress level;
- Proposed power law model can be generally applied to other creep data.

7. FIELD TESTS

7.1. Introduction

This chapter aims at applying power law model to four kinds of field tests. Three of them are performed at Texas A&M University riverside campus National Geotechnical Experimental Site (TAMU-NGES), and another one is performed at Houston area. While soil nail pullout test is carried out by this research team, spreading footing test, ground anchor pullout test and cyclic lateral load test were performed by former students of Dr. Jean-Louis Briaud. It should be noted there is one more field practice (San Jacinto Monument) mentioned in subsection 4.8.3.

7.2. Spreading Footing Test by Gibbens (1995), TAMU-NGES - Sand Site

Five spread footings were built at the sand site on TAMU-NGES (figure 7-1). They are two 3 x 3 x 1.2m footings, one 2.5 x 2.5 x 1.2m footing, one 1.5 x 1.5 x 1.2m footing, and one 1 x 1 x 1.2m footing. All five footings were founded at a depth of 0.76m in the sand. Five footings are named 3m footing (North), 3m footing (South), 2.5m footing, 1.5m footing, and 1m footing, respectively. An overall view of setup for testing is plotted in figure 7-2. More details could be found from Gibbens (1995).

Fortunately, the complete data set (raw data and reduced data) was obtained on a diskette kept by Dr. Jean-Louis Briaud, and it is successfully extracted to plot load-settlement curve, strain-time curve (log-log scales), and n value-stress level curve, presented in each subsection as follows.

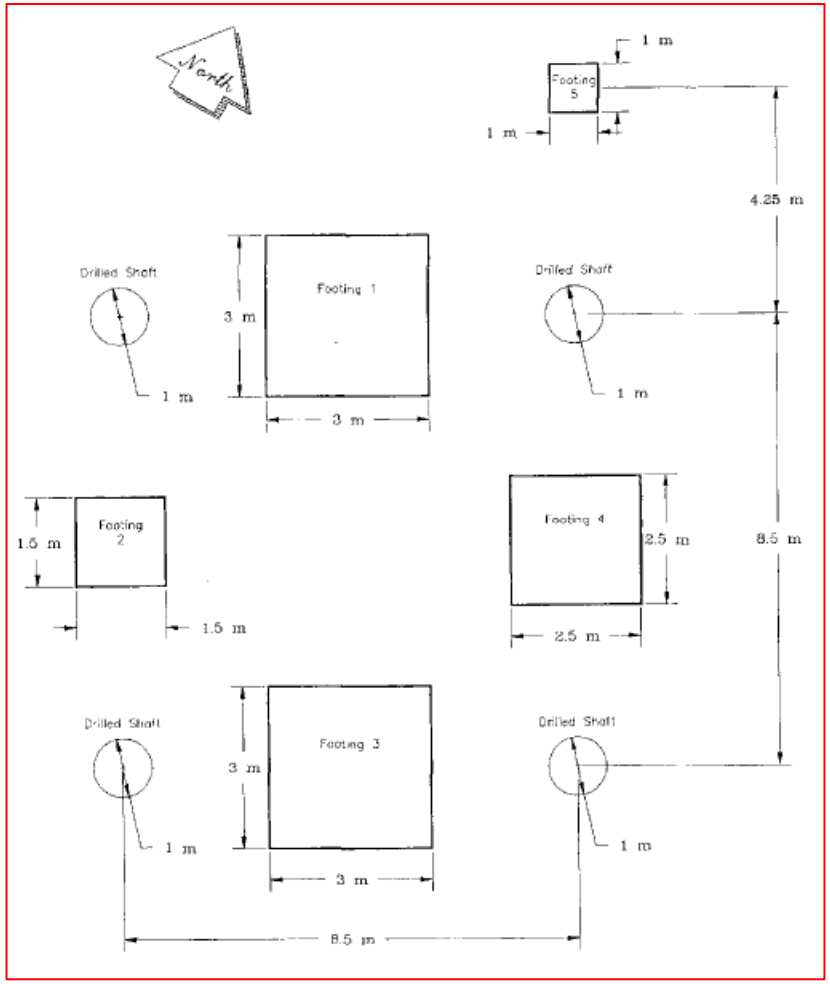

Figure 7-1. Spread footing layout, after Gibbens (1995)

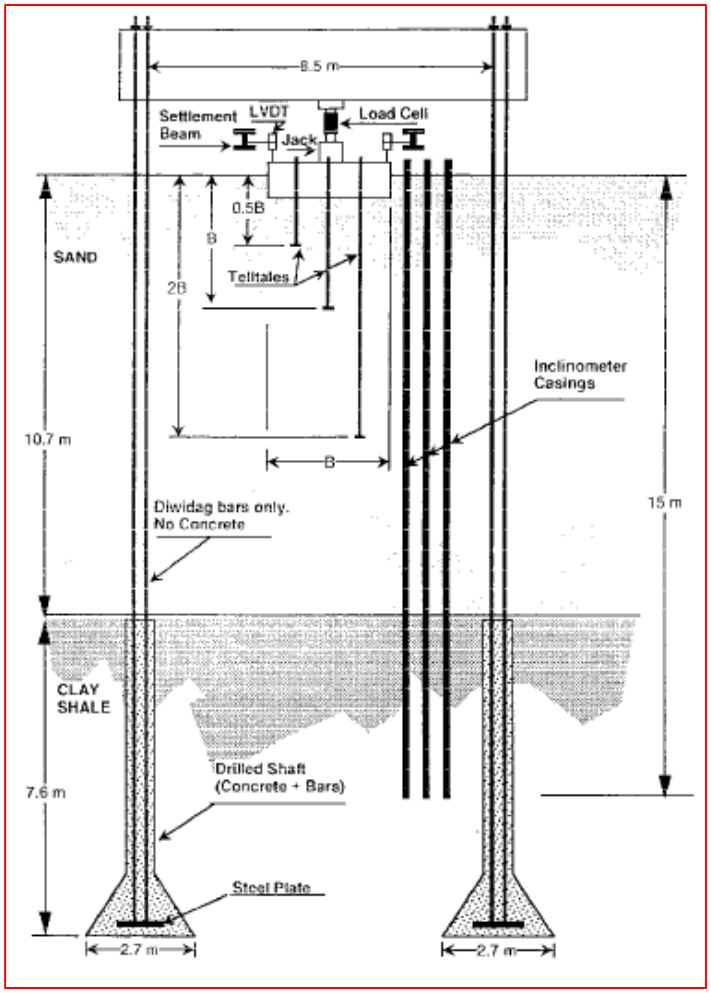

Figure 7-2. Spread footing test setup, after Gibbens (1995)

7.2.1. Load-settlement Curve

Initially, the wood reference beam was adopted. It was not until finishing testing on 1m footing, 1.5m footing, part of 2.5m footing and part of 3m footing (South) that it was found out the wood beam was creeping due to self-weight, which resulted in bad data. After that, the steel beam was adopted as reference beam to finish testing on remaining part of 2.5m footing, remaining part of 3m footing (South) and whole part of 3m footing (North).

Because of it, 1m footing, 3m footing (South) and 3m footing (North) were chosen to illustrate here. Data of 1.5m footing and 2.5m footing would be mentioned if necessary.

Loading protocols are shown in table 7-1 to table 7-3. In most cases, load increment and duration of each sustained load is equal, while unequal duration may impact n value, explained in later subsection. It should be noted that settlement during each sustained load was recorded starting at 1min instead of 0min.

Table 7-1. Loading protocol, 1m footing, after Gibbens (1995)

1m footing			
Loading/Unloading-Reloading MN	MN	Duration minutes	Note
0, 0.02, 0.04, 0.05, 0.07, 0.09	0.09	1, 3, 5, 7, 15, 20, 25, 30	Wood Beam
	0.18	1, 3, 5, 7, 15, 20, 25, 30	
	0.27	1, 3, 5, 7, 15, 20, 25, 30	
	0.36	1, 3, 5, 7, 15, 20, 25, 30	
	0.53	1, 3, 5, 7, 15, 20, 25, 30	
	0.71	1, 3, 5, 7, 15, 20, 25, 30	
0.71, 0.36, 0.07, 0.01, 0.36, 0.71	0.71	1, 3, 5, 7, 15, 20, 25, 30	
	0.8	1, 3, 5, 7, 15, 20, 25, 30, 60, 120, …, 1440	
	0.89	1, 3, 5, 7, 15, 20, 25, 30	
	0.98	1, 3, 5, 7, 15, 20, 25, 30	
	1.07	1, 3, 5, 7, 15, 20, 25, 30	
	1.16	1, 3, 5, 7, 15, 20, 25, 30	
	1.25	1, 3, 5, 7, 15, 20, 25, 30	
	1.34	1, 3, 5, 7, 15, 20, 25, 30	
1.34, 0.62, 0.13, 0, 0.62, 1.34, 1.42	1.42	1, 3, 5, 7, 15, 20, 25, 30	
	1.51	1, 3, 5, 7, 15, 20, 25, 30	
	1.6	1, 3, 5, 7, 15, 20, 25, 30	
	1.69	1, 3, 5, 7, 15, 20, 25, 30	
	1.78	1, 3, 5, 7, 15, 20, 25, 30	
1.78, 0.89, 0.09, 0			

Table 7-2. Loading protocol, 3m footing (South), after Gibbens (1995)

3m footing (South)			
Loading/Unloading-Reloading MN	MN	Duration minutes	Note
0, 0.09, 0.18, …, 0.45, **0.53**, 0.62, …, 0.89	0.89	1, 3, 5, 7, 15, 20, 25, 30	Wood Beam
	1.78	1, 3, 5, 7, 15, 20, 25, 30	
	2.67	1, 3, 5, 7, 15, 20, 25, 30	
	3.56	1, 3, 5, 7, 15, 20, 25, 30	
	4.45	1, 3, 5, 7, 15, 20, 25, 30	
4.45, 2.67, 0.89, 0, 0.89, 2.67, 4.45	4.45	1, 3, 5, 7, 15, 20, 25, 30, 60, 120, …, 1440	
4.45, 2.67, 0.89, 0, 0.89, 1.78, 2.67, 3.56	**3.56**	1, 3, 5, 7, 15, 20, 25, 30, 60, 120, …, 1320	Steel Beam
3.56, 4.45, 5.34	5.34	1, 3, 5, 7, 15, 20, 25, 30	
	6.23	1, 3, 5, 7, 15, 20, 25, 30	
	7.12	1, 3, 5, 7, 15, 20, 25, 30	
	8.01	1, 3, 5, 7, 15, 20, 25, 30	
8.01, 5.34, 2.67, 0, 2.67, 5.34, 8.01, 8.9	8.9	1, 3, 5, 7, 15, 20, 25, 30	
8.9, 6.23, 2.67, 0			

Table 7-3. Loading protocol, 3m footing (North), after Gibbens (1995)

3m footing (North)			
Loading/Unloading-Reloading MN	MN	Duration minutes	Note
0, 0.09, 0.18, …, 0.45, **0.53**, 0.62, …, 0.89	0.89	1, 3, 5, 7, 10, 15, 20, 25, 30	
	1.78	1, 3, 5, 7, 10, 15, 20, 25, 30	
	2.67	1, 3, 5, 7, 10, 15, 20, 25, 30	
	3.56	1, 3, 5, 7, 10, 15, 20, 25, 30	
	4.45	1, 3, 5, 7, 10, 15, 20, 25, 30	
4.45, 2.67, 0.89, 0, 0.89, 1.78, ..., 3.56, 4.45	4.45	1, 3, 5, 7, 10, 15, 20, 25, 30, 60, 120, …, 1380	
	5.34	1, 3, 5, 7, 10, 15, 20, 25, 30	Steel
	6.23	1, 3, 5, 7, 10, 15, 20, 25, 30	Beam
	7.12	1, 3, 5, 7, 10, 15, 20, 25, 30	
	8.01	1, 3, 5, 7, 10, 15, 20, 25, 30	
8.01, 5.34, 2.67, 0, 2.67, 5.34, 8.01, 8.9	8.9	1, 3, 5, 7, 10, 15, 20, 25, 30	
	9.79	1, 3, 5, 7, 10, 15, 20, 25, 30	
9.79, 7.12, 3.56, 0, 3.56, 7.12, 9.79, 10.24	10.24	1, 3, 5, 7, 10, 15, 20, 25, 30	
10.24, 7.12, 3.56, 0			

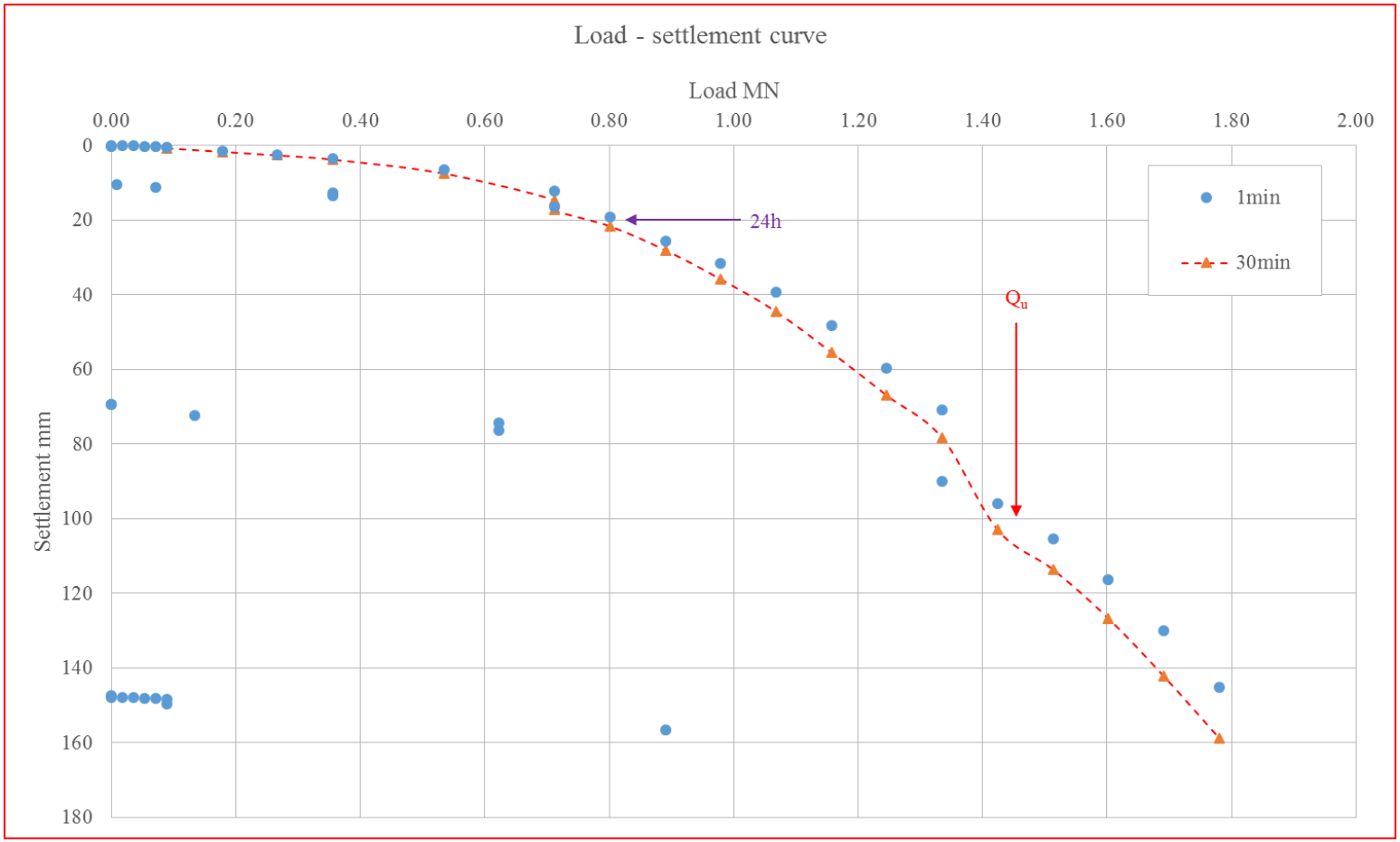

Figure 7-3. Load-settlement curve of 1m footing, after Gibbens (1995)

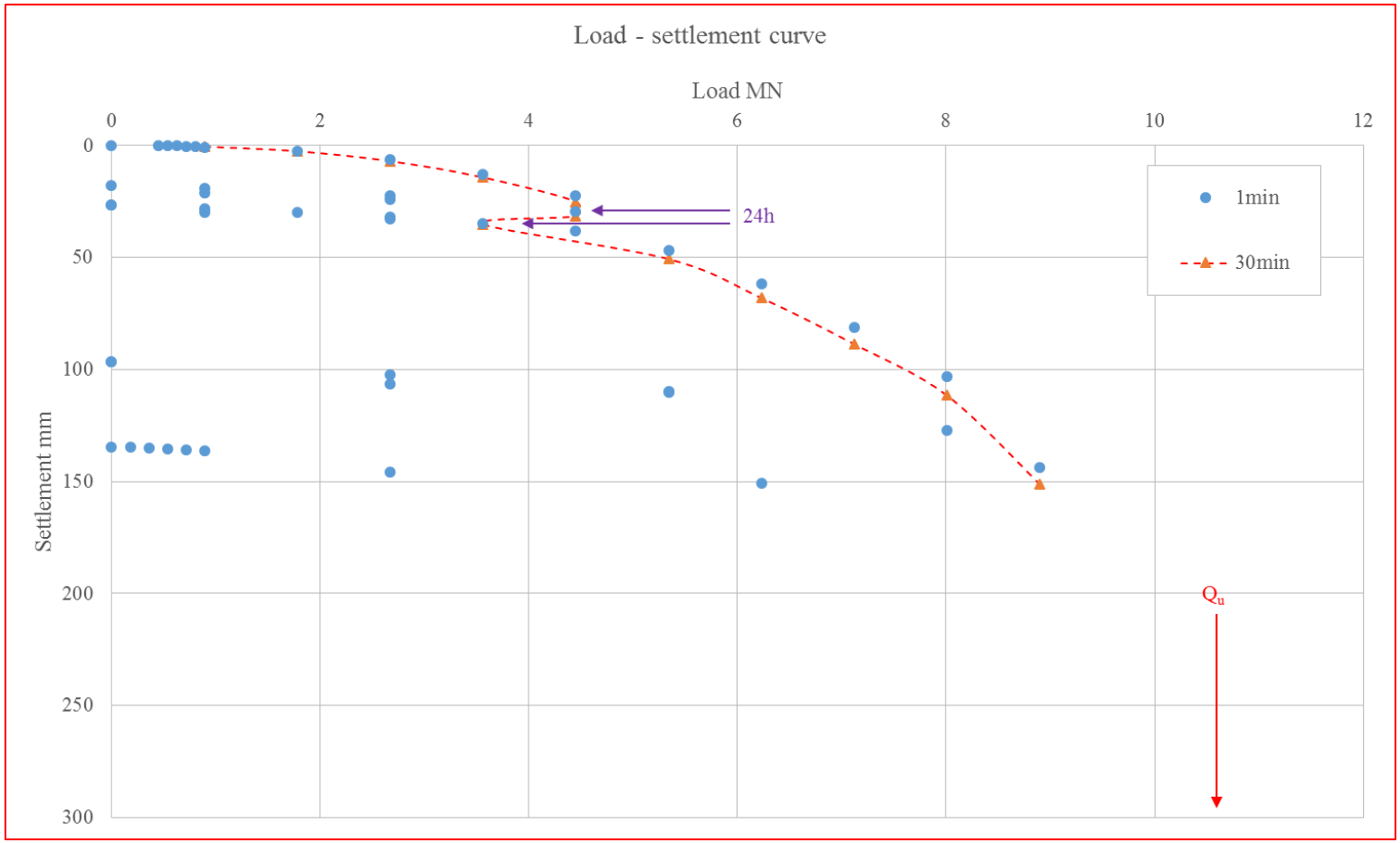

Figure 7-4. Load-settlement curve of 3m footing (South), after Gibbens (1995)

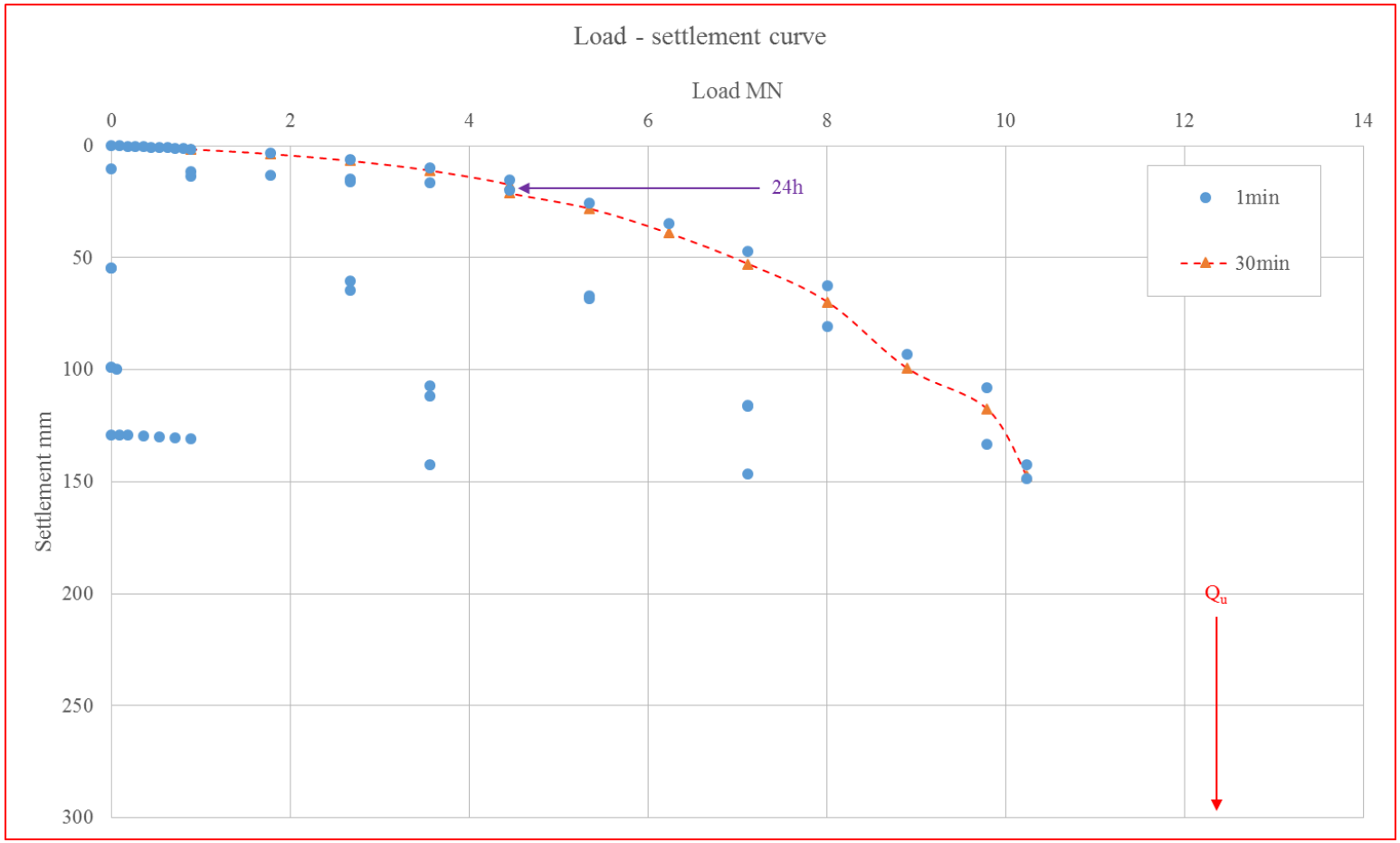

Figure 7-5. Load-settlement curve of 3m footing (North), after Gibbens (1995)

Load-settlement curve is plotted in figure 7-3 to figure 7-5. Ultimate load (Q_u) is defined to be the load corresponding to settlement at 30min equal to one tenth of B, where B is width of footing. The value of Q_u is acquired by extrapolating in all footings except 1m footing.

Connecting settlement at 30min under each sustained load provides a curve called "30 minute creep curve". In similar, connecting the starting points (at 1min) under each sustained load provides a curve called "1 minute creep curve". It is worth noting that both curves of 1m footing, 3m footing (South) and 3m footing (North) are not smooth. It implicitly supports that unequal duration (24h versus 30min) and unload-reload cycle have an impact on creep curves, namely, on n value.

7.2.2. Strain-time Curve

Three telltales per footing (figure 7-2) were installed to monitor settlement of soil layer at depth of 0.5B, B and 2B, where B is width of footing. Regarding bad data caused by wood beam, only data with 24h duration (monitored by LVDT) was corrected with reference to data monitored by 2B telltale, based on the assumption that soil layer at 2B depth didn't creep. The idea was supported by the good agreement of settlement monitored by LVDT and 2B telltale after steel beam was adopted for 2.5m footing and 3m footing (South) (figure 7-6). Gibbens (1995) pointed out that the somewhat erratic nature of LVDT data in bottom right corner of figure 7-6 was attributed to particularly small movements recorded.

Strain-time curve (log-log scales) is plotted in figure 7-7 to figure 7-9. In general, it is a straight line with n value as the slope. However, there is a seating problem at the first few low sustained load where n value is unavailable (i.e., not a straight line). To remind, seating problem also exists in laboratory tests.

Special attention should be paid to three phenomena:

- N value before and after an unload-reload cycle;
- N value before and after 24h duration, while 30min duration is generally adopted;
- N value after preloading;

For 1m footing, n value is drastically reduced at sustained load 0.71MN after unload-reload cycle, compared to n value at the same previous sustained load (0.71MN) before unload-reload cycle; n value is significantly reduced at sustained load 1.42MN after unload-reload cycle, compared to n value at previous sustained load 1.34MN before unload-reload cycle. Similar findings could be made from 3m footing (South) and 3m footing (North). Besides, for 1m footing, n value is appreciably reduced at sustained load 0.89MN with 30min duration, compared to n value at previous sustained load 0.8MN with 24h duration, however, n value at following sustained load 0.98MN with 30min duration is almost close to n value at sustained load 0.8MN with 24h duration. Similar findings could be made from other footings.

For 3m footing (South), n value is tremendously reduced at sustained load 3.56MN with 22h duration, compared to n value at previous sustained load 4.45MN with 24h duration. This is combination preloading with unload-reload cycle.

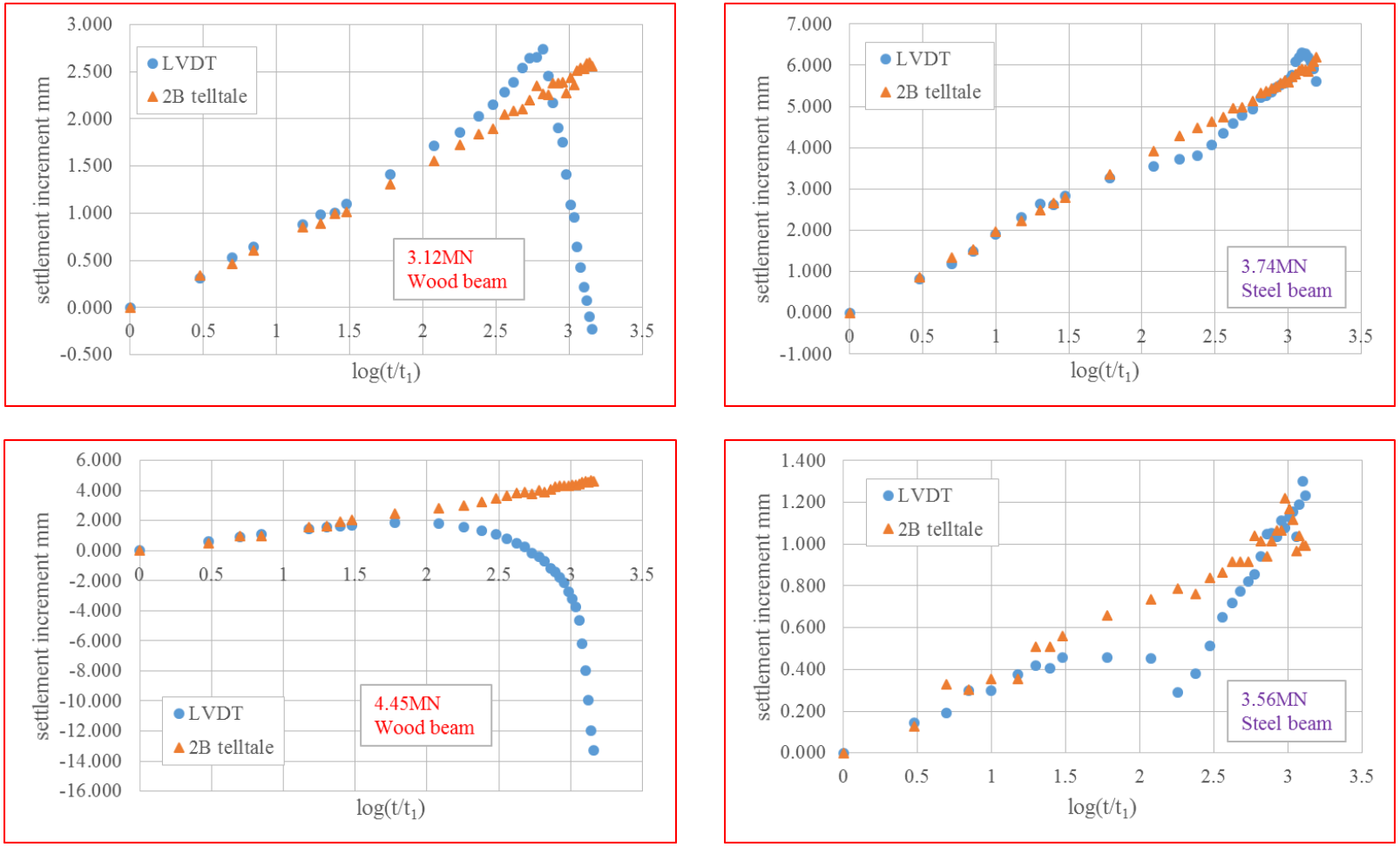

Figure 7-6. Settlement by LVDT and 2B telltale, 2.5m footing (top row) and 3m footing (South) (bottom row), after Gibbens (1995)

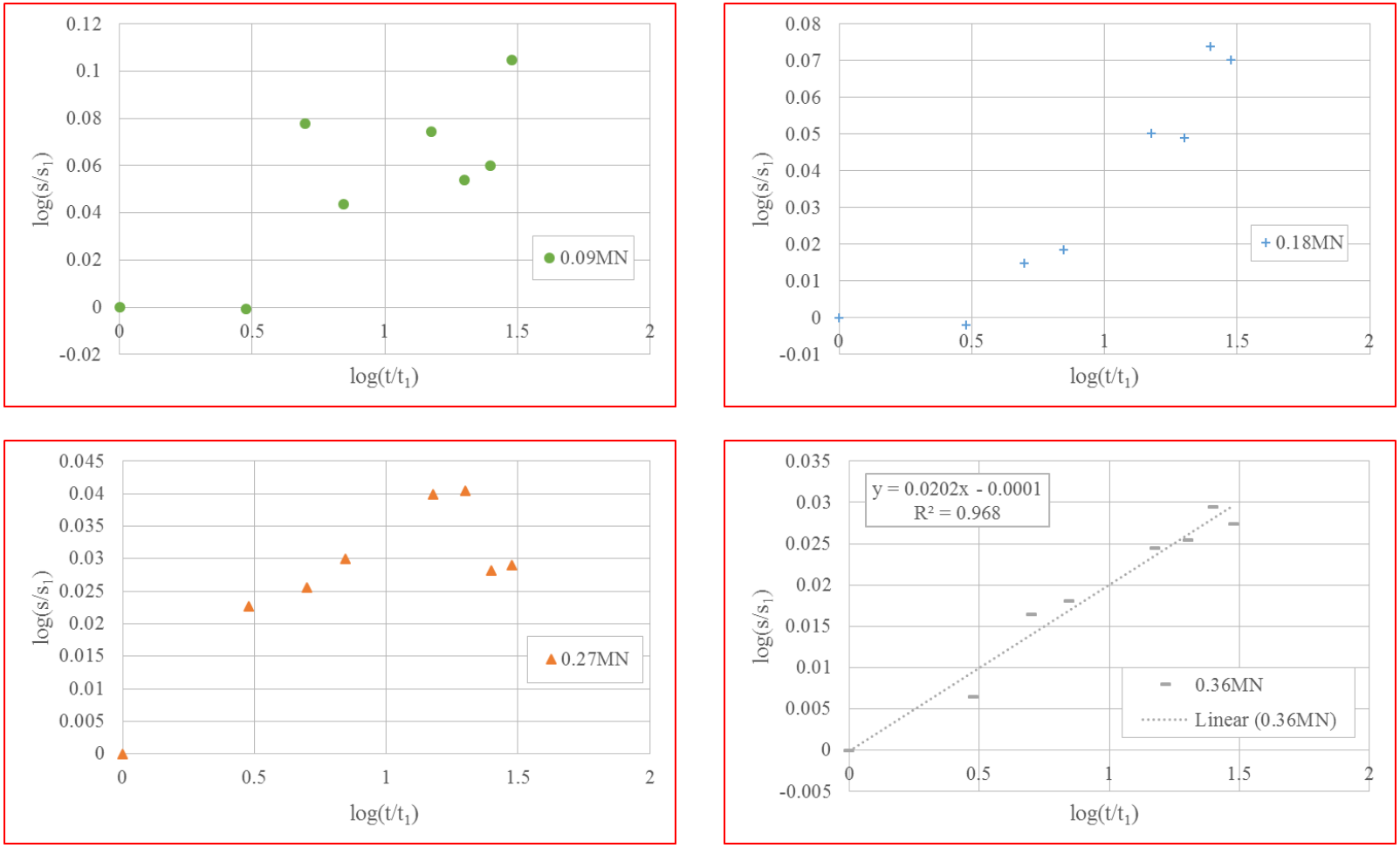

Figure 7-7. Strain-time curves (log-log scales), 1m footing, after Gibbens (1995)

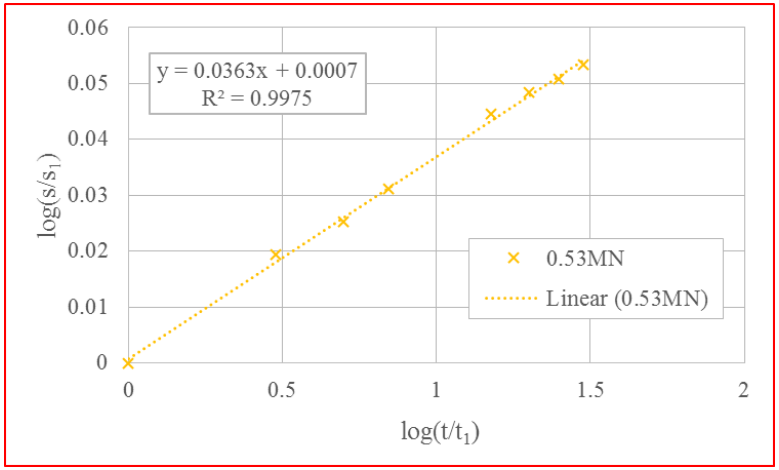

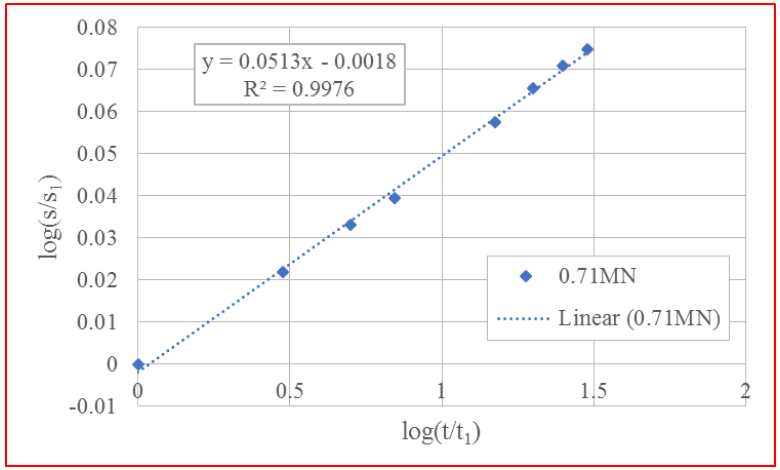

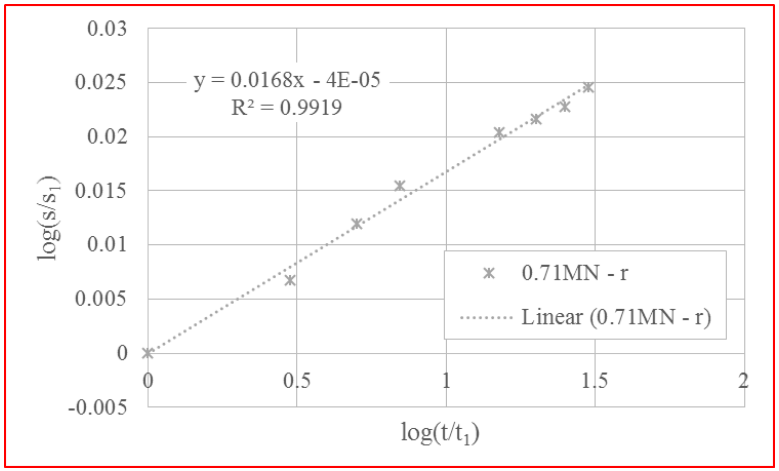

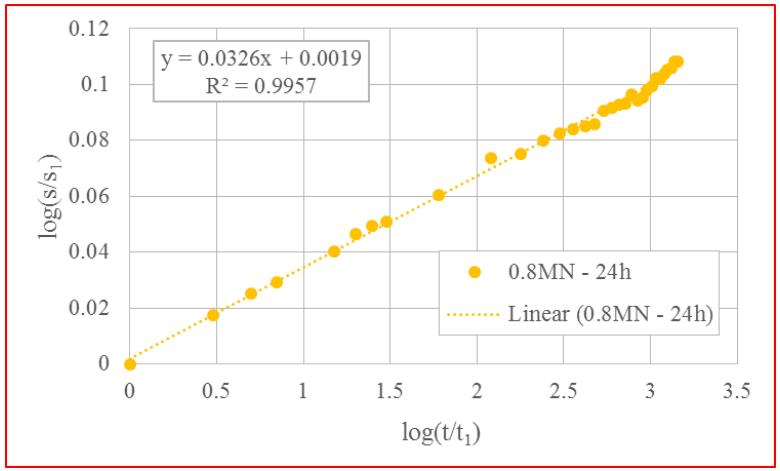

Figure 7-7 Continued

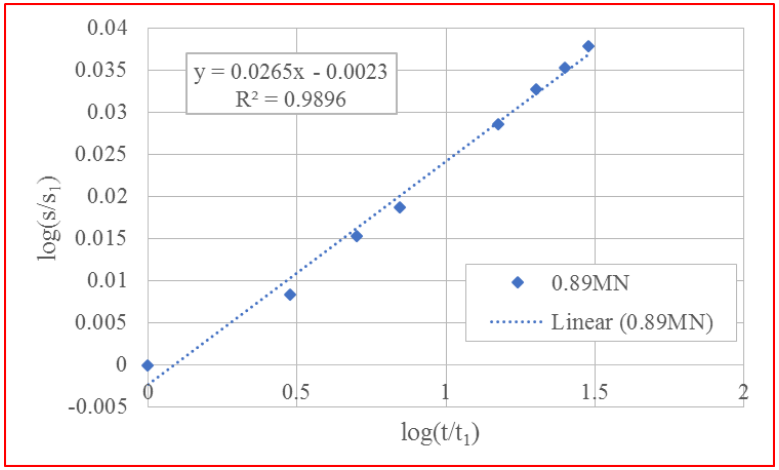

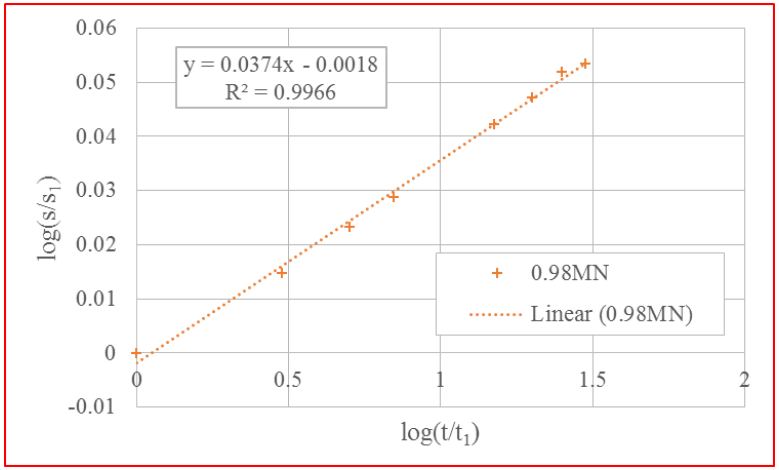

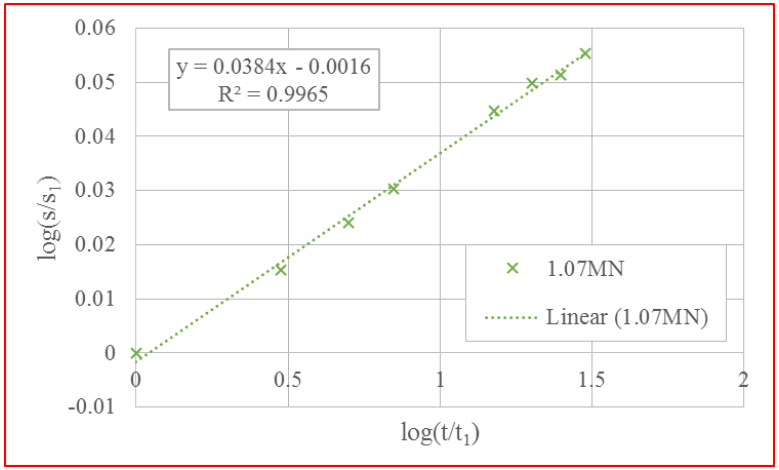

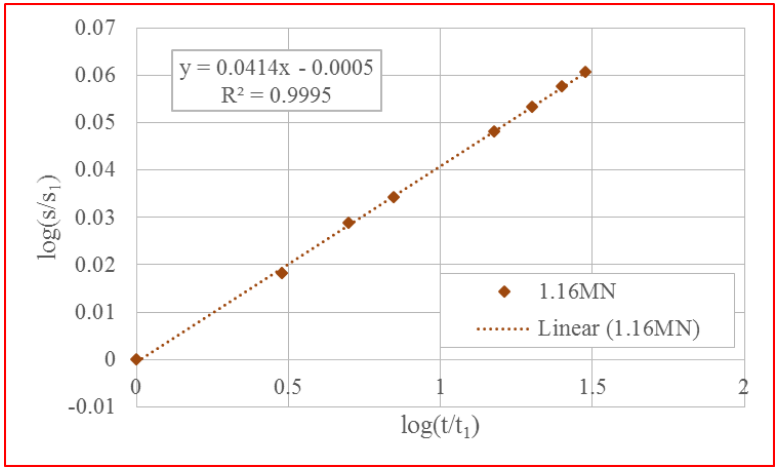

Figure 7-7 Continued

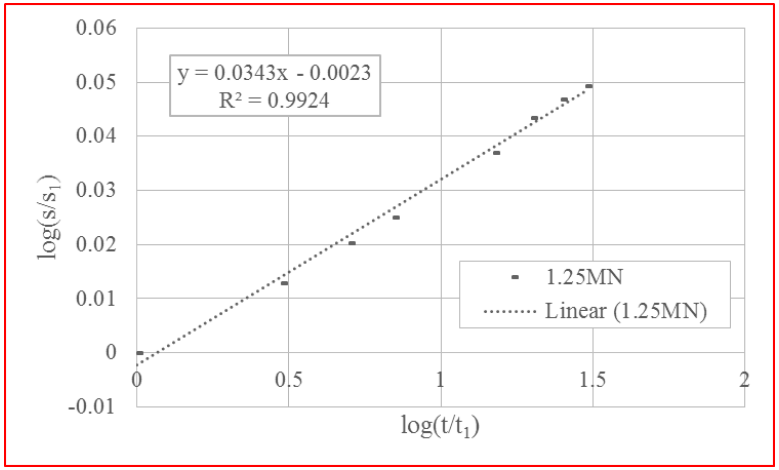

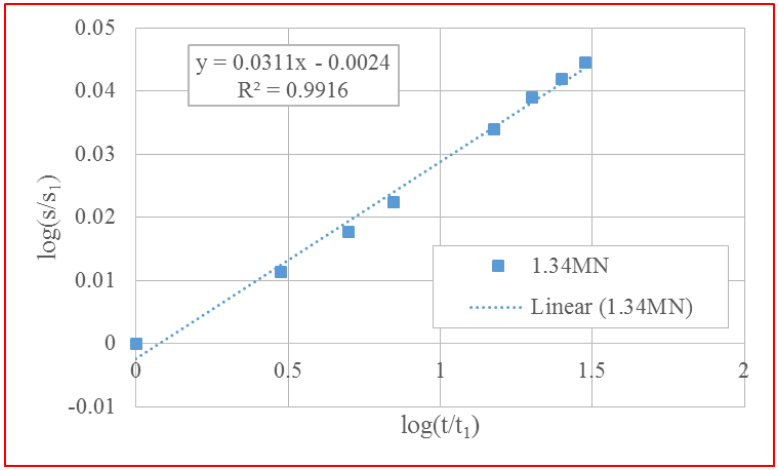

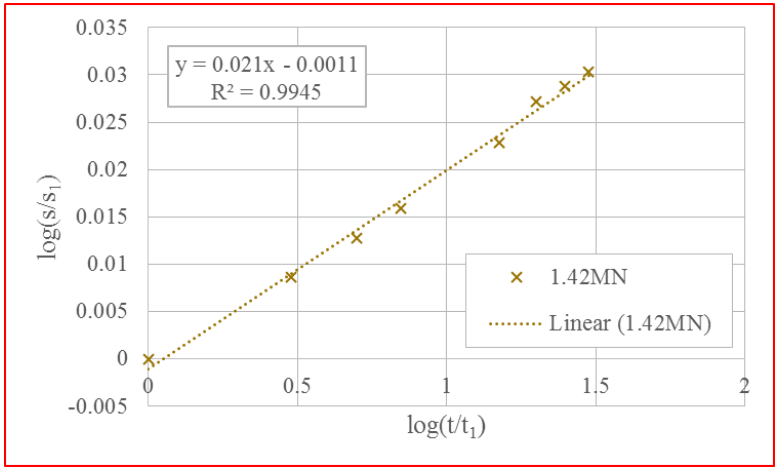

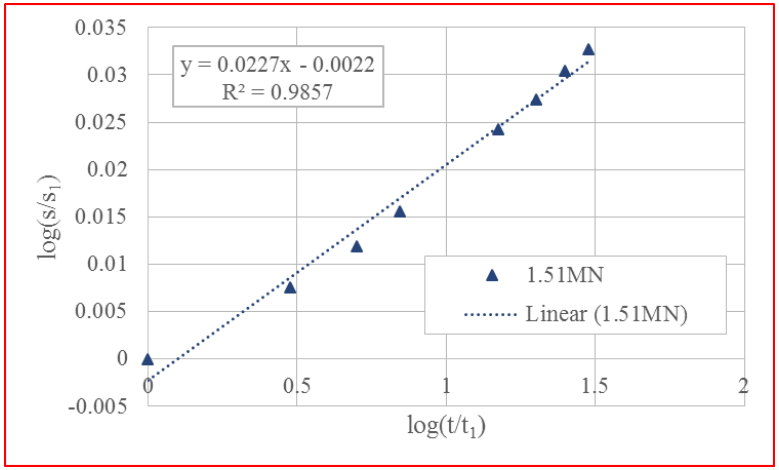

Figure 7-7 Continued

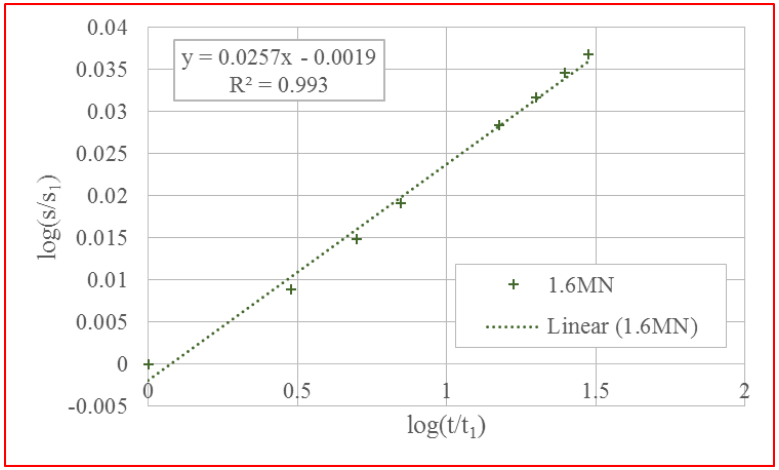

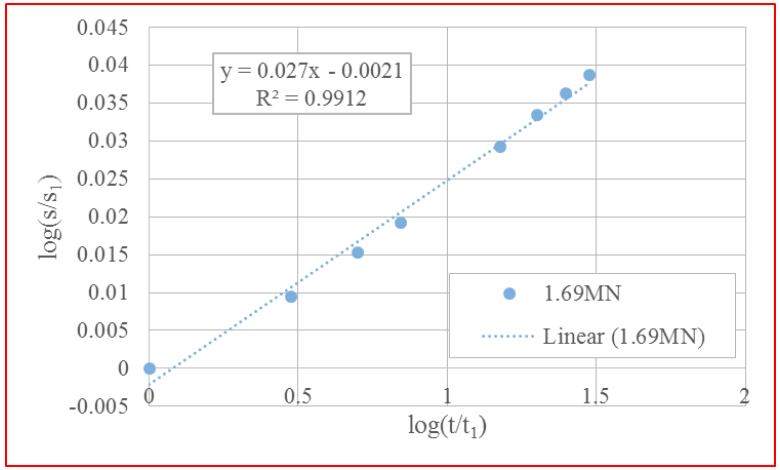

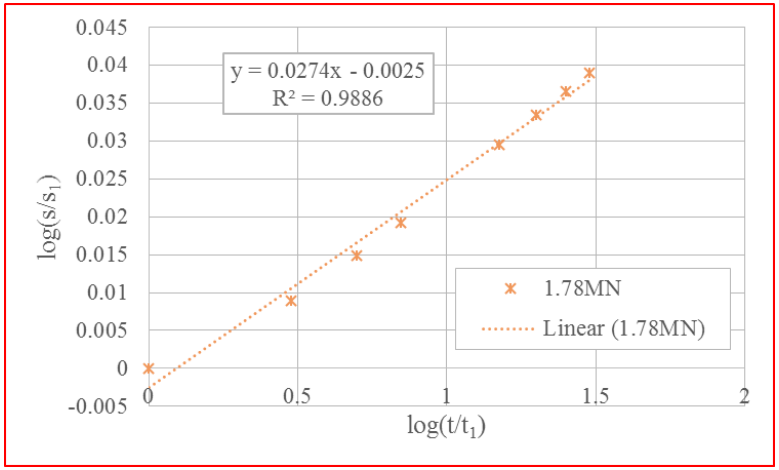

Figure 7-7 Continued

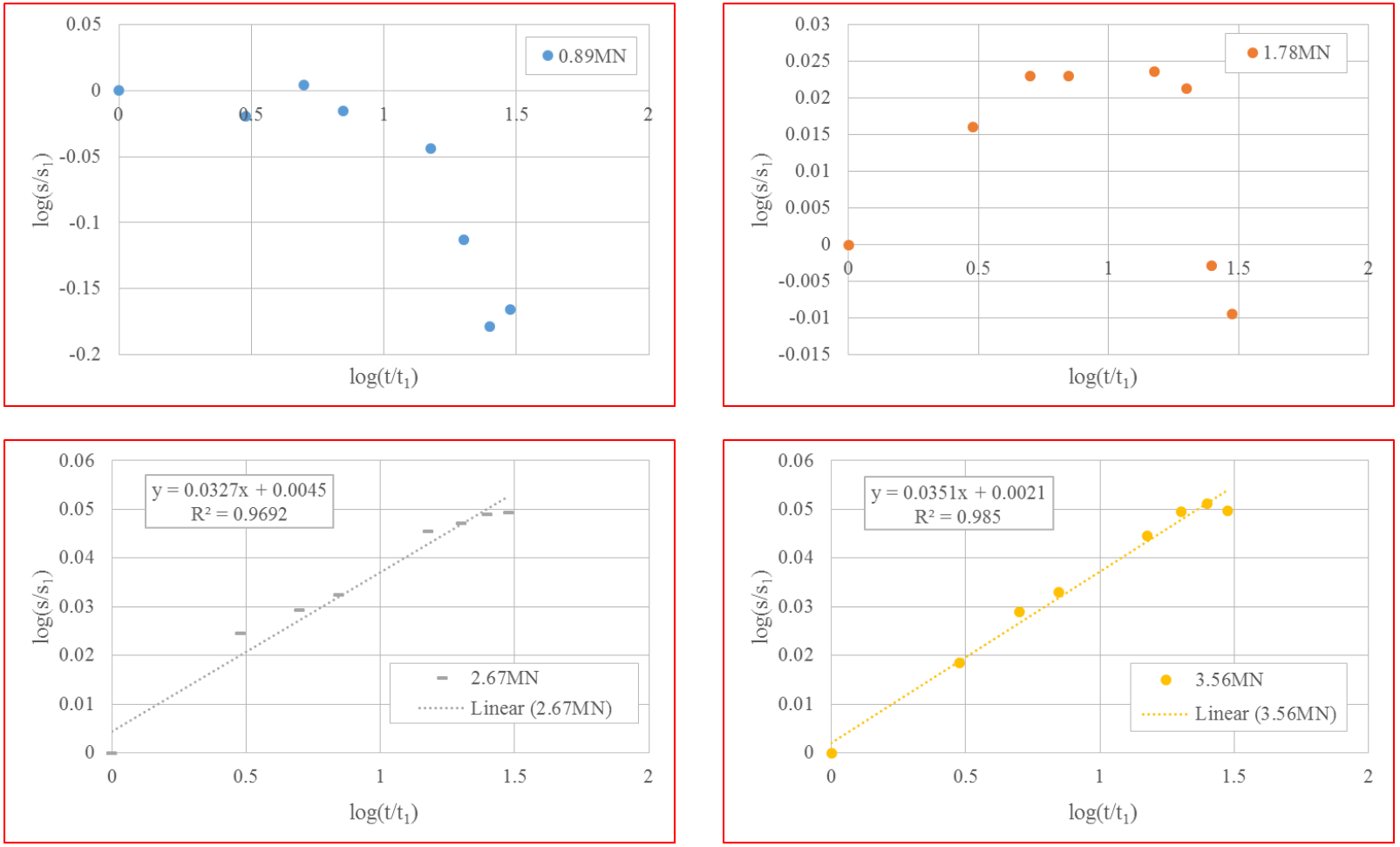

Figure 7-8. Strain-time curves (log-log scales), 3m footing (South), after Gibbens (1995)

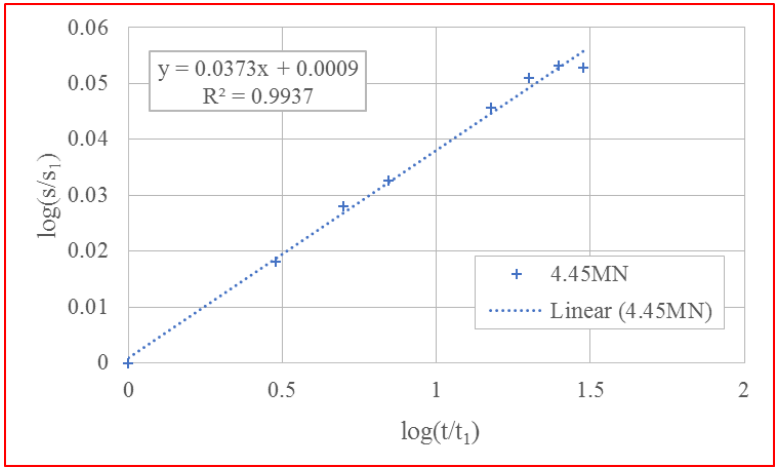

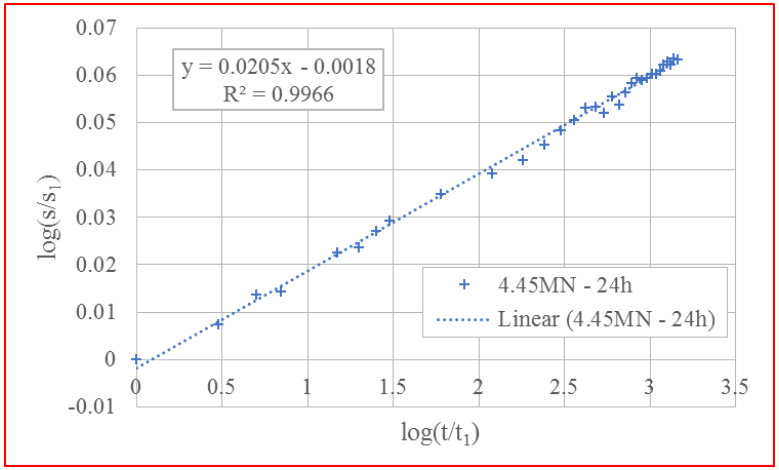

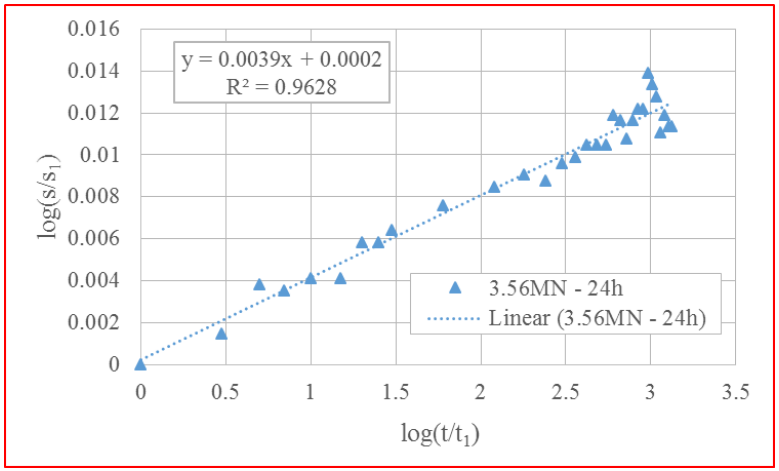

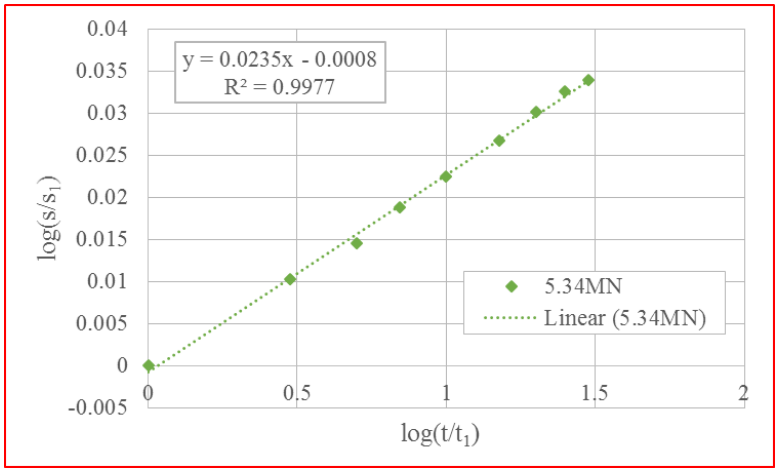

Figure 7-8 Continued

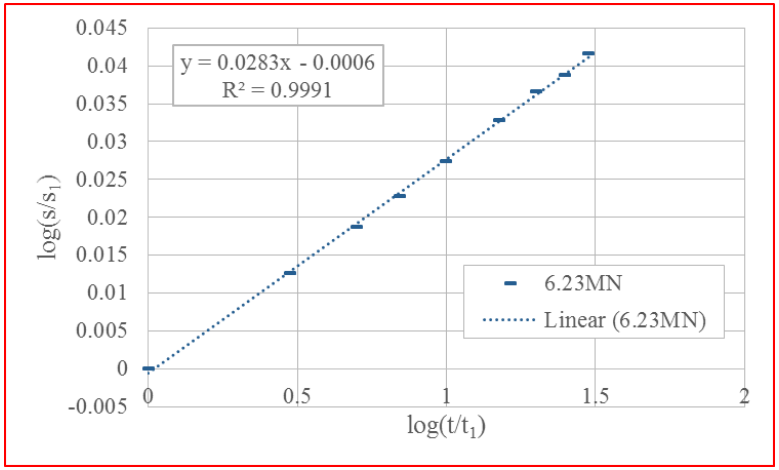

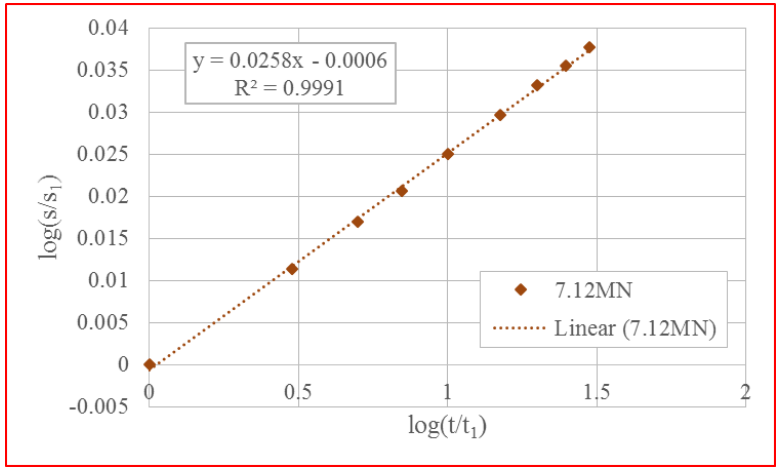

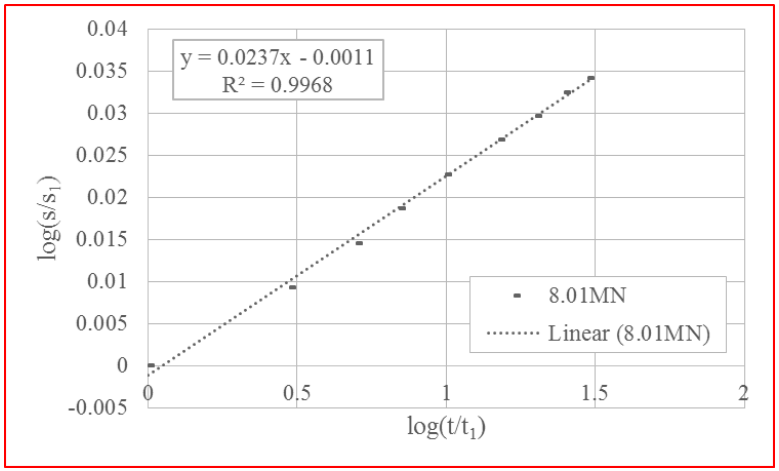

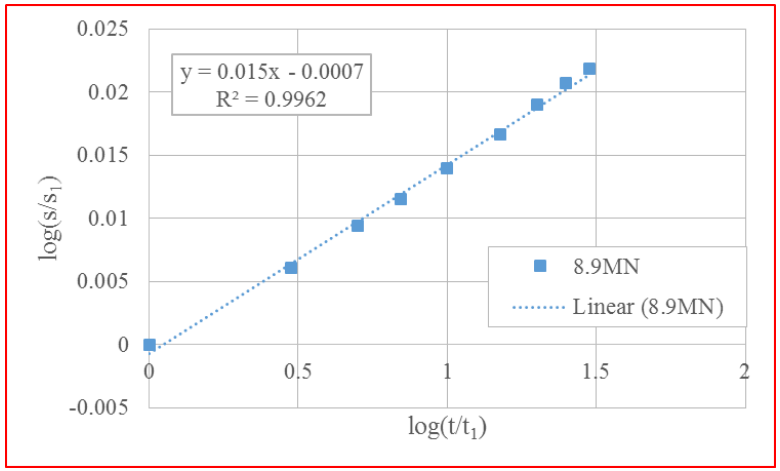

Figure 7-8 Continued

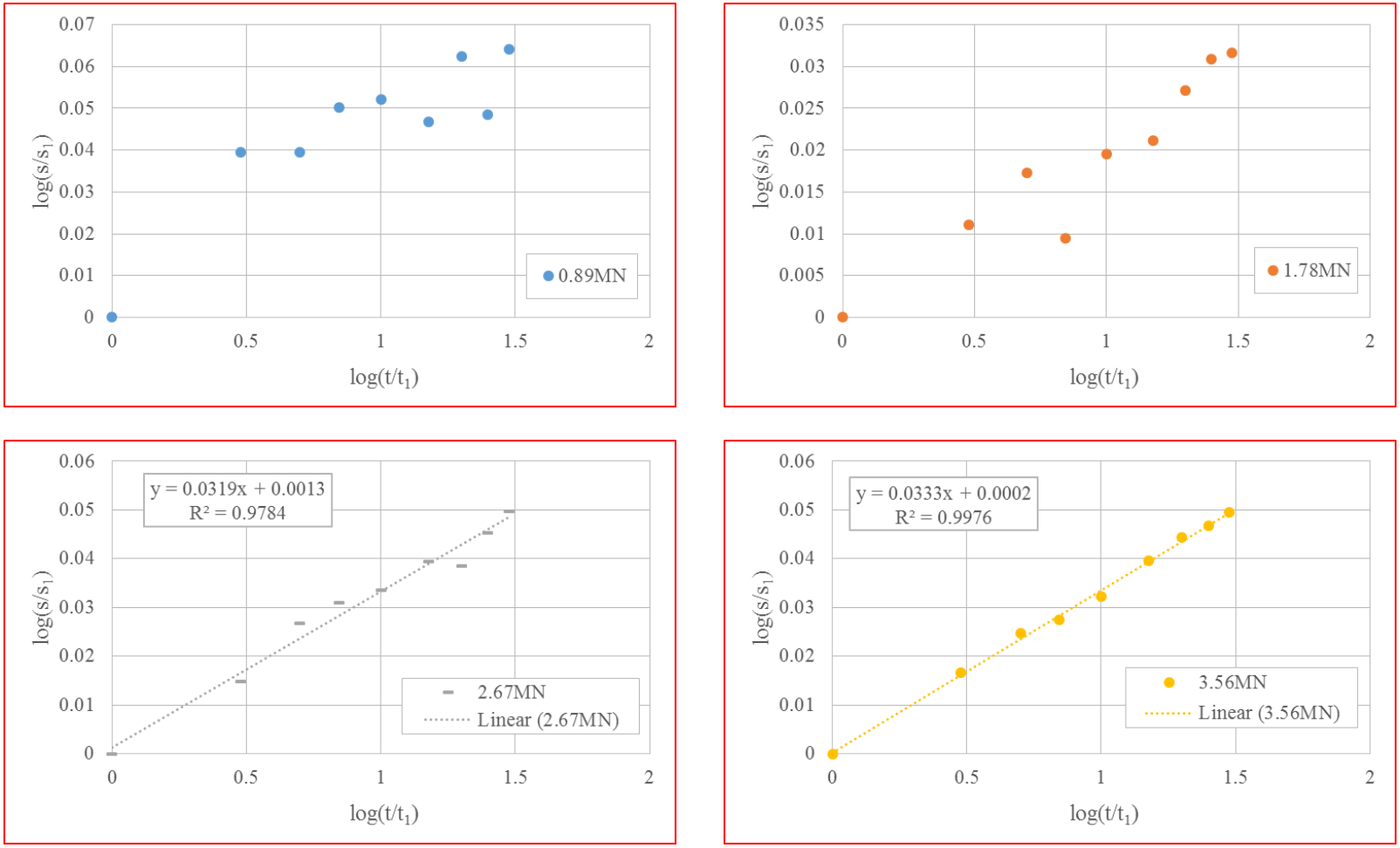

Figure 7-9. Strain-time curves (log-log scales), 3m footing (North), after Gibbens (1995)

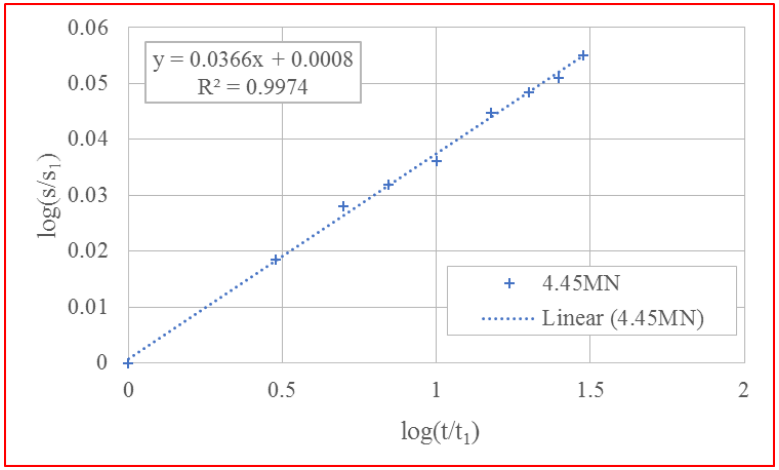

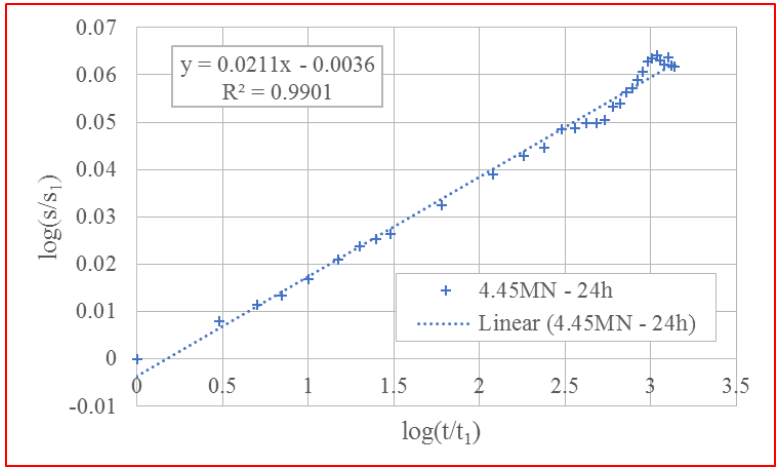

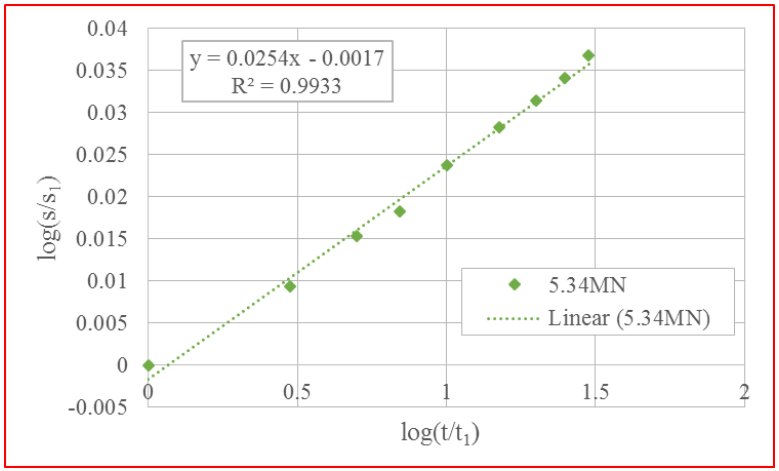

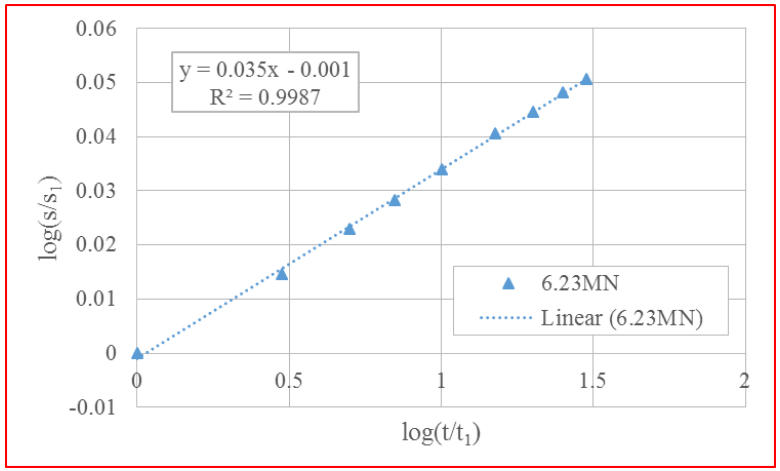

Figure 7-9 Continued

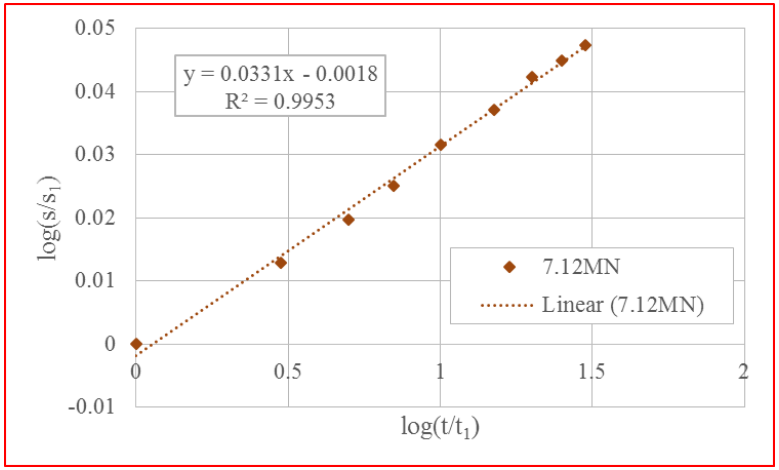

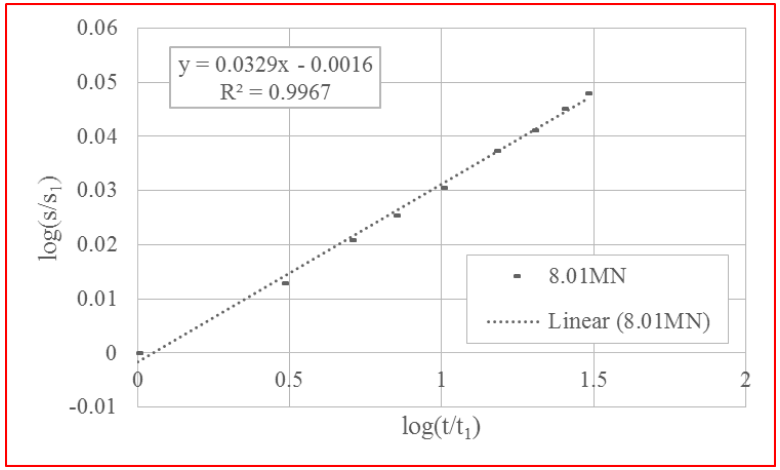

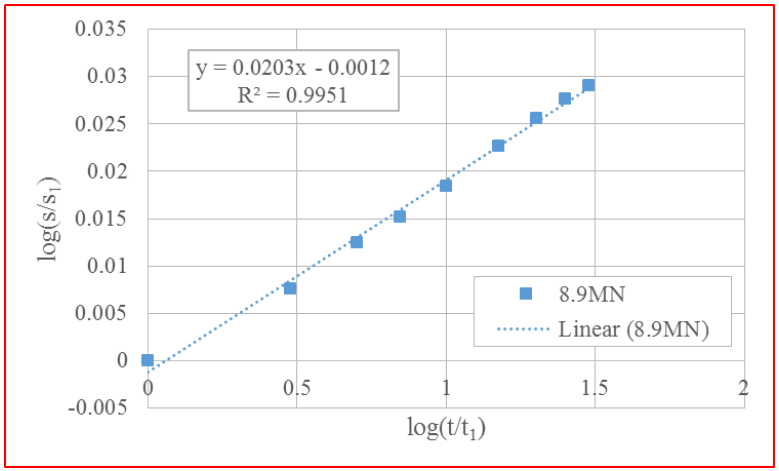

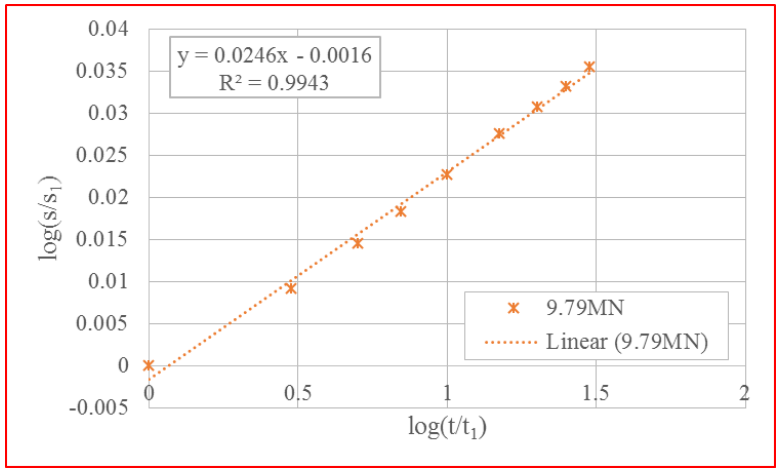

Figure 7-9 Continued

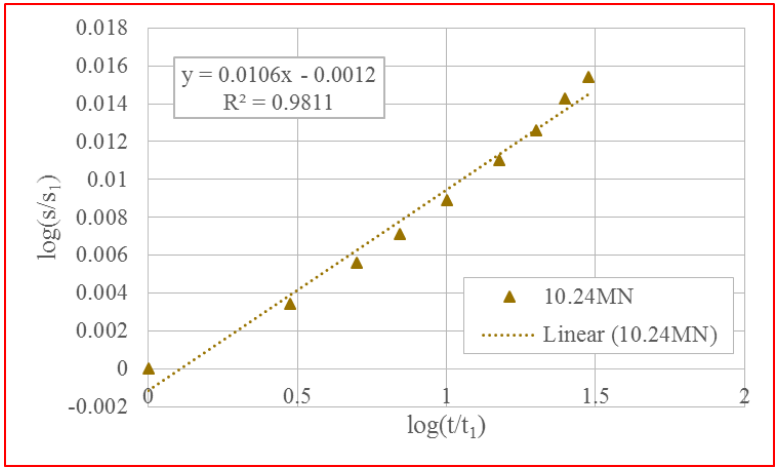

Figure 7-9 Continued

7.2.3. N Value-load Level Curve

N value-load level curve is plotted in figure 7-10 to figure 7-12. It is hard to agree that n value is independent of load level as presented in laboratory tests (figure 5-23, for instance). Briaud and Gibbens (1999) drew the conclusion that load history will have notably impact on n value. As pointed out in subsection 7.2.2, it is because n value is impacted by unload-reload cycle, unequal duration (24h versus 30min), and preloading. There are two more factors that will have an effect on n value: the chosen s_1 and wood beam creep due to self-weight.

If the load was sustained more than once (whether unload-reload cycle or preloading), to be consistent, s_1 corresponding to settlement at 1min at the first time (load was sustained) should be adopted to obtain n value. If s_1 is chosen as settlement at 1min at each time respectively, n value will be smaller. More details have been presented in subsection 5.4.5.

As mentioned earlier, only data with 24h duration was corrected when wood beam was adopted as reference beam. It is not surprising that n value of 30min duration with wood beam will be kind of weird. For example, n value of 1m footing is increasing with load level before the first unload-reload cycle.

It is worth noting that n value is gradually approaching (recovering) to a constant value after unload-reload cycle or 24h duration, even though n value at sustained load immediately following unload-reload cycle or 24h duration is significantly reduced. If n value without unload-reload cycle, 24h duration and wood beam is plotted as figure 7-13. It is in virtually constant.

Figure 7-10. N value-load level curve, 1m footing, after Gibbens (1995)

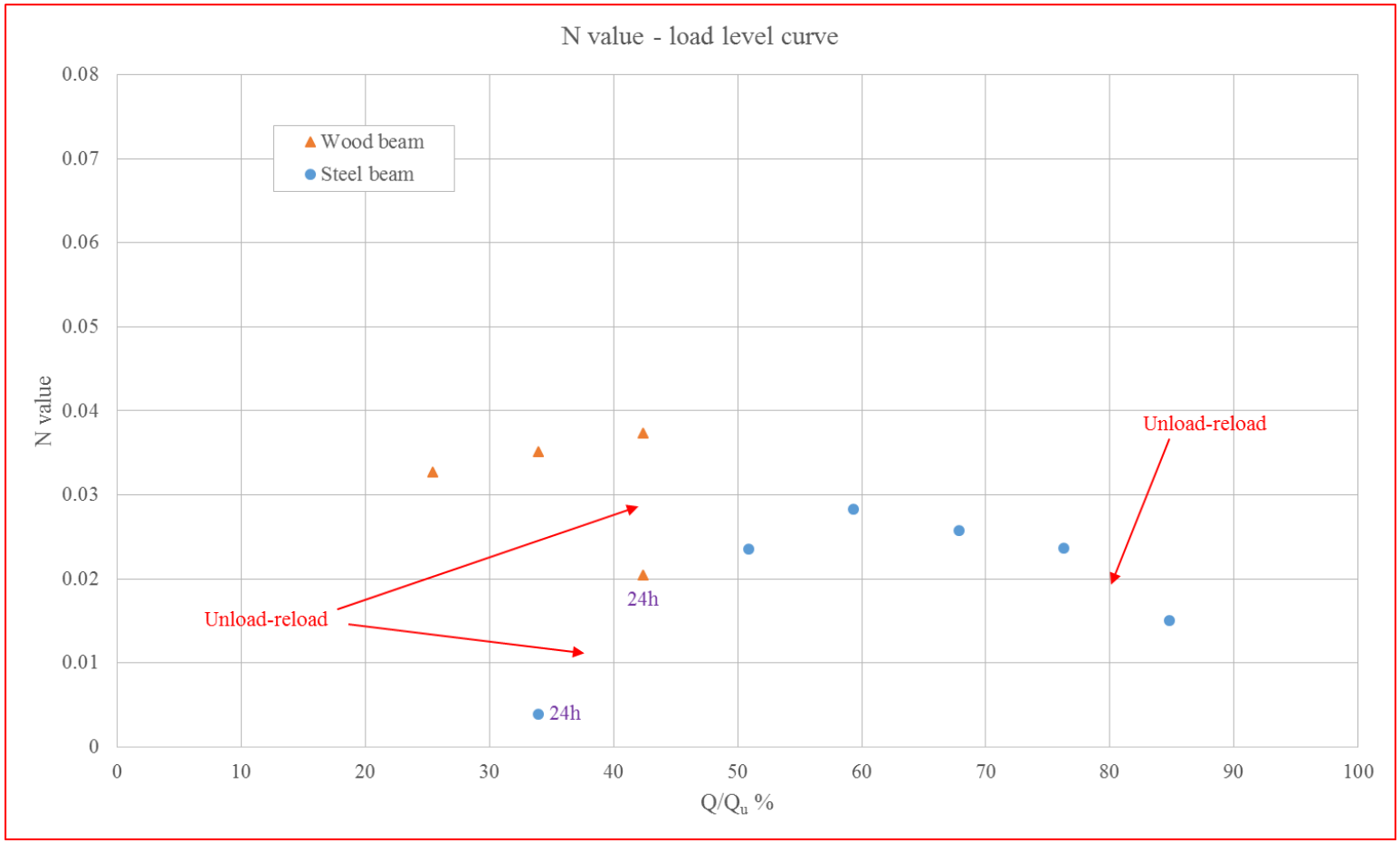

Figure 7-11. N value-load level curve, 3m footing (South), after Gibbens (1995)

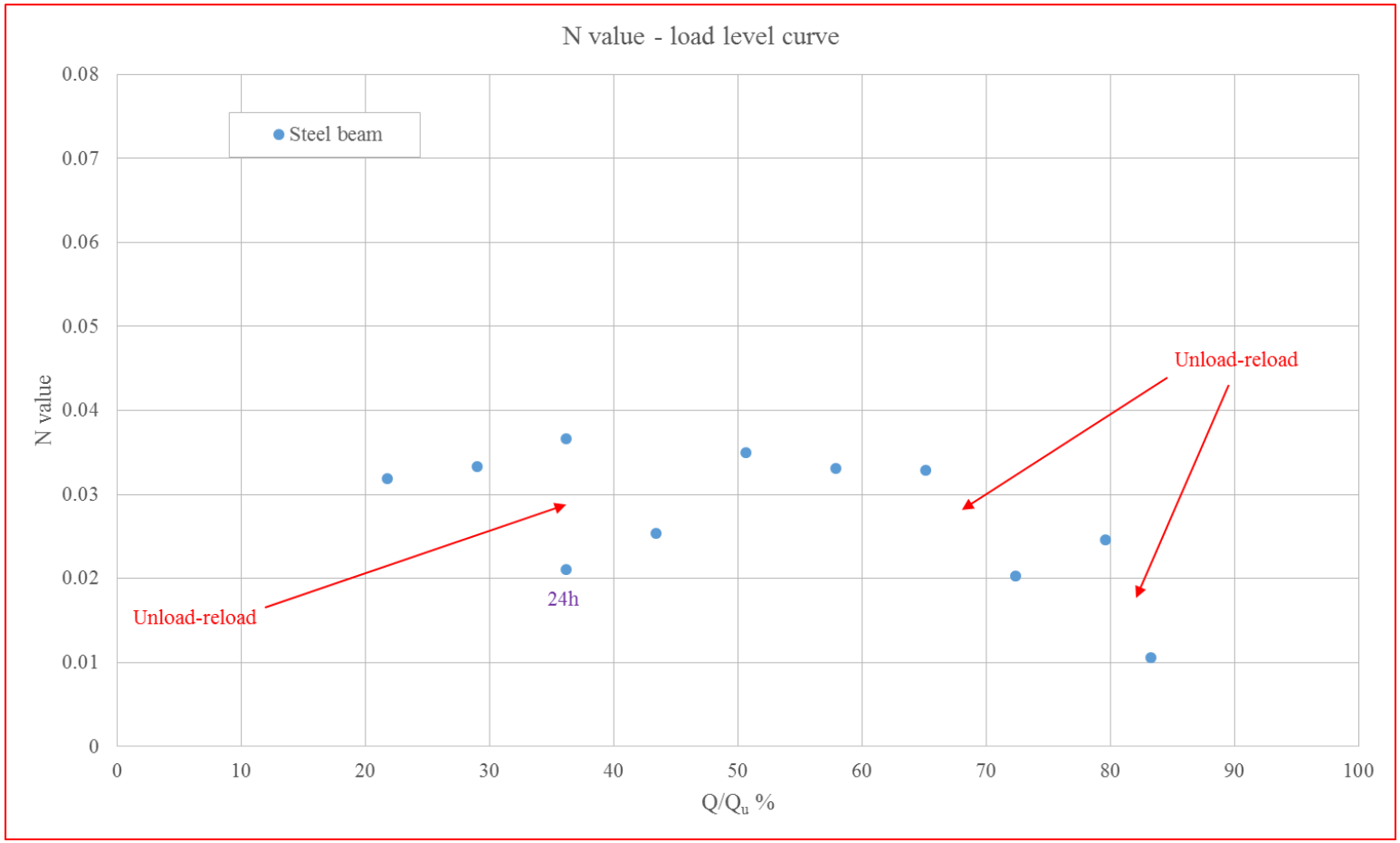

Figure 7-12. N value-load level curve, 3m footing (North), after Gibbens (1995)

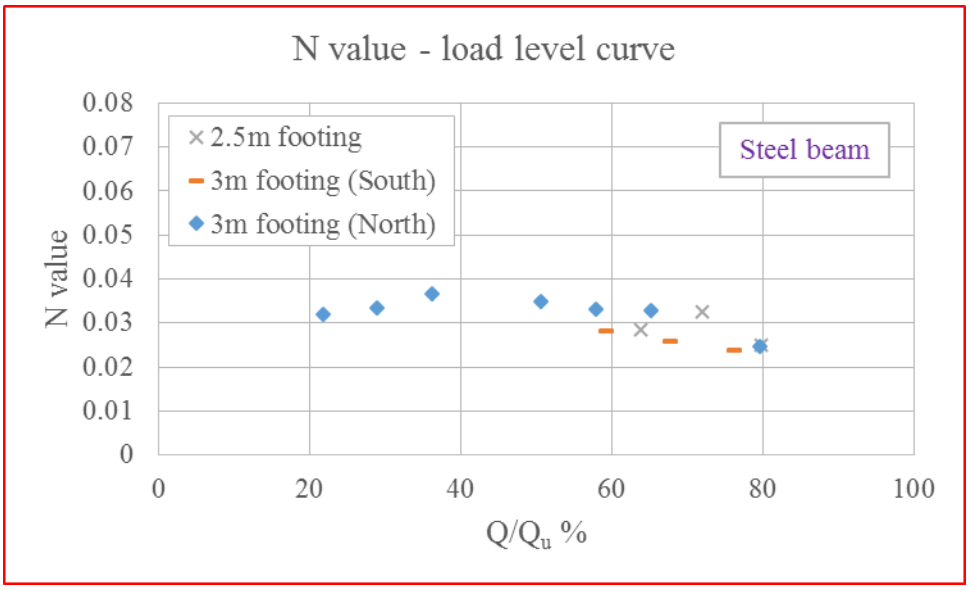

Figure 7-13. N value-load level curve, without unload-reload cycle, 24h duration, steel beam, after Gibbens (1995)

7.2.4. Verification Test in Laboratory

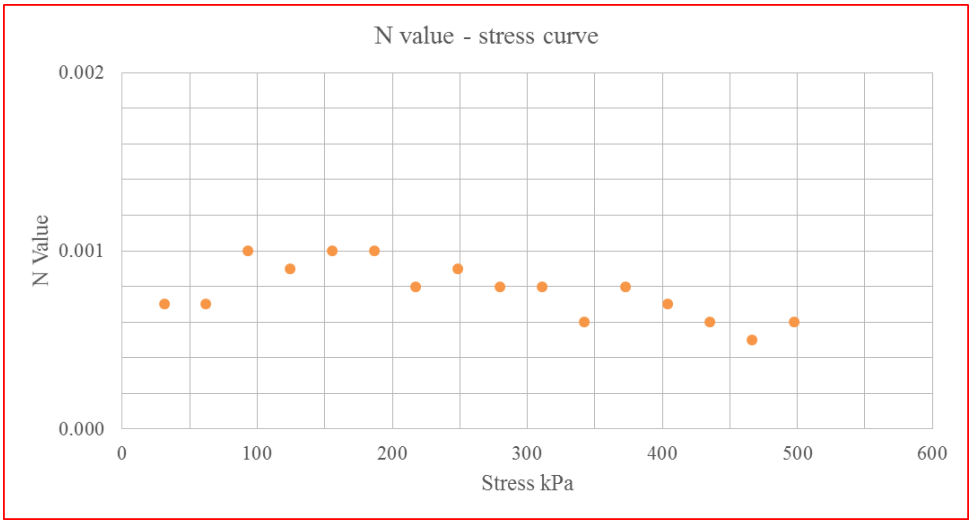

Figure 7-14. 30min duration, equal load increment

To verify the viewpoint that n value at sustained load following unload-reload cycle and 24h duration will be appreciably reduced, 1D consolidation test on wet sand were conducted. The reason to choose 1D consolidation test rather than triaxial creep test is that it is load increment test. And the reason to choose wet sand is that it won't swell and takes only a few seconds rather than more than 10min to consolidate, compared to clay.

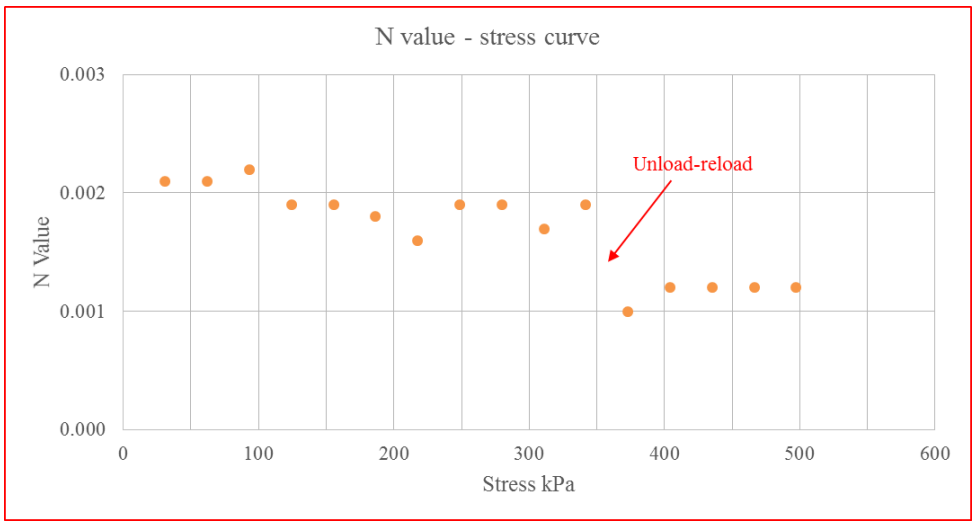

Figure 7-15. 30min duration, equal load increment with one unload-reload cycle

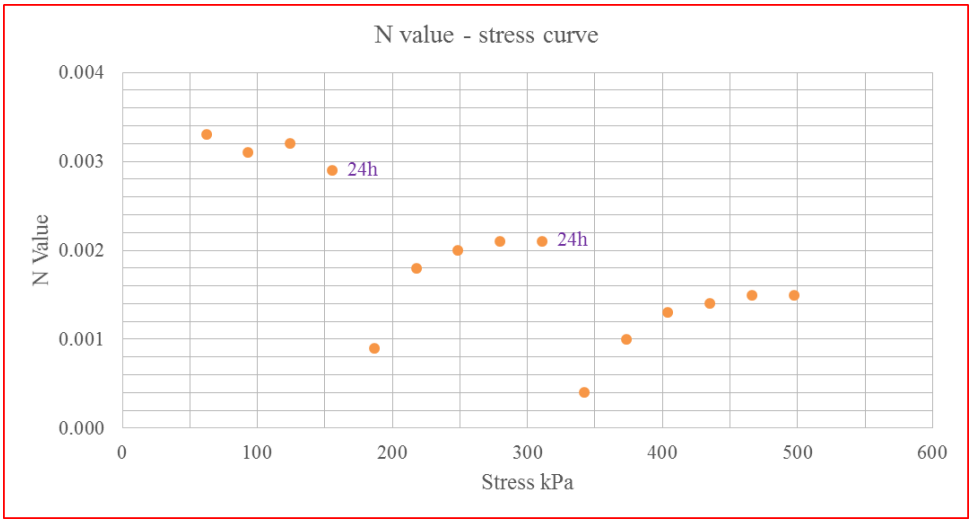

Figure 7-16. 30min duration in general with two 24h duration, equal load increment

The first test (figure 7-14) is loading from 15.5kPa to 497.3kPa with equal stress increment 15.5kPa (corresponding to 1kg dead weight), and the duration of each sustained stress is 30min.

The second test (figure 7-15) is same to the first test, except there is one unload-reload cycle after 341.9kPa. It is unloading from 341.9kPa to 1.5kPa, waiting 5sec, and then reloading from 1.5kPa to 373kPa.

The third test (figure 7-16) is same to the first test, except the duration at 155.4kPa and 310.8kPa is 24h rather than 30min.

Attention should be paid to the trend of n value rather than the number of n value, because it is not the same soil (wet sand is purchased instead of samples from TAMU-NGES - sand site) and mechanism is also different, while field tests are more related to deviatoric strain and 1D consolidation test is more related to hydrostatic strain.

N value is essentially independent of stress when there is no unload-reload cycle and unequal duration. N value at sustained stress following unload-reload cycle or larger duration (24h/30min = 48times in this case) will be significantly reduced. Though, after one to three sustained stress following, n value is approaching (recovering) to a new constant. However, the new constant n value is still smaller than the previous constant n value is because s_1 is chosen reference to the very beginning of test (i.e., zero deformation) (figure 3-8) so that the impact of unload-reload cycle and unequal duration is still taken into account.

Actually, the impact from unload-reload cycle and unequal duration is quite similar to the impact of swelling during 1D consolidation test and 1D compression test. As it has been explained before that n value is tremendously impacted at low stress levels, and it gradually recovers to be normal at high stress levels.

7.3. Ground Anchor Pullout Test by Suroor (1998), TAMU-NGES - Clay Site

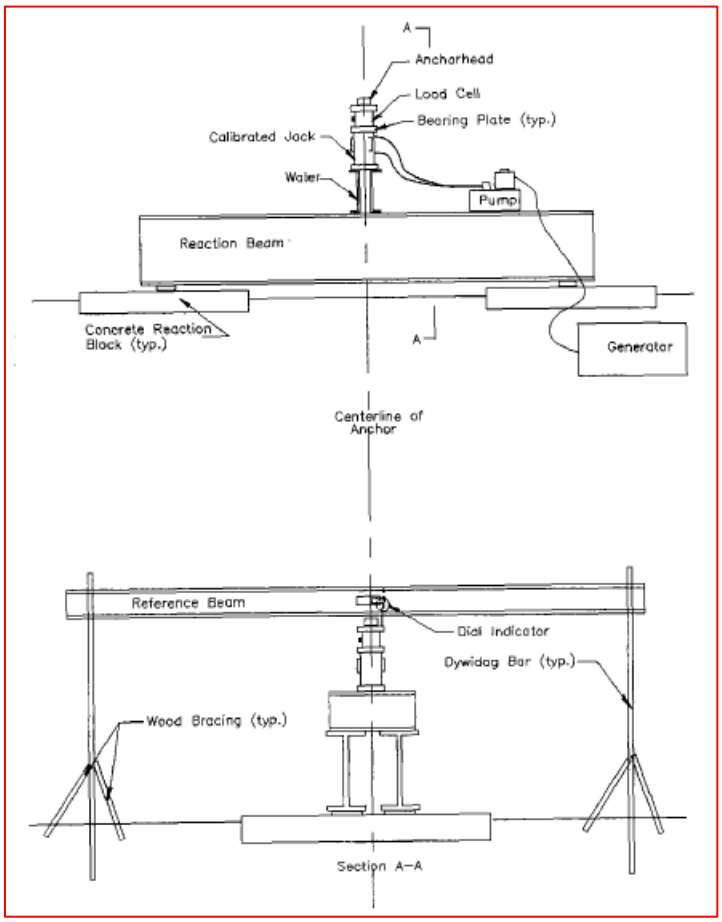

Figure 7-17. Ground anchor pullout test setup, after Powers (1993)

Ten ground anchors were installed at the clay site on TAMU-NGES in 1991. Powers (1993) tested all ten anchors at the same year, however, data is not available for analysis of n value. It should be pointed out that there are lock-off loads for anchor 1 (523kN) and anchor 2 (606kN) after tests finished in 1991. In other words, anchor 1 and anchor 2 were creeping six years (1991 to 1997) while movement was not monitored.

Suroor (1998) retested anchor 1, anchor 2, anchor 7 and anchor 8 in 1997, and raw data was appended in the thesis. With regard to anchor 1 and anchor 2, the lock-off load was first released, then were retested following scheduled loading protocols.

An overall view of setup for testing is plotted in figure 7-17. More details could be found at Powers (1993), Suroor (1998), and Briaud (1998).

7.3.1. Load-movement Curve

Table 7-4. Loading of all anchors, after Suroor (1998)

Phase	Load kN			
	Anchor 1	Anchor 2	Anchor 7	Anchor 8
AL	43.4	61.7	36.4	53.7
P1	107.0	119.0	80.7	67.1
P2	217.5	229.3	160.4	144.9
P3	315.8	336.4	239.9	214.7
P4	422.0	442.2	325.4	287.0
P5	527.6	550.6	407.3	374.4
P6	632.9	655.2	487.3	435.5
P7	732.3	763.2	582.5	506.9
P8	834.2	863.7	646.7	583.7
P9	934.5	967.8	740.9	660.0
P10	1034.5	1062.6	822.8	737.5
P11	1129.7	1158.7	904.9	**871.7**
P12	1222.5	1260.7	987.0	**1010.6**
P13	1310.5	1284.1	1058.4	**1152.7**
P14			1152.4	

Loading of all anchors is presented in table 7-4. In most cases, load increment is equal. Loading protocol is presented in table 7-5 to table 7-8. In general, the duration could be taken as equal. It is worth noting that there is unload-reload cycle before and after each sustained load, which will tremendously impact n value.

Load-movement curve is plotted in figure 7-18. Because there are so many unload-reload cycles, only monotonic curve is plotted. It seems there are some errors in the data because residual movement is somehow recovering at high load, especially for anchor 2 and anchor 8. Besides, it is almost no movement until failure, and the reason is so many unload-reload cycles.

Table 7-5. Loading protocol, anchor 1, after Suroor (1998)

Stage	Anchor 1	
	Loading	Duration minutes
S1	AL, P1	0
S2	AL, P1, P2	0, 1, 2, 3, 4, 5, 6, 10, 15
S3	AL, P1, P2, P3	0, 1, 2, 3, 4, 5, 6, 10
S4	AL, P1, P2, …, P4	0, 1, 2, 3, 4, 5, 6, 10
S5	AL, P1, P2, …, P5	0, 1, 2, 3, 4, 5, 6, 10
S6	AL, P1, P2, …, P6	0, 1, 2, 3, 4, 5, 6, 10
S7	AL, P1, P2, …, P7	0, 1, 2, 3, 4, 5, 6, 10
S8	AL, P1, P2, …, P8	0, 1, 2, 3, 4, 5, 6, 10
S9	AL, P1, P2, …, P9	0, 1, 2, 3, 4, 5, 6, 10, 15, 20
S10	AL, P1, P2, …, P10	0, 1, 2, 3, 4, 5, 6, 10
S11	AL, P1, P2, …, P11	0, 1, 2, 3, 4, 5, 6, 10
S12	AL, P1, P2, …, P12	0, 1, 2, 3, 4, 5, 6, 10
S13	AL, P1, P2, …, P13	0, 1, 2, 3, 4, 5, 6

Table 7-6. Loading protocol, anchor 2, after Suroor (1998)

Stage	Anchor 2	
	Loading	Duration minutes
S1	AL, P1	0
S2	AL, P1, P2	0, 1, 2, 3, 4
S3	AL, P1, P2, P3	0, 1, 2, 3, 4
S4	AL, P1, P2, …, P4	0, 1, 2, 3, 4, 5, 6, 10
S5	AL, P1, P2, …, P5	0, 1, 2, 3, 4, 5, 6, 10
S6	AL, P1, P2, …, P6	0, 1, 2, 3, 4, 5, 6, 10
S7	AL, P1, P2, …, P7	0, 1, 2, 3, 4, 5, 6, 10
S8	AL, P1, P2, …, P8	0, 1, 2, 3, 4, 5, 6, 10
S9	AL, P1, P2, …, P9	0, 1, 2, 3, 4, 5, 6, 10
S10	AL, P1, P2, …, P10	0, 1, 2, 3, 4, 5, 6, 10
S11	AL, P1, P2, …, P11	0, 1, 2, 3, 4, 5, 6, 10, 15, 20, 25, 30, 40, 50, 60
S12	AL, P1, P2, …, P12	0, 1, 2, 3, 4, 5, 6, 10, 15, 20, 25, 30
S13	AL, P1, P2, …, P13	0, 1, 2, 3, 4, 5, 6, 10, 15, 20, 25

Table 7-7. Loading protocol, anchor 3, after Suroor (1998)

Stage	Anchor 7	
	Loading	Duration minutes
S1	AL, P1	0, 1, 2, 3
S2	AL, P1, P2	0, 1, 2, 3
S3	AL, P1, P2, P3	0, 1, 2
S4	AL, P1, P2, …, P4	0, 1, 2, 3
S5	AL, P1, P2, …, P5	0, 1, 2, 3, 4, 5, 6, 10
S6	AL, P1, P2, …, P6	0, 1, 2, 3, 4, 5, 6, 10
S7	AL, P1, P2, …, P7	0, 1, 2, 3, 4, 5, 6, 10
S8	AL, P1, P2, …, P8	0, 1, 2, 3, 4, 5, 6, 10, 15, 20
S9	AL, P1, P2, …, P9	0, 1, 2, 3, 4, 5, 6, 10, 15
S10	AL, P1, P2, …, P10	0, 1, 2, 3, 4, 5, 6, 10, 15, 20, 25
S11	AL, P1, P2, …, P11	0, 1, 2, 3, 4, 5, 6, 10, 15, 20, 25, 30
S12	AL, P1, P2, …, P12	0, 1, 2, 3, 4, 5, 6, 10, 15, 20, 25, 30
S13	AL, P1, P2, …, P13	0, 1, 2, 3, 4, 5, 6, 10, 15, 20, 25, 30
S14	AL, P1, P2, …, P13	0, 1, 2, 3, 4, 5, 6, 10, 20, 30

Table 7-8. Loading protocol, anchor 4, after Suroor (1998)

Stage	Anchor 8	
	Loading	Duration minutes
S1	AL, P1	0
S2	AL, P1, P2	0, 1, 2
S3	AL, P1, P2, P3	0, 1, 2, 3, 4, 5, 6, 10
S4	AL, P1, P2, …, P4	0, 1, 2, 3, 4, 5, 6, 10
S5	AL, P1, P2, …, P5	0, 1, 2, 3, 4, 5, 6, 10
S6	AL, P1, P2, …, P6	0, 1, 2, 3, 4, 5, 6, 10
S7	AL, P1, P2, …, P7	0, 1, 2, 3, 4, 5, 6, 10
S8	AL, P1, P2, …, P8	0, 1, 2, 3, 4, 5, 6, 10
S9	AL, P1, P2, …, P9	0, 1, 2, 3, 4, 5, 6, 10
S10	AL, P1, P2, …, P10	0, 1, 2, 6, 10, 15
S11	AL, P1, P2, …, P11	0, 1, 2, 3, 4, 5, 6, 10, 15, 20
S12	AL, P1, P2, …, P12	0, 1, 2, 3, 4, 5, 6, 10, 15, 20, 25, 30
S13	AL, P1, P2, …, P13	0, 1

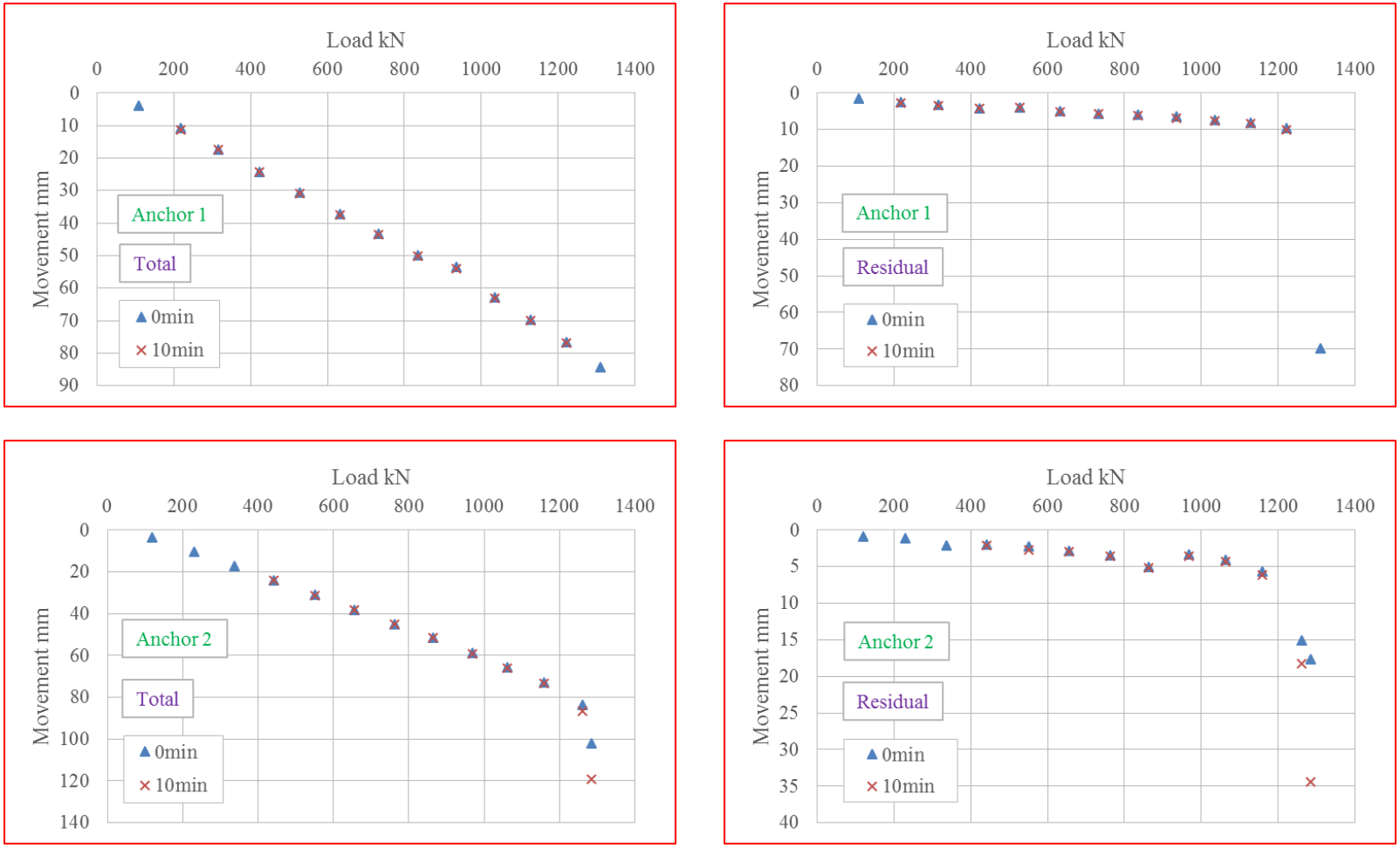

Figure 7-18. Load-movement curve (monotonic), after Suroor (1998)

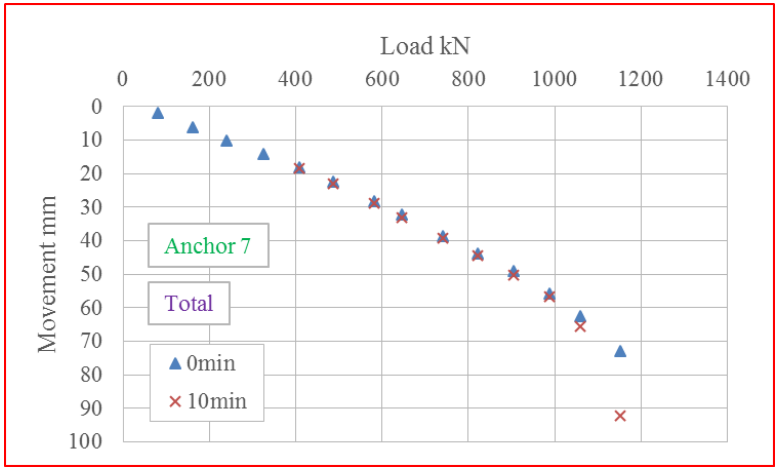

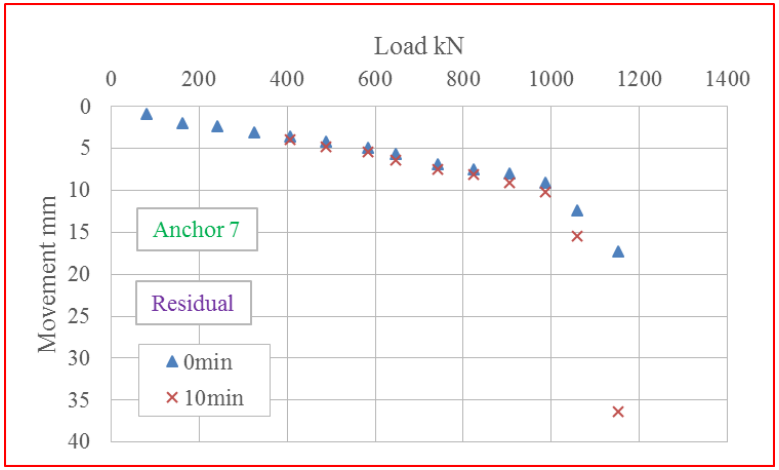

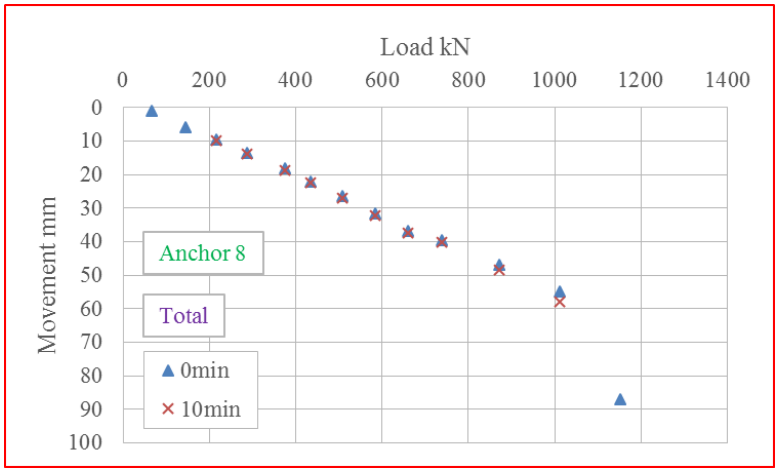

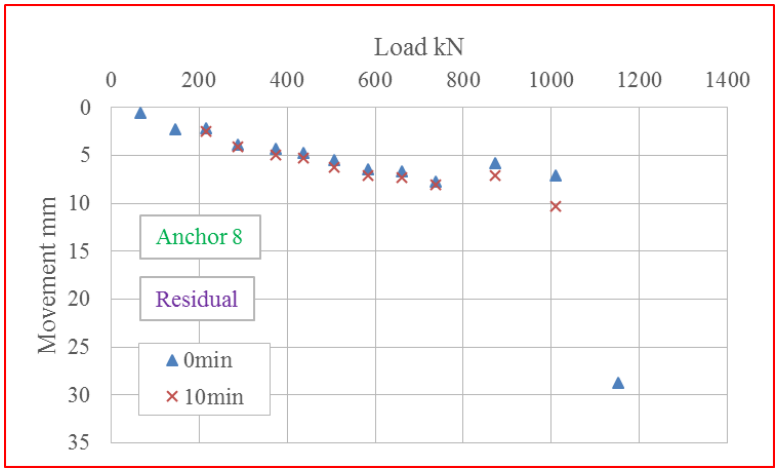

Figure 7-18 Continued

7.3.2. Movement-time Curve

Movement-time curve (log-log scales) is plotted in figure 7-19 to figure 7-22. At some sustained load, there is no movement during 10min duration, and strain-time curve is not plotted.

It is hardly to get any n value until approaching failure for anchor 1 and anchor 2, it is not surprising because both anchors were creeping six years with sustained load at load level 60% of ultimate load Q_u, where Q_u is defined to be the load corresponding to residual movement at 10min equal to 30mm. Thus, on one hand, for load level lower than 60%, the movement will be tiny (i.e., n value is negligible) because of the effect of preloading. On the other hand, for load level somewhat higher than 60%, it has already been demonstrated in section 7.2 that n value at sustained load following a long duration (6yr/10min = 315360times in this case) will drastically reduce.

With regard to anchor 7 and anchor 8, n value is obtained at all sustained loads except low loads where seating problem exists and loads where residual movement is somehow decreasing instead of increasing. However, generally, n value is appreciably lower than that from triaxial creep test in laboratory (figure 5-23), because of so many unload-reload cycles.

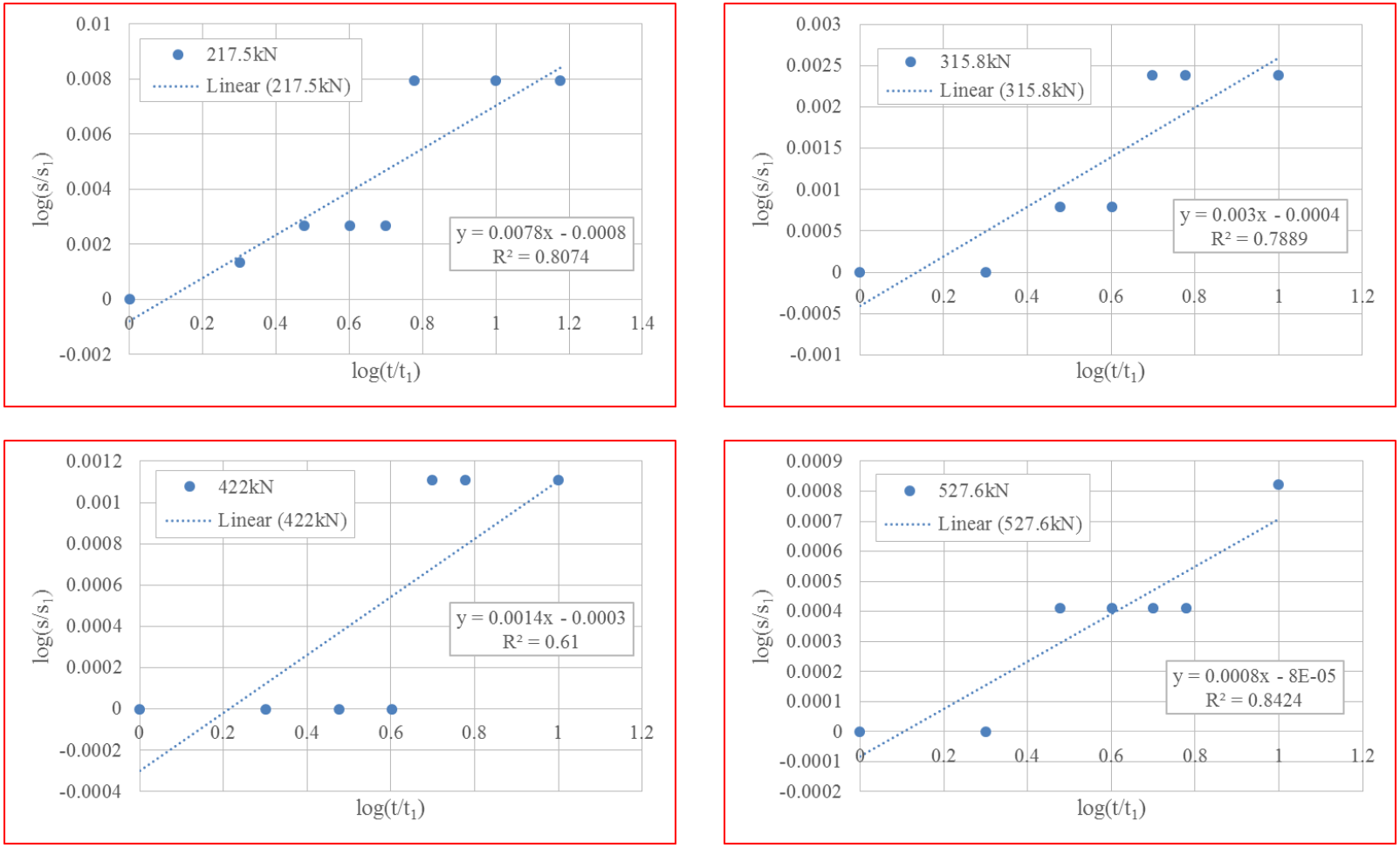

Figure 7-19. Movement-time curves (log-log scales), anchor 1, after Suroor (1998)

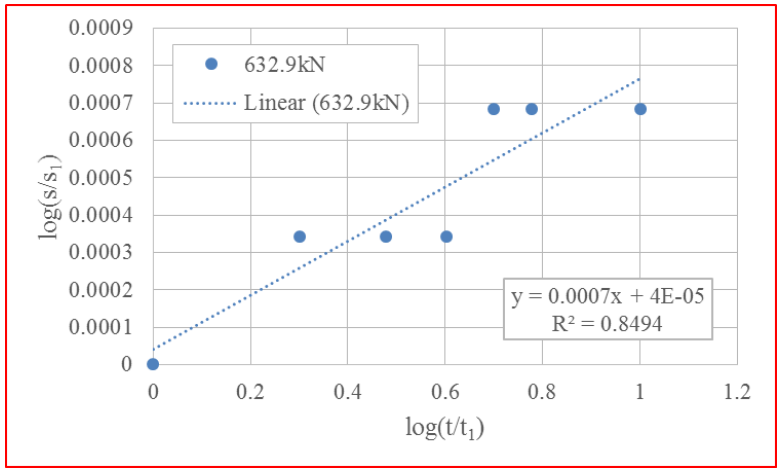

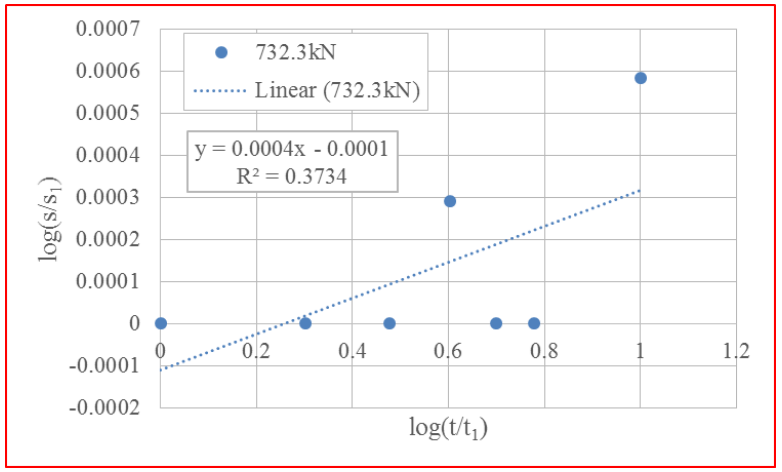

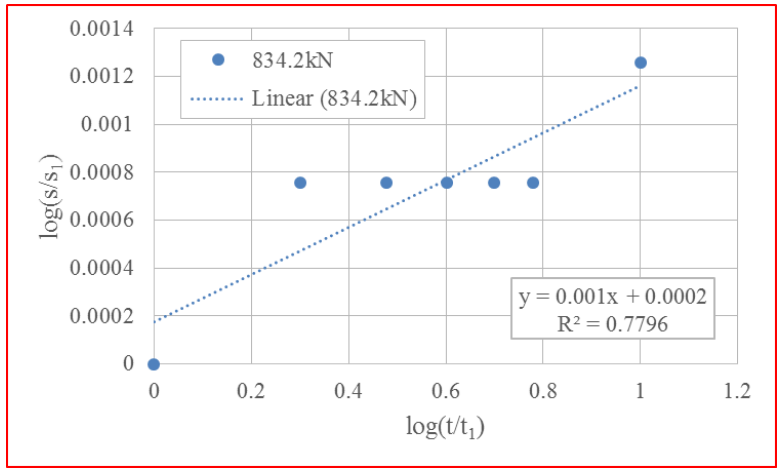

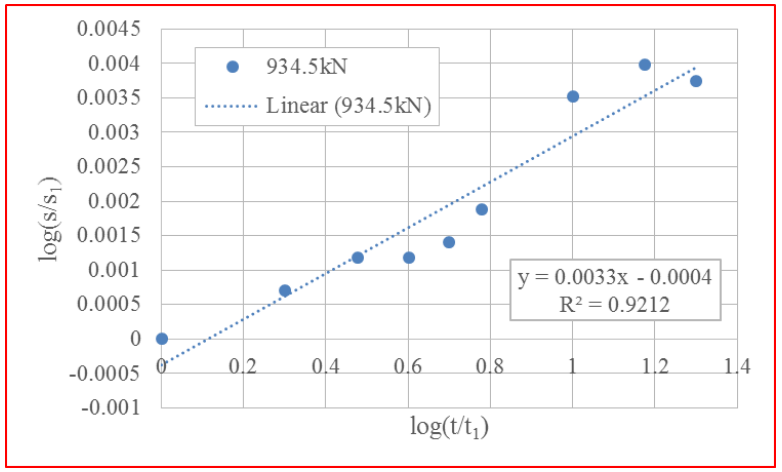

Figure 7-19 Continued

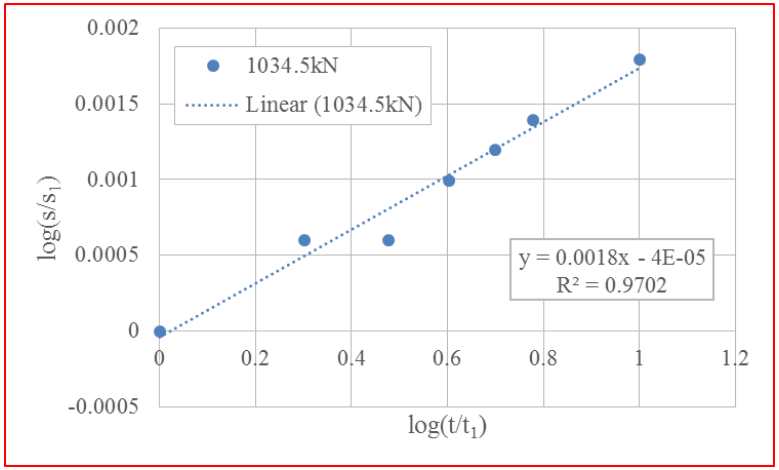

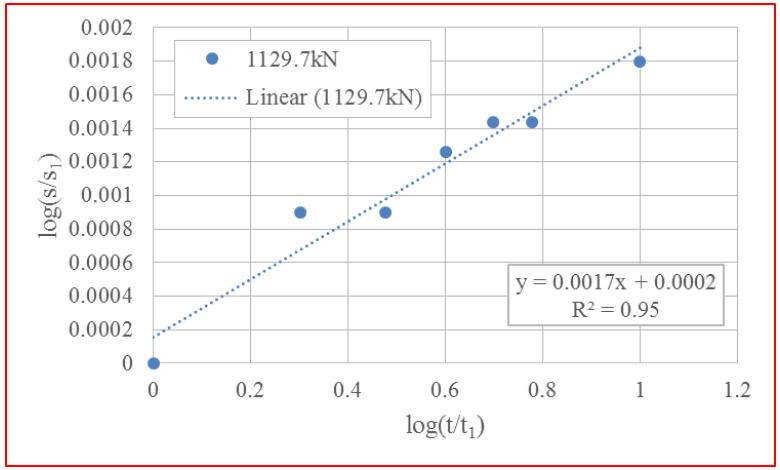

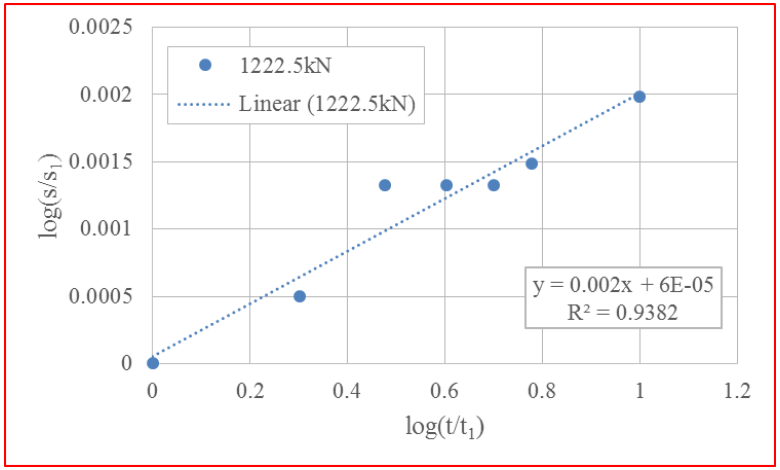

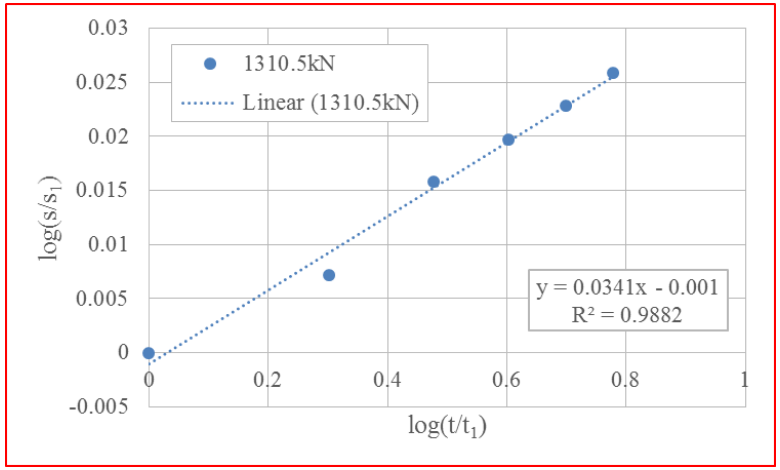

Figure 7-19 Continued

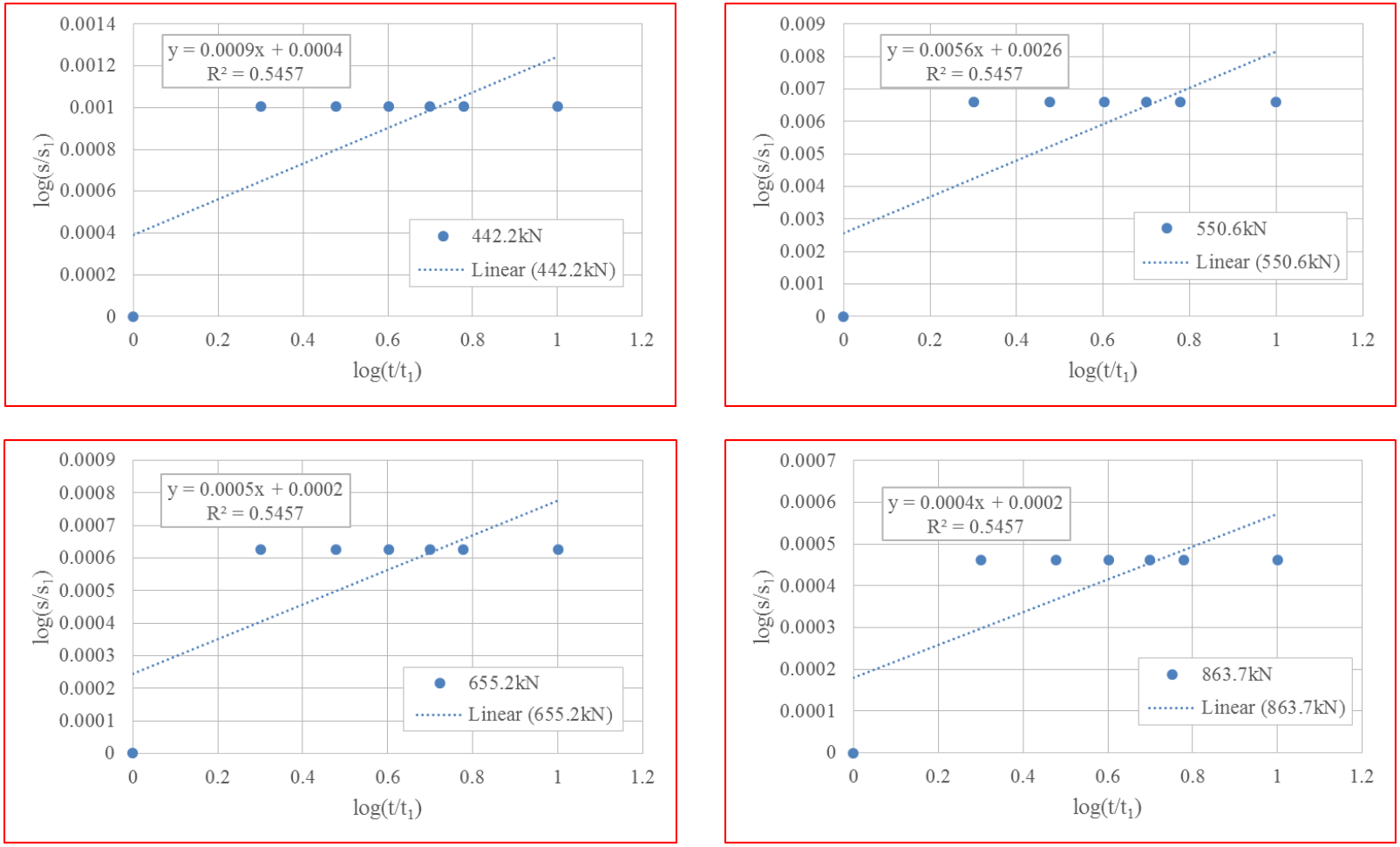

Figure 7-20. Movement-time curves (log-log scales), anchor 2, after Suroor (1998)

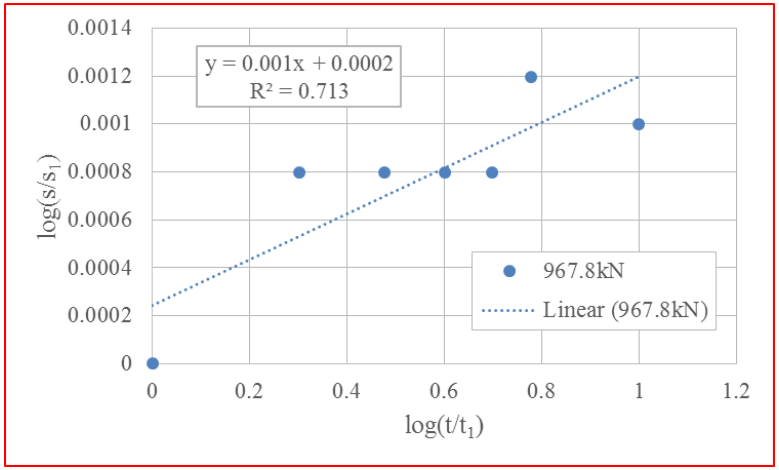

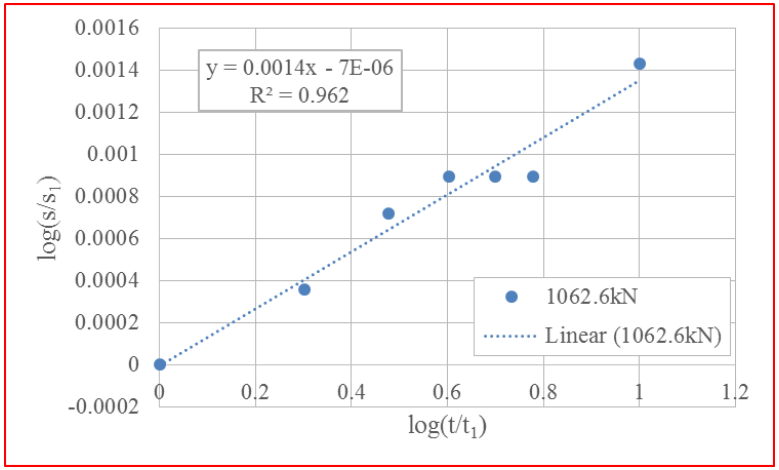

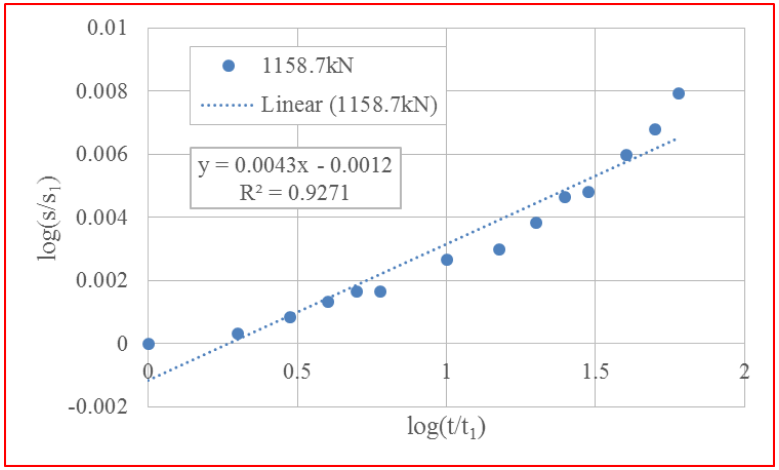

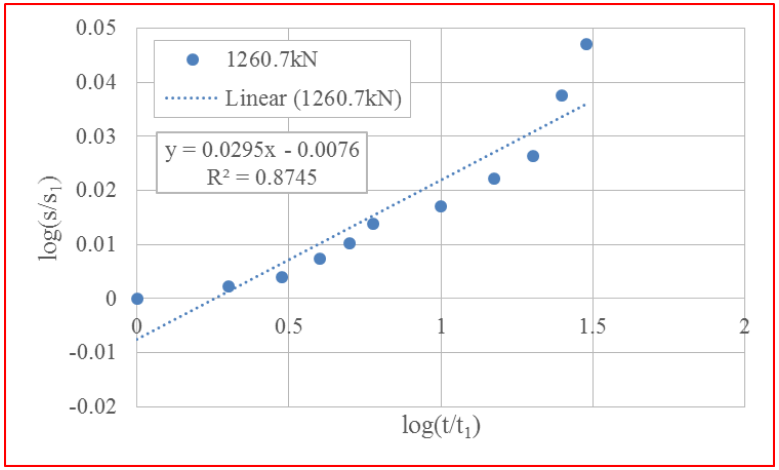

Figure 7-20 Continued

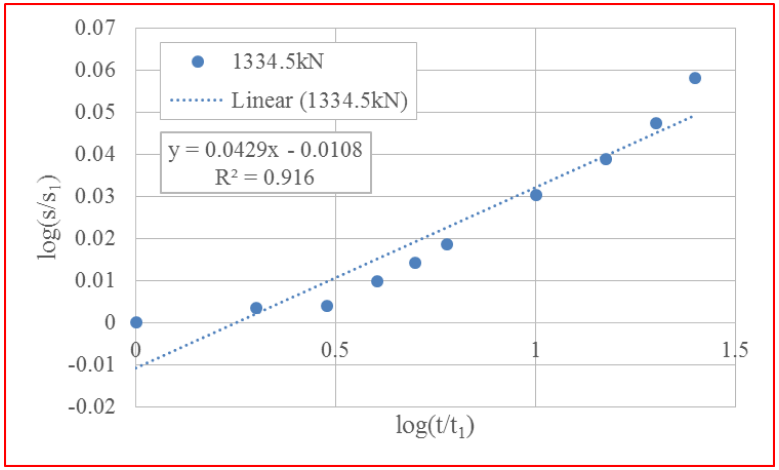

Figure 7-20 Continued

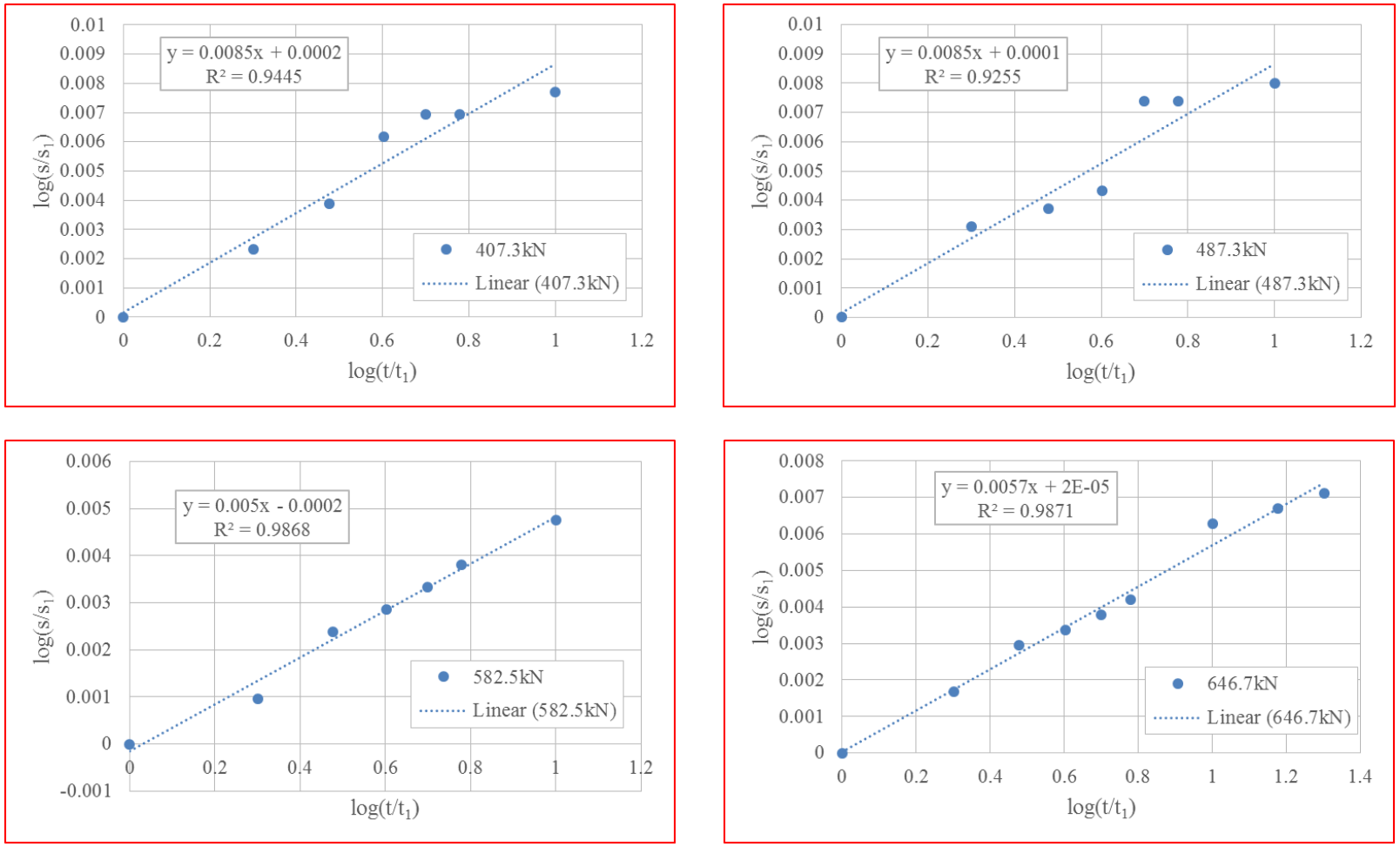

Figure 7-21. Movement-time curves (log-log scales), anchor 7, after Suroor (1998)

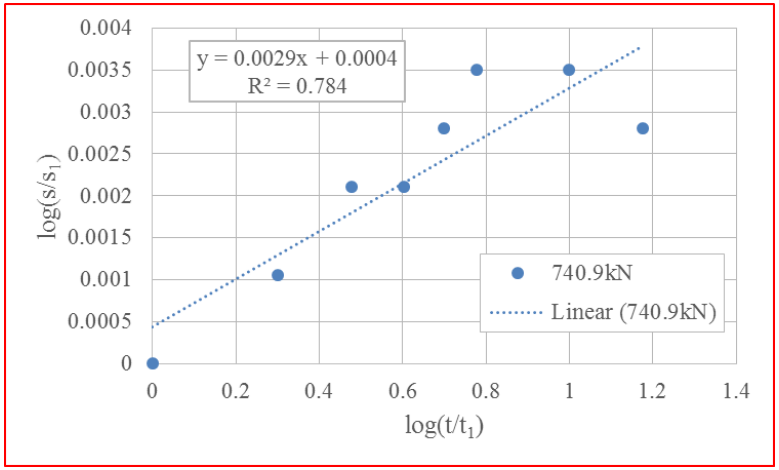

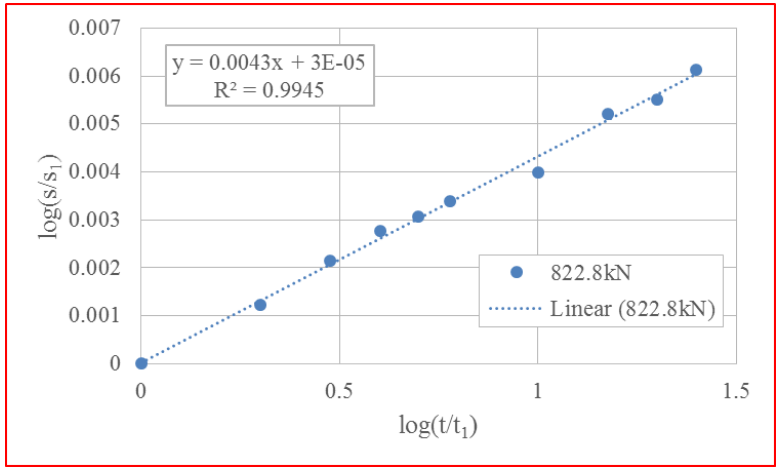

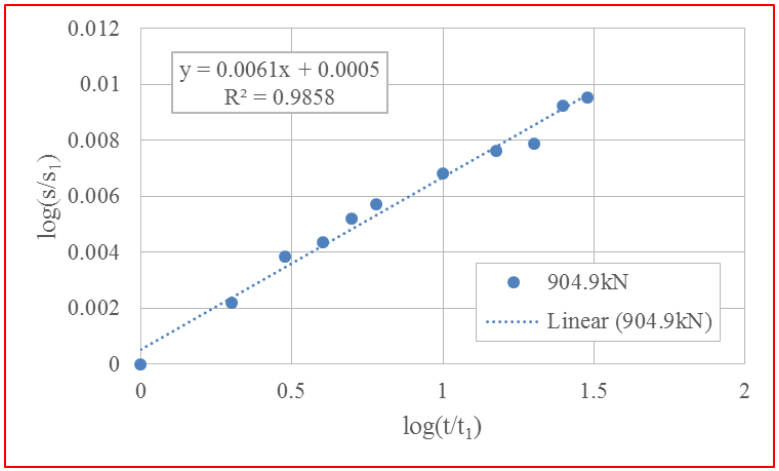

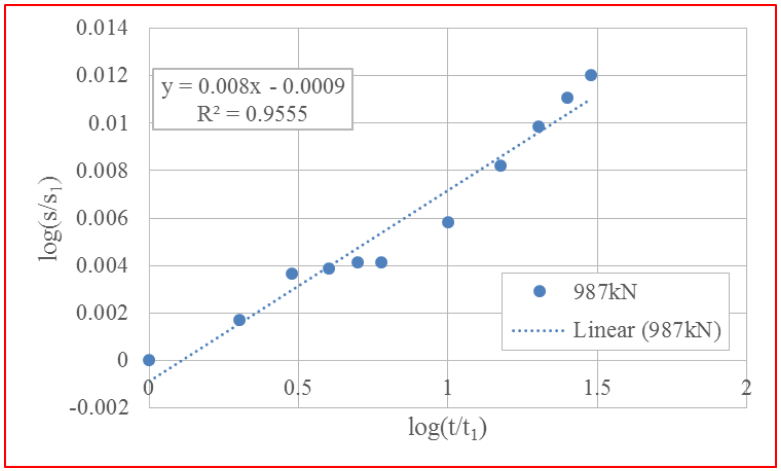

Figure 7-21 Continued

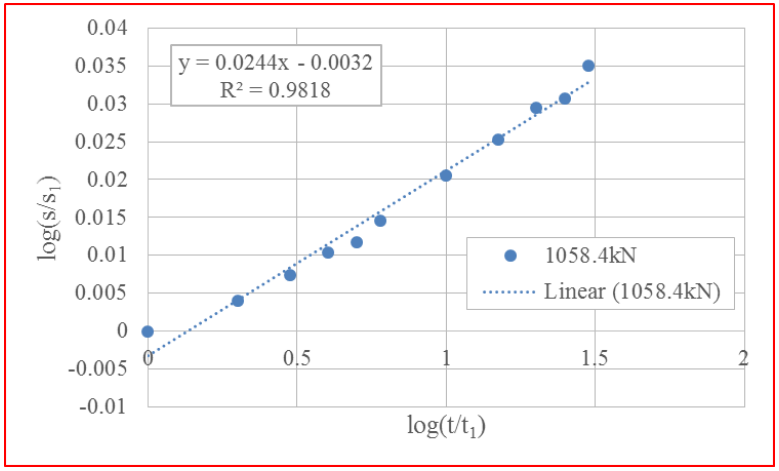

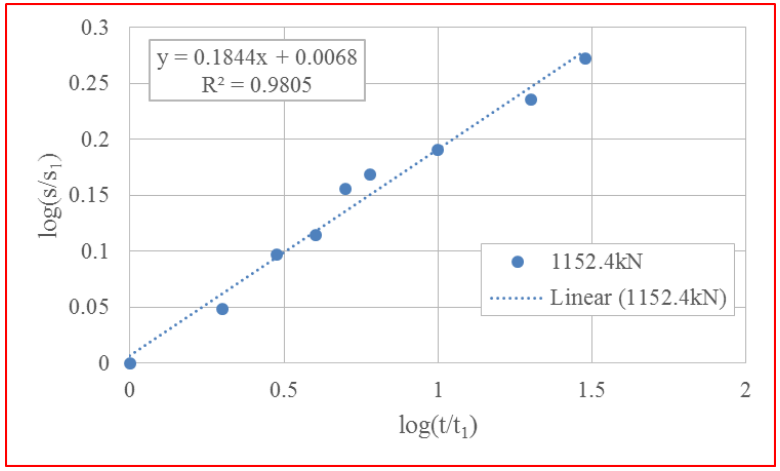

Figure 7-21 Continued

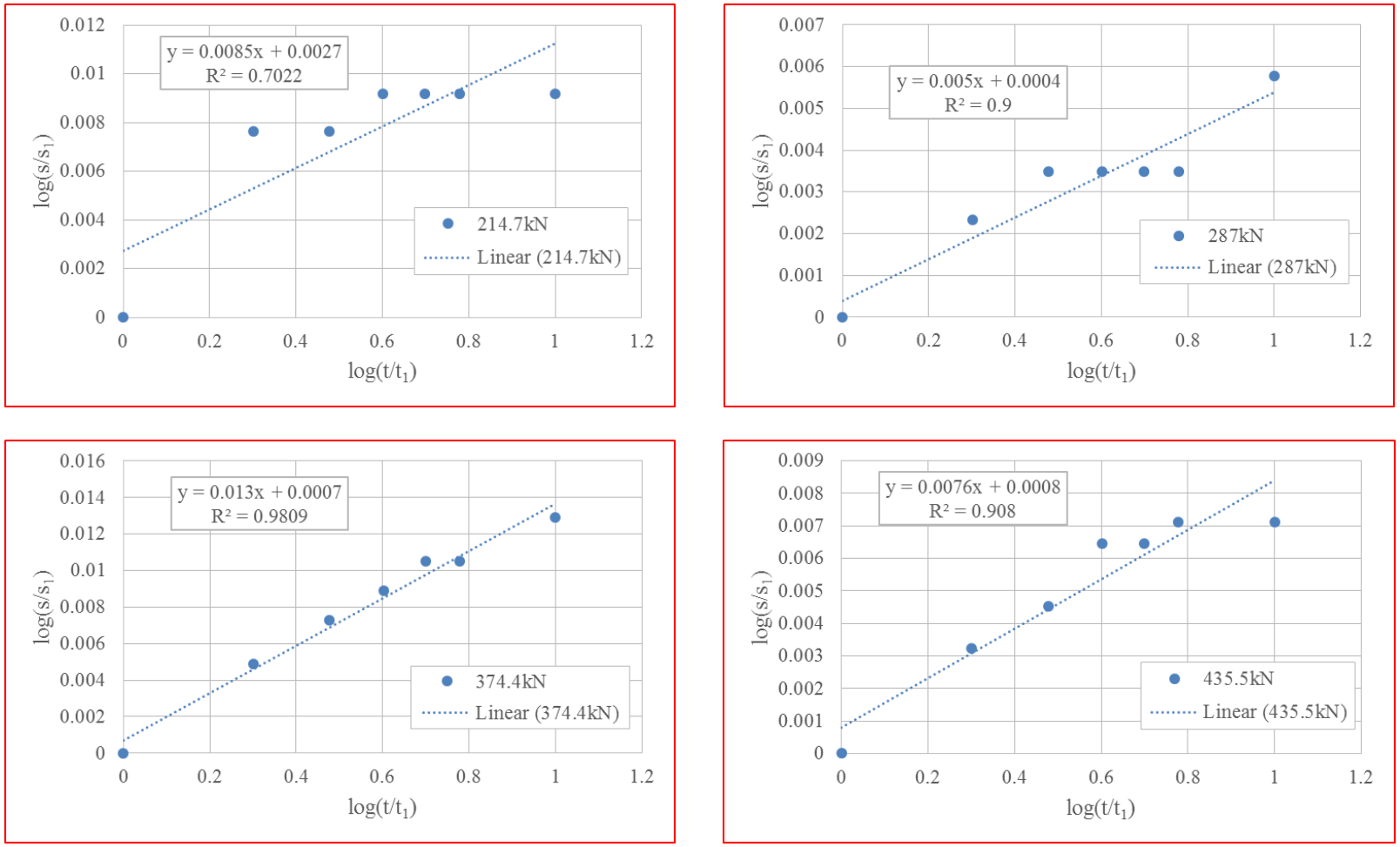

Figure 7-22. Movement-time curves (log-log scales), anchor 8 after Suroor (1998)

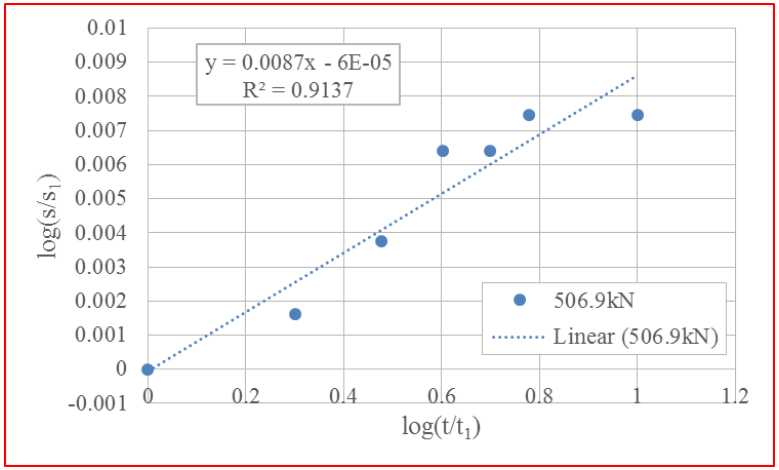

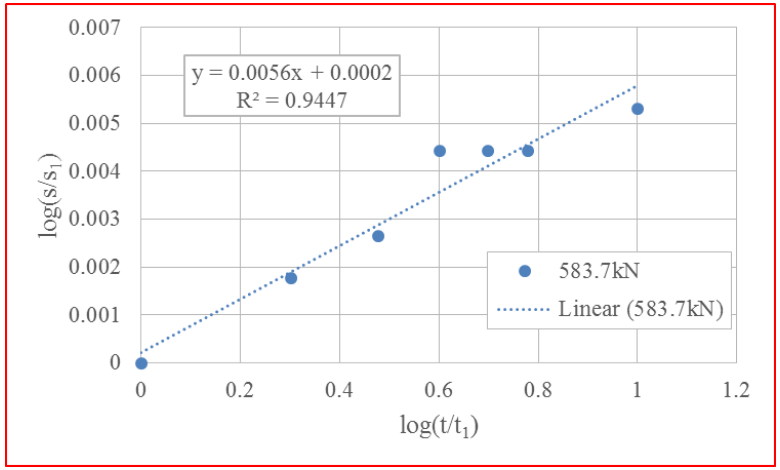

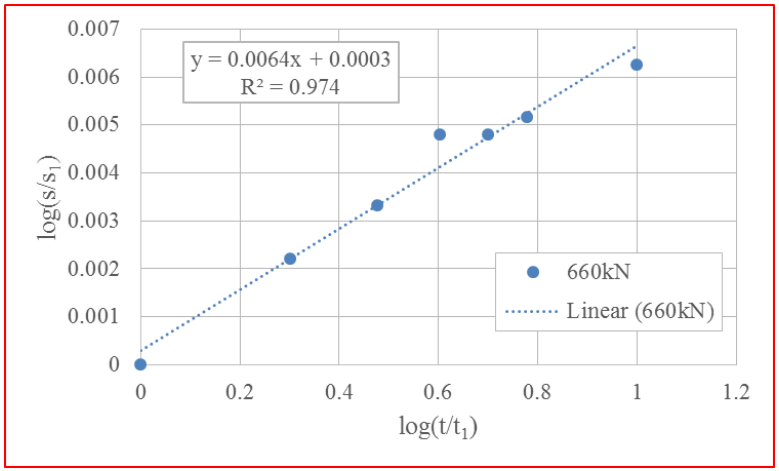

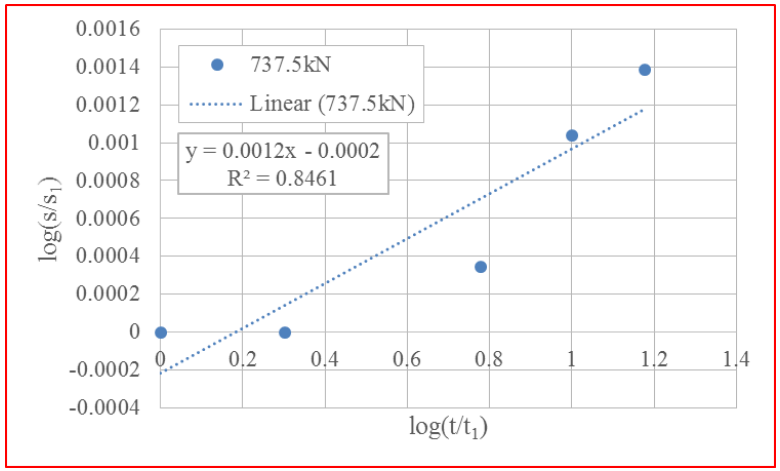

Figure 7-22 Continued

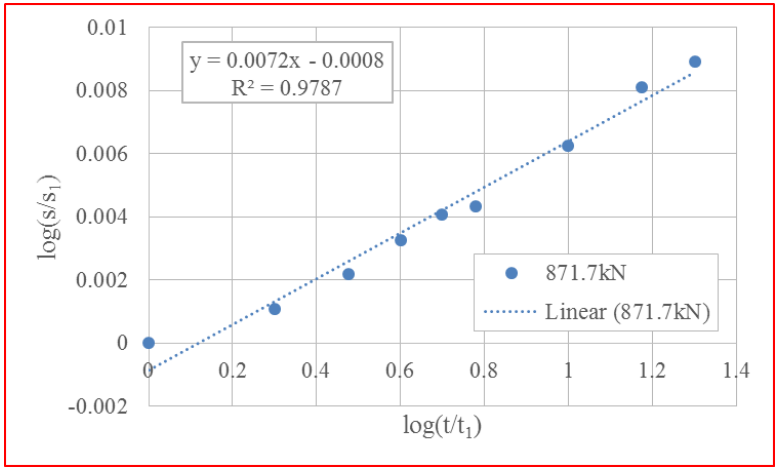

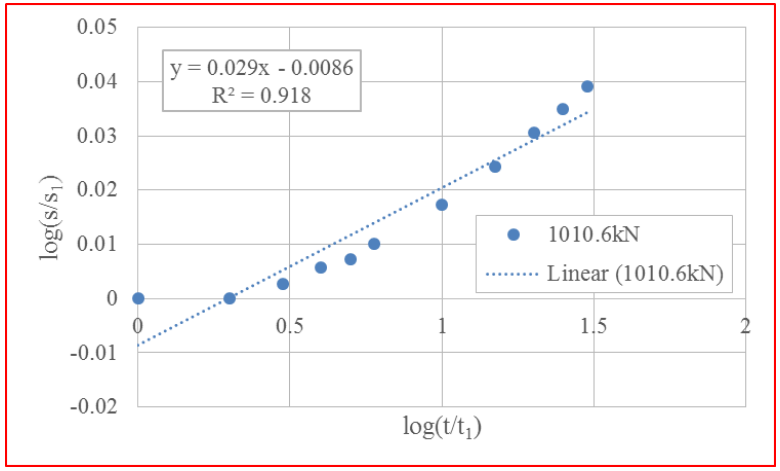

Figure 7-22 Continued

7.3.3. N Value-load Level Curve

N value-load level curve is plotted in figure 7-23. N value from anchor 7 and anchor 8 is still independent of load level. Because of six years creeping, n value from anchor 1 and anchor 2 is lower than that from anchor 7 and anchor 8. Besides, n value from anchor 7 and anchor 8 is significantly lower than that from triaxial creep test in laboratory (figure 5-23) because of unload-reload cycles, as it is thought n value whether from laboratory tests and field tests will be same for a given soil, which will be demonstrated in following section.

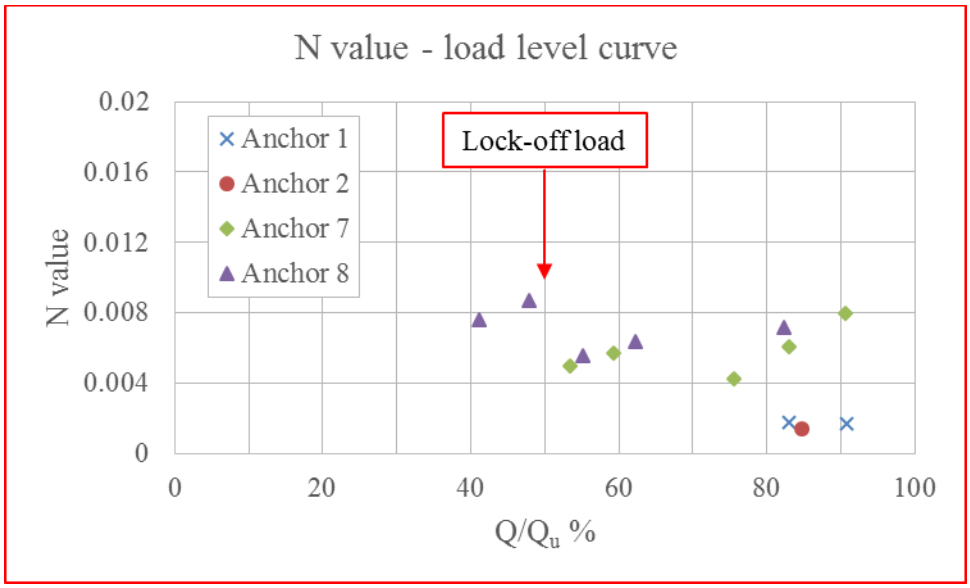

Figure 7-23. N value-load level curve, all anchors, after Suroor (1998)

7.4. Soil Nail Pullout Test, TAMU-NGES - Clay Site

A bunch of nails were installed at the clay site on TAMU-NGES in 2013. Data of one nail with 2.13m (7ft) bonded length and 178mm (7inch) diameter of borehole is presented here for illustration. The reason to pick this nail is that there is equal duration and without unload-reload cycle in its loading protocol.

An overall view of setup for testing is plotted in figure 7-24.

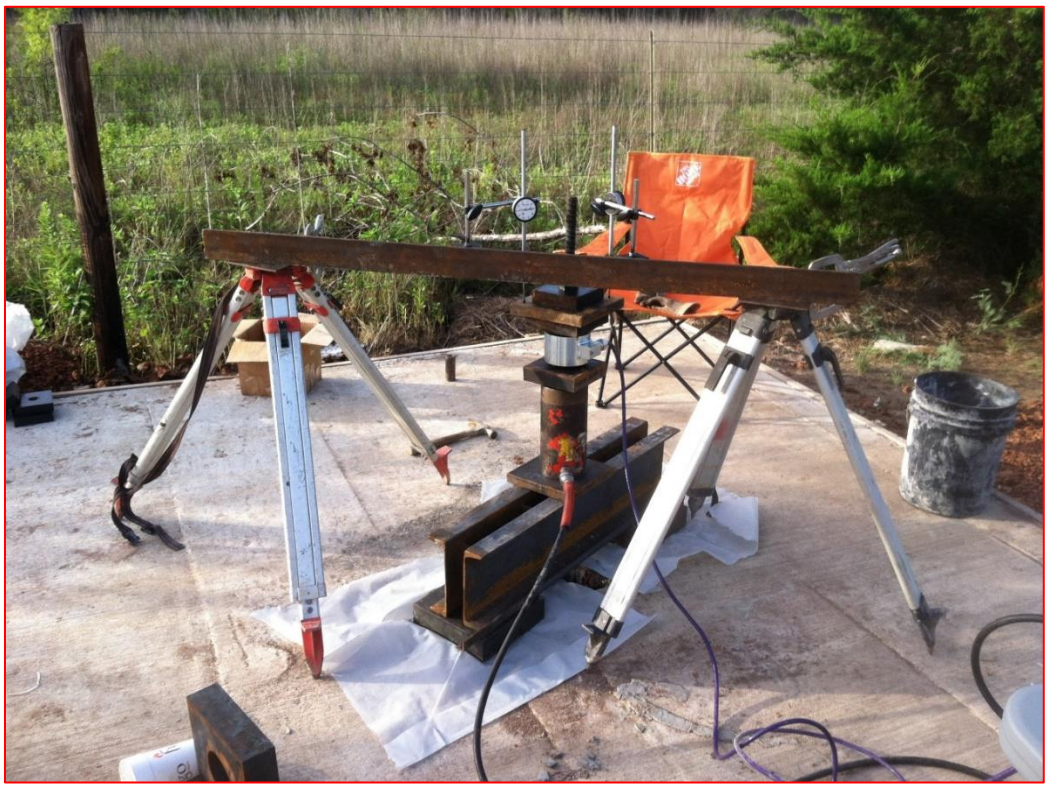

Figure 7-24. Soil nail pullout test setup

7.4.1. Load-movement Curve

Loading protocol is presented in table 7-9, and it is equal duration and without unload-reload cycle. Load-movement curve is plotted in figure 7-25. Because steel is elongated during the test, this elastic movement needs to be subtracted from total movement to reach residual movement.

Table 7-9. Loading protocol, soil nail pullout test

Loading/Unloading kN	kN	Duration minutes
0, 8.7, 25.7	25.7	1, 2, 3, 4, 5, 6, 10
	42.8	1, 2, 3, 4, 5, 6, 10
	59.8	1, 2, 3, 4, 5, 6, 10
	76.8	1, 2, 3, 4, 5, 6, 10
	93.9	1, 2, 3, 4, 5, 6, 10
	110.9	1, 2, 3, 4, 5, 6, 10
	128	1, 2, 3, 4, 5, 6, 10
	136.5	1
136.5, 110.9, 93.9, 59.8, 42.8, 0		

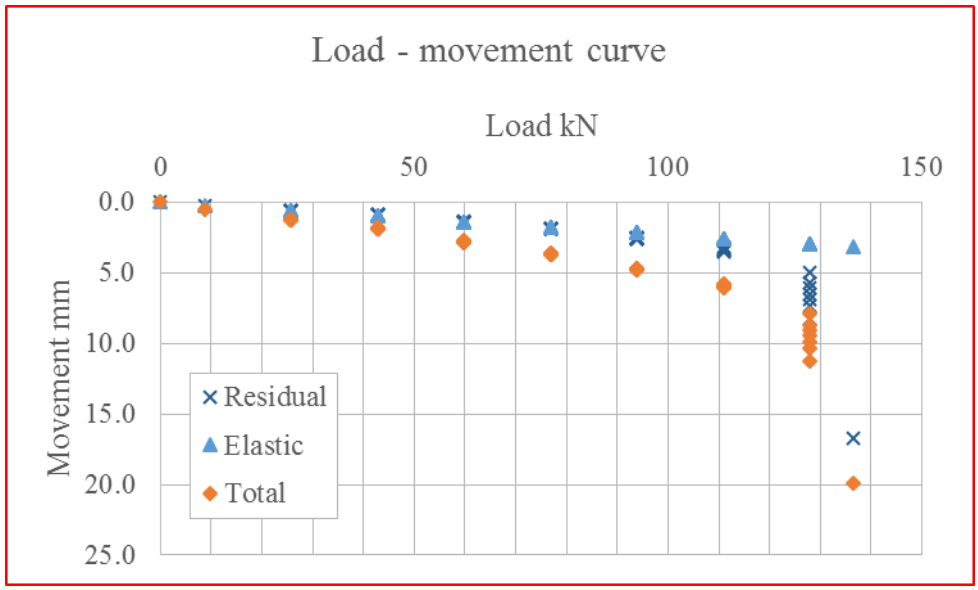

Figure 7-25. Load-movement curve, soil nail pullout test

Load-movement curve could be plotted with load level as long as Q_u is known. Here a different method is adopted to estimate Q_u, rather than based on load corresponding to movement of a predefined value.

Load-movement curve could be converted to friction-s/D curve to compare stress-strain curve obtained in laboratory test. The conversion is as follows:

$$f = \frac{Q}{L_B \cdot D \cdot \pi}$$
$$s / D = \frac{s}{D} \qquad (7\text{-}1)$$

Where,

f: Friction or bond strength;

Q: Load;

L_B: Bonded length, 2.13m;

D: Diameter of borehole, 178mm;

s: Movement.

Then, normalization curve (see subsection 5.4.2) could be adopted to fit friction-s/D curve to estimate maximum friction (further to calculate $Q_u = f_{\max} \cdot L_B \cdot D \cdot \pi$) and stress level at which creep failure happens (figure 5-27).

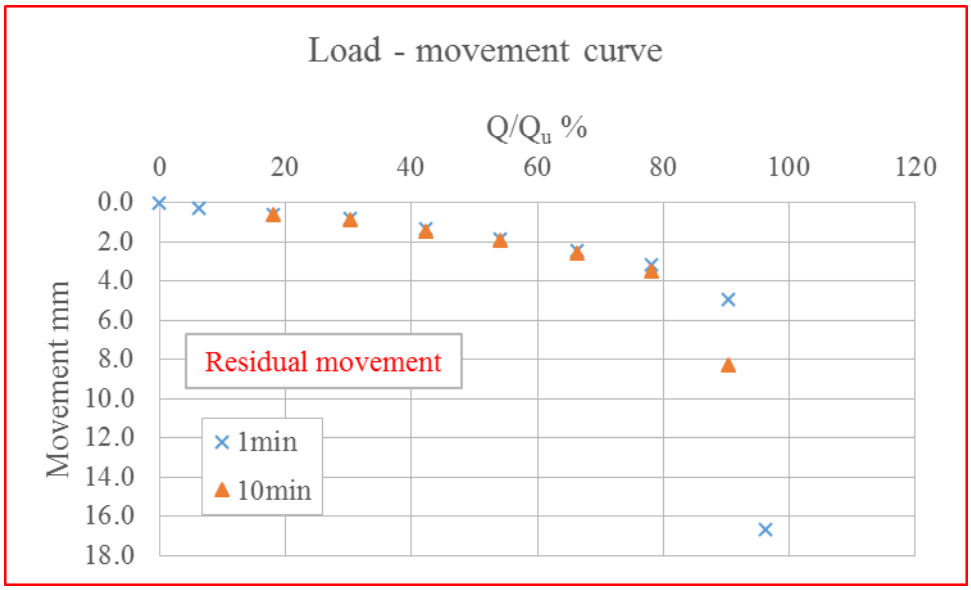

Figure 7-26. Load-movement curve

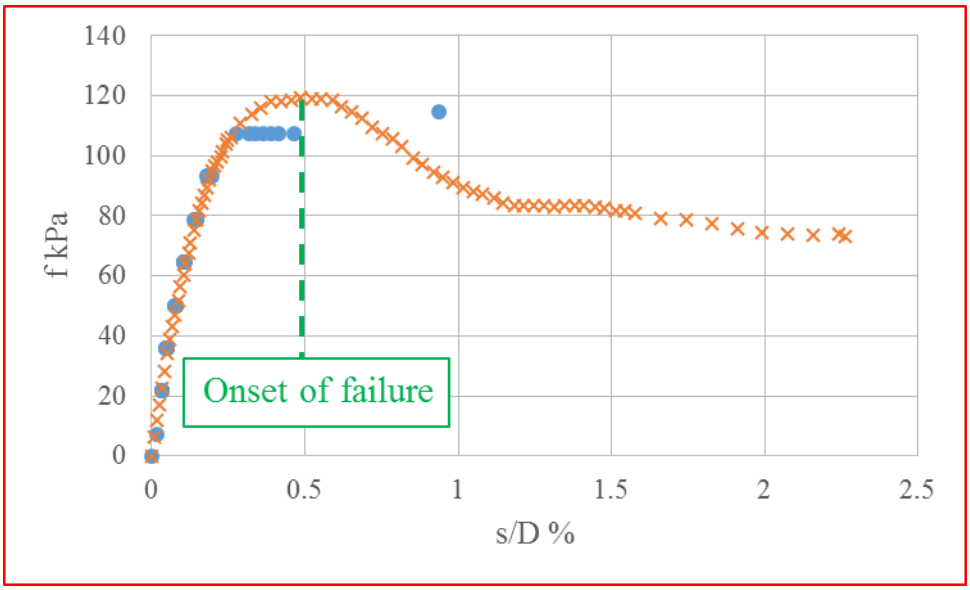

Figure 7-27. Estimating Q_u and stress level of creep failure with normalization curve

It should be noted that this fitting is based on the fact "1 minute creep curve" (because it didn't record "0 minute" data) of equal load increment test adopted in field tests is unique when there is equal duration and without unload-reload cycle. It won't work for load-movement curve of ground anchor pullout test in section 7.3 because of unload-reload cycles.

7.4.2. Movement-time Curve

Movement-time curve is plotted in figure 7-28. Still, there is seating problem that will impact n value at low loads. N value at sustained load corresponding to creep failure is remarkably higher. To compare, in usual, n value is hardly to acquire at sustained stress corresponding to creep failure at triaxial creep test in laboratory.

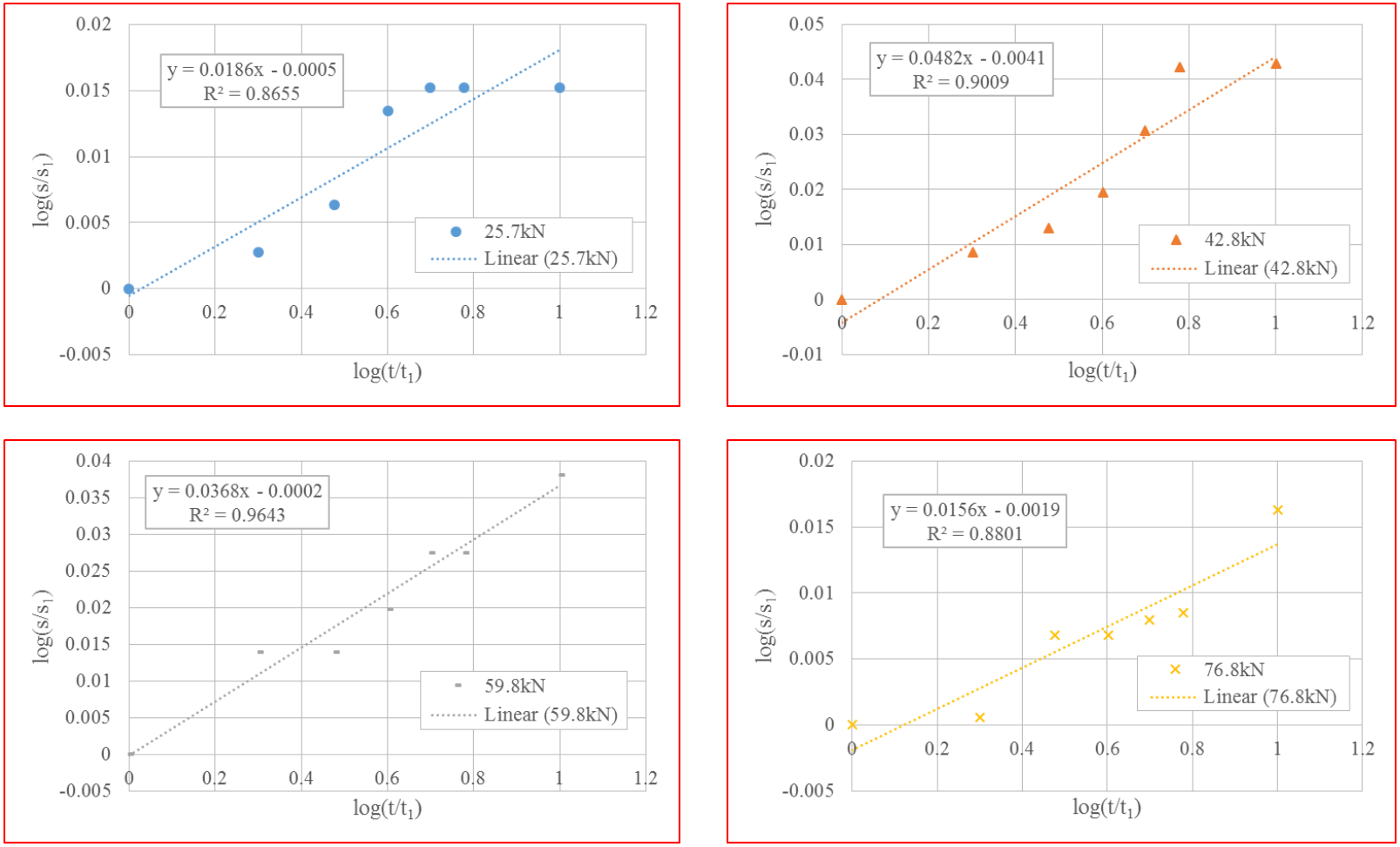

Figure 7-28. Movement-time curves (log-log scales), soil nail pullout test

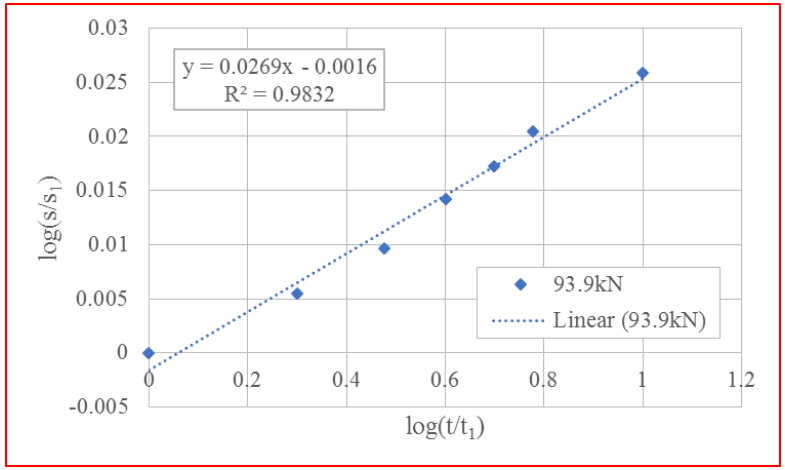

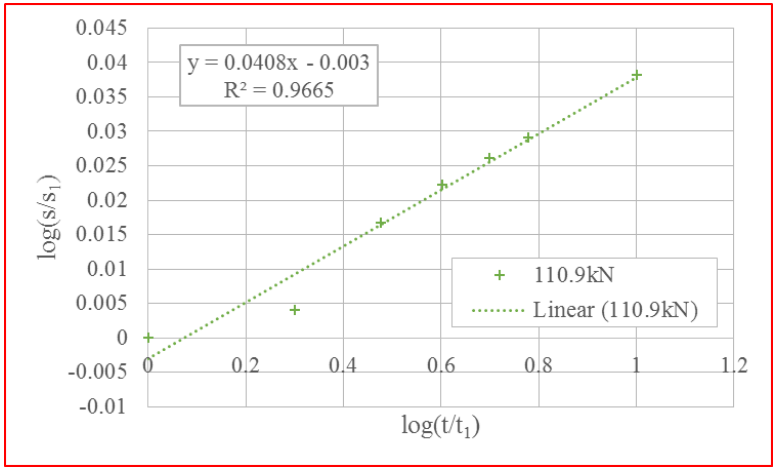

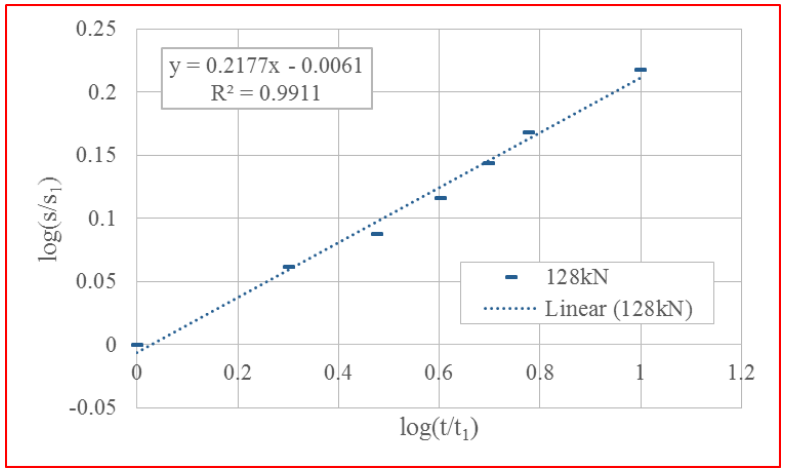

Figure 7-28 Continued

7.4.3. N Value-load Level Curve

N value-load level curve is plotted in figure 7-29. The most important finding is that n value obtained in field test is close to, if not same to, n value obtained in laboratory test (figure 5-23), which demonstrates that n value could be taken as a soil property.

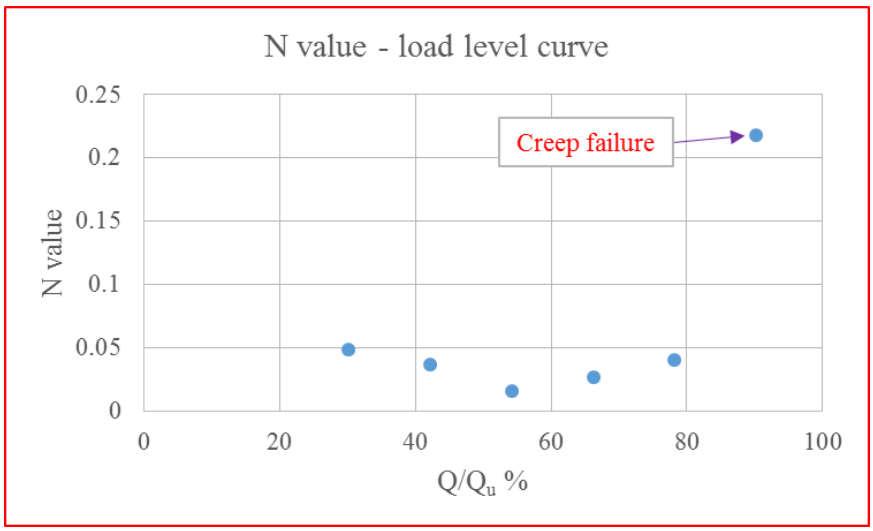

Figure 7-29. N value-load level curve, soil nail pullout test

N value is also basically independent of load level, though it is somehow lower at some sustained load. Besides, it is interesting that a much higher n value is obtained corresponding to creep failure, not only at soil nail pullout test but also at ground anchor pullout test (figure 7-21). In the meanwhile, there is no way acquire n value corresponding to creep failure from triaxial creep test in laboratory. Two possible

reasons are: a), the adjustment of the machine in laboratory is much slower than the speed of tester pumping in field; b), if deformation at 30min and 40min (because the first 20~30min is the lagging adjustment of machine) corresponding to creep failure at triaxial creep test is adopted to obtain n value, then compared to n value corresponding to creep failure in field test, it seems that they are in good agreement.

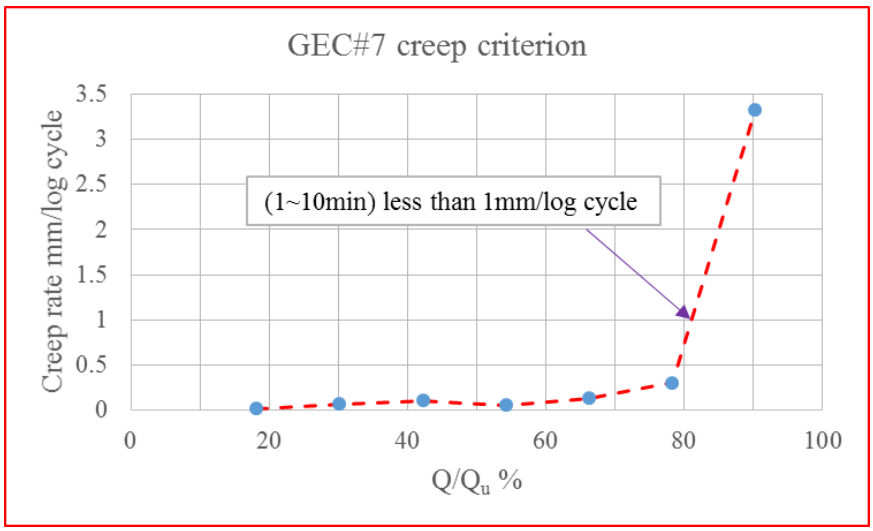

Figure 7-30. Creep failure criterion of GEC#7 (FHWA, 2003, 2015)

Creep failure criterion for soil nail pullout test from GEC#7 (FHWA, 2003, 2015) is less than 1mm between 1min to 10min (figure 7-30) or less than 2mm between 6min to 60min (the maximum duration required for creep test in GEC#7).

It is readily easy to convert between creep criterion of GEC#7 and power law model,

$$\frac{s_{10}}{s_1}=\left(\frac{t_{10}}{t_1}\right)^n=10^n\le\frac{s_1+1mm}{s_1}$$

$$\Rightarrow s_1\le\frac{1mm}{10^n-1}$$

$$\frac{s_{60}}{s_6}=\left(\frac{t_{60}}{t_6}\right)^n=10^n\le\frac{s_6+2mm}{s_6}=\frac{s_1\cdot\left(\frac{t_6}{t_1}\right)^n+2mm}{s_1\cdot\left(\frac{t_6}{t_1}\right)^n}=\frac{s_1\cdot 6^n+2mm}{s_1\cdot 6^n} \quad (7\text{-}2)$$

$$\Rightarrow s_1\le\frac{2mm}{\left(10^n-1\right)\cdot 6^n}$$

In this case, given n value-stress (load) level curve, creep criterion of GEC#7 is converted to restrict s_1 further E_1.

In another way, normalization curve which is adopted to predict the time to creep failure or long-term deformation after a specific duration, could also be converted to creep criterion of GEC#7. To recall, x-axis of normalization curve is strain/strain at failure,

$$\frac{strain}{strain\ at\ \ failure}\cdot estimated\ strain\ at\ \ failure=\frac{movement}{Diameter} \quad (7\text{-}2)$$

Where,

$\frac{strain}{strain\ at\ \ failure}$: Obtained from normalization curve, adopted in power law model;

$estimated\ strain\ at\ \ failure$: 0.5%~1% (figure 7-27);

$movement$: Monitored movement in field test, while difference between movement at 10min and movement at 1min less than 1mm required by GEC#7 ;

$Diameter$: Diameter of borehole.

In this case, after multiplying diameter of borehole and estimated strain at failure (1% for instance), normalized strain difference tabulated in table 5-1 and table 5-2 will yield movement difference, which could be compared to creep criterion of GEC#7. Again, it demonstrates deformation caused by creep will be tremendously reduced by prestressing (preloading).

7.5. Cyclic Lateral Load Test on Piles in Sand by Little (1988), Houston Area

Full scale cyclic lateral load tests were performed on six single piles in sand in Houston area, the data is adopted here to study the equation between cycle and creep. Only data of pile #2 is presented here for illustration, more details could be found at Little and Briaud (1988).

7.5.1. Load-deflection Curve

The load-deflection curve is plotted in figure 7-31. The load increment is constant, and each load is sustained for 6sec. 20 unload-reload cycles are performed at two selected load levels. At the first selected load level, the first 10 cycles are completely unloading and the second 10 cycles are partially unloading to 50% of the selected load; at the second selected load level, the first 10 cycles are partially unloading to 50% of the selected load and the second 10 cycles are completely unloading.

7.5.2. Deflection-time Curve

Deflection-time curve is plotted in figure 7-32. Still, there is seating problem that

will impact n value at low loads. However, all curves are straight lines, which again demonstrate that the proposed power law model is also feasible for application in cyclic lateral field load test.

7.5.3. N Value-stress Curve

N value-stress curve is plotted in figure 7-33. It is obvious that cycles tremendously reduce n value at loads after cycles and it will take a few loads for n value to reach a new constant. The same phenomena have been explained in the impact of swelling in 1D consolidation test and 1D compression test, the impact of cycles and unequal duration in spread footing test on sand performed by Gibbens (1995). It is all because s_1 is chosen reference to the very beginning of test (i.e., zero deformation) (figure 3-8).

It is the fact that n value will reach a new constant after a series of cycles. However, it is found the approach of n value after the first series of cycles is interrupted by the second series of cycles in figure 7-33. In this case the conclusion may be drawn that two selected load levels for cycles are too close that the second series of cycles are impacted by the first series of cycles.

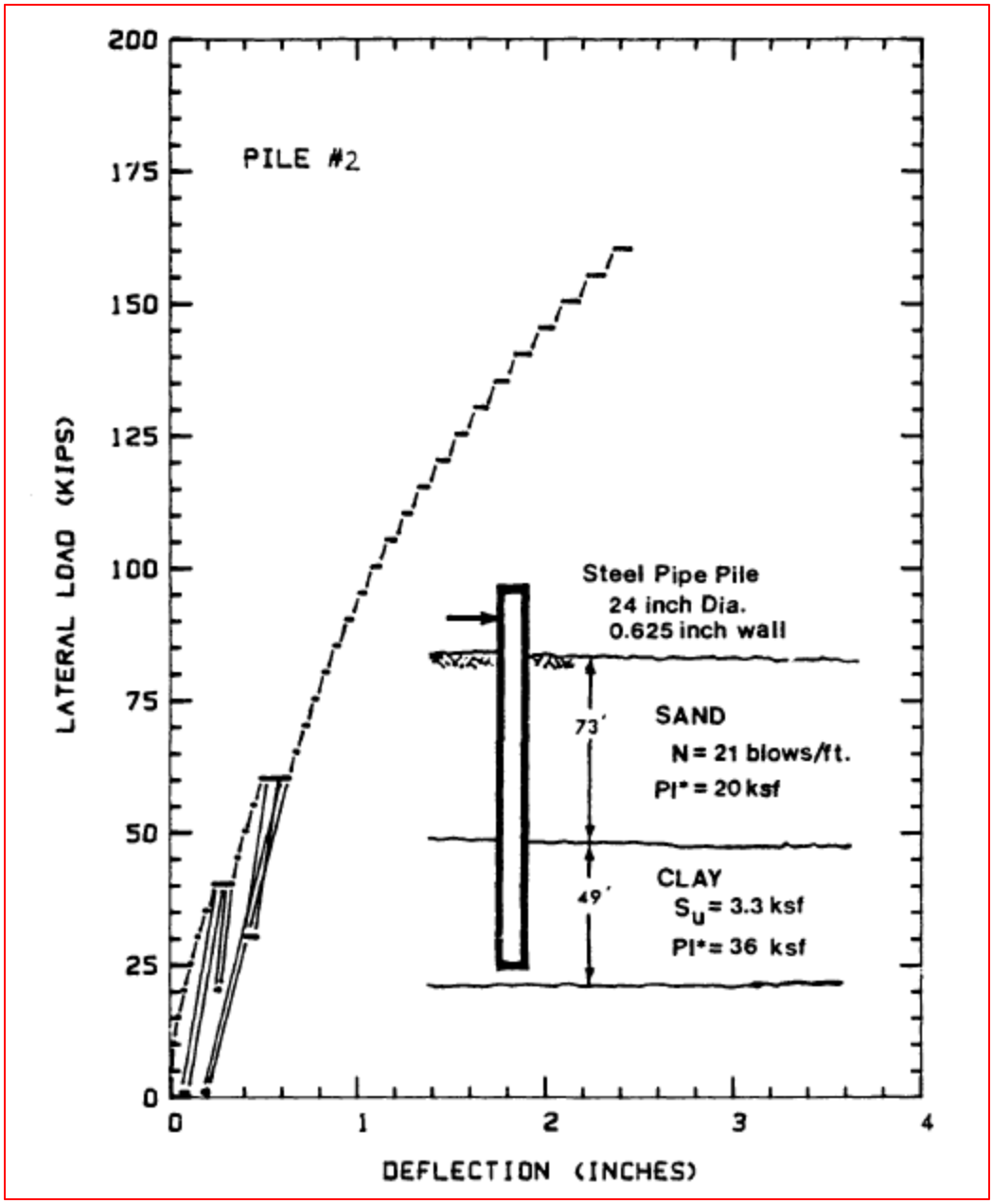

Figure 7-31. Load-deflection curve, cyclic lateral load test (Little and Briaud, 1988)

Note: 1kip=4.45kN, 1inch=25.4mm, 1ksf=47.88kPa, 1ft=0.3m

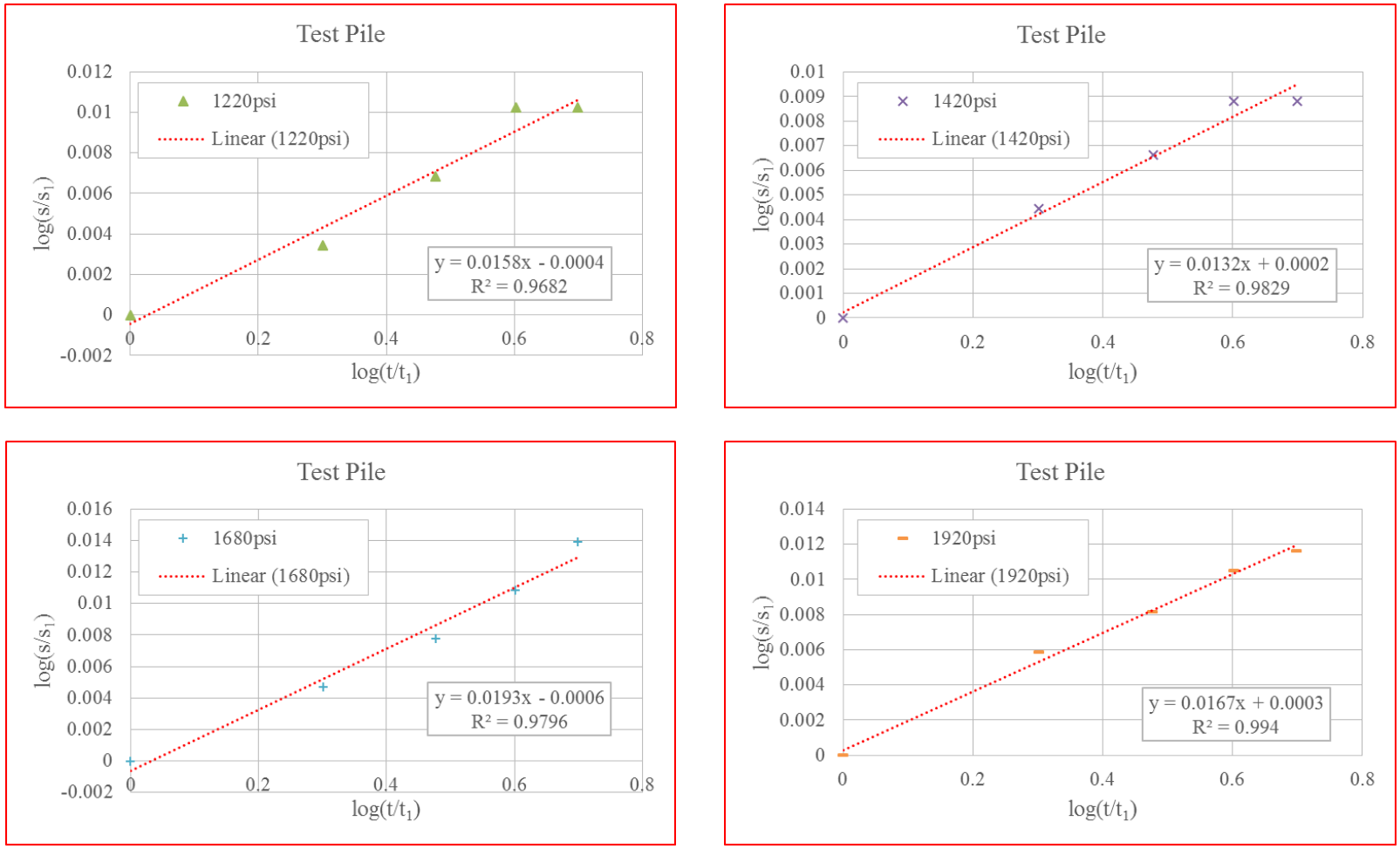

Figure 7-32. Deflection-time curves (log-log scales), cyclic lateral load test, after (Little and Briaud, 1988)

Note: 1psi=6.89kPa

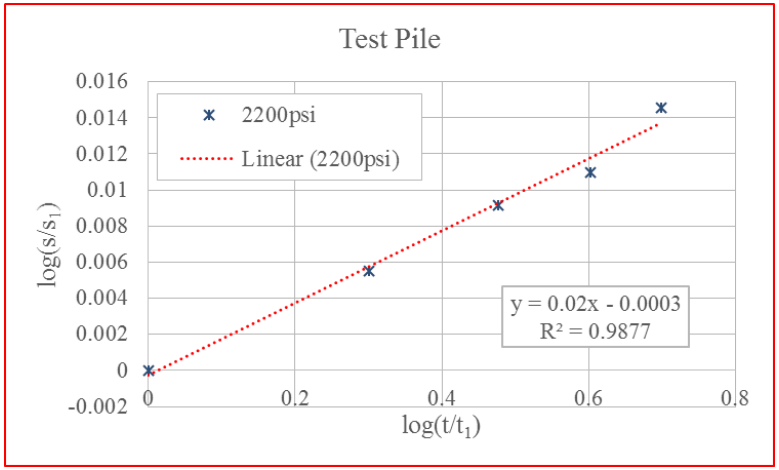

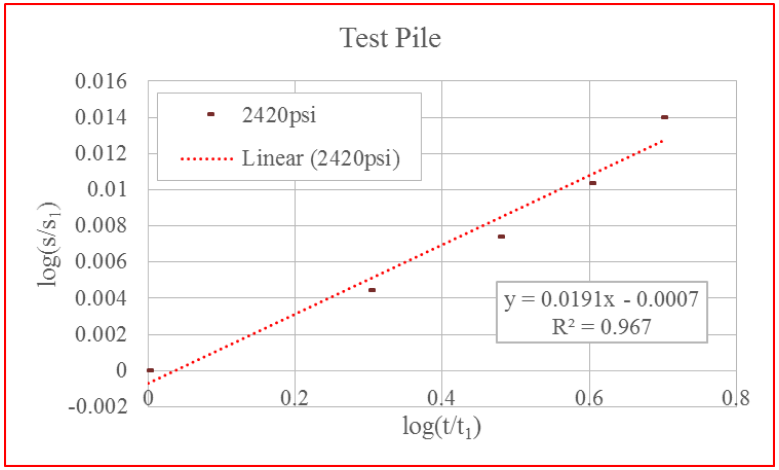

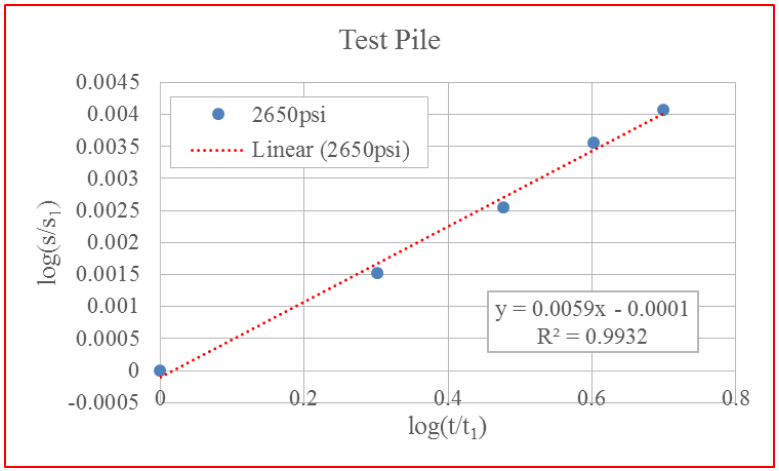

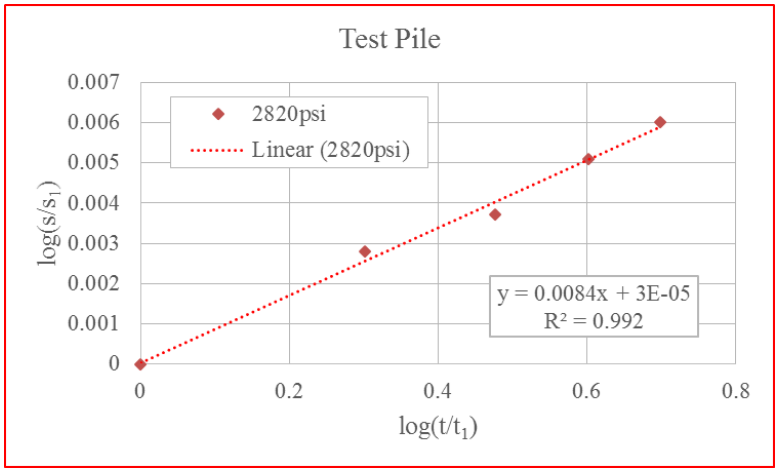

Figure 7-32 Continued

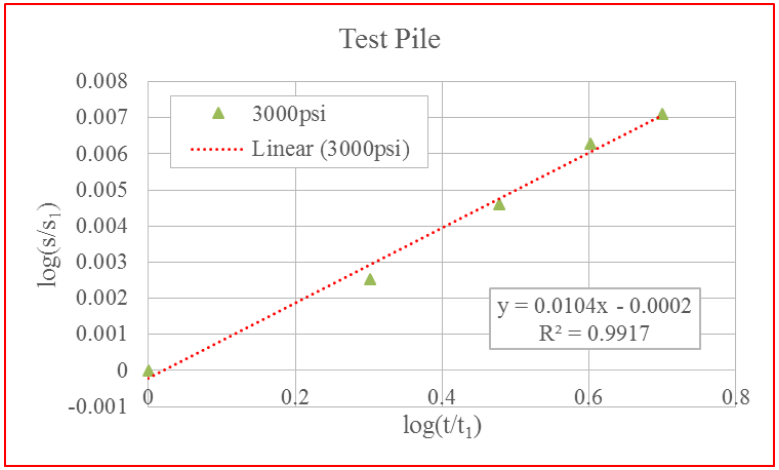

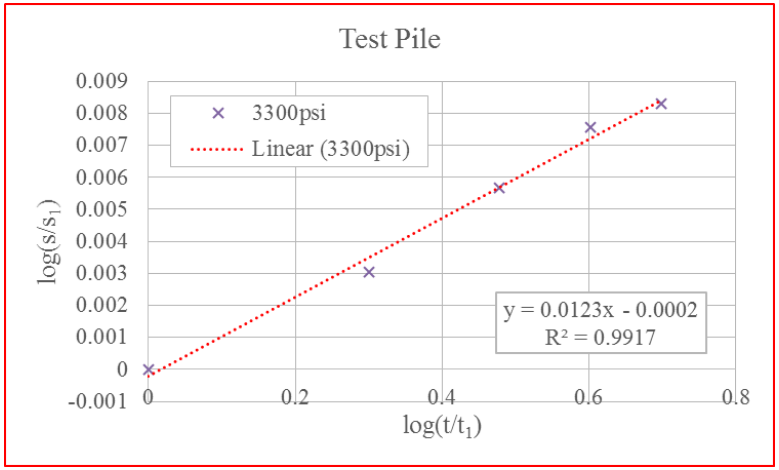

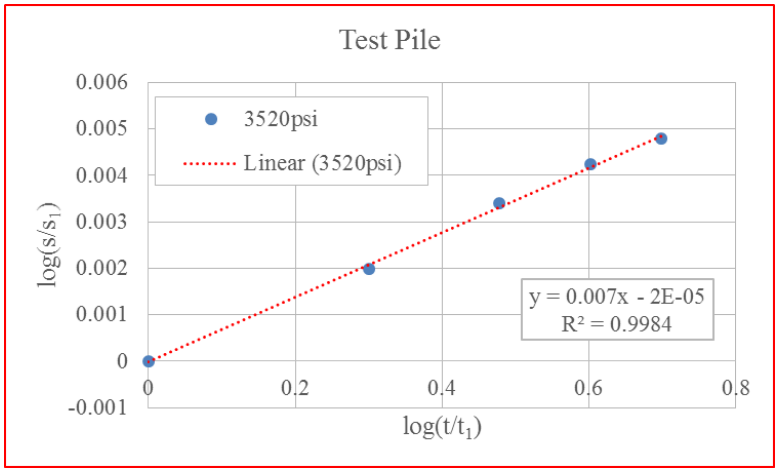

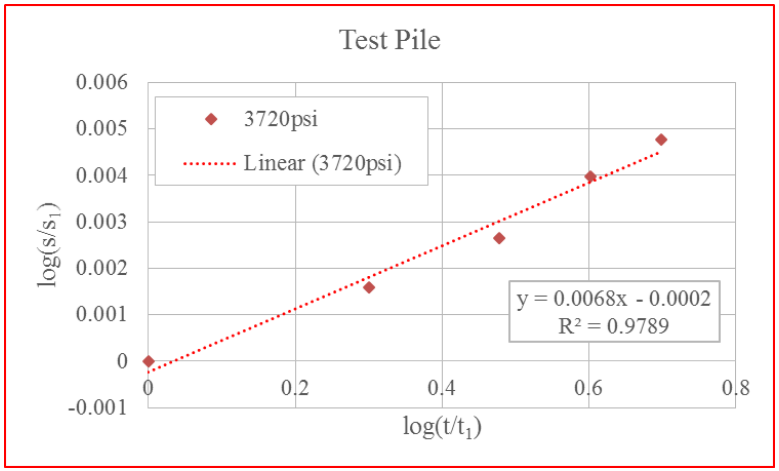

Figure 7-32 Continued

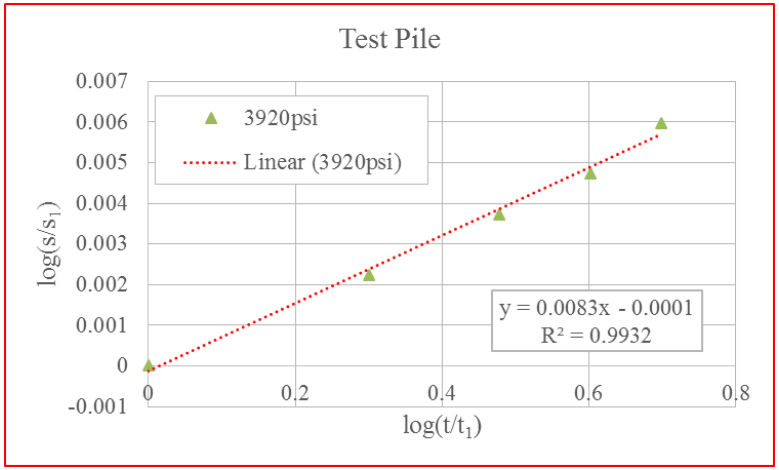

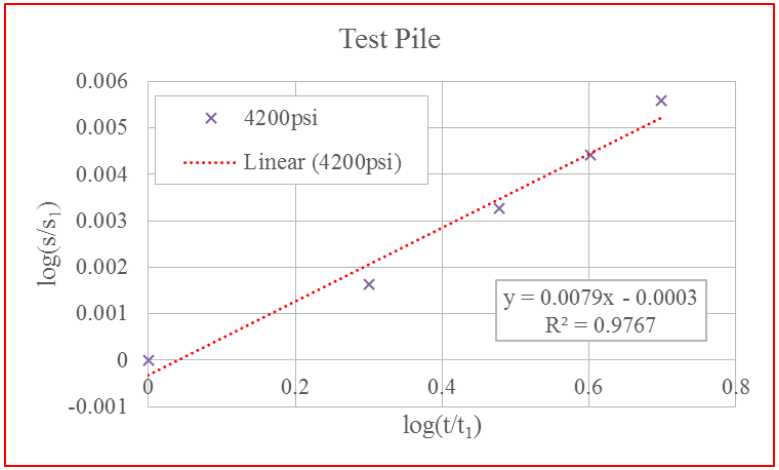

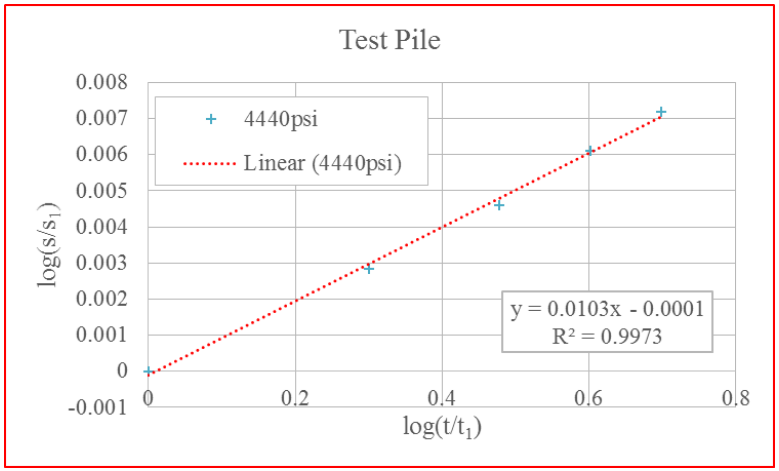

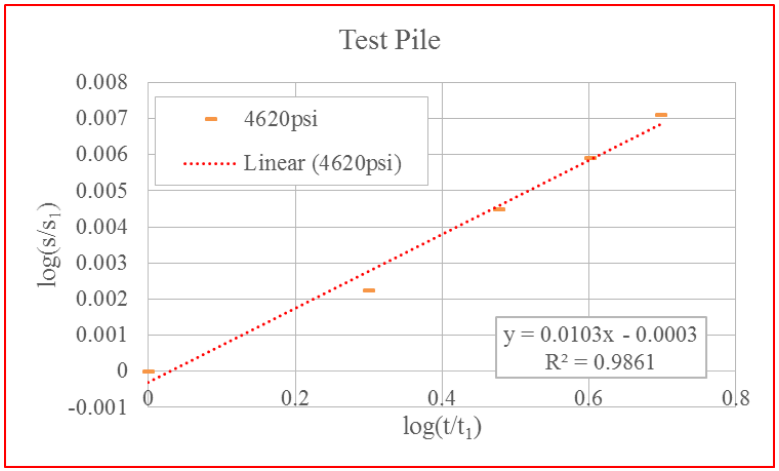

Figure 7-32 Continued

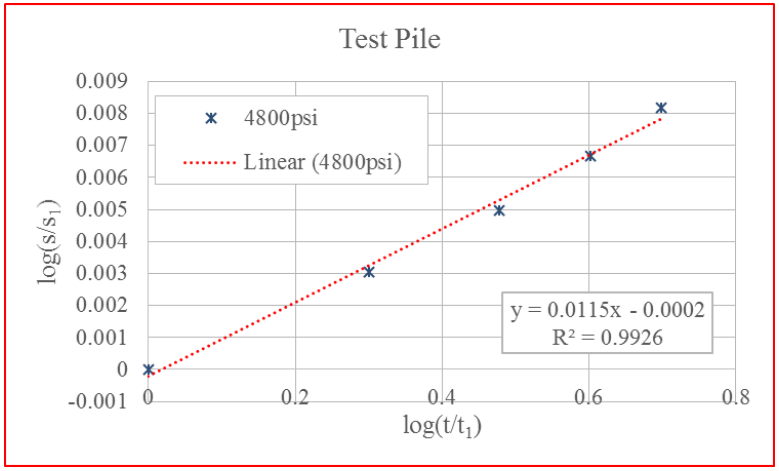

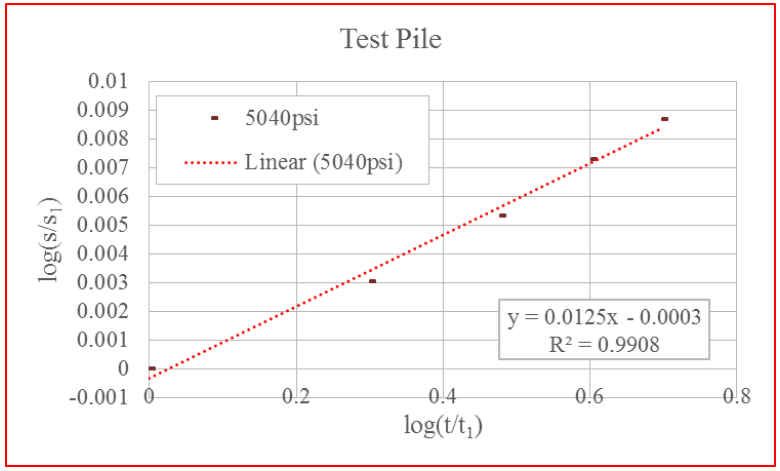

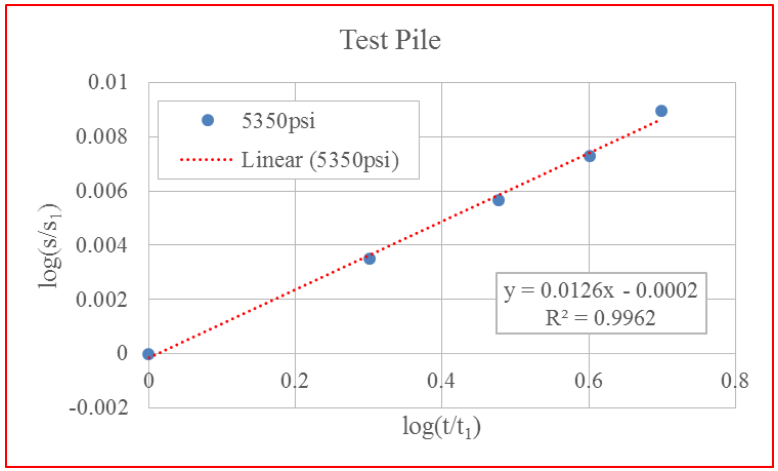

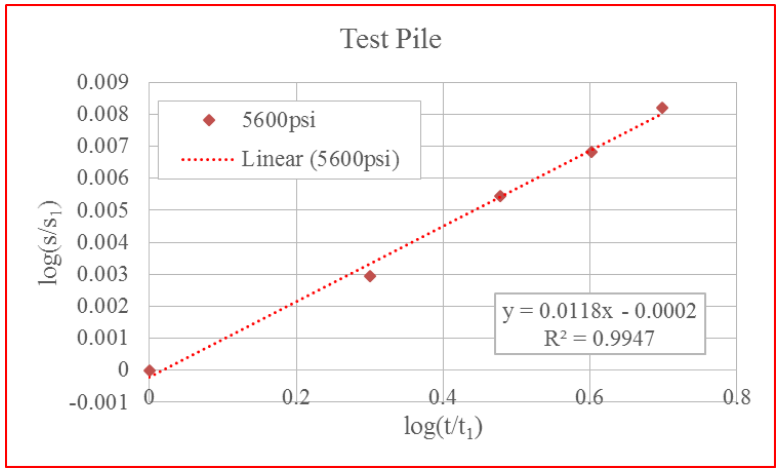

Figure 7-32 Continued

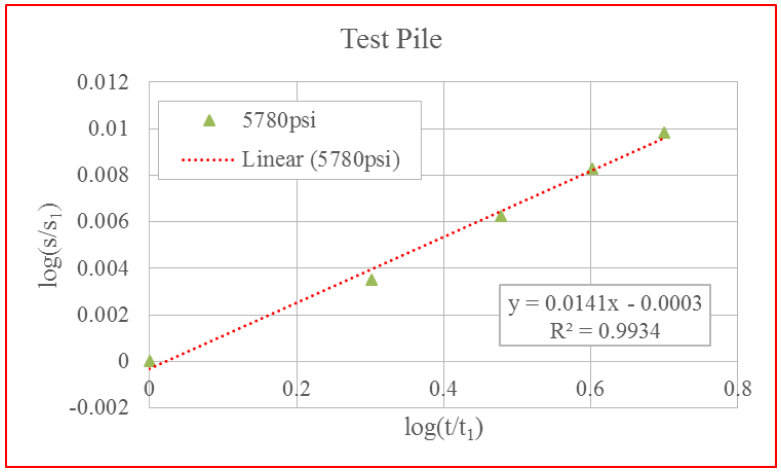

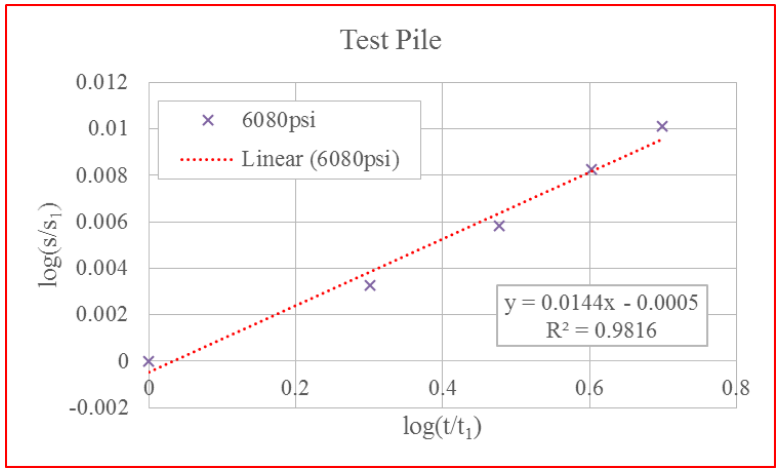

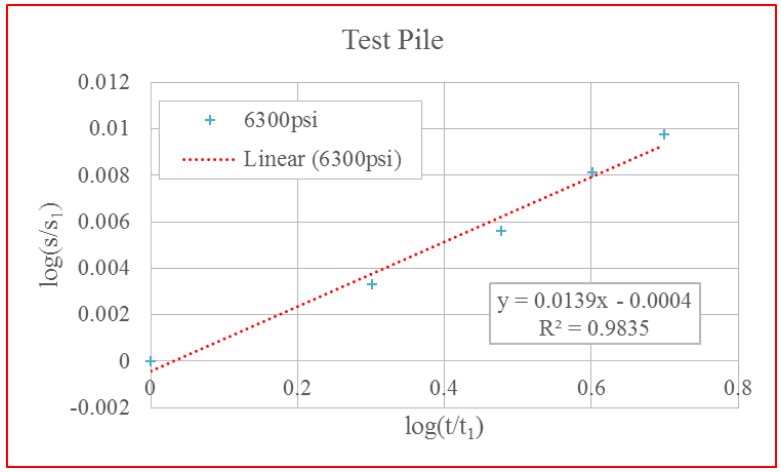

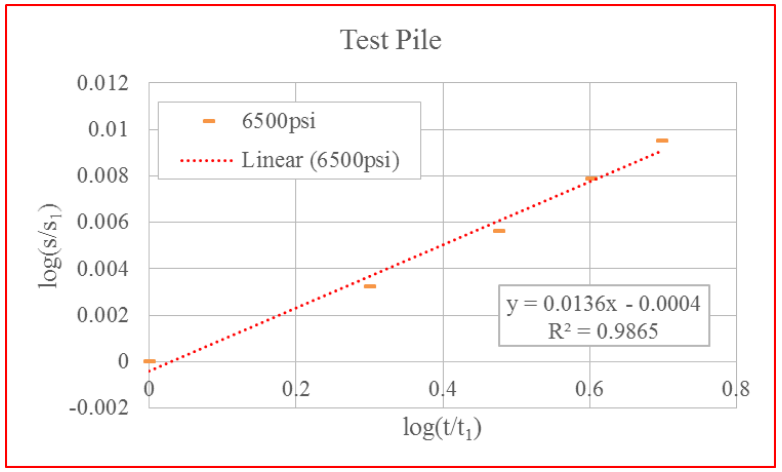

Figure 7-32 Continued

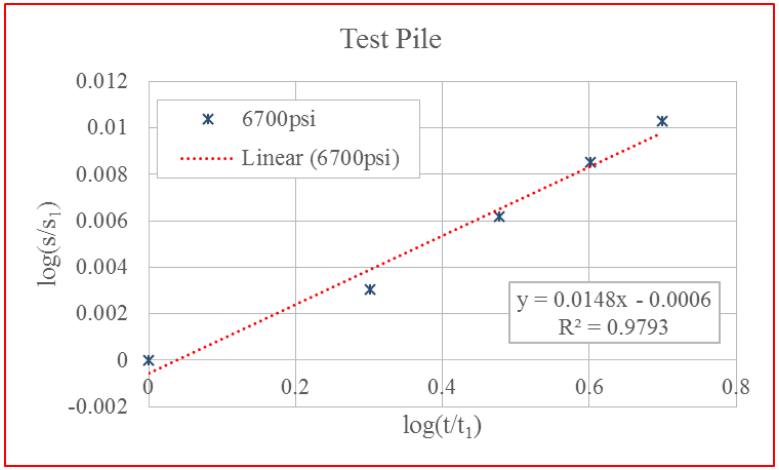

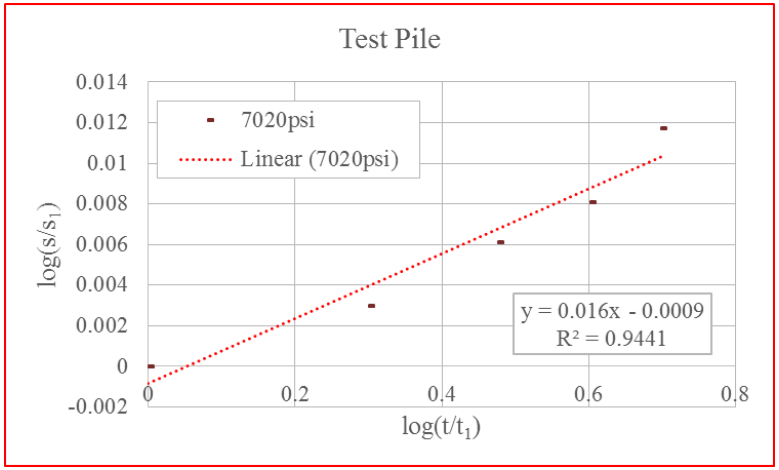

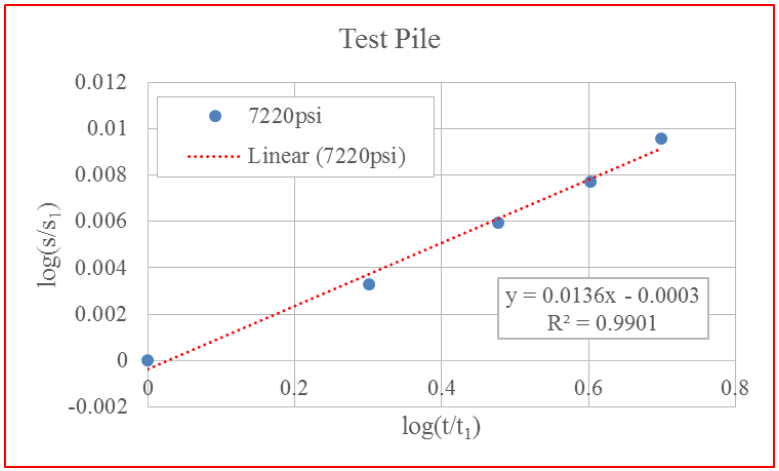

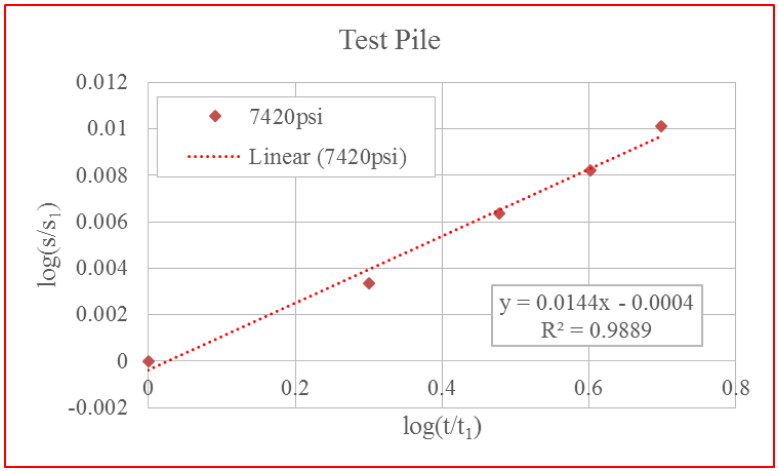

Figure 7-32 Continued

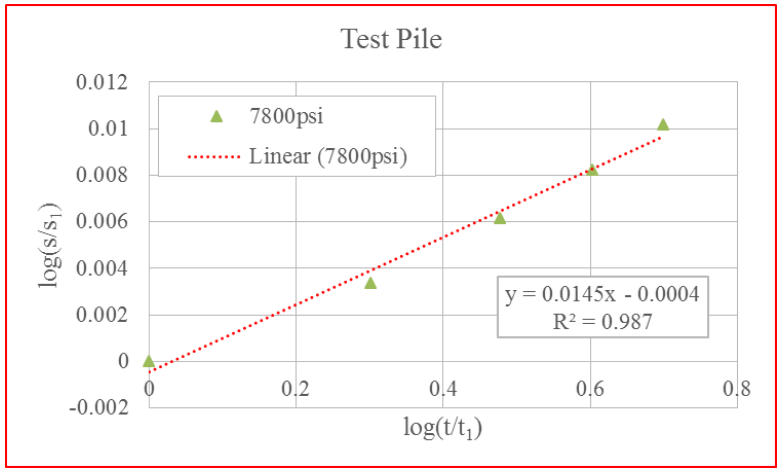

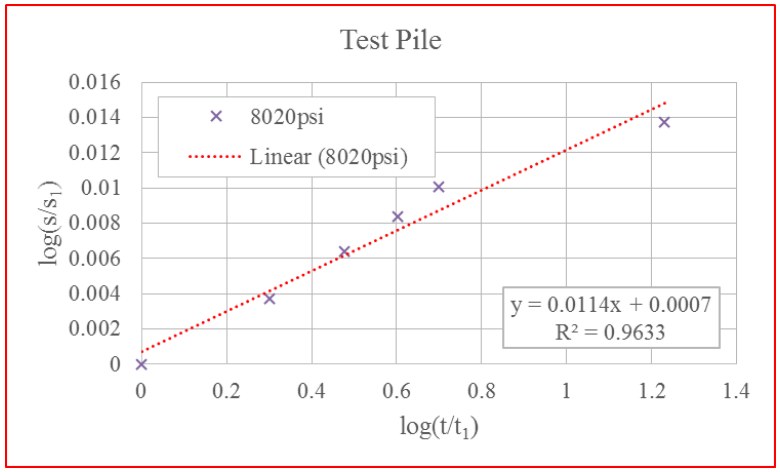

Figure 7-32 Continued

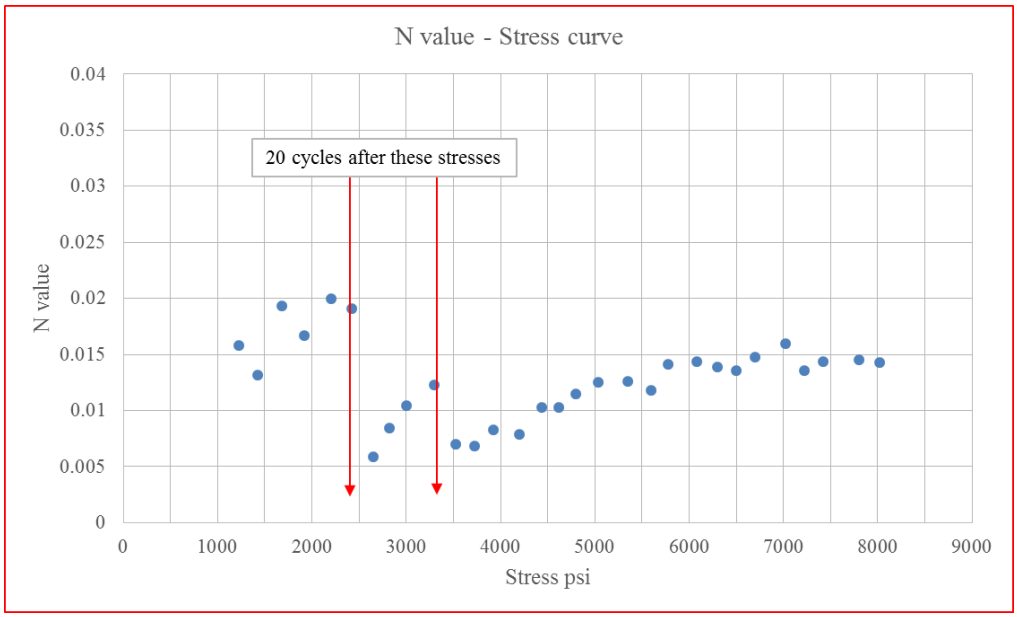

Figure 7-33. N value-stress curve, cyclic lateral load test, after (Little and Briaud, 1988)

Note: 1psi=6.89kPa

7.5.4. Cycle versus Creep

Creep can accumulate strain, which can be described as the power law model (equation 3-10). Cycle can also accumulate strain, which can be described by the equation below (Little and Briaud, 1988).

$$\frac{E}{E_1} = N^a \tag{7-3}$$

Where,

N: Number of cycles (not n value) and N is equal to 1 when there is no cycles;

E_1: Secant modulus E when N=1;

a: Exponent.

Combining equation 3-10 and equation 7-3, which yields,

$$\frac{t}{t_1} = N^b \tag{7-4}$$

Where,

b: Exponent, the slope when plotting the equation 7-4 in log-log scales;

t_1: Reference time for creep, in usual, t=1min;

t: Time for creep.

The equation 7-4 is the relation between creep and cycle. The creep time to accumulate the same accumulated strain caused by 20 cycles is calculated with power law model, plotted in figure 7-34 and figure 7-35.

However, the result is not that acceptable for the second 10 cycles at second load level (figure 7-35), it is caused by the inconsistence between completely unloading (big cycles) and partially unloading (small cycles). Big cycles and small cycles could be converted into each other as long as the same accumulated strain is reached, as plotted in figure 7-36 and figure 7-37. It is worth noting that at firs load level (low stress level), there is no much difference between big cycle and small cycle, while at second load level (medium stress level) there is a difference between big cycle and small cycle.

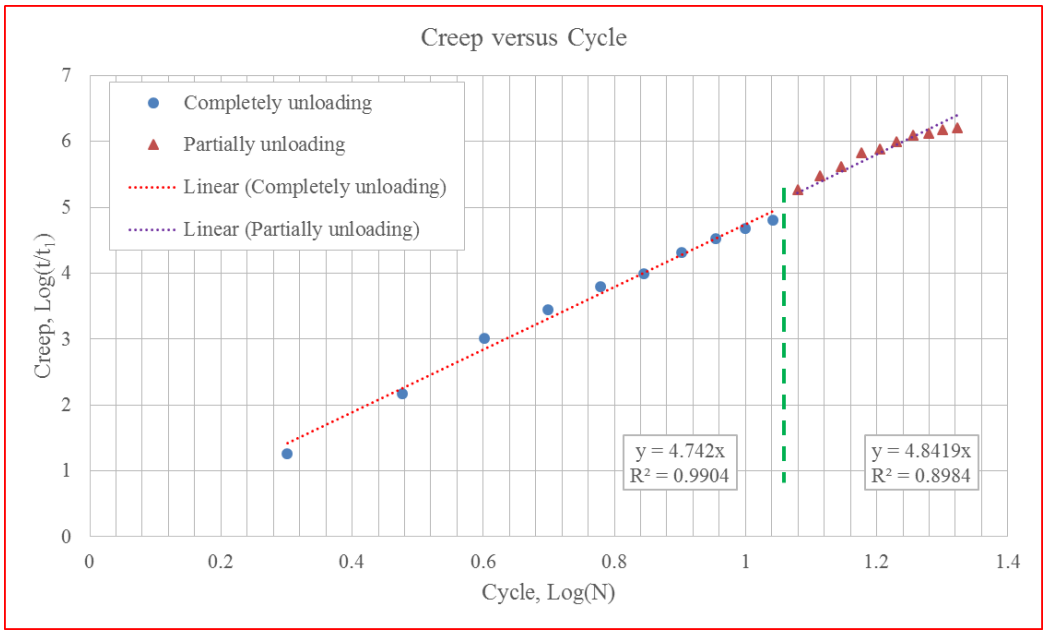

Figure 7-34. Creep versus cycle, at first load level

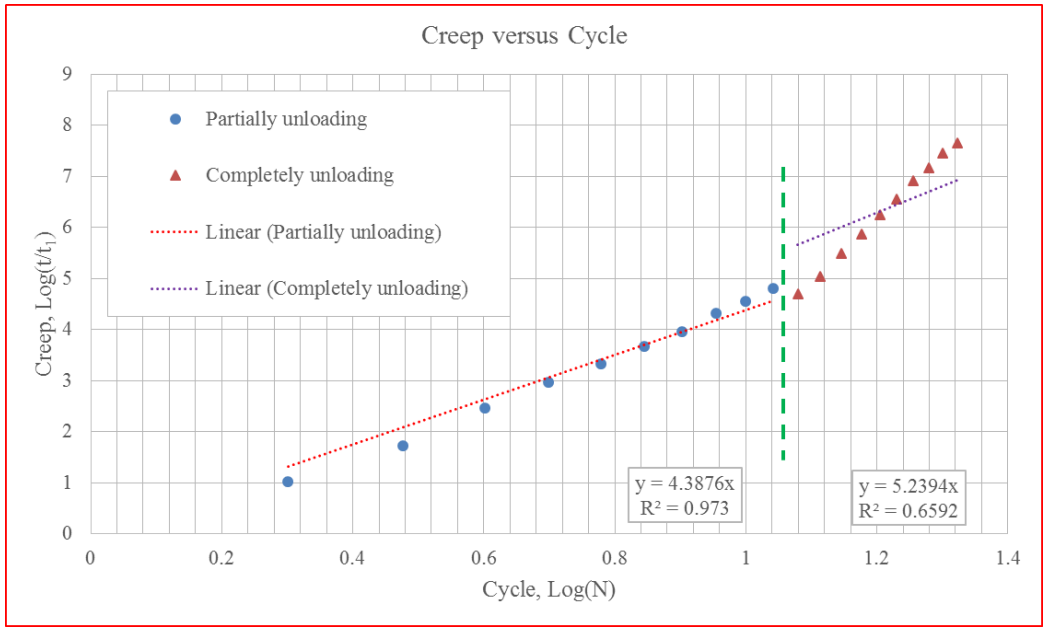

Figure 7-35. Creep versus cycle, at second load level

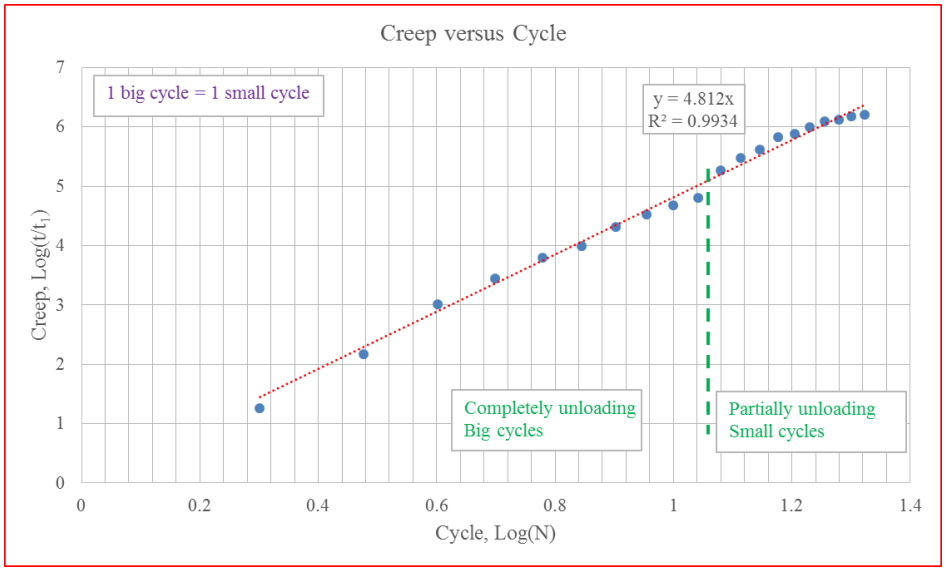

Figure 7-36. Creep versus cycle, at first load level, converting 1 big cycle to 1 small cycle

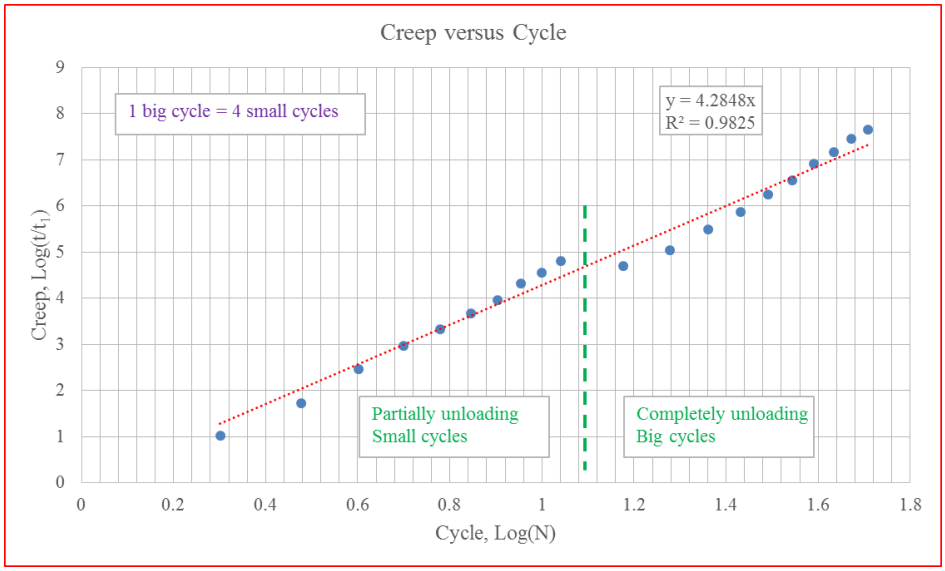

Figure 7-37. Creep versus cycle, at second load level, converting 1 big cycle to 4 small cycles

7.6. Conclusion

In this chapter the proposed power law model was applied to field tests. Several findings are made here:

- With regard to load increment test in field tests, n value will be significant impacted by unequal duration and unload-reload cycles. Without the impact from these factors, n value is independent of load level;
- N value at sustained load following a long duration will be drastically reduced, however, it will gradually recovers to a new constant value;
- N value at sustained load following a unload-reload cycle will be appreciably reduced, however, it will gradually approaches to a new constant value;
- For equal load increment field test with equal duration and without unload-reload cycle, n value from field test is close to, if not same to, n value from triaxial creep test in laboratory for a given soil, which demonstrates that n value could be taken as a soil property;
- The conversion, whether from creep criterion of GEC#7 to power law model or from power law model (normalization curve) to creep criterion of GEC#7, is readily simple.
- There is an equation between creep and cycle, because both can accumulate strain. However, this equation will depend on load level because cycle is not independent of load level.

8. NUMERICAL IMPLEMENTATION

8.1. Introduction

This chapter aims at stating numerical implementation of the proposed power law model. Because it is hard to write a new constitutive model to incorporate power law model, the power law model is manually added into numerical simulation, that is, in general, the following three steps are adopted to implement the power law model in numerical simulation:

Step one: conduct numerical simulation without creep;

Step two: choose the appropriate laboratory tests and/or field tests to acquire the n value;

Step three: manually update the deformation of gridpoints in numerical simulation in step one with power law model.

8.2. Triaxial UU Creep Test

Triaxial UU creep test on sample from borehole N3 at depth 2.4~3m is taken as the example to illustrate the numerical implementation.

8.2.1. 0 Minute Creep Curve

The numerical simulation is conducted with FLAC^{3D} (Itasca, 2006). The model of the sample is a cube with unit dimensions. Cam-clay model is adopted to describe the soil behavior with the following properties:

Shear modulus: 7000kPa

Maximum elastic bulk modulus: 30MPa

Soil constant: 7.72

Slope of normal consolidation line: 0.1

Slope of elastic swelling line: 0.04

Reference pressure: 1kPa

Preconsolidation pressure: 55kPa

Specific volume at reference pressure on normal consolidation line: 3.78

"0 minute creep curve" from numerical simulation is plotted in figure 8-1, while compared to measured creep curve and "0 minute creep curve" estimated with normalization curve (see subsection 5.4.2 and figure 5-21). The agreement between numerical data and measured data is quite good at most stress levels.

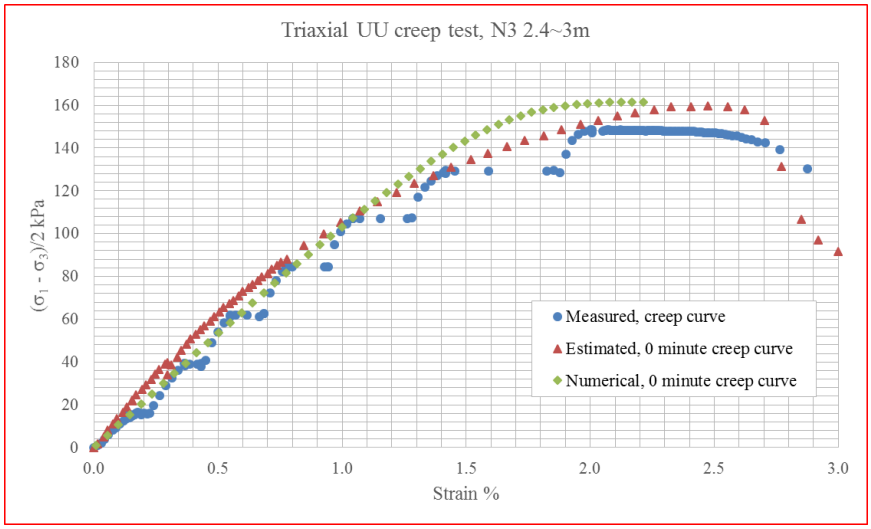

Figure 8-1. Numerical simulation of "0 minute creep curve", triaxial UU creep test, N3 2.4~3m

8.2.2. Creep Curve

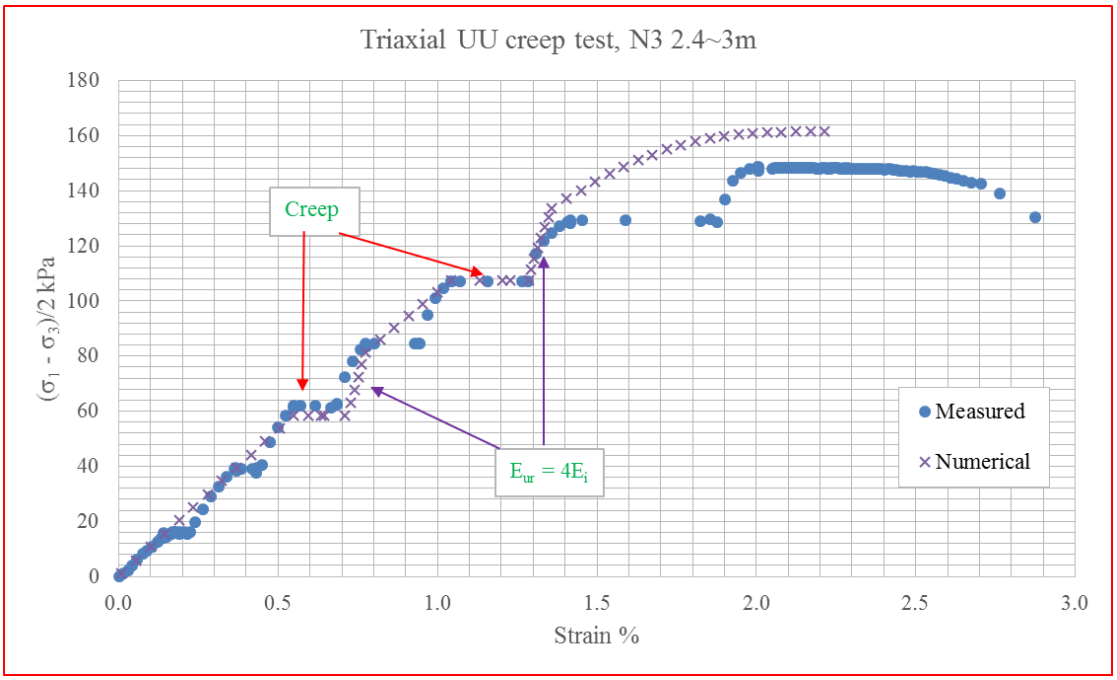

Figure 8-2. Numerical simulation of creep curve, triaxial UU creep test, N3 2.4~3m

N value from triaxial UU creep test (see subsection 5.4.3 and figure 5-23) is adopted in power law model. Two stress levels (40% and 70% of peak stress) are chosen for numerical simulation of creep curve. The procedure is described as below:

First, when the chosen stress level is reached, the simulation is paused and deformation of gridpoints is manually updated with power law model;

Second, switch the modulus from tangent modulus to unload-reload modulus, because the deformation accumulated by creep could also be accumulated by prestressing or preloading (see subsection 5.4.5 and figure 5-30), thus, it is necessary to

change the modulus after manually updating deformation with power law model. Restart the simulation;

Third, when the curve intersects with “0 minute creep curve”, switch the modulus back to tangent modulus from unload-reload modulus.

The result is plotted in figure 8-2, and the numerical data agrees very well with the measured data, which demonstrates the approach of this implementation works.

However, if deformation by creep is in concern, it is not necessary to calculate it (step three in section 8.1) in numerical simulation, because it is manually added into simulation

8.3. One-Dimensional (1D) Consolidation Test

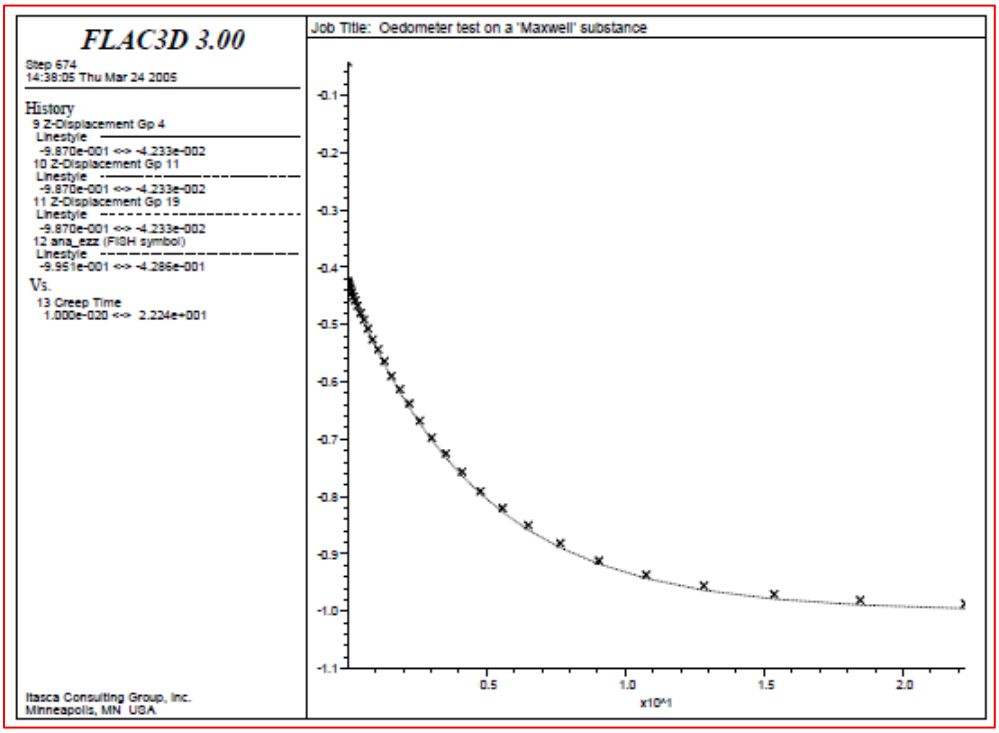

Figure 8-3. 1D consolidation test, numerical simulation and conventional method, from Itasca (2005)

There are three ways to calculate long-term deformation in 1D consolidation test: conventional method (see subsection 4.8.2), numerical simulation (with FLAC^{3D}), and power law model.

It has been demonstrated that the agreement is excellent between conventional method and numerical simulation with classical viscoelastic model in FLAC^{3D} (figure 8-3). Only primary consolidation is taken into account and the time corresponding to end

of consolidation is infinite. In other words, there is no way to take secondary compression into consideration in numerical simulation.

The fictitious example in subsection 4.8.2 is further discussed herein. On one hand, since the result from conventional method is identical to numerical simulation with classical viscoelastic model, there is no need to conduct numerical simulation; on the other hand, the only way to incorporate power law model into simulation is manually adding, while the result is exactly same with that calculated by hand (i.e., without simulation), there is also no need to conduct numerical simulation.

However, the time corresponding to end of primary consolidation, which is one parameter for calculation with power law model (see equation 4-4), needs to be addressed. It is found that it may be reasonable to assume it to be equal to the time corresponding to 95% degree of consolidation.

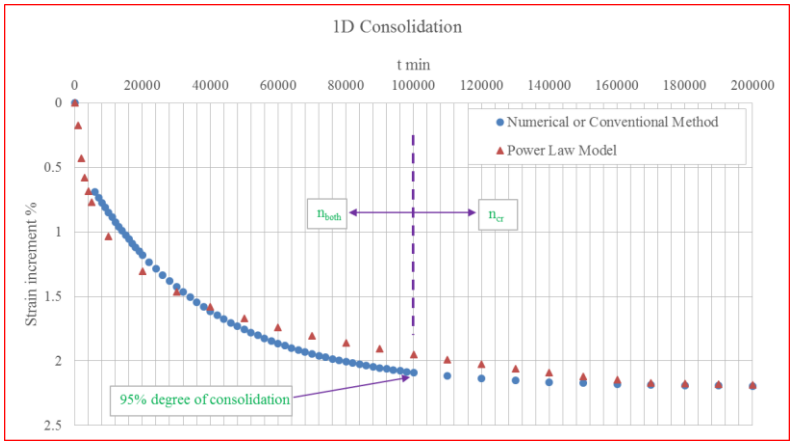

Figure 8-4. 1D consolidation test, numerical and power law model

8.4. Application in Practice

As previously stated, the proposed power law model is to describe time dependent behavior of soil in global level, and it seems that there is no need to incorporate the model in numerical simulation. If researchers prefer to implement the model in numerical simulation, the method presented in section 8.2 and 8.3 could be followed.

Thus, in practice, for example, embankments, foundations, retaining systems, etc., if time dependent behavior of soil is in concern, the following approach is suggested:

Step one: conduct numerical simulation (or calculation by hand) without taking time dependent behavior into account;

Step two: choose the appropriate laboratory tests and/or field tests to acquire the n value. That is to say, if the condition of the analyzed object is more close to oedometer test, n value from oedometer test needs to be adopted, otherwise, n value from triaxial creep test needs to be adopted;

Step three: calculate long-term deformation with power law model by hand or by simulation with the implementation approach described in previous sections (i.e., manually added).

9. CONCLUSIONS AND RECOMMENDATIONS

A power law model is proposed to describe time dependent behaviors of soils in this dissertation. The model is fully demonstrated through two kinds of laboratory tests on three different soils, data from literature, four kinds of field tests and one field practice.

This dissertation fulfills all objectives: a), validate TxDOT's design approach; b), study the time and possibility for creep failure at various stress level; c), predict long-term deformation in practice; d), propose some methods to reduce deformation caused by creep;

9.1. TxDOT's Design Approach

The objective of validating TxDOT's design practice is fulfilled by:

- The proposed power law model is feasible to describe time dependent behaviors of high PI clay, low PI clay, and sand. And creep behavior should not be directly associated with the presence of high plasticity clays;
- Both time for creep failure at any stress level and long-term deformation after duration of interest of engineer could be estimated with the power law model. Creep deformation should not be a concern when the ratio of service load of TxDOT's design over the ultimate load is one third (figure 5-24 and figure 5-25).

9.2. Creep Failure

The objective of studying creep failure is fulfilled by:

- Different from views of previous researchers, the criterion of creep failure is to exceed critical strain, namely, strain corresponding to estimated peak stress (critical strain is obtain by strain corresponding to peak stress from conventional triaxial shear test multiplying a ratio). Meanwhile, it seems creep failure can happen at any stress level as long as enough time is given. However, there will a stress threshold corresponding to a selected time which engineers are interested in;
- There is a unique curve (named “normalization curve”) to describe stress-strain curve until the peak stress for a given soil. It can be used to estimate peak stress in triaxial creep test when creep failure happens that results in the peak stress is unknown. It should be noted that estimated peak stress is obtained by multiplying peak stress from conventional triaxial shear test by a ratio, and in most cases this ratio is not equal to unit which previous researchers implicitly assumed it to be unit;
- Normalization curve could also be adopted to forecast ultimate load in field tests (figure 7-27);
- N value at different holding stresses could be compared by normalizing holding stresses over estimated peak stress, and n value-stress level curve is plotted. It is found that n value is in virtually independent of stress level;

- Time and possibility for creep failure at any stress level could be predicted based on normalization curve and n value-stress level curve;
- For equal load increment field test with equal duration and without unload-reload cycle, n value from field test is close to, if not same to, n value from appropriate laboratory tests for a given soil, which demonstrates that n value could be taken as a soil property;
- It is readily simple to convert, whether from creep criterion of GEC#7 to power law model or from power law model (normalization curve) to creep criterion of GEC#7;
- It is noticed that the duration of loading protocol in GEC#7 is unequal, namely page "E-9" in 2003 version GEC#7 and page 249 and 354 in 2015 version GEC#7, which is not quite reasonable because according the outcome of this research the deformation during 60min at 1.5DTL (i.e., design test load) will largely reduce the deformation during 10min at the load immediately following. It is suggested to revise the loading protocol in GEC#7 to keep the duration at all loading steps equal to obtain valuable results;

9.3. Long-term Deformation in Practice

The objective of predicting long-term deformation in practice is fulfilled by:

- Whether with consolidation or without consolidation, long-term deformation in practice is readily predicted with the power law model, and n value is

obtained from appropriate laboratory tests (triaxial tests or 1D tests) or field tests;

- If the appropriate laboratory test to obtain n value is triaxial tests, the long-term deformation could be predicted with normalization curve and n value-stress level curve, while the normalization curve will convert stress-strain curve in laboratory test to load-movement curve in practice;
- If the appropriate laboratory test to obtain n value is 1D tests, two n values (n_{both} and n_{cr}) needs to be obtained from 1D tests, while the time corresponding to end of primary consolidation (t_{eop}) will link laboratory tests to field practices;
- The power law model could be manually added into numerical simulation to implement the prediction of long-term deformation in practice;

9.4. Methods to Reduce Creep Deformation

The objective of proposing methods to reduce creep deformation is fulfilled by:

- Long-term deformation caused by creep could be readily estimated with power law model. When the time of interest (t) is certain, one way to reduce creep deformation is to limit S_1, since n value is independent of load level. It is clear that the lower the stress level, the lower the S_1. Therefore, creep deformation will be reduced by limiting the stress level;

- The second way to reduce creep deformation is prestress. It has been demonstrated creep deformation and n value will be largely reduced by an appreciably high prestressing ratio (figure 5-32);
- The third way to reduce creep deformation is by cycles, because both creep and cycles will accumulate deformation, it has been found there is an equation between creep and cycles in Chapter seven.

9.5. Recommendations for Future Research

The following recommendations are put forward for further research on this topic or similar topics:

- It is thought that n value from triaxial consolidated-drained (CD) creep test would be more suitable for predicting long-term deformation. And there should be two n values (n_{both} and n_{cr}) after applying power law model to triaxial CD creep test;
- The pressuremeter test (PMT) is close to pure shear test, while the mean stress is constant. However, there is excess pore pressure induced during the test, and if consolidation is defined as the deformation change with the dissipation of excess pore pressure, there should be two n values (n_{both} and n_{cr}) from PMT with a long duration. In usual, the duration of PMT is 30min at each step, n value obtained from PMT will be likely to be n_{both} for most soils except sand, and the long-term deformation prediction based on this n value will be possible to be precise at the early part of the prediction and not

suitable for long-term. If excess pore pressure could be able to dissipate rapidly in 30min (e.g., sand), two n values should be acquired in PMT, and the long-term deformation prediction would be accurate;

- Leaning Tower of Pisa is another case history that is worth to study with the proposed power law model, however, it is not included in this dissertation because of limited time;
- Creep is continuous deformation under constant stress, and relaxation is continuous stress releasing under constant strain. The microscope mechanism is quite similar. The proposed power law model may also work for relaxation, and it may be possible n value from creep test and relaxation test are the same, which further demonstrates n value could be taken as a soil property. Besides, it may be the combination of creep deformation and stress relaxation in practice. It will be very worthy to conduct the research on stress relaxation.

REFERENCES

Adachi, T., and Takase, A. (1981). "Prediction of long term strength of soft sedimentary rock". Proc. Int. Symp. on Weak Rock, Tokyo, pp. 21-24.

Arulanandan, K., Shen, C. K., and Young, R. B. (1971). "Undrained creep behaviour of a coastal organic silty clay". Geotechnique, 21(4), 359-375.

ASTM Standard (2007). "Standard Test Method for Unconsolidated-Undrained Triaxial Compression Test on Cohesive Soils". D2850-03a.

ASTM Standard (2011). "Standard Test Methods for One-Dimensional Consolidation Properties of Soils Using Incremental Loading". D2435/D2435M.

Bishop, A. W. (1966). "The strength of soils as engineering materials". Geotechnique, (16), 91-130.

Bishop, A. W. (1967). "Progressive failure with special reference to the mechanism causing it". In Proc. Geotech. Conf., Oslo, Vol. 2, pp. 142-150.

Bishop, A. W., and Lovenbury, H. T. (1969). "Creep characteristics of two undisturbed clays". In Proceedings of 7th International Conference of Soil Mechanics and Foundation Engineering, Vol. 1, pp. 29-37.

Bjerrum, L. (1967). "The third Terzaghi lectures; Progressive failure in slopes of overconsolidated plastic clay and shales". Journal of the Soil Mechanics and Foundations Division, 93(5), 1-49.

Briaud, J.-L. (1997). "The National Geotechnical Experimentation Sites at Texas A&M University: Clay and Sand". Report No.: NGES-TAMU-007.

Briaud, J.-L. (2013). “Geotechnical Enginearing : Unsaturated and Saturated Soils”. John Wiley and Sons Publishers, New York.

Briaud, J.-L., and Garland, E. (1985). “Loading rate method for pile response in clay”. Journal of Geotechnical Engineering, 111(3), 319-335.

Briaud, J.-L., and Gibbens, R. (1997). “Large scale load tests and data base of spread footings on sand”. Report No. FHWA-RD-97-068.

Briaud, J.-L., and Gibbens, R. (1999). “Behavior of Five Large Spread Footings in Sand”. Journal of Geotechnical and Geoenvironmental Engineering, 125(9), 787-796.

Briaud, J.-L., Griffin, R., Yeung, A., Soto, A., Suroor, A., and Park, H. (1998). “Long-term behavior of ground anchors and tieback walls”. Report No. FHWA/TX-99/1391-1. August, 1998.

Briaud, J.-L., and Lim, Y. (1997). “Soil-nailed wall under piled bridge abutment: simulation and guidelines”. Journal of geotechnical and geoenvironmental engineering, 123(11), 1043-1050.

Briaud, J.-L., Nicks, J., Rhee, K., and Stieben, G. (2007). “San Jacinto monument case history”. Journal of Geotechnical and Geoenvironmental Engineering, 133(11), 1337-1351.

Briaud, J.-L., Powers, W. F., and Weatherby, D. E. (1998). “Should grouted anchors have short tendon bond length?”. Journal of geotechnical and geoenvironmental engineering, 124(2), 110-119.

Briaud, J.-L., Smith, B., Rhee, K. Y., Lacy, H., and Nicks, J (2009). “The Washington monument case history”. International Journal of Geoengineering Case histories. http://casehistories.geoengineer.org, Paper ID: IJGCH, 1(3), 3.

Briaud, J.-L., Koohi, Y., Nicks, J., and Jung, I. (2015). “San Jacinto monument: new soil data and analysis including subsidence”. Journal of Geotechnical and Geoenvironmental Engineering, 141(6), 04015023.

Campanella, R. G., and Vaid, Y. P. (1974). “Triaxial and plane strain creep failure of an undisturbed clay”. Canadian Geotechnical Journal, 11(1), 1-10.

Casagrande, A. (1949). “Discussion of the paper on excavation slopes by Binger and Thompson, symposium on the Panama Canal-the sea level project”. Trams. Amer. Sot. Civ. Eng. 114: 870, 874.

Casagrande, A., and Wilson, S. D. (1951). “Effect of rate of loading on the strength of clays and shales at constant water content”. Geotechnique, 2(3), 251-263.

Chandler, R. J., and Skempton, A. W. (1974). “The design of permanent cutting slopes in stiff fissured clays”. Geotechnique, 24(4), 457-466.

Christensen, R. W., Wu, T. H., and Mencl, V. (1964). “Analysis of Clay Deformation as a Rate Process”. Journal of Soil Mechanics & Foundations Division, 90(6411).

Clough, G. W., Kuck, W. M., and Kasali, G. (1979). “Silicate-stabilized sands”. Journal of Geotechnical and Geoenvironmental Engineering, 105(1).

Dornfest, E.M., Nelson, J.D. and Overton, D.D. (2007). “Case history and causes of a progressive block failure in gently dipping bedrock”. Proceedings of the First North American Landslide Conference, Colorado.

FHWA (2003). “Geotechnical engineer circular No. 7: soil nail walls”. Report No: FHWA0IF-03-17, Department of Transportation.

FHWA (2015). “Geotechnical engineer circular No. 7: soil nail walls”. Report No: FHWA-NHI-14-007, Department of Transportation.

Galvan, M. (2012). “TxDOT Briadge Division, Proposal meeting RMC5 - 0-6784”.

Gibbens, R. M. (1995). “Load tests on five large spread footings on sand and evaluation of prediction methods”. MS thesis, Texas A&M University.

Havel, F. (2004). “Creep in Soft Soils”. PhD dissertation, Norwegian University of Science and Technology.

Henkel, D. J. (1957). “Investigations of two long-term failures in London Clay slopes at Wood Green and Northolt”. Proceedings of the 4th International Conference in Soil Mechanics and Foundation Engineering, London, England, Vol. 2, pp. 315-320.

Hunter, G. and Khalili, N. (2000). “A simple criterion for creep induced failure of over-consolidated clays”. Pro. GeoEng 2000 Conference, Melbourne.

Itasca. (2005). “Fast lagrangian analysis of continua in 3-dimensions, version 3.0, manual”. Minnesota: Itasca.

Karimpour, H., and Lade, P. V. (2013). “Creep behavior in Virginia Beach sand”. Canadian Geotechnical Journal, 50(11), 1159-1178.

Konikow, L. F. (2013). “Groundwater depletion in the United States (1900-2008)”. US Department of the Interior, US Geological Survey.

Kubena, M. E., and Briaud, J.-L. (1989). “Tension Capacity of Two Drilled and grouted Piles”. Texas A&M University, Department of Civil Engineering Report, 5887-2.

Kuhn, M. R., and Mitchell, J. K. (1992). “Modelling of soil creep with the discrete element method”. Engineering computations, 9(2), 277-287.

Kuhn, M. R., and Mitchell, J. K. (1993). “New perspectives on soil creep”. Journal of Geotechnical Engineering, 119(3), 507-524.

Kwok, C. Y., and Bolton, M. D. (2010). “DEM simulations of thermally activated creep in soils”. Géotechnique, 60(6), 425-433.

Ladanyi, B. (1972). “An engineering theory of creep of frozen soils”. Canadian Geotechnical Journal, 9(1), 63-80.

Ladd, C. C., Foot, R., Ishihara, K. Schlosser, F. and Poulos, H. J. (1977). “Stress-Deformation and Strength Characteristics”. Proceedings 9th of International Conference of Soil Mechanics and Foundation Engineering, Tokyo, 421-494.

Lefebvre, G. (1981). “Fourth Canadian Geotechnical Colloquium: Strength and slope stability in Canadian soft clay deposits”. Canadian Geotechnical Journal, 18(3), 420-442.

Lefebvre, G. Z., and Rochelle, P. L. (1974). “The analysis of two slope failures in cemented Champlain clays”. Canadian Geotechnical Journal, 11(1), 89-108.

Little, R. L., and Briaud, J.-L. (1988). “Full scale cyclic lateral load tests on six single piles in sand”. Texas A&M University. Report No. TAMU-RR-5640.

Lo, K. Y., and Lee, C. F. (1974). “An evaluation of the stability of natural slopes in plastic Champlain clays”. Canadian Geotechnical Journal, 11(1), 165-181.

Lo, K. Y., and Morin, J. P. (1972). “Strength anisotropy and time effects of two sensitive clays”. Canadian Geotechnical Journal, 9(3), 261-277.

Mesri, G., and Shahien, M. (2003). “Residual Shear Strength Mobilized in First-Time Slope Failures”. Journal of Geotechnical and Geoenvironmental Engineering, 129(1), 12-31.

Mitchell, R. J. (1970). “On the yielding and mechanical strength of Leda clays”. Canadian Geotechnical Journal, 7(3), 297-312.

Mitchell, J. K. (1993). “Fundamentals of soil behavior”. 2nd Edition, New York: Wiley.

Murayama, S., and Shibata, T. (1961). “Rheological properties of clays”. Proceedings of 5th International Conference of Soil Mechanics and Foundation Engineering, Paris, France, Vol. 1, pp. 269-273.

Nelson, J. D., and Thompson, E. G. (1977). “A theory of creep failure in overconsolidated clay”. Journal of the Geotechnical Engineering Division, 103(11), 1281-1294.

Noda, T., Fernando, G., and Asaoka, A. (2000). “Delayed failure in soft clay foundations”. Soils and foundations, 40(1), 85-97.

Pestana, J. M., and Whittle, A. J. (1995). “Compression Model for Cohesionless Soils”. Geotechnique, 45(4):611-631.

Pestana, J. M., and Whittle, A. J. (1998). “Time Effects in the Compression of Sands”. Geotechnique, 48(5):695-701.

Philibert, A. (1976). “Etude de la résistance au cisaillement d'une argile Champlain”. Master thesis, Université de Sherbrooke.

Pusch, R. (1978). “Creep Mechanisms in Clay”. No. Research Rpt 1978: 10Monograph.

Saito, M., and Uezawa, H. (1961). “Failure of soil due to creep”. In Fifth International Conference of Soil Mechanics and Foundation Engineering, Paris, pp. 315-318.

Sanzeni, A., Whittle, A., Germaine, J., and Colleselli, F. (2012). “Compression and Creep of Venice Lagoon Sands”. Journal of Geotechnical and Geoenvironmental Engineering, 138(10):1266–1276.

Singh, A., and Mitchell, J. K. (1968). “General stress-strain-time function for soils”. Journal of Soil Mechanics and Foundations Div, ASCE, Vol. 94 (SM1), pp. 21-46.

Singh, A., and Mitchell, J. K. (1969). “Creep potential and creep failure of soils”. In Soil Mechanics and Foundation Engineering Conference Proceeding, Mexico, Vol. 1, pp 379-383.

Skempton, A. W. (1964). “Long-term stability of clay slopes”. Geotechnique, (14), 77-102.

Skempton, A. W., and Hutchinson, J. (1969). “Stability of natural slopes and embankment foundations”. In Soil Mech and Fdn Eng Conf Proc/Mexico/.

Skempton, A. W. (1970). “First-time slides in over-consolidated clays”. Geotechnique, 20(3), 320-324.

Skempton, A. W. (1977). “Slope stability of cuttings in brown London clay”. In Proceedings of the 9th International Conference on Soil Mechanics and Foundation Engineering, Vol. 3, pp. 261-270.

Sowers G. F. (1979). “Introductory Soil Mechanics and Foundations: Geotechnical Engineering”. 4th Edition, Macmillan, New York.

Stark, T. D., and Eid, H. T. (1994). “Drained residual strength of cohesive soils”. Journal of Geotechnical Engineering, 120(5), 856-871.

Suroor, A. H. M. (1998). “Delayed failure of overconsolidated clays under sustained loads”. MS thesis, Texas A&M University.

Tavenas, F., Des Rosiers, J. P., Leroueil, S., La Rochelle, P., and Roy, M. (1979). “The use of strain energy as a yield and creep criterion for lightly overconsolidated clays”. Geotechnique, 29(3), 285-303.

Tavenas, F., and Leroueil, S. (1977). “Effects of stresses and time on yielding of clays”. Proceedings of the 9th International Conference on Soil Mechanics and Foundation Engineering, Vol. 1, pp. 319-326.

Ter-Stepanian, G. (1975). “Creep of a clay during shear and its rheological model”. Geotechnique, 25(2), 299-320.

Terzaghi, K. (1936). “Stability of slopes of natural clay”. Proceedings of the 1st International Conference of Soil Mechanics and Foundation Engineering, Cambridge, Mass. Vol. 1, pp. 161-165.

Van Asch, T. J., and Van Genuchten, P. M. B. (1990). “A comparison between theoretical and measured creep profiles of landslides”. Geomorphology, 3(1), 45-55.

Varnes, D. J. (1982). “Time-deformation relations in creep to failure of earth materials”. Proc. of the 7th Southeast Asian Geotechnical Conference, Vol. 2, pp. 107-130.

Vermeer, P. A., and Neher, H. P. (1999). “A Soft Soil Model that Accounts for Creep”. In Proceedings of the International Symposium Beyond 2000 in Computational Geotechnics (pp. 249-261).

Wong, R. C., and Varatharajan, S. (2014). “Viscous Behavior of Clays in One-dimensional Compression”. Canadian Geotechnical Journal, 51(7): 795-809.

Yin, J. H., and Graham, J. (1989). “Viscous-elastic-plastic Modelling of One-dimensional Time-dependent Behavior of Clays”. Canadian Geotechnical Journal, 26(2):199-209.

Yin, J. H., and Graham, J. (1994). “Equivalent Times and One-dimensional Elastic Viscoplastic Modelling of Time-dependent Stress-strain Behavior of Clays”. Canadian Geotechnical Journal, 31(1):42-52.

Yin, J. H., and Graham, J. (1996). “Elastic Visco-plastic Modelling of One-dimensional consolidation”. Geotechnique, 46(3):515-527.

Yin, J. H. (1999). “Non-Linear Creep of Soils in Oedometer Tests”. Geotechnique, 49(5):699-707.